ANTIBODY AFFINITY AND AFFINITY DISTRIBUTIONS

DETERMINATION IN ELISA AND BIOSENSOR

CIP-GEGEVENS KONINKLIJKE BIBLIOTHEEK, DEN HAAG

Pathak, Sulbha Sanjeev

Antibody affinity and affinity distributions.
Determination in ELISA and biosensor/
Sulbha Sanjeev Pathak; [ill.: Tar M. van Os]. - Rotterdam:
Erasmus Universiteit, Afdeling Immunologie. - Ill.
Thesis Rotterdam. - With ref.
ISBN 90-73436-27-3
NUGI 743
Subject headings: antibodies; affinity / enzym immunoassay/
biosensor

ANTIBODY AFFINITY AND AFFINITY DISTRIBUTIONS

DETERMINATION IN ELISA AND BIOSENSOR

ANTISTOF AFFINITEIT EN AFFINITEITSDISTRIBUTIES

BEPALING IN ELISA EN BIOSENSOR

PROEFSCHRIFT

ter verkrijging van de graad van doctor
aan de Erasmus Universiteit Rotterdam
op gezag van de rector magnificus
Prof. Dr. P.W.C. Akkermans M. A.
en volgens besluit van het College voor Promoties.
De openbare verdediging zal plaatsvinden op
woensdag 20 december 1995 om 11.45 uur.

door

Sulbha Sanjeev Pathak

geboren te Sangli, India

PROMOTIE-COMMISSIE:

Promotor: Prof. dr. R. Benner

Co-promotor: dr. H.F.J. Savelkoul

Overige leden: Prof. dr. H.G. van Eijk
Prof. dr. J.J. Haaijman
Prof. dr. H.J. Neijens

IMMUNOLOGIE
ROTTERDAM

The studies described in this thesis were performed at the Department of Immunology, Erasmus University Rotterdam.

Publication of this thesis was partly sponsored by Fisons Applied Sensor Technology, Cambridge, UK

Illustrations: Tar M. van Os
Printing: Ridderprint, Ridderkerk

To raise new questions, new possibilities, to regard old problems from a new angle makes a real adventure in science.
Where change is the only constant
(Einstein)

To Sanjeev and Gauri

Contents

INTRODUCTION

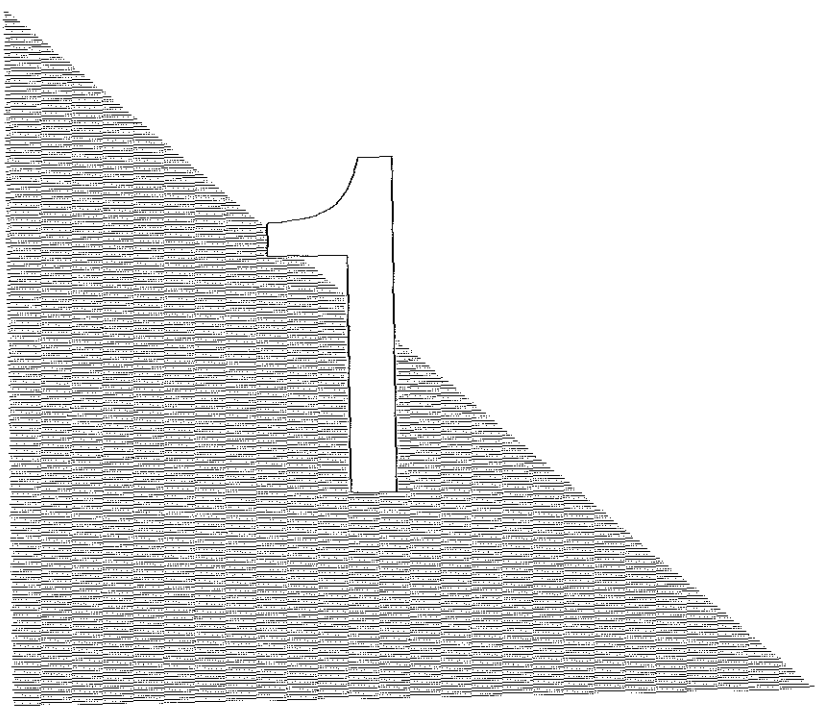

Introduction

अश्वंम् नैव, गजंम् नैव
व्याघ्रंम नैवच् नैवच्
अजापुत्रो बलिंम् दध्यात्
देवो दुर्बल घातकः

CHAPTER 1

Introduction

Neither the horse, nor the elephant, definitely not the tiger, but the weak and defenceless lamb is chosen for sacrifice - states a sanskrit observation coined about 1500 years ago (adjacent page). The ability to defend oneself against external and internal aggressors is indispensable for survival. Some form of self-defence is a basic requirement needed to protect oneself from a world of pathogens that is forever evolving. In mammals, the body's defence system is highly evolved. In them, the non-specific innate immune system and the specific adaptive immune system are linked together to form a formidable integrated host defence mechanism.

1.1 Humoral immunity: the role of B cells

In mammalian adults, bone marrow is the major site of the generation of B lymphocytes[194, 195]. The antigen-independent phase of B-cell maturation also takes place in the bone marrow, where lymphoid progenitors commit to the B cell lineage and subsequently differentiate into surface immunoglobulin M positive (IgM^+) B cells[208]. The differentiation of B lymphocytes from committed precursor cells to Ig secreting plasma cells is a multiple-step procedure that can be defined by changes in the expression pattern of lineage-specific genes[98, 152]. Mature B cells exit from the bone marrow and migrate to peripheral lymph nodes and other peripheral lymphoid organs, where the antigen-dependent phase of development takes place if the B cells encounter their specific antigen[146]. The terminal differentiation of B cells to antibody-secreting plasma cells takes place in these organs[98]. These plasma cells are end cells with the sole function of producing antibodies - the effectors of humoral immunity.

1.2 Helper T cells in humoral immunity

T lymphocytes are also produced by the bone marrow stem cells, but mature in the thymus. $CD4^+$ T cells regulate the humoral immune response by selectively inducing antigen-specific B cells to differentiate and secrete antibodies with different effector functions determined by the various Ig heavy chain isotypes[149]. Antibody responses to protein antigens require specific recognition of the same antigen complex by both B lymphocytes and $CD4^+$ T lymphocytes. Such antigens are called T dependent (TD) antigens and the T cells involved are referred to as T helper (Th) cells[277]. Protein antigens are processed by antigen-presenting cells (APC) and presented to Th cells in the context of MHC class II molecules along with costimulatory signals. The APC also produce IL-1. Together, these two events activate the T cells. Cross-linking of antigen receptors on cell surface along with help from activated Th cells activates the B cells. B cells can also obtain help directly from T cells by acting

as antigen-specific APC. T cell help has two components - release of cytokines and additional signals which require cell to cell contact, i.e. cognate help[reviewed in 197]. In cognitive interaction, T-B cells exchange a series of signals that result in selection, proliferation and differentiation of the B cells. Apart from MHC class II molecules, certain membrane molecules such as CD40L (gp39), CD28, CTLA-4 expressed by T cells and CD40 and B7/B7-1 (CD80), B7-2 (CD86) on B cells are important in T-B interaction[113, 144, 149, 150]. CD28 is constitutively expressed on T cells while CD40L and CTLA-4 are expressed only on activated T cells[64]. B7-1/B7-2, on the other hand, are activation antigens not constitutively expressed while the expression of CD40 is upregulated with the activation of B cells[25, 62]. CD28-B7 interaction is important in T cell stimulation, prevention of anergy and is thought to be indispensable in T-B costimulation[134, 272]. CD40-CD40L interaction, in particular, has a role in activation of B cells, isotype switching, the latter resulting in B cells expressing isotypes other than IgM, and memory development[73, 89, 131, 244]. One of the important aspects of the Th cell-B cell interaction is the receptor directed polar release of a variety of helper cytokines in the immunological synapse, resulting in high concentrations of these cytokines at the B cell membrane[143, 199]. The balance of cytokines produced profoundly influences the nature and magnitude of the immune response.

Table 1 Th subsets: cytokine secretion by Th1 and Th2 type $CD4^+$ cells

Cytokine	Th1	Th2
IFN-γ	+ +	-
IL-2	+ +	-
LT	+ +	-
TNF-α	+ +	+
GM-CSF	+ +	+
IL-3	+	+
IL-4	-	+ +
IL-5	-	+ +
IL-6	-	+ +
IL-9	-	+ +
IL-10	-	+
IL-13	±	+

Th subsets

Th cells can be divided into two major and distinct effector subsets based on their cytokine production profile (Table 1) and therefore their function[183, 184]. The two subsets mediate distinct immune responses; Th1 type cells are important in cell-mediated immunity, while Th2 type cells are known to

augment the antibody response[102, 224, 253]. However, this distinction is not absolute, and some Th cells secrete both Th1 and Th2 cytokines[77, 185] and have been called the Th0 cells. It is suggested that these Th0 cells can differentiate into Th1 or Th2 phenotype after antigenic stimulation[68, 250] or alternatively could be a third effector Th cell population[205, 269].

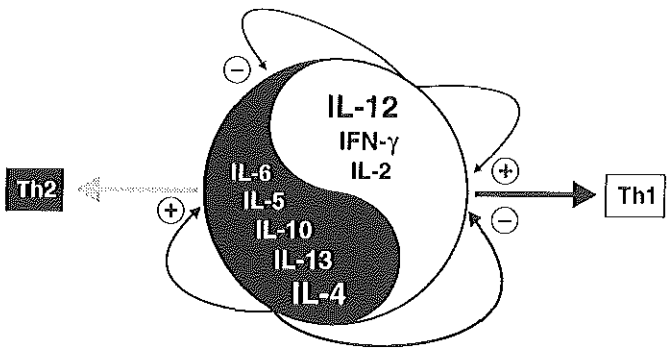

Figure 1 Th1 and Th2 cell generation is regulated by the equilibrium between different groups of cytokines. The Th1 and Th2 responses are maintained by both positive and negative feedback mechanisms (modified from Trinchieri, 1993).

It is established that cytokines are involved in the regulation of the different Th subsets. IFN-γ stimulates the proliferation of Th1 clones and inhibits the proliferation of Th2 clones. Even Th2 clones exposed to IL-2 and IL-4 are inhibited from proliferation by IFN-γ. However, it does not influence the cytokine production by these clones[75, 76, 77]. Recently, endogenously produced IL-12 was shown to be an obligatory cytokine for the generation of Th1 cells[105, 271]. It also has an indirect effect in that it induces IFN-γ production by T cells and NK cells in co-operation with TNF and IL-1. IL-4, on the other hand, inhibits the production of IL-2 and IFN-γ by naive $CD4^+$ and $CD8^+$ T cells that are stimulated with soluble CD3 in combination with APC[260]. Also, IL-4 directs the development of Th0 cells to Th2 cells resulting in an increased IL-4 production[2, 252, 255]. IL-10 and IL-13, like IL-4, are produced by Th2 cells[58, 67]. IL-10 inhibits the production of cytokines - especially IFN-γ - by Th1 cells and promotes the development of Th2 type cells[301]. IL-13 is similar to IL-4 in its action and is a multi-potent cytokine[59]. Both IL-10 and IL-4 are powerful inhibitors of IL-12 production[271]. A balance of cytokines produced by T cells thus influences the development of Th subsets as summarized in Figure 1. Several cytokines and other molecules secreted by APC - especially IL-10, IL-12 and prostaglandin E_2 produced by macrophages - also influence of the pathways of Th cell differentiation[60, 76, 78].

1.3 Specificity and diversity

The three remarkable and unique features of the immune system are specificity, diversity and memory[276]. The vertebrate immune system is capable of specifically recognizing and responding to an enormous number of antigens. This immune recognition and interaction with antigen is mediated by the surface Ig (sIg) and T cell receptor molecules expressed on the surface of the B and T lymphocytes, respectively.

Ig polypeptides consist of separate structural domains: a variable (V) domain that forms the antigen binding site, and three or four constant region domains (C) that mediate various effector functions[230] (Figure 2). The specific antigen-binding activity of Ig is conferred by the complementarity determining regions (CDR) of the V domain[120, 196, 292]. Both heavy (H) and light (L) chains of the Ig molecule make extensive contacts with the antigen, though frequently the contact made by the H chain is more extensive[29]. The antigen-binding specificity and affinity can be influenced by the variability in the residues involved in the V_L-V_H contact[1]. According to a generally held view, the driving force in protein association reactions arises from an increase in the entropy of ordered water molecules displaced from the interface upon complex formation i.e. hydrophobic interactions are thought to be an important driving force in protein associations[115]. However, recent work on free and lysozyme bound Fv fragments (a heterodimer consisting of only V_H and V_L domains) of anti-lysozyme antibody D1.3 suggests that a large number of water molecules form an integral part of antigen-antibody interface and improve complementarity by filling in voids not occupied by amino acid residues. Strict complementarity is achieved not by antibody residues alone, but by the participation of an intricate network of buried and solvent-accessible water molecules in and around the interface[24, 175]. The general consensus is that Van der Waal's interactions, hydrogen bonds and to a lesser extent salt bridges mediate the binding between antibody and antigen[24].

The total number of different Ig molecules that the immune system of an individual can produce is called the antibody specificity repertoire or the B cell repertoire. The creation of this primary repertoire does not require exposure to antigen. The diversity of the primary antibody repertoire is achieved through three different phenomena: diversity present in the germline multi-gene families, combinatorial diversity and junctional diversity. This primary repertoire is created by V(D)J recombination of the germline sequences. Following antigenic challenge, a process of somatic hypermutation further increases the specificity and the diversity of the immune response[21]. In mammals, though the average affinity of the serum antibodies often increases 10 to 30 fold, individual clones showing an affinity increase of between 10^3-fold or more may appear during the course of the immune response[290]. Additionally, further diversity in the nature of the immune response is achieved by the process of isotype switching.

By switching H chain C domains, class switch recombination permits the same variable or binding domain to be deployed to several different biological fronts[153].

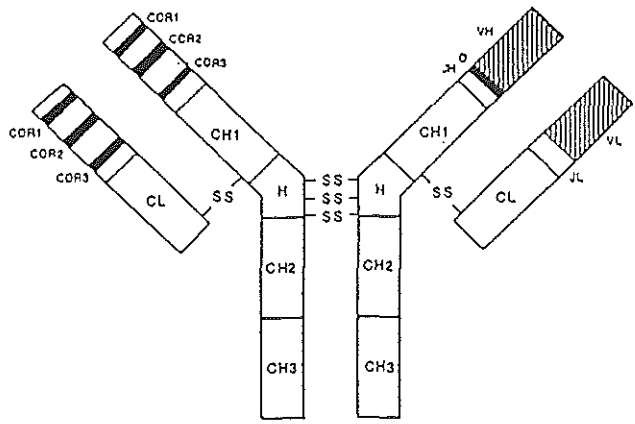

Figure 2 Structure of an IgG molecule V_H, C_H, V_L and C_L domains are shown as boxes and the hinge region is denoted H. Location of CDR regions and V_H, D_H, J_H, V_L and J_L gene segments are indicated by different shadings.

1.3.1 The V(D)J recombination

The immune system uses DNA-targeting enzyme systems to modify antigen receptor genes in the development of lymphoid cells[43, 268]. Three loci undergo rearrangement before Ig molecules can be produced (H chain, κ and λ). The variable domain exon encodes the antigen-binding pocket of the Ig molecule. It is assembled by integration of different subexons: V (variable) and J (joining) fragments for the κ and λ chain and V, D (diversity) and J fragments for each heavy chain[26]. Any one V region can join to any D or J region, so that an enormous diversity of antigen receptors can be generated from a relatively small number of germline subexons[55, 222]. V(D)J recombination is the combinatorial process by which developing lymphocytes begin to generate an enormous range of binding specificities from a limited amount of genetic information. The assembly process is tightly regulated, occurring in a preferred temporal order: D_H joins to J_H before V_H joins D_HJ_H; μ segments rearrange before κ[7, 204, 215, 240]. Junctional diversity further serves to increase the repertoire as the joining of the coding ends of the V(D)J subexons is imprecise. DNA recombination events occur during the integration of these fragments[285]. The joining does not occur at a fixed position; the amount of sequence contributed by each germline segment (V, D, and J) can vary by a small (usually less than 10) number of residues[176, 214, 286]. Moreover, random or templated additions[154, 268], as well as duplications contribute to increasing the repertoire[6, 49].

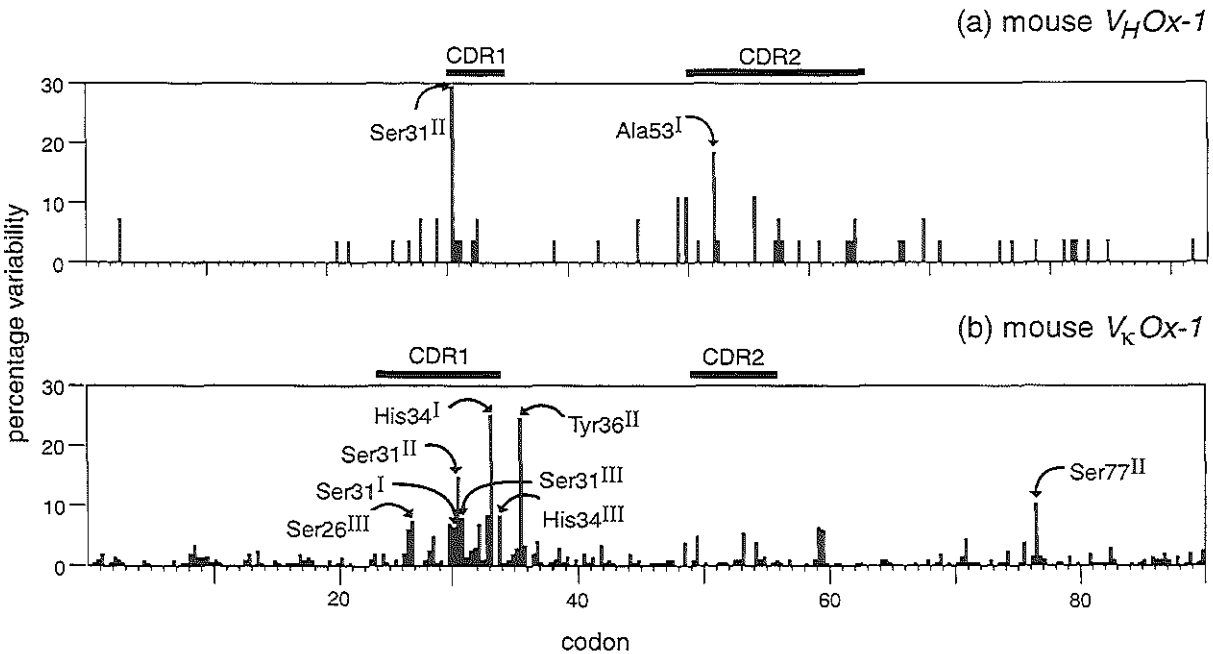

Figure 3 Pattern of hypermutation in Ig V genes of anti-pHOx antibodies. Variability is shown at each nucleotide position. Certain individual hotspots are marked with their codon designation, with the particular base position in the codon indicated by roman numeral. (a) Shows the mouse V_HOx-1 gene; variability calculated from 68 sequences selected by the antigen (b) Shows the mouse V_κOx-1 gene; variability was calculated from 166 sequences selected by the antigen (modified from Betz et al., 1993).

1.3.2 Somatic hypermutation

Extensive analysis of fetal liver B lymphocytes and human cord blood cells shows that the primary B cell repertoire in both man and mouse is essentially unmutated[39, 182, 201, 273, 287], while the repertoire of IgM-expressing peripheral blood B cells as well as the peripheral memory B cell pool is diversified by hypermutation[106, 232, 287]. In both these species antigenic activation by TD antigen is necessary to induce hypermutation in B cells. The somatic mutations accumulate only during the antigen dependent expansion of B-cell clones[11, 202]. During the course of a TD antigen-specific immune response, the strength of the binding between the antigen and serum antibodies increases with time[61, 116]. This phenomenon is referred to as affinity maturation[236]. Such maturation results from specific alterations of the structure of the antibody molecules[249] (Figures 3 and 4). The predominant mechanism of affinity maturation is hypermutation of V region genes coupled to antigenic selection[129, 177]. This somatic mutation occurs within restricted stretches of the DNA and serves to further diversify the genes encoding the antibody molecules[17, 95, 125, 286]. Somatic hypermutation acts specifically on rearranged Ig V, D and J gene elements and their immediate 5′ and 3′ flanking regions. Such mutations have not been detected in the C regions of somatically mutated antibodies and only rarely outside a region of about 1 kb surrounding the rearranged V region gene elements[28, 79, 125, 148]. In non-rearranged V genes, mutations have been found only occasionally or not at all[84, 225, 288].

The mutation rate may vary depending on the stage of differentiation of the B cells. A rate of 10^{-5}/base pair/generation may occur at the pre-B-cell stage allowing for a marginal increase in the pre-immune and early immune response repertoire[282]. However, nucleotide exchanges are estimated to be introduced at the very high rate of around 10^{-3}/base pair/generation in the rearranged V genes of antigenically stimulated cells[5, 11, 129, 177]. This rate implies that one mutation is introduced per second of a mitotic cycle! The expression of V-region genes in the effector phase of the secondary response along with the rare occurrence of mutations in myelomas and hybridomas[32] suggests that the hypermutation mechanism is up- and down-regulated in a stage-dependent manner[5].

Point mutations are the major class of somatic mutations seen in the murine antibody[17, 28, 42, 80, 188, 286], though some deletions, insertions and potential recombination events have also been reported[53, 79, 125]. Silent mutations not expressed at the protein level are spread over the entire V region and represent a neutral background resulting from the nature of the intrinsic mutational process[21, 45, 172, 202, 228]. Characteristic nucleotide substitution preferences called mutational hotspots are observed in both V_H and V_L genes[20, 85]. Indeed, recent work indicates certain codon positions (represented by amino acids at position 30, 31, 50, 55 and 90, 113) are often mutated, even in response to

different antigens[31, 53, 72, 82, 186, 237]. Position 113 in particular may play a role in determining antibody specificity in general, since it is modified by somatic mutation in a variety of antibodies[53, 213, 235, 262]. The hypermutation process seems to exhibit a preference for transitions over transversions[81, 82, 119, 148, 283]. It also manifests strand polarity - a low frequency of mutation is seen for thymine and cytosine while adenine and guanine mutate with a comparatively higher frequency[21]. Also, fewer mutations are found 5′ of V(D)J as compared to the 3′ region[284].

Any mutation that causes a change in the CDR of an antibody molecule directly affects the antigen-antibody binding since these regions are in direct contact with the antigen. Determination of the crystal structure of the complex between Fab of an anti-2-phenyloxazolone (phOX) antibody and its hapten showed that many of the mutations were in the border of CDR1 and FRW (Frame work) II regions. The amino acids at position 34 (His) and 36 (Phe) in CDR1 seem to be particularly prone to mutation. Alzari et al.[8] have established that amino acids at these two positions are directly in contact with the hapten and therefore important in phOx-antiphOx interaction. Affinity measurements showed that amino acid exchanges in these positions resulted in an 8- to 10-fold increase in affinity[10]. Similar preference for mutations in particular positions of the V genes have also been reported for other antigens[37, 174, 229, 295]. Some CDR residues close to the antigen but not directly in contact with it as well as some amino acids in the FRW that can influence CDR conformation and/or orientation may also undergo mutations[71, 145, 220, 228, 241].

In the case of phOx, a clear mutational drift is observed in antibodies in the later stages of the immune response. A change from two point mutations per chain in the early stages to eight mutations in the tertiary response exemplifies this mutational drift[14, 64]. In the secondary or later stages of the immune response, a repertoire shift towards other germline gene combinations is observed[13], perhaps because it is increasingly difficult to improve the kinetics of binding as affinity increase through somatic mutations may reach saturation[241]. The later stages of the immune response may then be dominated by antibodies bearing a different, kinetically more favorable, antigen-binding site[14, 70].

Despite intensive efforts, the mechanism of the hypermutation process remains unclear. The signal for the location of the mutational target seems to be generated by the rearrangement of V and J gene segments. For full activation of the mechanism, signals associated with both V and J regions may be required, since DJ rearrangements in the inactive IgH loci exhibit about ten times less somatic mutations than do their active counterparts[5, 206, 213].

Productively and non-productively rearranged Ig loci containing a V gene element are mutated to a similar extent[84, 104, 198]. Although it has been suggested that somatic mutation is linked to the origin of DNA replication[207],

it has been shown that though B cell proliferation is clearly necessary for induction of hypermutation, by itself it is not sufficient to induce hypermutation[294]. It is generally believed that the molecular mechanism involved in the generation of somatic mutations is random introduction of point mutations in rearranged V genes[173]. However, the predominance of mutations in the CDR regions and the high rate of substitutional to silent mutations argue against a random mechanism. Also, although only some somatic mutations have a significant effect on the affinity for antigen[15, 94], there seems to be a very limited fluctuation in the pattern of somatic mutations between individual mice[147]. A templated mechanism of somatic hypermutation has therefore been suggested. But, the fact that somatic modifications are introduced in introns and sometimes as much as those in the CDR would argue against a templated mechanism as well[79, 82]. The elucidation of the mechanism must await further experimentation. It seems certain that the effective targeting event is not the result of a single DNA-binding factor but rather a complex series of interactions involving more than one element scattered over a large DNA region[19].

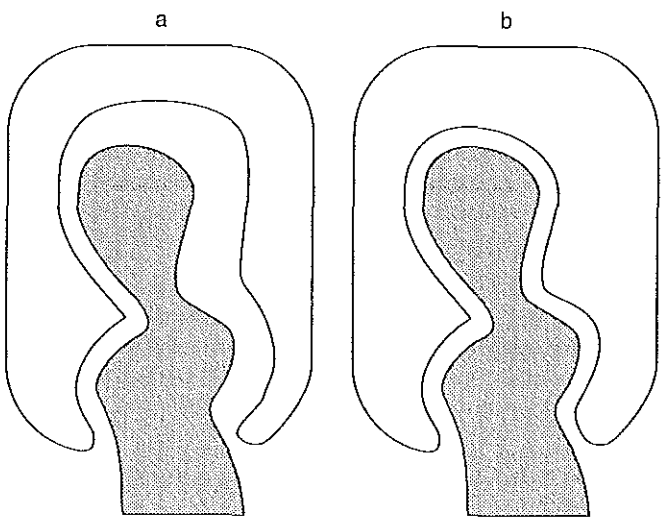

Figure 4 Schematic representation of the consequences of hypermutation. (a) Antibody produced early in the primary immune response. (b) Antibody produced in late secondary responses. Complementary improves as a result of hypermutation; consequently, the affinity of the antibody for the antigen also increases.

The time at which hypermutation occurs, relative to the process of heavy chain switch, is not clear. In human tonsillar germinal centers (GC), most centroblasts have already deleted their μ heavy chain genes, indicating that switch signals are delivered before centrocytes are selected and induced to differentiate[164]. Sequence analysis of individual V region genes expressed by the progeny of individual precursor cells allows the construction of genealogical trees. Such experiments indicate that somatic mutations can be introduced both before and

after the isotype switch[5, 177, 212]. The recovery of sequences with identical switch recombination sites, but different patterns of somatic mutations as well as the appearance of somatic mutations in the V regions before class switch recombination suggests that hypermutation is active both before and after the switch[166, 227].

Berek and Milstein[15] have analyzed the phenomenon of affinity maturation in the murine model. They established that 7 days after primary immunization, practically no somatic mutations are found in the V-region. Similar results have also been reported for other antigens[52, 170, 295]. However, in the case of lymph node GC, the earliest time point at which mutated sequences have been detected is between 4 and 6 days after primary immunization, indicating a more rapid onset of hypermutation in the lymph node[147, 164, 289]. The frequency of somatic mutations rapidly increases during the second week after immunization[12]. As certain V-region residues are critical for binding a given antigen, specific mutations are repeatedly selected[15, 289]. By day 14 almost all sequences contained somatic mutations[95].

Sequence analysis of secondary and tertiary response antibodies has shown that the affinity maturation in the memory response is caused by a further increase in the number of somatic mutations[15], suggesting the reactivation of the hypermutation mechanism after antigenic stimulation[10, 202]. In contrast, in transfer experiments[56, 235] and by *in vitro* activation of $sIgG^+$ cells[178], it has been shown that memory cells proliferate and differentiate into plasma cells without activation of the hypermutation process. It seems therefore possible that there are two different types of memory cells: larger $sIgM^+$ blast cells corresponding to long-term memory cells, that could stay in the follicles for prolonged periods of time, and which could undergo further rounds of mutation and small resting memory cells that have undergone isotype switching, desist from further hypermutation and finally leave GC[10, 251]. There is some evidence for both types of cells.

It is generally accepted that somatic hypermutation and affinity maturation occurs during the proliferative phase of the B cells in the GC[111, 163]. Cells with increased affinity have a proliferative advantage and are allowed to expand and/or differentiate[35, 48], while low affinity variants are pushed into the pathway to apoptosis[155, 157]. The salient features of somatic hypermutation are summarized in Table 2.

1.3.3 Class switch recombination

In mice, the class switch recombination allows the variable-domain exon to be switched from Igμ-type heavy chain to any of six alternative constant domain

Table 2 Salient features of somatic hypermutation

- Somatic hypermutation occurs in the germinal centers and is observed only for TD antigens.
- The process of hypermutation seems to begin 4-7 days after the primary immunization.
- Hypermutation occurs during a small window in the proliferative stage of B cells in the germinal centers. Nucleotide exchanges may be introduced at a rate of 10^{-3}/base pair/generation.
- It occurs in restricted stretches of DNA on rearranged V(D)J regions. Mutations are more frequent in the CDR regions directly in contact with the epitope than in the FR regions.
- Point mutations are the major class of mutations observed.
- Characteristic nucleotide substitution preferences called mutational hotspots are observed both in V_H and V_L regions.
- Transitions (AT→GC) are preferred over transversions (AT→CG). The process also exhibits strand polarity, low frequency of mutation of thymine but not adenine and similarly of cytosine but not guanine.
- High affinity clones are preferentially expanded, while low affinity or altered specificity clones undergo apoptosis.
- The process of hypermutation occurs in a step-wise manner, brief bursts of high of mutation rates interspersed between periods of mutation free growth [128].

exons (γ1, γ2a, γ2b, γ3, α and ε). The fully assembled and expressed V_H gene is coupled to a new C_H gene so that the antigenic specificity of the antibody remains unchanged, but the effector functions vary[153]. The switch generally takes place after a committed B lymphocyte has been stimulated by an antigen or mitogen[50, 122, 190], but there remains evidence that it can also occur during early stages in B cell development[3, 101].

The genes encoding the different heavy chain isotypes are located in the C_H locus on chromosome 12 in mice. They are clustered at the 3′ end of the V-region gene segment in the order 5′-Cμ-Cδ-Cγ3-Cγ1-Cγ2b-Cγ2a-Cα-Cε-3′. The entire locus spans about 200 kb[231]. The constant region genes except for Cδ are flanked by switch regions at the 5′ end. They vary in length from 1 kb (Sε) to 10 kb (Sγ1) and share homology with each other, being composed of tandem repeats that vary both in length and sequences[63, 96, 101].

The primary mechanism for switching involves intrachromosomal recombination, with looping out and deletion of the C_H genes between the sites of recombination[47, 101, 108]. In both man and mouse, switching is preceded by transcription of the unrearranged C gene segment to which the cell will be switching and there is a strict correlation between the expression of specific C_H germline transcripts and subsequent switching to the corresponding gene[118, 226, 233, 247]. These germ-line transcripts appear not to be translated and are referred to as sterile transcripts. They are initiated at multiple sites 2 kb 5′ to the S region, and proceed through the S region and the C segment [151, 160, 246]. Recent experiments have shown that if a DNA segment which contains the promoter and first exon (germ-line exon) of the germline transcript is deleted, switching does not occur on that chromosome, indicating that transcription of germ-line

transcripts is probably necessary for switching[57].

Role of cytokines and adhesion molecules in isotype switching to IgG1 and IgE

Unlike hypermutation, heavy chain class switch recombination is not a stochastic event[66]. IL-4 was reported to be needed for the isotype switch to IgG1 and IgE[46, 107, 218, 219, 278]. IFN-γ, on the other hand, inhibits expression of both γ1 and ε germline transcripts induced by LPS and IL-4[18, 226]. Three protein complexes, one of which is constitutively expressed, have been shown to bind to a 179-base pair LPS/IL-4 responsive germ-line epsilon promoter[210]. The early B cell-specific transcription factor (BSAP) is found to be involved in the formation of this constitutively expressed complex. Moreover, this BSAP binding site is essential for IL-4 and LPS induced germ-line ε transcription and class switching to Cε gene. Recently, Delphin and Stavnezer[57] have identified three transcription factors that appear to regulate induction of transcription of mouse germline ε promoter. Mutation in any of the sequence elements that bind these factors, within the context of the germline ε promoter abolishes or reduces induction by IL-4. Similar sites are also found in the mouse germline γ1 promoter.

Recent studies indicate that B cells switched to IgG1 can further switch to IgE by the process of a second looping out and deletion called sequential isotype switching. A large body of evidence favors such a mechanism. During the process of isotype switching to IgE, many B cells stain doubly positive for sIgG1 and sIgE[239]. Other studies showed that LPS stimulation of IgM positive B cells leads to the formation of IgE positive cells with IgG1 positive cells as intermediates[171, 234]. Cytoplasmic staining of the intermediates revealed IgG1 and IgE double positive B cells suggesting co-secretion by the double positive cells. Recently, Van Ommen et al.[274] have shown that sequential isotype switching to IgE indeed occurs in not only primary, but also secondary responses of IL-4 treated mice. In human B cells, on the other hand, isotype switch to the ε locus seems to occur either directly from μ to ε, or by a double step sequential switching from μ to ε via γ or even by a triple step sequential switch from μ to ε via the α and γ genes[299] (Figure 5).

Currently, it is agreed that two separate signals are necessary and sufficient to induce isotype switching to IgG1 and IgE. The first signal is provided by IL-4 or IL-13, the second is provided by the physical interaction of B cells and activated T cells[27, 47]. Adhesion molecules are thought to have an important role in this process. CD40-CD40L interaction has a central role in isotype switching. *In vitro* experiments with murine cDNA for CD40L have shown that it can induce B cell proliferation and IgE production in the presence of IL-4. In humans, CD23-CD21 interaction seems to play a key role in the generation of IgE. CD23 interacts with CD21 on B cells driving them to IgE production.

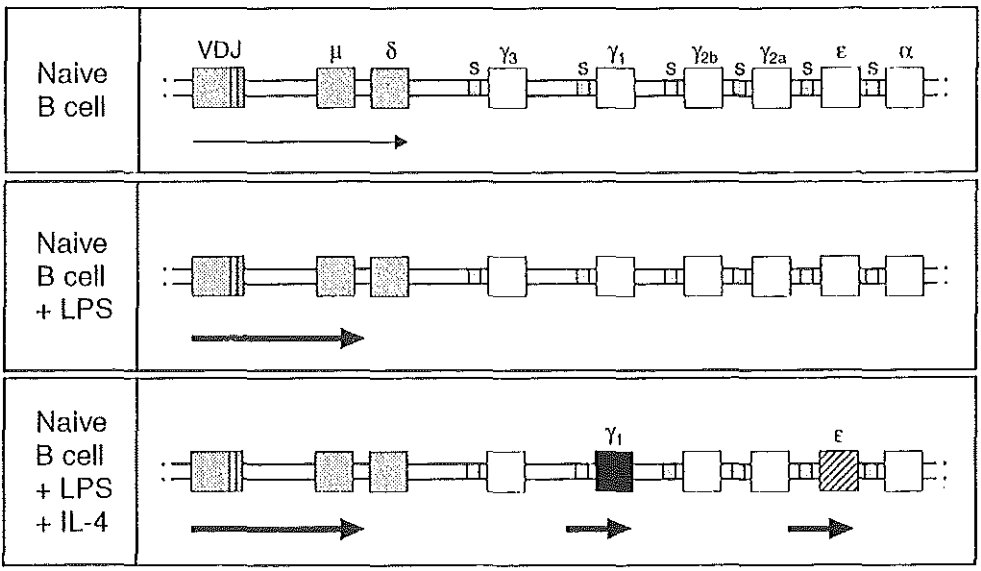

Figure 6 Murine isotype switching. Resting naive B cells ($sIgM^+ IgD^+$) transcribe the μ and δ loci at a low rate. LPS induces IgM secretion. In the presence of IL-4, Cγ1 and Cε are transcribed at a low rate preceding switching to IgG1 and IgE (modified from Janeway and Travers, 1994).

1.4 Memory

Immunologic memory is defined as the ability to generate a more effective immune response after a secondary encounter with antigen and can be evoked months or years after an initial antigenic encounter[33, 40, 41]. Memory cells exhibit higher affinity receptors[296] and have lower activation thresholds than virgin cells[216, 276]. The development of B cell memory is a T cell dependent process[88]. At the serum level, memory antibody responses are characterized by the rapidity of the response, increased magnitude and time span of the response, presence of antibodies of a higher average binding affinity and of isotypes other than IgM.

1.4.1 Phenotype of memory B and T cells

The origin of memory B cells is controversial. One theory suggests that plasma cells and memory B cells originate from the same daughter cell[38]. An opposing theory states that different precursor B cells are programmed to give rise to memory cells and plasma cells within a clone prior to antigenic exposure[127]. The controversy regarding their lineage awaits resolution though these theories

do agree that at some point the B cell lineages diverge to give memory cells and plasma cells. Memory B cells can be distinguished from the naive cells on the basis of cell surface markers[44, 209, 242] (Table 3). Moreover, memory B cells express surface Ig molecules of a higher affinity than the naive cells due to the process of affinity maturation[16]. They are also more efficient in antigen trapping and processing[276].

Table 3 Phenotypic characteristics of memory B cells

Marker	Naive cells	Memory cells
CD44 (Pgp-1)	low	high
MEL-14 (L-Selectin)	low	high
sIgD	+	-
PNA	high	low
J11D	high	low
M17	-	+

The development of memory T cells out of naive T cells is accompanied by a number of cell-surface changes that may affect T cell triggering, interactions with B cells or other APC, and recirculation[51, 140, 162]. A plethora of surface molecules have been proposed as markers for memory T cells[87, 162, 242]. CD45 is one of them. It is expressed on all leucocytes in different isoforms due to alternative splicing[267]. In humans, the CD45RA isoform is supposed to occur on naive cells while the CD45RO isoform is proposed to be the marker for memory cells[22, 217, 238, 261]. However, the work of Bell and Sparshott[9] and Michie et al.[180] suggests that CD45RO may not be stably expressed over long periods of time, and the memory phenotype may revert to the naive phenotype. In the murine model the CD45RB isoform has been used to distinguish functionally distinct subsets of T cells. Memory T cells express low levels of this isoform, while naive cells express high levels (Table 4). Additionally, murine memory T cells express high levels of adhesion molecules[36, 161, 200, 245] and low levels of the lymphocyte homing receptor L-Selectin (MEL-14)[30, 192, 254]. Differentiation of naive and memory cells on the basis of cytokine production *in vitro* following *in vivo* boosting has also been investigated[34,88]. However, distinguishing such responses need consideration of phenotype, activation state, and analysis of function, making the interpretation of data difficult[88].

1.4.2 Mechanisms of immunological memory

Two different mechanisms have been postulated to account for immunological

memory. The conventional model holds that specialized, long-lived 'memory cells' harbor memory[38, 41]. However, the formal demonstration of long-lived antigen specific memory cells has proved difficult. Most of the older studies

Table 4 Phenotypic characteristics of memory T cells

Marker	Naive cells	Memory cells
CD44 (Pgp-1)	low	high
MEL-14 (L-Selectin)	high	low
CD45RB	high	low
CD11a/CD18 (LFA-1)	low	high
CD54 (ICAM-1)	low	high

demonstrate the persistence of memory in the absence of cell division. Schittek and Rajewsky[221] have demonstrated the persistence of memory in absence of cell division in mice by using techniques to label proliferating cells. Also, long-lasting T cell memory for *M. tuberculosis* has been demonstrated in mice treated with cyclophosphamide or ionizing radiation[193]. In a recent study, however, Mullbacher[187] has demonstrated that $CD8^+$ memory T cells reactive to influenza virus can persist for 25 weeks in the absence of antigen.

The second model assumes that memory is critically dependent on continuous stimulation by the antigen, which results in the persistence of effector-type or activated clones[23, 65, 92, 191, 267]. In adoptive transfer experiments memory B cells have been shown to decay rapidly in the absence of antigen, while they survived indefinitely when transferred with the antigen[93, 191]. Similar dependence was reported for T cell memory as well[92]. Follicular dendritic cells (FDC) are proposed to play a critical role in immune memory responses. FDC within the primary follicles and GC serve as antigen depot and constantly restimulate B cells[117, 189, 265, 266]. However, FDC cannot process antigen and therefore cannot participate in maintenance of T cell memory. But, it has been shown that B cells can become effective as APC when interacting with FDC in an antigen-specific manner[90, 134]. The fact that the survival of the memory cells is dependent on the presence of antigen, does not necessarily imply the memory cells engage in a chronic proliferative response to the antigen. Also, the possibility that long-lived memory cells eventually become independent of the antigen cannot be excluded[223], and unequivocal results regarding the necessity of antigen for survival of memory B cells remains elusive.

Current evidence suggests that memory cells have a more rapid turnover than virgin cells[180, 270]. Chromosomal lesions that preclude cell division were

followed with time after irradiation in CD45RA (naive phenotype) and CD45RO (memory phenotype) T cells. The CD45RO with dicentric chromosomes disappeared from circulation within 1 year, while CD45RA cells survived for several years without cell division. Other adoptive transfer experiments also support the notion that naive T cells and B cells in mice have a long life spans[243, 279]. The life span of memory cells and hence the decay of the memory response may be related to the expression of molecules such as bcl-2[191], but the factors that influence bcl-2 levels in memory cells are also not known.

1.5 The germinal center

It is generally accepted that the GC is the defined anatomical site of:

i. clonal expansion of B cells[109, 110, 139],
ii. somatic hypermutation in B cell Ig V-region genes[12, 121],
iii. selection of B cells on the basis of their ability to receive antigen-specific signals[157],
iv. induction of differentiation pathways to memory cells[48, 126] or plasma cells[132, 263], and,
v. Ig isotype switching[129, 135].

The main constituents of GC are activated B lymphocytes, FDC, tingible body macrophages and $CD4^+$ T lymphocytes[35, 103, 112, 211, 248, 281]. The Th cells have a Th2-like phenotype in that they produce IL-4[34] and seem to be largely specific for the immunizing antigen[74, 181]. It was generally believed that T lymphocytes do not require the GC micro-environment to establish memory[143] and that the T cell antigen receptor genes are incapable of hypermutation[55, 97, 276, 291]. Recently, however, Zheng et al.[300] have presented direct evidence that the small population of antigen-specific T cells that are recruited in splenic GC acquire mutations in the variable region of the α-chains but not the β-chains. It is therefore tempting to suggest that mutational diversification and selection of T cells may also be accomplished in the GC.

The recruitment of virgin B cells into TD responses is confined to the first few days after exposure to antigen; the response is subsequently maintained by memory B cell clones[91]. Virgin B cells do not respond to antigen localized on FDC but can be activated outside the follicles[91, 280], and form GC[91, 138, 169]. By the second day following primary immunization with a TD antigen, antigen binding T cells may be found within the periarteriolar lymphatic sheath (PALS)[109, 110, 169]. By the fourth day of the response, antigen-specific B cell blasts begin to fill the FDC network of the lymphoid follicle, initiating the GC reaction[123, 137, 138, 258]. The GC response reaches a maximum by day 10-12 of the primary response and in the absence of further free antigen, the GC decline in size until they are no longer apparent - 3 weeks after immunization[109, 156, 168]. The analysis of GC B cells shows that the somatic diversification of the

antibody repertoire takes place during clonal expansion[111].

1-2 days after secondary immunization, pre-existing GC dissociate prior to new GC formation[100, 259]. Antigen in the form of immune complex is transported into draining lymph nodes and may be seen on the FDC within hours[260]. New GC with cells bearing PNA^{hi} phenotype begin to develop 2-4 days later. Day 3-5 post-immunization, immune complex coated bodies (iccosomes) are released into the micro-environment of the GC[257] and the GC response peaks at day 10[48, 259]. GC are initiated by a small number of precursor cells i.e. GC are oligoclonal in origin[109, 111, 139, 142, 159]. On an average only three B cell blasts colonize each follicle after a single immunization. Stathmokinetic[298] and tritiated thymidine[99] or 5-bromo-2-deoxyuridine-uptake studies[159] estimate the cell cycle time of GC blasts to 6-7 hrs.

It is central to the function of follicles that the antigen is taken up by the FDC in the form of immune complexes and can be held in a non-degraded form for more than a year[159, 179, 264]. FDC are also postulated to be important for the maintenance of memory. Follicular B cells can take up antigen from FDC, process it and present it in the context of MHC class II molecules to $CD4^+$ T cells in the GC[133]. Also, FDC show the presence of passively adsorbed MHC class II molecules. Peptides held in these passively adsorbed molecules can be recognized by GC T cells[90].

A large proportion of the proliferating centrocytes die in the GC. This is seen by the presence of intensely condensed chromatin and nuclear fragmentation that characterizes cells undergoing apoptosis[293]. These condensed nuclear fragments (tingible bodies) are derived from cells which have been recently in cycle. The tingible bodies become labeled within a few hours of starting an infusion of tritiated thymidine[69]. Recent studies by Ziegner et al.[297] suggest that a strong selection for high affinity variants takes place during the proliferative stage of B cell development in the GC and not only in the centrocyte stage. They isolated single germinal centers and sequenced L chains characteristic of phOx-specific antibodies of mice immunized with phOx. A proportion of analyzed GC showed B cells in which practically all sequences carry the amino acid substitutions characteristic of high affinity phOx antibodies. The pattern and distribution of somatic mutations in the V_kOx1 L chain suggest that selection for affinity already occurs during the proliferative stage. Further work is needed to establish how this selection takes place. Whether FDC can actively participate in the initial proliferative phase is questionable[203], since mature FDC become apparent only in the late proliferative phase of the GC reaction, when B cells differentiate into memory cells[167]. In the early phase, competition for progressively diminishing amounts of the free antigen[236], rather than antigen presented on the FDC may determine which B cell clones expand[10].

Recent experiments show that FDC influence B cell differentiation and survival by engaging adhesion receptors on the B cells[130]. The selected cells receive signals via soluble CD23 and IL-1α, express bcl-2, are rescued from apoptosis and ultimately leave the GC[83, 155, 158]. Studies by MacLennan et al.[164] suggest that this interaction with CD23 and IL-1α induces the differentiation to plasma blasts and ultimately to plasma cells, while CD40 signals are necessary for the development of memory B cells[73, 89]. Physiologically, the plasma blasts are still in cell cycle when they leave the follicles and migrate to sites where they differentiate to non-dividing plasma cells[165]. The signalling system that induces this migration has not been identified yet. It is suggested that a proportion of affinity selected centrocytes may even re-enter the GC and go through further cycles of proliferation and V region gene mutation[156].

Direct evidence that somatic hypermutation is activated in the GC is still fragmentary, particularly in relation to the exact stage or stages of the process of activation[86]. It has been suggested that the hypermutation in GC precursor cells is triggered in the outer T cell area (PALS)[136]. However, sequence analysis of NP-specific B cells isolated from PALS-associated foci suggested that the hypermutation mechanism is not activated in these cells[111]. It was therefore thought that B cells populating the follicles and initiating the GC reaction may be derived from a different B cell subset. Berek et al.[12] have suggested that the hypermutation mechanism may already be activated before the B cells migrate into primary follicles, so that the first somatic mutations may accumulate during B cell proliferation in the PALS. Recent work by Ziegner et al.[297] substantiates this observation. Interestingly, they found the presence of expanded but unmutated B cell clones in a substantial proportion of GC, leading to the proposition that somatic mutation, like isotype switch, is not a necessary step in the development of GC, but an option that a developing clone may implement. Alternatively, it is also possible, that the B cells have to reach a certain critical clone size, before the process of hypermutation is switched on[4, 124]. Further work using precise markers for GC maturity needs to be done before a firm hypothesis can be put forward.

1.6 The aim of the experimental work

The aim of the work presented in this thesis was to gain insights in the process of affinity maturation of murine IgG1 and IgE antibody responses at the serum level. The increase in affinity of the antibodies later in the immune response is due to the process of hypermutation and antigen driven selection in the GC. GC are also thought to be the site of isotype switching. Interleukin 4 (IL-4) is known to have a crucial role in the development of GC, rescue of antigen-selected B cells from apoptosis and their continued proliferation. In mice it is also known to selectively induce isotype switching to IgG1 and IgE. We were therefore interested in studying the influence of IL-4 treatment on the process of affinity maturation at the serum level in the murine model. The ultimate hope

was that the insights gained could help extend our studies to humans.

Affinity refers to the strength of the interaction between a single combining site of an antibody and an antigenic determinant and can be expressed in thermodynamic terms such as association constant or free energy change. The term average affinity (also referred to as avidity) is used to describe the binding strength of a population of polyclonal antibodies with a polyvalent antigen. Thermodynamically speaking, the association constant can only be interpreted rigorously for an equilibrium in homogeneous solutions. When using non-homogeneous methods, however, other experimental factors may influence the state of equilibrium, and the stability of the complex is therefore best described by an appropriate operational parameter that is strictly dependent on the experimental conditions employed. Such determinations may be best described as functional affinity.

The experimental determination of the affinity of an antibody for its antigen is of considerable importance. It is the basic parameter which helps in characterizing the molecule. The most ideal method of determination of affinity requires the capability of measuring the bound and free fraction of one of the reactants at equilibrium, without in any way disturbing the equilibrium, and preferably without labeling either of the reactants. Equilibrium dialysis is considered one of the most unequivocal methods of affinity determination, but has many limitations. Until now, determination of average affinity and affinity distributions of the antigen-specific serum antibodies has proved to be difficult especially for large proteinic antigens.

To enable us to investigate the processes of affinity maturation, it was necessary to develop suitable reagents and appropriate assay systems that could determine affinity of the antigen-specific antibodies in small volumes of the sample, even when present in small concentrations and in the presence of a large amount of other non-specific proteins. Chapter 2 of this thesis is focussed on methods of determination of concentration and affinity in ELISA. The theoretical background of ELISA, critical factors influencing the applicability of ELISA as well as the need for quality control of the reagents are discussed in chapter 2.1. After developing a Terasaki-ELISA that allows the concentration determination of total and antigen-specific IgE antibodies in extremely small volumes of the sample (chapter 2.2), we proceeded to apply this system for affinity determinations as well. In chapter 2.3 we demonstrate the application of Terasaki-ELISA to the determination of affinity of antigen-specific antibodies in culture supernatants, ascitic fluids as well as serum samples. During our investigations on monoclonal IgE mixtures we observed that some IgE mixtures showed a functional affinity much higher than either of the components. Chapter 2.4 summarizes our observations. In chapter 2.5 we demonstrate the applicability of the equations developed in chapter 2.3 to the microtitre system as well. The application of an inhibition ELISA to study the affinity distributions

of polyclonal immune responses is also demonstrated.

The advent of biosensor technology promises the opportunity to determine affinity of antigen-specific antibodies in real time. In chapter 3.1, we describe the application of biosensor technology to concentration and affinity determinations of antigen-specific monoclonal and polyclonal antibodies. Various parameters that can influence measurements in the biosensor were investigated, and are discussed in chapter 3.2. It has been established that prolonged IL-4 treatment reduces the antigen-specific IgG1 and IgE responses in mice[275]. On the other hand, IL-4 is known to be important in the GC reaction[34]. The last part of chapter 3 (3.3) gives the results of our investigations on the effect of prolonged IL-4 treatment on the process of affinity maturation in antigen-specific IgG1 responses.

To summarize, this thesis addresses the following questions -

- Is it possible to determine the affinity and affinity distributions of serum antibodies in ongoing immune responses?
- Does affinity maturation occur in primary and secondary IgG1/IgE responses and what is the extent of this maturation?
- Does prolonged IL-4 treatment affect this process of affinity maturation?

1.7 References

1. Abergel C., Tipper J.P., Padlan E.A. (1994) Structural significance of sequence variability in antibody complementarity-determining regions. Res. Immunol. 145:49.
2. Abeshira-Amar O., Gilbert M., Joliy M., Theze J., Jankovic D.L. (1992) IL-4 plays a dominant role in the differential development of Th0 into Th1 and Th2 cells. J. Immunol. 148:3820.
3. Abney E.R., Cooper M.D., Kearney J.F., Lawton A.R., Parkhouse R.M. (1978) Sequential expression of Ig on developing mouse B lymphocytes: a systematic survey that suggests a model for the generation of Ig isotype diversity. J. Immunol. 120:2041
4. Agur Z., Mazor G., Meilson I. (1991) Maturation of the humoral immune response as an optimization problem. Proc. R. Soc. Lond. B. 245:147.
5. Allen D., Cumano A., Dildorp R., Kocks C., Rajewsky K., Rajewsky N., Roes J., Sablitzky F., Siekvitz M. (1987) Timing, genetic requirements and functional consequences of somatic hypermutation during B-cell development. Immunol. Rev. 96:5.
6. Alt F.W. and Baltimore D. (1982) Joining of Ig heavy chain gene segments: implications with evidence of D-J_H fusion. Proc. Natl. Acad. Sci. USA 79:4118.
7. Alt F.W., Yancopoulus G.D., Blackwell T.K., Wood C., Thomas E., Boss M., Coffman R., Rosenberg N., Tonegawa S., Baltimore D. (1984) Ordered rearrangement of immunoglobulin heavy chain variable region. EMBO J. 3:1209.
8. Alzari P.M., Spinelli S., Mariuzza R.A., Boulot G., Polajak R.J., Jarvis J.M., Milstein C. (1990) Three dimensional structure determination of anti-phenyloxazolone antibody. The role of somatic mutation and heavy/light chain pairing in the maturation of an immune response. EMBO J. 9:3807.
9. Bell E.B. and Sparshott S.M. (1990) Interconversion of CD45R subsets of $CD4^+$ T cells *in vivo*. Nature 348:163.
10. Berek C. (1992) The development of B cells and the B-cell repertoire in the micro-environment of the germinal center. Immunol. Rev. 126:5.
11. Berek C. (1993) Somatic mutation and memory. Curr. Opin. Immunol. 5:218.

12. Berek C., Berger A., Apel M. (1991) Maturation of the immune response in germinal centers. Cell 67:1121.
13. Berek C., Griffiths G.M., Milstein C. (1985) Molecular events during maturation of the immune response to oxazolone. Nature 316:412.
14. Berek C., Jarvis J.M., Milstein C. (1987) Activation of memory and virgin B cell clones in hyperimmune animals. Eur. J. Immunol. 17:1121.
15. Berek C. and Milstein C. (1987) Mutation drift and repertoire shift in the maturation of the immune response. Immunol. Rev. 96:23.
16. Berek C. and Milstein C. (1988) The dynamic nature of the antibody repertoire. Immunol. Rev. 105:5.
17. Bernard O., Hozumi N., Tonegawa S. (1978) Sequences of mouse immunoglobulin light-chain genes before and after somatic changes. Cell 15:1133.
18. Berton M.T., Uhr J.W., Vitetta E.S. (1989) Synthesis of germline gamma immunoglobulin heavy-chain transcripts in resting B cells: induction by interleukin 4 and inhibition by interferon gamma. Proc. Natl. Acad. Sci. USA 86:2829.
19. Betz A.G., Milstein C., Gonzalez-Fernandez A., Pannell R., Larson T., Neuberger M. (1994) Elements regulating somatic hypermutation of an immunoglobulin κ gene: Critical role for the intron enhancer/matrix attachment region. Cell 77:239.
20. Betz A.G., Neuberger M.S., Milstein C. (1993b) Discriminating intrinsic and antigen-selected mutational hotspots in immunoglobulin V genes. Immunol. Today 14:405.
21. Betz A.G., Rada C., Panell R., Milstein C., Neuberger M.S. (1993a) Passenger transgenes reveal intrinsic specificity of the antibody hypermutation mechanism: clustering, polarity and specific hotspots. Proc. Natl. Acad. Sci. USA 90:2385.
22. Beverley P.C.L. (1990a) Human T cell memory. Curr. Top. Microbiol. Immunol. 159:111.
23. Beverley P.C.L. (1990b) Is T-cell memory maintained by crossreactive stimulation? Immunol. Today 11:203.
24. Bhatt T.N., Bentley G.A., Boulot G., Greene M.I., Tello D., Dall'Acqua W., Souchon H., Schwarz F.P., Mariuzza R.A., Poljak R.J. (1994) Bound water molecules and conformational stabilization help mediate an antigen-antibody association. Proc. Natl. Acad. Sci. USA 91:1089.
25. Bjork P., Axelsson B., Pulie S. (1991) Expression of CD43 during activation of human B lymphocytes. Scand. J. Immunol. 33:211.
26. Blackwell T.K. and Alt F.W. (1988) Immunoglobulin genes. In: 'Molecular Immunology', Hames B.D. and Glover D.M. (Eds), IRL Press, Oxford, England, p. 70.
27. Bonnefoy J-Y., Gauchat J-F., Life P., Graber P., Mazzei G., Aubry J-P. (1995) Pairs of surface molecules in human IgE regulation: CD23-CD21 and CD40-CD40L. (Eur. Resp. J., in press)
28. Bothwell A.L.M., Paskind M., Reth M., Imanishi-Kari T., Rajewsky K., Baltimore D. (1982) Somatic variants of murine immunoglobulin lambda chain. Nature 298:380.
29. Braden B.C. and Poljak R.J. (1995) Structural features of the reactions between antibodies and protein antigens. FASEB J. 9:9.
30. Bradley L.M., Duncan D.D., Tonkonogy S., Swain S.L. (1992) Long-term $CD4^+$ memory T cells from the spleen lack MEL-14, the lymph node homing receptor. J. Immunol. 148:324.
31. Brown M., Stenzel-Poore M., Stevens S., Kondoleon S.K., Ng J., Bachinger H.P., Rittenberg M.B. (1992) Immunologic memory to phosphocholine keyhole limpet haemocyanin. Recurrent mutations in the lambda 1 light chain increase affinity for antigen. J. Immunol. 148:339.
32. Bruggeman M., Muller H-J., Burger C., Rajewsky K. (1986) Idiotypic selection of an antibody mutant with changed hapten binding specificity, resulting from a point mutation in position 50 of heavy chain. EMBO J. 5:1561.
33. Burnet F.M. and Fenner F. (1949) The production of antibodies. MacMilan and Co., London. p. 1.
34. Butch A.W., Chung G-H., Hoffman J.W., Nahm M. (1993) Cytokine expression by germinal center cells. J. Immunol. 150:39.
35. Butcher E.C., Rouse R.V., Coffman R.L., Nottenburg C.N., Hardy R.R., Weissman I.L. (1982) Surface phenotype of Peyer's patch germinal center cells: Implications for the role of germinal

centers in B cell differentiation. J. Immunol. 129:2698.
36. Butterfield K.C., Fathman C.G., Budd R.C. (1989) A subset of memory CD4$^+$ T cells identified by expression of Pgp-1. J. Exp. Med. 173:763.
37. Bye J.M., Carter C., Cui Y., Gorick B.D, Songsivilai S. (1992) Germline variable region gene segment derivation of human monoclonal anti-Rh(D) Antibodies. Evidence for affinity maturation by somatic hypermutation and repertoire shift. J. Clin. Invest. 90:2481.
38. Byers V.S. and Sercarz E.E. (1968) The X-Y-Z scheme of immunocyte maturation. IV. The exhaustion of memory cells. J. Exp. Med. 127:307.
39. Cai J., Humphries C., Richardson A., Tucker P.W. (1992) Extensive and selective mutation of a rearranged V_H5 gene in human B cell chronic lymphocytic leukaemia. J. Exp. Med. 176:1073.
40. Celada F. (1967) Quantitative studies of the adoptive immunological memory in mice. II. Linear transmission of cellular memory. J. Exp. Med. 125:199.
41. Celada F. (1971) The cellular basis of immunologic memory. Proc. Allergy 15:223.
42. Chein N.C., Pollock R.R., Desaymard C., Scharff M.D. (1988) Point mutations cause the somatic diversification of IgM and IgG2a anti-phosphorylcholine antibodies. J. Exp. Med. 167:954.
43. Chen J. and Alt F.W. (1993) Gene rearrangement and B cell development. Curr. Opin. Immunol. 5:194.
44. Christoph T., Rickert R., Rajewsky K. (1994) M17: a novel gene expressed in germinal centers. Int. Immunol. 6:1203.
45. Clarke S., Rickert R., Wloch M.K., Staudt L., Gerhard W., Weigert M. (1990) BALB/c secondary responses to the Sb site of influenza virus haemagglutinin and unequal number of V_H and V_κ mutations. J. Immunol. 145:2286.
46. Coffman R.L. and Carty J. (1986) A T cell activity that enhances polyclonal IgE production and its inhibition by interferon-gamma. J. Immunol. 136:949.
47. Coffman R.L., Lebman D., Rothman P. (1993) Mechanisms of immunoglobulin isotype switching. Adv. Immunol. 54:229.
48. Coico R.K., Bhogal B.S., Thorbecke G.J. (1983) Relationship of germinal centers in lymphoid tissue to immunologic memory. VI. Transfer of B cell memory with lymph node cells fractionated according to their receptors for peanut agglutinin. J. Immunol. 131:2254.
49. Cook G.C. and Tomlinson I.M. (1995) The human immunoglobulin V_H repertoire. Immunol. Today 16:237.
50. Coutinho A., Benner R., Bjorklund M., Forni L., Holmberg D., Ivars F., Martinez A.C., Pettersson S. (1982) A 'trans' perspective on the control of immunoglobulin C gene expression. Immunol. Rev. 67:87.
51. Croft M., Bradley L.M., Swain S.L. (1994) Naive versus memory D4 T cell response to antigen. Memory cells are less dependent on accessory cell costimulation and can respond to many antigen-presenting cell types including resting B cells. J. Immunol. 152:2675.
52. Cumano A. and Rajewsky K. (1985) Structure of primary anti(4-hydroxy-3-nitrophenyl)acetyl (NP) antibodies in normal and idiotypically suppressed C57BL/6 mice. Eur. J. Immunol. 15:512.
53. Cumano A. and Rajewsky K. (1986) Clonal recruitment and somatic mutation in the generation of immunological memory to the hapten NP. EMBO J. 5:2459.
54. Damle N.K., Klussman K., Leytze G., Mydral S., Aruffo A., Ledbetter J.A., Linsley P.S. (1994) Costimulation of T lymphocytes with integrin ligands intercellular adhesion molecule-1 or vascular cells adhesion molecule-1 induces functional expression of CTLA-4 a second receptor for B7. J. Immunol. 152:2686.
55. Davies M.M. and Bjorkmann P.J. (1988) T-cell antigen receptor genes and T-cell recognition. Nature 334:395.
56. Dell C.L., Lu Y.X., Claflin J.L. (1989) Molecular analysis of clonal stability and longevity in B-cell memory. J. immunol. 143:3364.
57. Delphin S. and Stavnezer J. (1995) Characterization of interleukin-4 (IL-4) responsive region in the immunoglobulin heavy chain germline ε promoter: Regulation by NF-IL-4 a C/EBP family

member and NF-κB/p50. J. Exp. Med. 181:181.
58. Doherty T.M., Kastelein R., Menon S., Andrade S., Coffman R.L. (1993) Modulation of murine macrophage function by IL-13. J. Immunol. 151:7151.
59. Doyle A.G., Montaner L.J., Minty A.J., Caput D., Ferrara P., Gordan S. (1994) Interleukin-13 alters the activation state of murine macrophages *in vitro*: comparison with interleukin-4 and interferon-gamma. Eur. J. Immunol. 24:1441.
60. Duncan D.D. and Swain S.L. (1994) Role of antigen-presenting cells in the polarized development of helper T cell subsets: evidence for differential cytokine production by Th0 cells in response to antigen presentation by B cell and macrophages. Eur. J. Immunol. 24:2506.
61. Eisen H.N. (1966) The immune response to a simple antigenic determinant. In: 'The Harvey Lectures'. Series 60, Academic Press, N.Y. p. 1.
62. Engel P., Gribben J.G., Freeman G.J., Zhou L.J., Nozawa Y., Abe M., Nadler L.M., Wakasa H., Tedder T.F. (1994) The B7-2 (B70) costimulatory molecule expressed by monocytes and activated B lymphocytes is the CD86 differentiation antigen. Blood 84:1402.
63. Esser C. and Radbruch A. (1990) Immunoglobulin class switching: molecular and cellular analysis. Annu. Rev. Immunol. 8:717.
64. Even J., Griffiths J.M., Berek C., Milstein C. (1985) Light chain germ-line genes and the immune response to 2-phenyloxazolone. EMBO J. 4:3439.
65. Feldbush T.L. (1973) Antigen modulation of the immune response. The decline of immunological memory in the absence of continuing antigenic stimulation. Cell. Immunol. 8:435.
66. Finkelman F.D., Holmes J., Katona I.M., Urban Jr. J.F., Beckman M.P., Park L.S., Schooley K.A., Coffman R.L., Mosmann T.R., Paul W.E. (1990) Lymphokine control of *in vivo* IgE responses. J. Immunol. 140:1022.
67. Fiorentino D.F., Bond M.W., Mosmann T.R. (1989) Two types of mouse helper T cell. IV. Th2 clones secrete a factor that inhibits cytokine production by Th1 clones. J. Exp. Med. 170:2081.
68. Firestein G.S., Roeder, W.D., Laxer, J.A, Townsend K.S., Weaver C.T., Hom J.T., Linton J.M., Torbett B.E., Glasebrook, A.L. (1989) A new murine $CD4^+$ T cell subset with an unrestricted cytokine profile. J. Immunol. 143:518.
69. Fliedner T.M. (1967) On the origin of tingible bodies in germinal centers in immune responses. In: 'Germinal centers in immune responses.' Cottier H., Odartchenko N., Schindler R. and Congdon C.C. (Eds), Springer-Verlag, Berlin. p. 218.
70. Foote J. and Milstein C. (1991) Kinetic maturation of an immune response. Nature 352:530.
71. Foote J. and Winter G. (1992) Antibody framework residues affecting the conformation of the hypervariable loops. J. Mol. Biol. 224:486.
72. Ford J.E., McHeyer-Williams M.G., Lieber M.R. (1994) Analysis of individual immunoglobulin lambda light chain genes amplified from single cells is inconsistent with variable region gene conversion in germinal-center B cell somatic mutation. Eur. J. Immunol. 24:1816.
73. Foy T.M., Laman J., Ledbetter J., Aruffo A., Claasen E., Noelle R.J. (1994) gp39-CD40 interactions are essential for germinal center formation and development of B cell memory. J. Exp. Med. 180:157.
74. Fuller K.A., Kanagawa O., Nahm M.H. (1993) T cells within germinal centers are specific for the immunizing antigen. J. Immunol. 151:4505.
75. Gajewski T.F. and Fitch F.W. (1988) Antiproliferative effect of IFN-γ in immune regulation I. IFN-γ inhibits the proliferation of Th2 but not Th1 murine HTL clones. J. Immunol. 140:4245.
76. Gajewski T.F. and Fitch F.W. (1991) Differential activation of murine Th1 and Th2 clones. Res. Immunol. 142:19.
77. Gajewski T.F., Joyce J., Fitch F.W. (1989) Antiproliferative effect of IFN-γ in immune regulation III. Differential selection of Th1 and Th2 murine helper T lymphocyte clones using recombinant IL-2 and recombinant IFN-γ. J. Immunol. 143:15.
78. Gajewski T.W., Pinnas M., Wong T., Fitch F.W. (1991) Murine Th1 and Th2 clones proliferate optimally in response to distinct antigen-presenting cell populations. J. Immunol. 146:1750.
79. Gearhart P.J. and Bogenhagen D.F. (1983) Clusters of point mutations are found exclusively

around rearranged V genes. Proc. Natl. Acad. Sci. USA 80:3439.
80. Gearhart P., Johnson N.D., Douglas R., Hood L. (1981) IgG antibodies to phosphorylcholine exhibit more diversity than their IgM counterparts. Nature 291:29.
81. Golding G.B., Gearhart P.J., Glickman B.W. (1987) Patterns of somatic mutations in immunoglobulin variable genes. Genetics 115:169.
82. Gonzalez-Fernandez A., Gupta S., Pannell R., Neuberger M.S. (1994) Somatic mutation of immunoglobulin lambda chains: A segment of the major intron hypermutates as much as the complementarity determining regions. Proc. Natl. Acad. Sci. USA 91:12614.
83. Gordon J., Flores-Romo L., Cairns J.A., Millsum M.J., Lane P.J., Johnson G.D., MacLennan I.C.M. (1989) CD23: a multi-functional receptor/lymphokine? Immunol. Today 10:153.
84. Gorski J., Rollini P., Mach B. (1983) Somatic mutations of immunoglobulin variable genes are restricted to the rearranged V gene. Science 220:1179.
85. Gram H., Marconi L.-A., Barbas C.F. III, Collet T.A., Lerner R.A. (1992) *In vitro* selection and affinity maturation of antibodies from a naive combinatorial immunoglobulin library. Proc. Natl. Acad. Sci. USA 89:3576.
86. Gray D. (1991) Understanding germinal centers. Res. Immunol. 142:237.
87. Gray D. (1993) Immunological memory. Annu. Rev. Immunol. 11:49.
88. Gray D. (1994) Regulation of immunological memory. Curr. Opin. Immunol. 6:425.
89. Gray D., Dullforce P., Jainandunsing S. (1994) Memory B cell development but not germinal center formation is impaired by *in vivo* blockade of CD40-CD40 ligand interaction. J. Exp. Med. 180:141.
90. Gray D., Kosco M., Stockinger B. (1991) Novel pathways of antigen presentation for the maintenance of memory. Int. Immunol. 3:141.
91. Gray D., MacLennan I.C.M., Lane P.J.L. (1986) Virgin B cell recruitment and the lifespan of memory during antibody responses to DNP haemocyanin. Eur. J. Immunol. 16:641.
92. Gray D. and Matzinger P. (1991) T cell memory is short lived in the absence of antigen. J. Exp. Med. 174:969.
93. Gray D. and Skarvall H. (1988) B cell memory is short-lived in the absence of antigen. Nature 336:70.
94. Gray D., Skarvall H., Liu Y-J., MacLennan I.C.M., Leanderson T. (1990) Hypermutation and memory B cells: The role of germinal centers. In: 'Somatic hypermutation in V-regions.' Steele E.J. (Ed), CRC Press, Boca Raton, FL. p. 83.
95. Griffiths C.M., Berek C., Kaartinen M., Milstein C. (1984) Somatic mutation and the maturation of the immune response to 2-phenyloxazolone. EMBO J. 4:3439.
96. Gritzmacher C.A. (1989) Molecular aspects of heavy-chain class switching. Crit. Rev. Immunol. 9:173.
97. Hackett J. Jr., Stebbins C., Rogerson B., Davies M.M., Storb U. (1992) Analysis of a T cell receptor gene as a target of somatic hypermutation mechanism. J. Exp. Med. 176:225.
98. Hagman J. and Grossched R. (1994) Regulation of gene expression at early stages of B-cell differentiation. Curr. Opin. Immunol. 6:222.
99. Hanna Jr. M.G. (1964) An autoradiographic study of the germinal center on spleen white pulp during early intervals of the immune response. Lab. Invest. 13:95.
100. Hanna Jr. M.G., Congdon C.C., Wust C.J. (1966) Effect of antigen dose on lymphatic tissue germinal centers. Proc. Soc. Exp. Biol. Med. 121:286.
101. Harriman W., Volk H., Defranoux N., Wabl M. (1993) Immunoglobulin class switch recombination. Annu. Rev. Immunol. 11:361.
102. Hayakawa K. and Hardy R.R. (1991) Murine $CD4^+$ T cell subsets. Immunol. Rev. 123:145.
103. Heinen E., Cormann N., Kinet-Denoel C. (1988) The lymph follicle, a hard nut to crack. Immunol. Today 9:240.
104. Hozumi N., Wu G.E., Muriaso H., Roberts L., Vetter D., Fife W.L., Whiteky M., Sadowski P. (1981) RNA splicing mutation in an aberrantly rearranged immunoglobulin gamma1 gene. Proc. Natl. Acad. Sci. USA 78:7019.
105. Hseih C.S., Macatonia S.E., Tripp C.S., Wolf S.F., O'Garra A., Murphy K.M. (1993) Development of Th1 $CD4^+$ T cells through IL-12 produced by Listeria-induced macrophages.

Science 260:547.
106. Huang C., Stewart A.K., Schwartz R.S., Stollar B.D. (1992) Immunoglobulin heavy chain gene expression in peripheral blood lymphocytes. J. Clin. Invest. 89:1331.
107. Isakson P.C., Pure E., Vitetta E.S., Krammer P.H. (1982) T cell-derived B cell differentiation factor(s). Effect on the isotype switch of murine B cells. J. Exp. Med. 155:734.
108. Jack H.M., McDowell M., Steinberg C.M., Wabl M. (1988) Looping out and deletion mechanism for the immunoglobulin heavy-chain class switch. Proc. Natl. Acad. Sci. USA 85:1158.
109. Jacob J., Kassir R., Kelsoe G. (1991a) In situ studies of the primary immune response to (4-hydroxy-3-nitrophenyl)acetyl. I. The architecture and dynamics of responding cell populations. J. Exp. Med. 173:1165.
110. Jacob J. and Kelsoe G. (1992) *In situ* studies of the primary immune response to (4-hydroxy-3-nitrophenyl)acetyl. II. A common clonal origin for periarteriolar lymphoid sheath-associated foci and germinal centers. J. Exp. Med. 176:679.
111. Jacob J., Kelsoe G., Rajewsky K., Weiss U. (1991b) Intraclonal generation of antibody mutants in the germinal centers. Nature 354:389.
112. Jacobson E.B., Caporale L.H., Thorbecke G.J. (1974) Effect of thymus cell injections on germinal center formation in lymphoid tissues of nude (thymusless) mouse. Cell. Immunol. 13:416.
113. Janeway Jr. C.A. and Bottomly K. (1994) Signals and signs for lymphocyte responses. Cell 76:275.
114. Janeway Jr. C.A. and Travers P. (1994) Immunobiology. The immune system in health and disease. Blackwell Scientific Publications, Oxford. p. 1.
115. Janin J. and Chothia C. (1975) Principles of protein-protein recognition. Nature 256:705.
116. Jerne N.K. (1951) Avidity based on rabbit skin responses to diphtheria toxin-antitoxin mixtures. Acta. Path. Microbiol. Scand. [Suppl.] 87:2.
117. Jones P.D. and Ada G.L. (1987) Persistence of influenza virus-specific antibody secreting cells and B-cell memory after primary murine influenza virus infection. Cell. Immunol. 109:53.
118. Jung S., Rajewsky K., Radbruch A. (1993) Shutdown of class switch recombination by deletion of a switch region control element. Science 259:984.
119. Kaartinen M., Kulp S., Makela O. (1990) Characteristics of selection-free mutations and effects of subsequent selection. In: 'Somatic mutation in V-regions.' Steele E.J. (Ed), CRC Press, Boca Raton, FL. p. 105.
120. Kabat E.A., Wu T.T., Bilofsky H. (1977) Unusual distribution of amino acids in complementarity-determining (hypervariable) segments of heavy and light chains of immunoglobulins and their possible roles in specificity of antibody combining sites. J. Bio. Chem. 252:6609.
121. Kallberg E., Gray D., Leanderson T. (1993) Analysis of somatic mutation activity in multiple Vk genes involved in the response to 2-phenyl-5-oxazolone. Int. Immunol. 5:573.
122. Kearney J.F. and Lawton A.R. (1975) B lymphocyte differentiation induced by lipopolysaccharide. I. Generation of cells synthesizing four major immunoglobulin classes. J. Immunol. 115:67.
123. Kelsoe G. and Zeng B. (1993) Sites of B-cell activation *in vivo*. Curr. Opin. Immunol. 5:418.
124. Kepler T.B. and Perelson A.S. (1993) Cyclic re-entry of germinal center B cells and the efficiency of affinity maturation. Immunol. Today 14:415.
125. Kim S., Davies M., Sinn E., Patten P., Hood L. (1981) Antibody diversity: Somatic hypermutation of rearranged V_H genes. Cell 27:573.
126. Klaus G.G.B., Humphrey J.H., Kunkle A., Dongworht D.W. (1980) The follicular dendritic cell: Its role in antigen presentation in the generation of immunological memory. Immunol. Rev. 53:3.
127. Klinman N.R. and Linton P.-J. (1990) The generation of B cell memory: a working hypothesis. Curr. Top. Microbiol. Immunol. 159:19.
128. Kocks C. and Rajewsky K. (1988) Stepwise intraclonal maturation of antibody affinity through somatic hypermutation. Proc. Natl. Acad. Sci. USA 85:8206.

129. Kocks C. and Rajewsky K. (1989) Stable expression and somatic hypermutation of antibody V regions in B-cell developmental pathways. Annu. Rev. Immunol. 7:537.
130. Koopman G., Keehnen R.M.J., Lindhout E., Newman W., Shimuzu Y., Van Seventer G.A., De Groot C., Pals S.T. (1994) Adhesion through the LFA-1 (CD11a/CD18)-ICAM-1 (CD54) and VLA-4 (CD49d)-VCAM-1 (CD106) pathways prevents apoptosis in germinal center B cells. J. Immunol. 152:3760.
131. Korthauer U., Graf D., Mages H.W., Briere F., Padayachee M., Malcolm S., Ugazio A.G., Notarangelo L.D., Levinsky R.J., Kroczek R.A. (1993) Defective expression of T-cell CD40 ligand causes X-linked immunodeficiency with hyper-IgM. Nature 361:541.
132. Kosco M.H., Burton G.F., Kapasi Z.F., Szakal A.K., Tew J.G. (1989) Antibody-forming cell induction during an early phase of germinal center development and its decay with aging. Immunology 68:312.
133. Kosco M.H., Szakal A.K., Tew J.G. (1988) *In vivo* obtained antigen presented by germinal center B cells to T cells *in vitro*. J. Immunol. 140:354.
134. Kosco-Vilbois M.H., Gray D., Scheidegger D., Julius M. (1993) Follicular dendritic cells help resting B cells to become effective antigen-presenting cells: induction of B7/BB1 and upregulation of major histocompatibility complex class II molecules. J. Exp. Med. 178:2055.
135. Kraal G., Weissman I.L., Butcher E.C. (1982) Germinal center B cells: antigen specificity and changes in heavy chain class expression. Nature 298:377.
136. Kroese F.G.M., Seijen H.G., Nieuwenhuis P. (1991) The initiation of the germinal center activity. Res. Immunol. 142:249.
137. Kroese F.G.M., Timens W., Nieuwenhuis P. (1990) Germinal center reaction and B lymphocytes: Morphology and function. Curr. Top. Pathol. 84:103.
138. Kroese F.G.M., Wabbena A.S., Nieuwenhuis P. (1986) Germinal center formation and follicular antigen trapping in the spleen of lethally X-irradiated and reconstituted rats. Immunology 57:99.
139. Kroese F.G.M., Wabbena A.S., Seijen H.G., Nieuwenhuis P. (1987) Germinal centers are oligoclonal in origin. Eur. J. Immunol. 17:1609.
140. Kulper H., Brouwer M., De Boer M., Parren P., Van Lier R.A. (1994) Differences in the responsiveness to CD3 stimulation between naive and memory $CD4^+$ T cells cannot be overcome by CD28 costimulation. Eur. J. Immunol. 24:1956.
141. Kupfer A., Mosmann T.R., Kuper H. (1991) Polarized expression of cytokines in cell conjugates of helper T cells and splenic B cells. Proc. Natl. Acad. Sci. USA 88:775.
142. Kuppers R., Zhao-Hohn M., Hansmann M.-L., Rajewsky K. (1993) Tracing B cells development in human germinal centers by molecular analysis of single of cells picked from histological sections. EMBO J. 12:4955.
143. Lane P., Bordet C., Hubele S., Scheidegger D., Muller U., McConell F., Kosco-Vilbois M. (1994) B cell function in mice transgenic for mCTLA4-H gamma 1: lack of germinal centers correlated with poor affinity maturation and class switching despite normal priming of $CD4^+$ T cells. J. Exp. Med. 179:819.
144. Lanier L.L., O'Fallon S., Somoza C., Phillips J.H., Linsley P.S., Okumura K., Ito D., Azumo M. (1995) CD80 (B7) and CD86 (B70) provide similar costimulatory signals for T cell proliferation, cytokine production and generation of CTL. J. Immunol. 154:97.
145. Lavole T.B., Drohan W.N., Smith-Gill S.J. (1992) Experimental analysis by site-directed mutagenesis of somatic mutation effects on affinity and fine specificity in antibodies specific to lysozyme. J. Immunol. 148:503.
146. Law C-L. and Clarke E.A. (1994) Cell-cell interactions that regulate the development of B-lineage cells. Curr. Opin. Immunol. 6:238.
147. Leanderson T., Kallberg E., Gray D. (1992) Expansion, selection and mutation of antigen-specific B cells in germinal centers. Immunol. Rev. 126:47.
148. Lebecque S.G. and Gearhart P.J. (1990) Boundaries of somatic mutation in rearranged immunoglobulin genes: 5′ boundary is near the promoter, and 3′ boundary is approximately 1 kb from V(D)J gene. J. Exp. Med. 172:1717.
149. Lederman S., Yellin M.J., Covey L.R., Cleary A.M., Callard R., Chess L. (1993) Non-antigen

signals for B-cell growth and differentiation to antibody secretion. Curr. Opin. Immunol. 5:439.
150. Lederman S., Yellin, M.J., Inghirami G., Lee J.J., Knowles D.M., Chess L. (1992) Molecular interactions mediating T-B lymphocyte collaboration in human lymphoid follicles: Roles of T-B activating molecule (5c8 antigen) and CD40 in contact-dependent help. J. Immunol. 149:3817.
151. Lehman D.A., Nomura D.Y., Coffman R.L., Lee F.D. (1990) Molecular characterization of germ-line immunoglobulin A transcripts produced during transforming growth factor type beta-induced isotype switching. Proc. Natl. Acad. Sci. USA 87:3962.
152. Li Y.-S., Hayakawa K., Hardy R.R. (1993) The regulated expression of B-lineage associated genes during B cell differentiation in bone marrow and fetal liver. J. Exp. Med. 178:951.
153. Lieber M.R. (1991) Site-specific recombination in the immune system. FASEB J. 5:2934.
154. Lieber M.R., Hesse J.E., Lewis S., Bosma G., Rosenberg N., Mizzuchi K., Bosma M., Gellert M. (1988) The defect in murine severe combined immune deficiency: joining of signal sequences but not coding segments in V(D)J recombination. Cell 55:7.
155. Liu Y.-J., Cairns J.A., Holder M.J., Abbot S.D., Jansen K.U., Bonnefoy J.-Y., Gordon J., MacLennan I.C.M. (1991a) Recombinant 25kDa CD23 and interleukin-1 alpha promote the survival of germinal center B cells: evidence for bifurcation in the development of centrocytes rescued from apoptosis. Eur. J. Immunol. 21:1107.
156. Liu Y.-J., Johnson J.D., Gordon J., MacLennan I.C.M. (1992) Germinal centers in T-cell dependent antibody responses. Immunol. Today 84:103.
157. Liu Y.-J., Joshua D.E., Williams G.T., Smith C.A., Gordon C.A., MacLennan I.C.M. (1989) Mechanism of antigen driven selection in the germinal center. Nature 342:929.
158. Liu Y.-J., Mason D.Y., Johnson G.D., Abbot S., Gregory C.D., Hardie D.C., Gordon J., MacLennan I.C.M. (1991b) Germinal center cells express bcl-2 protein after activation by signals which prevent their entry in apoptosis. Eur. J. Immunol. 21:1905.
159. Liu Y.-J., Zhang J., Lane P.J.L., Chan E.Y.-T., MacLennan I.C.M. (1991c) Sites of specific B cell activation in primary and secondary responses to T cell-dependent and T cell-independent antigens. Eur. J. Immunol. 21:2951.
160. Lutzker S., Rothman P., Pollock R., Coffman R., Alt F.W. (1988) Structure and expression of germ-line Ig gamma 2b transcripts. Mol. Cell. Biol. 8:1849.
161. MacDonald H.R., Budd R.C., Cerottini J.C. (1990) Pgp-1 (Ly 24) as a marker of murine memory T lymphocytes. Curr. Top. Microbiol. Immunol. 159:97.
162. Mackay C.R. (1993) Immunological memory. Adv. Immunol. 53:217.
163. MacLennan I.C.M. (1991) The center of hypermutation. Nature 354:352.
164. MacLennan I.C.M. (1994) Germinal centers. Annu. Rev. Immunol. 12:117.
165. MacLennan I.C.M. and Chan E.Y.-T. (1991) The origin of bone marrow plasma cells. In: 'Epidemiology and Biology of Multiple Myeloma.' Obrams G.I. and Potter M. (Eds), Springer-Verlag, Berlin, p. 129.
166. MacLennan I.C.M. and Gray D. (1986) Antigen driven selection of virgin and memory B cells. Immunol. Rev. 91:61.
167. MacLennan I.C.M., Johnson G.D., Liu Y.-J., Gordon J. (1991) The heterogeneity of follicular reactions. Res. Immunol. 142:253.
168. MacLennan I.C.M., Liu Y.-J., Ling N.R. (1988) B cell proliferation in follicles, germinal center formation and the site of neoplastic transformation in Burkitt's lymphoma. Curr. Top. Microbiol. Immunol. 141:138.
169. MacLennan I.C.M., Liu Y.-J., Oldfield S., Zhang J., Lane P.J.L. (1990) The evolution of B cell clones. Curr. Top. Microbiol. Immunol. 159:37.
170. Malipiero U.V., Levy N.S., Gearhart P.J. (1987) Somatic mutation in anti-phosphorylcholine antibodies. Immunol. Rev. 96:59.
171. Mandler R., Finkelman F.D., Levine A.D., Snapper C.M. (1993) IL-4 induction of IgE class switching by lipopolysaccharide-activated murine B cells occurs predominantly through sequential switching. J. Immunol. 150:407.
172. Manser T. (1990a) Regulation, timing, and mechanism of antibody V gene somatic hypermutation: lessons from the arsonate system. In: 'Somatic Hypermutation in V-regions.'

Steele E.J. (Ed), CRC Press, Boca Raton, FL. p. 41.
173. Manser T. (1990b) The intraclonal diversity and control of antibody isotype switch recombination. Int. Immunol. 2:893.
174. Manser T., Wysocki L.J., Margolies M.N., Gefter M.L. (1987) Evolution of antibody variable region structure during the immune response. Immunol. Rev. 96:141.
175 Mariuzza R.A. and Poljak R.J. (1993) The basics of binding: mechanisms of antigen recognition and mimicry by antibodies. Curr. Opin. Immunol. 5:50.
176. Max E.E., Seidman J.G., Leder P. (1979) Sequences of five potential recombination sites encoded close to an immunoglobulin κ constant regions. Proc. Natl. Acad. Sci. USA 76:3450.
177. McKean D.M., Huppi K., Bell M., Staudt L., Gerhard W., Weigert M. (1984) Generation of antibody diversity in the immune response of BALB/c mice to influenza virus haemagglutinin. Proc. Natl. Acad. Sci. USA 81:3180.
178. McHeyzer-Williams M.G., Nossal G.J.V., Lalor P.A. (1991) Molecular characterization of single memory cells. Nature 350:502.
179. Merkenschlager M., Terry L., Edwards R., Beverley P.C.L. (1988) Limiting dilution analysis of proliferative responses in human lymphocyte population defined by the antibody UCHL-1: Implications for differential CD45 expression in T cell memory formation. Eur. J. Immunol. 18:1653.
180. Michie C.A., MacLean A., Alcock C., Beverley P.C.L. (1992) Lifespan of human lymphocyte subsets defined by CD45 isoforms. Nature 360:264.
181. Michie S.A. and Rouse R.V. (1988) Study of murine T cell migration using the Thy-1 allotype marker. Transplantation 46:98.
182. Mortari F., Newton J.A., Wang J.Y., Schroeder H.W. (1992) The human cord blood antibody repertoire. Frequent usage of the V_H7 gene family. Eur. J. Immunol. 22:241.
183. Mosmann T.R. and Coffman R.L. (1987) Two types of mouse helper T cell clones: Implications for immune regulation. Immunol. Today 8:223.
184. Mosmann T.R and Coffman R.L. (1989) Heterogeneity of cytokine secretion patterns and functions of helper T cells. Adv. Immunol. 46:111.
185. Mosmann T.R., Shumacher J.H., Street, N.F., Budd R., O'Garra A., Fong T.A.T., Bond M.W., Moore K.W.M., Sher A., Fiorentino D.F. (1991) Diversity of cytokine synthesis and function of mouse $CD4^+$ T cells. Immunol. Rev. 123:209.
186. Motoyama N., Okada H., Azuma T. (1991) Somatic mutation in constant region of mouse lambda 1 light chain. Proc. Natl. Acad. Sci. USA 88:7933.
187. Mullbacher A. (1994) The long term maintenance of cytotoxic T cell memory does not require the persistence of antigen. J. Exp. Med. 179:317.
188. Nossal G.J.V. (1992) The Molecular and cellular basis of affinity maturation in the antibody response. Cell 68:1.
189. Nossal G.J.V., Abbot A.P., Mitchell J., Lummus Z. (1968) Antigens in immunity. XV. Ultrastructural features of antigen capture in primary and secondary follicles. J. Exp. Med. 127:277.
190. Nossal G.J.V., Szenberg A., Ada G.L., Austin C.M. (1964) Single cell studies on 19S antibody production. J. Exp. Med. 119:485.
191. Nunez G., Hockenbury D., McDonnell T.J., Sorenson C.M., Korsmeyer S.J. (1991) Bcl-2 maintains B cell memory. Nature 353:71.
192. Ohgama J., Katoh M., Hirano M., Arase H., Arase-Fukushi N., Mishima M., Iwabuchi K., Ogasawara K., Onoe K. (1994) Functional studies on MEL-14^+ and MEL14^- T cells in peripheral lymphoid tissues. Immunobiol. 190:225.
193. Orme I.M. (1988) Characteristics and specificity of acquired immunologic memory to *Mycobacterium tuberculosis* infection. J. Immunol. 140:3589.
194. Osmond D.G. (1980) Production and differentiation of B lymphocytes in the bone marrow. In: 'Immunoglobulin genes and B cell differentiation.' Battisto J.R. and Knight J.L. (Eds), Elsevier, North Holland, N.Y. p. 135.
195. Osmond D.G. and Batten S.J. (1984) Genesis of B lymphocytes in the bone marrow; extravascular and intravascular localization surface IgM-bearing cells in mouse bone marrow

detected by electron-microscope radioautography after *in vivo* perfusion of ^{125}I anti-IgM antibody. Am. J. Anat. 170:349.
196. Padlan E.A. (1977) Structural implications of sequence variability in immunoglobulins. Proc. Natl. Acad. Sci. USA 74:2551.
197. Parker D. (1993) T-cell dependent B cell activation. Annu. Rev. Immunol. 11:331.
198. Pech M., Hochtl J., Schnell H., Zachau H.G. (1981) Differences between germ-line and rearranged V_k coding sequences suggest a localized mutation mechanism. Nature 291:668.
199. Poo W-J., Conrad L., Janeway Jr. C.A. (1988) Receptor-directed focusing of lymphokine release by helper T cells. Nature 332:378.
200. Preito J., Takei F., Gendelman R., Christenson B., Biberfield P., Patarroyo M. (1989) MALA-2 mouse homologue of the human adhesion molecule ICAM-1 (CD 54). Eur. J. Immunol. 19:1551.
201. Raaphorst F.M., Timmers E., Kenter M.J.H., Van Tol M.D.H., Vossen J.M., Schuurman R.K.B. (1992) Restricted utilisation of germ-line V_H3 genes and short diverse third complementarity-determining regions (CDR3) in human fetal B lymphocyte immunoglobulin heavy chain rearrangements. Eur. J. Immunol. 22:247.
202. Rada C., Gupta S.K., Gheradi E., Milstein C. (1991) Mutation and selection during the secondary response to 2-phenyl-oxazolone. Proc. Natl. Acad. Sci. USA 88:5508.
203. Rademakers L.H.P.M. (1991) Follicular dendritic cells in germinal center development. 37th Forum in Immunology. Res. Immunol. 142:257.
204. Reth M.G., Amirati P., Jackson S., Alt F.W. (1985) Regulated progression of a cultured pre-B-cell line to the B cell stage. Nature 317:353.
205. Rocken M., Saurat J.H., Heuser C. (1992) A common precursor for $CD4^+$ T cells producing IL-2 or IL-4. J. Immunol. 148:1301.
206. Roes J., Huppi K., Rajewski K., Sablitzky F. (1989) V gene rearrangement is required to fully activate the hypermutation mechanism in B cells. J. Immunol. 142:1022.
207. Rogerson B., Hackett J., Peters A., Haasch D., Storb U. (1991) Mutation pattern of immunoglobulin transgene sis compatible with a model of somatic hypermutation in which targeting a mutator is linked to the direction of DNA replication. EMBO J. 10:4331.
208. Rolink A. and Melchers F. (1993) B lymphopoiesis in the mouse. Adv. Immunol. 53:123.
209. Rose M.L., Birbeck M.S., Wallis V.J., Forrester J.A., Davies A.J.S. (1980) Peanut lectin binding properties of germinal centers of mouse lymphoid tissues. Nature 28:364.
210. Rothman P., Li S.C., Gorham B., Glimcher L., Alt F., Boothby M. (1991) Identification of a conserved LPS/IL-4 responsive element located at the promoter of germ-line ε transcripts. Mol. Cell. Biol. 11:5551.
211. Rouse V.R., Ledbetter J.A., Weissman I.L. (1982) Mouse lymph node germinal centers contain a selected subset of T cells - the helper phenotype. J. Immunol. 137:2395.
212. Rudikoff S., Pawlita M., Pumphrey J., Heller M. (1984) Somatic diversification of immunoglobulins. Proc. Natl. Acad. Sci. USA 81:2162.
213. Sablitzky E., Wildner G., Rajewwsky K. (1985) Sequence analysis of non-expressed immunoglobulin heavy chain loci in clonally related, somatically mutated hybridoma cells. EMBO J. 4:345.
214. Sakano H., Kurosawa Y., Weigert M., Tonegawa S. (1981) Identification and nucleotide sequence of a diversity DNA segment (D) of immunoglobulin heavy-chain genes. Nature 290:562.
215. Samelson L.E., Lindsten T., Fowlkes B.J., Van Den Elsen P., Terhorst C., Davies M.M., Germain R.N., Schwartz R.H. (1985) Expression of genes of the T-cell antigen receptor complex in precursor thymocytes. Nature 315:765.
216. Sanders M.E., Makgoba M.W., June C.H., Young H.A., Shaw S. (1989) Enhanced responsiveness of human memory cells to CD2 and CD3 receptor mediated activation. Eur. J. Immunol. 19:803.
217. Sanders M.E., Makgoba, M.W., Sharrow S.O., Stephany D., Springer T.A., Young H.A., Shaw S. (1988) Human memory T lymphocytes express increased levels of three cell adhesion molecules (LFA-3, CD2, LFA-1) and three other molecules (UCHL1, CDw29, Pgp-1) and have

enhanced IFN-γ production. J. Immunol. 140:1401.
218. Savelkoul H.F.J., Lebman D.A., Benner R., Coffman R.L. (1988) Increase of the precursor frequency and clonal size of murine immunoglobulin E-secreting cells by interleukin-4. J. Immunol. 141:749.
219. Savelkoul H.F.J., Seymour B.W.P., Sullivan L., Coffman R.L. (1991) IL-4 can correct defective IgE production in SJA/9 mice. J. Immunol. 146:1801.
220. Schildbach J.F., Near R.I., Bruccoleri R.E., Haber E., Jeffrey P.D., Novotny J., Sheriff S., Margolies M.N. (1993) Modulation of antibody affinity by a non-contact residue. Prot. Sci. 2:206.
221. Schittek B. and Rajewsky K. (1990) Maintenance of B cell memory by long-lived cells generated from proliferating precursors. Nature 346:749.
222. Schroeder H., Walter M., Hofker M., Ebens A., Van Dijk K., Liao L., Cos D., Milner E., Perlmutter R. (1988) Physical linkage of a human heavy chain variable region gene segment to diversity and joining region elements. Proc. Natl. Acad. Sci. USA 85:8196.
223. Scollay R. and Shortman K. (1985) Cell traffic in the adult thymus: cell entry and exit, birth and death. In: 'Recognition and Regulation in Cell-mediated immunity.' Watson J.D. and Marbrook J. (Eds), Marcel Dekker, N.Y., p. 3.
224. Scott P. (1993) Selective differentiation of $CD4^+$ T helper cell subsets. Curr. Opin. Immunol. 5:391.
225. Selsing E. and Storb U. (1981) Somatic mutation of antibody genes. Cell 25:47.
226. Severinson E., Fernandez C., Stavnezer J. (1990) Induction of germ-line immunoglobulin heavy-chain transcription by mitogens and interleukins prior to switch recombination. Eur. J. Immunol. 20:1079.
227. Shan H., Shlomick M., Weigert M. (1990) Heavy-chain switch does not terminate somatic mutation. J. Exp. Med. 172:531.
228. Sharon J. (1990) Structural correlates of high antibody affinity: three engineered amino acid substitutions can increase affinity of an anti-p-azophenylarsonate antibody 200-fold. Proc. Natl. Acad. Sci. USA 87:4814.
229. Sharon J., Gefter M., Wysocki L.J., Margolies M.N. (1989) Recurrent somatic mutation in mouse antibodies to p-azophenylarsonate increase affinity for hapten. J. Immunol. 142:596.
230. Shatz D.G., Oettinger M.A., Schlissel M.S. (1992) V(D)J recombination: molecular biology and regulation. Annu. Rev. Immunol. 10:359.
231. Shimuzu A., Takahashi N., Yaoita Y., Honjo T. (1982) Organization of the constant-region gene at the mouse immunoglobulin heavy chain. Cell 28:499.
232. Short J.A., Sethupati P., Zhai S.K., Knight K.L. (1991) V(D)J genes in V_Ha2 allotype suppressed rabbits. Limited germline V_H gene usage and accumulation of somatic mutations in D regions. J. Immunol.147:4014.
233. Sideras P., Mizuta T.R., Kanamori H., Suzuki N., Okamoto M., Kuze K., Ohno H., Doi S., Fukuhara S., Hasan M.S. (1989) Production of sterile transcripts of C gamma genes in IgM-producing human neoplastic B cell line that switches to IgG-producing cells. Int. Immunol. 1:631.
234. Siebenknotten G., Esser C., Wabl M., Radbruch A. (1992) The murine IgG1/IgE class switch program. Eur. J. Immunol. 22:1827.
235. Siekvitz M., Kocks C., Rajewsky K., Dildrop R. (1987) Analysis of somatic mutation and class switching in naive and memory B cells generating adoptive primary and secondary responses. Cell 48:757.
236. Siskind G.W. and Benacerraf B. (1969) Cell selection by antigen in the immune response. Adv. Immunol. 10:1
237. Slaughter C.A. and Capra J.D. (1983) Amino acid sequence diversity within the family of antibodies bearing a major anti-arsonate cross-reactive idiotype of the A strain mouse. J. Exp. Med. 158:1615.
238. Smith S.H., Brown M.H., Rowe D., Callard R.E., Beverley P.C.L. (1986) Functional subsets of human helper-inducer cells defined by a new monoclonal antibody, UHCL1. Immunology 58:63.

239. Snapper C.M., Finkelman F.D., Stefany D., Conrad D.H., Paul W.E. (1988) IL-4 induces co-expression of intrinsic membrane IgG1 and IgE by murine B cells stimulated with lipopolysaccharide. J. Immunol. 145:3654.
240. Snodgrass H.R., Dembic Z., Steinmetz M., Von Boehmer H. (1985) Expression of T-cell antigen receptor genes during fetal development in the thymus. Nature 315:232.
241. Spinelli S. and Alzari P.M. (1994) Structural implications of somatic mutations during the immune response to 2-phenoxyoxazolone. Res. Immunol. 145:41.
242. Sprent J. (1994) T and B memory cells. Cell 76:315.
243. Sprent J., Schaefer M., Hurd M., Surh C.D., Ron Y. (1991) Mature murine B and T cells transferred to SCID mice can survive indefinitely and many maintain a virgin phenotype. J. Exp. Med. 174:717.
244. Spriggs M.K., Armitage R.J., Stockbine L., Clifford D.N., Macduff B., Sato T.A., Malszewski C.R., Fanslow W.C. (1992) Recombinant human CD40 ligand stimulates B cell proliferation and immunoglobulin E secretion. J. Exp. Med. 176:1543.
245. Springer T.A., Dustin M.L., Kishimoto T.K., Marlin S.D. (1987) The lymphocyte function associated LFA-1, CD2, and LFA-3 molecules. Cell adhesion receptors of the immune system. Annu. Rev. Immunol. 5:223.
246. Stavnezer J., Radcliffe G., Lin Y.C., Nietupski J., Berggren L., Sitia R., Severinson E. (1988) Immunoglobulin heavy-chain switching may be directed by prior induction of transcripts from constant-region genes. Proc. Natl. Acad. Sci. USA 85:7704.
247. Stavnezer-Nordgren J. and Sirlin S. (1986) Specificity of immunoglobulin heavy chain correlates with activity of germline heavy chain genes prior to switching. EMBO J. 5:95.
248. Stein H., Gerdes J., Mason D.Y. (1982) The normal and malignant germinal center. Clinics in Haematol. 111:531.
249. Steiner L.A. and Eisen H.N. (1967) Sequential changes in the relative affinity of antibodies synthesized during the immune response. J. Exp. Med. 126:1161.
250. Street N.E., Schumacher J.H., Fong T.A.T., Bass H., Fiorentino D.F., Leverah J.A., Mosmann T.R. (1990) Heterogeneity of mouse helper T cells. Evidence from bulk cultures and limiting dilution cloning for precursors of Th1 and Th2 cell. J. Immunol. 144:1629.
251. Strober S. (1976) Maturation of B lymphocytes in rats. III. Two subpopulations of memory B cells in the thoracic duct lymph differ by size, turnover rate, and surface immunoglobulin. J. Immunol. 117:1288.
252. Swain S.L. (1991) Regulation of the development of distinct subsets of $CD4^+$ T cells. Res. Immunol. 142:14.
253. Swain S.L., Bradley L.M., Croft M., Tonkonogy S., Atkins G., Weinberg A.D., Duncan D.D., Hedrick S.M., Dutton R.W., Huston G. (1991) Helper T-cell subsets: phenotype, function and the role of lymphokines in regulating their development. Immunol. Rev. 123:115.
254. Swain S.L., Weinberg A.D., English M. (1990b) $CD4^+$ T cell subsets: Lymphokine secretion of memory cells and of effector cells that develop from precursors *in vitro*. J. Immunol. 144:1788.
255. Swain S.L., Weinberg A.D., English M., Huston G. (1990a) IL-4 directs the development of Th2-like helper effectors. J. Immunol. 145:3796.
256. Szakal A.K., Homes K.L., Tew J.G. (1983) Transport of immune complexes from the subcapsular sinus to lymph node follicles on the surface of nonphagocytic cells, including cells with dendritic morphology. J. Immunol. 131:1714.
257. Szakal A.K., Kosco M.H., Tew J.G. (1988) A novel *in vivo* follicular dendritic cell-dependent iccosome-mediated mechanism for delivery of antigen to antigen-processing cells. J. Immunol. 140:341.
258. Szakal A.K., Kosco M.H., Tew J.G. (1989) Microanatomy of lymphoid tissue during the induction and maintenance of humoral responses: structure function relationships. Annu. Rev. Immunol. 7:91.
259. Szakal A.K., Taylor J.K., Smith J.P., Kosco M.H., Burton G.F., Tew J.G. (1990) Kinetics of germinal center development in lymph nodes of young and aging immune mice. Anat. Rec. 227:475.

260. Tanaka T., Hu-Li J., Seder R.A., Fazekas de St. Groth B., Paul W.E. (1993) Interleukin-4 suppresses interleukin-2 and interferon-γ production by naive T cells stimulated by accessory cell-dependent receptor engagement. Proc. Natl. Acad. Sci. USA 90:5918.
261. Tedder T.F., Cooper M.D., Clement L.T. (1985) Human lymphocyte differentiation antigens HB-10 and HB11. II. Differential production of B cell growth and differentiation factors by distinct helper T cell subpopulations J. Immunol. 134:2989.
262. Teillaud J.-L., Desayamrd C., Ciutsi A.M., Haseltine B., Pollock R.A., Yelton D.E., Scharff M.D. (1983) Monoclonal antibodies reveal the structural basis of antibody diversity. Science 222:721.
263. Tew J.G., DiLosa R.M., Burton G.F., Kosco M.H., Kupp L.I., Masuda A., Szakal A.K. (1992) Germinal centers and antibody production in bone marrow. Immunol. Rev. 126:97.
264. Tew J.G. and Mandel T.E. (1979) Prolonged antigen half-life in the lymphoid follicles of specifically immunized mice. Immunology 37:69.
265. Tew J.G., Phipps R.P., Mandel T.E. (1980a) The follicular dendritic cell: long-term antigen retention during immunity. Immunol. Rev. 53:29.
266. Tew J.G., Phipps R.P., Mandel T.E. (1980b) The maintenance and the regulation of the humoral immune response: persisting antigen and the role of follicular antigen-binding dendritic cells as accessory cell. Immunol. Rev. 53:175.
267. Thomas M.L. (1989) The leucocyte common antigen family. Annu. Rev. Immunol. 7:339.
268. Tonegawa S. (1983) Somatic generation of antibody diversity. Nature 302:575
269. Torbett B.E., Laxter J.A., Glasebrook A.L. (1990) Frequencies of T cells secreting IL-2 and/or IL-4 among unprimed $CD4^+$ populations. Evidence that clones secreting IL-2 and IL-4 give rise to clones which secrete only IL-4. Immunol. Lett. 23:227.
270. Tough D.F. and Sprent J. (1994) Turnover of naive- and memory-phenotype T cells. J. Exp. Med. 179:1127.
271. Trinchieri G. (1993) Interleukin-12 and its role in the generation of Th1 cells. Immunol. Today 14:335.
272. Valle A., Aubry J-P., Durand I., Banchereau J. (1991) IL-4 and IL-2 upregulate the expression of antigen B7, the B cell counterstructure to T cell CD28: an amplification mechanism for T-B cell interactions. Int. Immunol. 3:229.
273. Van Es J.H., Gmelig Myeling F.H.J., Logtenberg T. (1992) High frequency of somatically mutated IgM molecules in the human adult blood B cell repertoire. Eur. J. Immunol. 22:2761.
274. Van Ommen R., Vredendaal A.E.C.M., Savelkoul H.F.J. (1994a) Secondary IgE responses *in vivo* are predominantly generated via gamma1-epsilon positive B cells. Scand. J. Immunol. 40:491.
275. Van Ommen R., Vredendaal A.E.C.M., Savelkoul H.F.J. (1994b) Prolonged *in vivo* IL-4 treatment inhibits antigen-specific IgG1 and IgE formation. Scand. J. Immunol. 40:1.
276. Vitetta E.S., Berton M.T., Burger C., Kepron M.M., Lee W.T., Yin X-M. (1991) Memory B and T cells. Annu. Rev. Immunol. 9:193.
277. Vitetta E.S., Fernandez B.R., Myers C.D., Sanders V.M. (1989) Cellular interactions in the humoral immune response. Adv. Immunol. 45:1.
278. Vitetta E.S., Ohara J., Myers C., Layton J., Krammer P.H., Paul W.E. (1985) Serological, biochemical, and functional identity of B cell stimulatory factor 1 and B cell differentiation factor for IgG1. J. Exp. Med. 161:1726.
279. Von Boehmer H. and Hafen K. (1993) The lifespan of naive alpha/beta T cells in secondary lymphoid organs. J. Exp. Med. 177:891.
280. Von Der Heide R.H. and Hunt S.V. (1990a) Immigration of thoracic duct B lymphocytes into established germinal centers in the rat. Eur. J. Immunol. 20:79.
281. Von Der Heide R.H. and Hunt S.V. (1990b) T lymphocytes in rat germinal centers belong to $ER3^+$ sub-population of $CD4^+$ cells. Immunology 69:542.
282. Wabl M., Burrows F.D., Von Gabain A., Steinberg C. (1985) Hypermutation at the immunoglobulin heavy chain locus in a pre-B cell line. Proc. Natl. Acad. Sci. USA 82:479.
283. Weber J.S., Berry J., Manser T., Claflin J.L. (1991) Position of the rearranged V kappa and its 5′ flanking sequences determines the location of somatic mutations in the J kappa locus.

J. Immunol. 146:3652.
284. Weber J.S., Berry J., Manser T., Claflin J.L. (1994) Mutations in Ig V(D)J genes are distributed asymmetrically and independently of the position of V(D)J. J. Immunol. 153:3594.
285. Weigert M., Perry R., Kelley D., Hunkapillar T., Schilling J., Hood L. (1980) The joining of V and J gene segments creates antibody diversity. Nature 283:497.
286. Weigert M.G., Cesari I.M., Yonkovich S.J., Cohn M. (1970) Variability in the light chain sequences of mouse antibody. Nature 228:1045.
287. Weiss U. and Rajewsky K. (1990) The repertoire of somatic antibody mutants accumulating in the memory compartment after primary immunization is restricted through affinity maturation and mirrors that expressed in the secondary response. J. Exp. Med. 172:1681.
288. Weiss U. and Wu G.E. (1982) Somatic mutations in unrearranged immunoglobulin gene segments encoding the variable region of lambda light chains. EMBO J. 6:927.
289. Weiss U., Zobelein G., Rajewsky K. (1992) Accumulation of somatic mutants in the B cell compartment after primary immunization with a T cell-dependent antigen. Eur. J. Immunol. 22:511.
290. Wilson M., Hsu E., Marcuz A., Courtet M., Du Pasquier L., Steinberg C. (1992) What limits affinity maturation of antibodies in *Xenopus* - the rate of somatic mutation or the ability to select mutants? EMBO J. 11:4337
291. Winoto A., Urban J.L., Lan N.C., Goverman J., Hood L., Hansburg D. (1986) Predominant use of V alpha gene segment in mouse T-cell receptor for cytochrome c. Nature 324:679.
292. Wu T.T. and Kabat E.A. (1970) An analysis of the sequences of the variable regions of Bence Jones proteins and myeloma light chains and their implications for antibody complementarity. J. Exp. Med. 132:211.
293. Wylie A.H., Morris R.G., Smith A.L., Dunlo D. (1984) Chromatin cleavage in apoptosis: association of condensed chromatin morphology and dependence on macromolecular synthesis. J. Pathol. 142:67.
294. Wysocki L.J., Creadon G., Lemann K.R., Cambier J.C. (1992) B cell proliferation initiated by Ia cross-linking and sustained by interleukins leads to cells switching but not somatic mutation. Immunology 75:116.
295. Wysocki L.J., Manser T., Gefter M. (1986) Somatic evolution of variable region structures during an immune response. Proc. Natl. Acad. Sci. USA 83:1847.
296. Yefenof E., Sanders V.M., Uhr J.W., Vitetta E.S. (1986) *In vitro* activation of murine antigen-specific memory B cells by a T-dependent antigen. J. Immunol. 137:85.
297. Ziegner M., Steinhauser G., Berek C. (1994) Development of antibody diversity in single germinal centers selective expansion of high affinity variants. Eur. J. Immunol. 24:2393.
298. Zhang K., MacLennan I.C.M., Liu Y-J., Lane P.J.L. (1988) Is rapid proliferation in B centroblasts linked to somatic mutation in memory B cell clones? Immunol. Letters 18:297.
299. Zhang K., Mills F.C., Saxon A. (1994) Switch circles from IL-4-directed ε class switching from human B lymphocytes. Evidence for direct, sequential and multiple step sequential switch form μ to ε Ig heavy chain gene. J. Immunol. 152:3427.
300. Zheng B., Xue W., Kelsoe G. (1994) Locus-specific somatic hypermutation in germinal center T cells. Nature 372:556.
301. Zlotnik A. and Moore K.W. (1991) Interleukin-10. Cytokine 3:366.

DETERMINATION OF CONCENTRATION AND AFFINITY IN ELISA

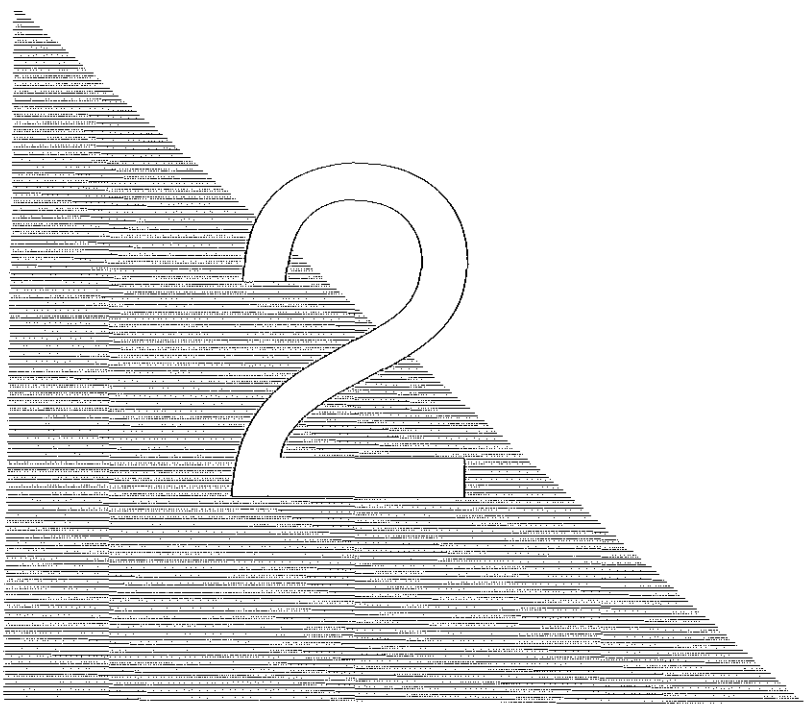

Determination of concentration and affinity in ELISA

CHAPTER 2.1

Quantitation of immunoglobulin concentration in ELISA

S.S. Pathak, A. Van Oudenaren and H.F.J. Savelkoul

Department of Immunology, Erasmus University Rotterdam, the Netherlands

1 Introduction

Enzyme-linked immunosorbent assay (ELISA) was first described by Engvall and Perlmann (1971) and Schuurs and Van Weemen (1977) and provides a safe and simple method of measuring antigen-specific and total immunoglobulins (Ig). ELISA fall under the category of heterogeneous immunosorbent assays in which (a) the bound and free fraction of Ig (ligand) are physically separated by a washing procedure and (b) the antigen (Ig) to be detected or determined is either directly or indirectly physically attached to a solid phase.

Various types of ELISA have been developed and described in literature. The commonly used ones can be divided into different categories depending upon -

a. The entity to be detected or determined, i.e. antigen or antibody specific, qualitative or (semi-) quantitative ELISA.
b. The set-up of the assay - direct, indirect, competitive, inhibitory, non-competitive, two-site (sandwich) or amplified assays.
c. The nature of the substrate employed - fluorogenic, chromogenic, luminogenic.
d. The amounts of reactants used - macro-ELISA performed in a tube, micro-ELISA employing a microtitre plate or micro-ELISA needing micro quantities (5 µl) of sample performed in Terasaki trays - Terasaki-ELISA.

Moreover, the solid phase used to adsorb the protein coat can be of various materials - glass, polypropylene, polyvinylchloride (PVC), polystyrene, polycarbonate, nitrocellulose, silicons etc., though only polystyrene or PVC microtitre plates are commercially available.

2 Set up of the assay

The majority of ELISA are performed in polystyrene microtitre plates using commercially available equipment facilitating easy and automatic handling of the system. A serum sample of 100 µl is used to determine the concentration of Ig (IgM, IgA, IgG) in moderately sensitive ELISA. However, if simultaneous detection of a number of Ig classes (especially rare ones like IgD and IgE), autoantibodies, anti-idiotypic antibodies etc. is required, a fairly large serum

sample is needed. This problem is more pronounced in longitudinal studies on sera of mice or children, where it is often difficult to acquire the amount of serum needed to perform the assay. In the case of monoclonal antibody production as well, only very small quantities of supernatants are available for the assay, since testing for Ig production is desired as soon as possible following fusion. We therefore adopted the Terasaki-ELISA performed in the 60 well Terasaki trays using 5 µl of sample per well, thus reducing the amount of serum or supernatant needed. One further advantage of this method is that very small amounts of coating and detecting reagents are required. The Terasaki trays are made of polystyrene, so that the adsorption characteristics of these plates can be expected to be essentially similar to those of polystyrene microtitre plates. For the determination of total Ig, we use a two-site (sandwich) ELISA system in which the antigen (Ig) is characterized by two geometrically and molecularly distinct binding sites for the two specific antibodies employed. Thus, the Ig is sandwiched between the known anti-isotypic catching antibody adsorbed to a solid phase and a detecting antibody, in effect rendering a much higher degree of specificity to the overall system. The catching as well as the detecting antibodies can be either identical or different but they must be heterologous to the Ig determined. For antigen-specific assays, we use the antigen as the catching moiety and a heterologous detecting antibody. After adsorbing the antigen or catching antibody to the solid phase, all subsequent incubations are done until equilibrium is established and competition can no longer occur between the labeled and unlabeled ligand involved. Moreover, all other reagents, except the sample, are in slight excess, so that only the Ig that is bound out of the sample is the limiting step. Thus, the signal obtained is directly related to the amount of Ig bound.

Other ELISA systems, whether competitive, homologous, one-site, homogeneous or non-equilibrium reaching, are well documented and will not be discussed here. The reader is referred to the available reviews (Wisdom, 1976; Schuurs and Van Weemen, 1977) and books (Voller et al., 1981; Avrameas et al., 1983; Bizollon, 1984). Some relevant points to consider before performing heterogeneous ELISA will be described here, after which essential parameters like sensitivity, detection limit and accuracy will be discussed.

3 Coating of the solid phase

3.1 Theoretical aspects

The coating of the solid phase can be done either by covalent coupling to the plastic matrix, or to grafted plastic surfaces or as is done generally, by simple adsorption. Most proteins adsorb to plastic surfaces, probably due to hydrophobic interactions between the nonpolar (glyco)protein moieties having a net charge of zero and the nonpolar plastic matrix. The rate and the extent of adsorption (and therefore coating) depends upon a number of different factors.

The more important ones being -

a. The nature of the molecule being adsorbed i.e. the net charge, hydrophobicity, size, molecular weight, diffusion coefficient, etc.
b. The concentration of the adsorbing molecule, determining the occupancy rate.
c. The nature of the coating buffer i.e. its composition, molarity and pH; but also the absence of detergents, adsorbed spacer molecules for peptide binding (e.g. poly-L-lysine) or agents permitting covalent coupling of highly charged molecules (e.g. glutaraldehyde).
d. The solid phase - the chemical nature of the solid phase will obviously influence the extent of adsorption, so will the ratio of surface, area to be coated to the volume of the coating solution (typically 1.5 ng/mm^2 or 6 x 10^9 molecules/mm^2, since a microtitre well is 33 mm^2 in surface this equals maximum immobilization of 50-150 ng/well). The shape of the wells resulting in shearing or stress forces can be critical. Large differences in the adsorbing properties of plates of different manufacturers and even among different batches from the same manufacturer have been observed.
e. The temperature and duration of adsorption (typically overnight at 4°C, 3 hrs at 37°C or even one minute in a microwave).

Langmuir proposed an equation to fit adsorption data which implies an equilibrium between protein molecules and a limited number of surface active sites on the solid phase. Both the equilibrium constant K_A and the maximal surface concentration of the adsorbed molecules can be calculated from the experimental data using the following equation:

$$\frac{1}{m} = \frac{1}{b} + \frac{1}{bK_A c}$$

Where c is the molar concentration of the protein in equilibrium with m grams of adsorbed protein per cm^2, b and K_A are constants. The value of b corresponds to the maximum amount of protein that can be adsorbed to solid phase (saturation). K_A is the association constant corresponding to the reaction:

$$P + S \underset{k_d}{\overset{k_a}{\rightleftharpoons}} PS \; ; \qquad K_A = \frac{k_a}{k_d}$$

Where, S represents surface active sites and P the protein to be adsorbed.

When only one kind of surface site is available and only these sites are occupied by the protein (no protein-protein association), a monolayer is formed according to this reaction. If two or more kinds of surface sites with different affinity for the protein are available, more complex reactions will take place.

The main criticism directed against this approach is that the equilibrium may not be a reversible one, as assumed by the Langmuir treatment. The basis for this criticism is the fact that several authors could not detect protein desorption from plastic solid phases other than plates (Cantarero et al., 1980). Morrisey (1977) and Lehtonen and Viljanen (1980) amongst others, on the other hand, have reported such desorption. Anything from 30 to 68% desorption has been reported. The underlying cause for this discrepancy might be that some proteins may indeed be irreversibly adsorbed or may undergo conformational change after being adsorbed, and thus escape detection by the enzyme used for the studies, viz., horseradish peroxidase. This question needs further study since desorption influences reliability of ELISA. It should be noted that in sandwich techniques, since a large excess of capturing antibody exists on the solid phase, even an important loss may not influence the final result.

The adsorptive characteristics of polystyrene for different proteins like albumin and Ig show that the adsorptive behaviour is not explainable only on the basis of simple charge differences and molecular weight and size. Adsorption is, however, dependent on the concentration of protein in the input solution and increases proportionally with temperature and incubation time. Beyond the range of concentrations where the proportion of protein adsorbed is independent of input, i.e. the region of independence, the kinetics of adsorption change and then seem to be inversely proportional to the protein size. The presence of competing proteins has no effect on the adsorptive characteristics of a given protein provided the total protein concentration of the mixture was within the range of independence. Up to a certain limit, a constant fraction of the proteins is adsorbed to plastic surfaces. For example, 80% of the IgM but only about 25% of BSA is adsorbed, with a limit of about 1.5 ng/mm^2 for both proteins, independent of the input. According to Butler (1981), the protein molecules at this limit become equidistantly distributed on the surface and the failure to exceed this coverage (about 1/3 of the surface) is due to steric hindrance. As these data were obtained from microtitre plates having an effective coating area of around 0.1 mm^2/µl, it would imply that at maximum 0.2 µg/ml of protein can be adsorbed before steric hindrance occurs. As a rule, under optimal working conditions a linear dose-response curve is obtained in ELISA. At higher inputs of analyte a deviation from this linearity can occur. This phenomenon is referred to the 'hook effect' and was originally used synonymously with the 'prozone phenomenon' (Nakamura et al., 1986). However, they are now recognized to be two independent phenomena. In ELISA, the 'hook effect' is commonly assumed to mean a release of coated antigen or antibody from the plate during the subsequent washing steps.

However, in reality, it is the result of the release of coated antigen or catching antibody into the solution during sample incubation. As a result, both the coated (Ag^c) and the free (Ag^{sol}) molecules compete for binding sites on the Ig molecule (Ab). Therefore, two different equilibria can be established leading to two different affinity constants (K_1 and K_2).

$$[Ag]^c + [Ag]^{sol} + [Ab] \rightleftharpoons [AgAb]^c + [AgAb]^{sol}$$

$$K_1 = \frac{[AgAb]^c}{[Ag]^c[Ab]} \qquad K_2 = \frac{[AgAb]^{sol}}{[Ag]^{sol}[Ab]}$$

The ratio between these two affinity constants determines the extent of the hook effect. As a result the plateau value of ELISA titration curves may be lowered by increasing (but non saturating) concentrations of the coat (Pesce et al., 1983).

The 'prozone phenomenon' is said to occur when a decreased instead of an increased signal is observed at higher levels of the analyte. It is presumed to be the result of monovalent binding between the detecting antibody or the conjugate and the analyte. It is thus a function of the affinity of the analyte and the detecting reagents, as well as the concentration, and is independent of the coat (Vos et al., 1987). Subsequent washings dissociate weakly bound ligands from the plate and cause 'bleeding'. Bleeding refers to a progressive loss of antibodies bound to the immobilized ligand due to dissociation of immune complexes containing antibodies with low affinities.

3.2 Practical aspects

The usefulness of an ELISA depends upon the coating efficiency and the reproducibility of the coat. Thus, it is essential to ensure sufficient adsorption of the protein to the plastic surface. Various strategies can be employed to achieve this.

a. Use of coating buffers - Engvall and Perlmann (1971) have suggested the use of a high pH - high ionic strength buffer (0.1 M Na_2CO_3, pH 9.6) for efficient coating of antibodies, which is perhaps the most widely used. Recent studies, however, have shown, that the method of passive adsorption of proteins - especially Ig - at this high pH leads to extensive protein denaturation. Only 10% of the adsorbed IgG was found to retain its activity under these conditions (Butler et al., 1992). PBS (10 mM Na or K phosphate buffer, pH 7.2 - 7.8) with 150 mM NaCl is also popular for coating of Ig, and is thought to cause much less protein denaturation. For antigen-specific

ELISA, on the other hand, a large variation in the binding of various proteinic antigens to plastic surfaces can be expected. The choice of a proper buffer can help increase the binding. A variety of buffers can therefore be employed. Scott et al. (1985) for example found that 0.1 M acetic acid increased the efficiency of coating of dietary antigens. For a new assay, a proper investigation to establish the most suitable buffer is thus necessary. This may not, however, increase the coating efficiency sufficiently and to further increase the binding of the proteins, pretreatment of either the proteins or the polystyrene surface can be attempted.

b. Pretreatment of proteins - Partial denaturation and/or aggregation of proteins by heat treatment may help increase the binding of proteins. For several antigens (myoglobin, ovalbumin, albumin, transferrine, ferritin) an increase in sensitivity of ELISA was obtained after cross-linking by a carbodiimide promoted condensation reaction. Pretreatment of the antibody with glutaraldehyde was found to increase its binding by 2 to 5 fold. Any kind of treatment of the proteins is likely to cause denaturation or partial unfolding of the molecule, and therefore change its antigenic properties. Proper controls must hence be included to avoid erroneous results.

c. Pretreatment of the polystyrene surface - Activation of the polystyrene surface can be achieved by different means. Kemeny et al. (1986) suggested ultraviolet irradiation of the plates. Boudet et al. (1991) have successfully coated small synthetic peptides to microtitre plates by exposing them to UV radiation for upto 20 min. Pretreatment of the plate with a freshly diluted 2% solution of glutaraldehyde for 2 hrs has been found to increase antibody binding significantly. Klasen and Rigutti (1983) have found activation of polystyrene by 0.025% glutaraldehyde lead to reliable coating even by water-insoluble proteins dissolved in urea. The effect of glutaraldehyde is pH-dependent and is less polymerizing at low pH (pH 5.0). Biotinylated microtitre plates are now also commercially available. These plates can be used to immobilize Ig via a streptavidin bridge. Ig thus immobilized have been found to retain a high degree of reactivity (Butler et al., 1992). Alternatively, streptavidin can be passively adsorbed to the microtitre plate, and biotinylated proteins used for coating. Such methods are especially useful when dealing with small, synthetic peptides (Ivanov et al., 1992).

   For small antigens or haptens, it is advisable to precoat the plates with a polylysine or polyaspartate spacer or to use a hapten carrier conjugate for coating. Cyanogen bromide has likewise been used to increase the coating efficiency. Linking of antigen to the plastic via an antibody bridge decreases the variation due to differing adsorption of different antigens. Furthermore, it may also increase the sensitivity of the assay and is therefore used by many workers (Urbanek et al., 1985).

   To detect antibodies directed against cell-surface antigenic determinants, it is possible to coat the cells in monolayers on the solid phase using glutaraldehyde (0.02%, 15 min at RT), especially since such low concentrations of glutaraldehyde do not alter the conformation of the antigenic determinants.

One note of caution is, however, necessary. Pretreatment of the proteins or the polystyrene surfaces may lead to allosteric changes in the coated molecule, and thus decrease its immunoreactivity.

d. Use of various time-temperature combinations - Overnight coating at 4°C as suggested by Engvall and Perlmann (1971) is most frequently used. Various time-temperature combinations have been suggested in literature. These vary from 1-2 hours at 37°C to few hours at elevated temperatures followed by overnight incubation at 4°C.

All ELISA incubation times, including coating time, can be reduced by exposing the plates to 2.45 GHz microwaves combined with air blowing. Such usage, however, has to be carefully regulated, as otherwise denaturation of the proteins can occur. Coating plates by allowing them to dry completely (37°C for 1 hr, 15 min with a fan) so as to ensure maximal coating was tried by us. However, we did not find any increase in the overall sensitivity of the assay, perhaps because drying promotes protein denaturation (unpublished results). Ansari et al. (1985) have also found that drying of plates following coating led to a decreased activity of the solid phase bound antibody.

The concentration of proteins to be used in the coating solution has of course to be empirically determined. Excessively high protein concentrations should be avoided as they are likely to cause multilayers of proteins on the solid phase due to protein-protein interaction. Also, competition between the immune serum and surface active sites for the antigen molecules may occur in ELISA. If this competition occurs, it will lead to affinity and concentration dependent desorption, leading to a non-linear dose-response curve.

Engvall (1980) has suggested 1-10 µg/ml as optimal concentration for coating of antigens and antibodies. This concentration can be used as a starting point. In our own experience with the microtitre system, we have observed that higher than optimal coating concentrations, leads to a lowering of the signal. This phenomenon could be explained by the formation of multiple protein-protein layers at higher coating concentrations with the consequent desorption during the ELISA.

The coated plates can be stored either wet in PBS with 1-2 mM NaN_3 at 4°C or dried in an exiccator for periods up to 4 weeks. In our experience, however, storing wet plates coated with monoclonal antibody at 4°C for more than 12-16 hrs leads to decreased sensitivity, probably because prolonged storing at a high pH leads to structural changes in the molecule or because of a time-related denaturation of the protein due to adsorption to plastic. However, we have observed that storing wet plates coated in PBS (pH 7.2) for upto 4 days has no undesirable effect on the ELISA.

After the coating has been completed, the trays are washed thoroughly -

generally with the same running buffer as is used in the rest of the steps. PBS is commonly used, though Tris buffered saline can also be employed.

The washing removes all the excess unadsorbed protein. Non-ionic detergents such as Tween 20 (TW20) are generally used in the wash-buffer as they lower the surface tension and thus prevent formation of new hydrophobic interactions between the added protein and the solid phase. The effect of washes on dissociation of immune complexes is dependent on the affinity of the antibodies employed. When antibodies are immobilized on the solid phase in concentration of 10^{-7} M (fairly typical for microtitre plates), low affinity antibodies (K_D = 10^5 - 10^6 M) may be rapidly dissociated and under-represented. With higher affinities (K_D = 10^8 - 10^9 M), however, activities are representative for concentrations.

All the remaining unoccupied binding sites are saturated with an unrelated, non-interfering protein to control non-specific adsorption. An extra protein coating aimed at saturating the plastic support not occupied by the antigen has also been suggested. BSA (1-5%), gelatin (0.02-0.1%), or casein either in combination with TW20 or alone are in common use. Schonheyder and Andersen (1984) as well as Pruslin et al., (1991) have shown that BSA post coating and addition of BSA to serum diluent decreases background readings and increases specific activity. However, batch to batch variation has often been found in BSA. The likelihood of the presence of contaminating bovine antibodies in BSA can also not be ignored. Reservations about its general applicability are therefore expressed (Smith et al., 1993). TW20 was found to be a satisfactory blocking agent in experiments with murine monoclonal antibodies and high-titre animal antisera. In contrast, high non-specific binding that was not abolished by TW20 was found to be a major problem in experiments with low-titre rabbit antisera as well as in some assays with human antibodies from patient sera. So, the most suitable blocking agent will depend upon the individual system, that is to say on the coat, the detecting reagent(s) and the nature of the sample, and will vary widely. Blocking of e.g. rat Ig immobilization confirms that small molecules (<10 kDa) block better than larger molecules (>30 kDa). Ig were found to be able to penetrate blocking layers of BSA giving high background levels and early failure of blocking with dilution.

4 Choice and preparation of the ligand

4.1 Theoretical aspects

Several characteristics of the enzyme to be conjugated to the detecting antibody need to be considered in choosing the enzyme (Table 1). These include the turnover number (i.e. the molecular activity), specific activity, detectability of the product, absence of substances likely to interfere with enzyme activity in the fluids to be measured, etc.

Table 1 Criteria for choice of enzyme label

1. Availability of low-cost purified homozygous enzyme preparations.
2. High specific activity or turnover number.
3. Presence of reactive residues through which the enzyme can be cross-linked to other molecules with minimal loss of enzyme and antibody activity.
4. Capability of producing stable conjugates.
5. Enzyme should be absent from biological test samples.
6. Assay method that is simple, cheap, sensitive, precise and not affected by factors present in the sample.
7. Enzyme, substrates, cofactors, etc. should not pose potential health hazards.

Table 2 lists some of the enzymes in common use. The size of the antibody-enzyme conjugated molecule can also influence the sensitivity of the ELISA system. The binding of the detection reagent at high concentrations of the primary antibody appears to be sterically inhibited in direct proportion to the size of the conjugate used, leading to a marked deviation from linearity in this region of the binding curve (Koertge and Butler, 1985). Conjugation reactions involving only proteins (enzymes and antibodies) can be carried out easily by using various bifunctional reagents as extensively reviewed (Tijssen, 1985).

Table 2 Comparison of some enzymes available for ELISA

Enzyme	pH optimum	Specific activity (U/mg)	Molecular weight (Da)	Practical Substrates	
				Visual	Fluorescent
Alkaline phosphatase	8-10	400	100,000	ONPP	MUF-P FM-P
Peroxidase	5-7	900	40,000	5-AS	NADH OPD HPA ABTS
β-Galacto-sidase	6-8	400	540,000	ONPG	MUF-G

Abbreviations : ABTS, 2,2-azino-di-(3 ethyl benzothiazolin sulfone-6) diammonium salt; 5-AS, aminosalicylic acid; FM-P, fluorescein methyl phosphate; HPA, hydroxyphenylacetic acid; MUF-G, methyl umbelliferyl galactose; MUF-P, methyl umbelliferyl phosphate; NADH, nicotinamide adenine dinucleotide; ONPG, ortho nitrophenyl galactose; ONPP, ortho nitrophenyl phosphate; OPD orthophenylene diamine.

Refer Table 3 for the most popular cross-linking methods. Generally speaking, use of an heterobifunctional cross-linker should be preferred since it gives rise to conjugates free from polymeric products that are observed when using a homobifunctional linker. It has been suggested that the sensitivity of the ELISA is partially influenced by the method by which the enzyme is coupled to the detecting antibody. Tsang et al. (1984) showed by using glutaraldehyde and sodium periodate coupled peroxidase-anti-human conjugates that the former

conjugates are more useful in quantitative assays where wide ranges are desirable. The latter conjugates, on the other hand, are more suited to qualitative assays where sensitivity is more important.

Table 3 Common methods used to prepare enzyme-antibody conjugates

Reactive group	Bifunctional reagent
Amino residues	glutaraldehyde 1,4-benzoquinone succinimidyl-3-(2-pyridyldithiopropionate)(SPDP)
Sulphydryl groups	N,N'-o-phenylenedimaleimide M-maleimidebenzoyl-N-hydroxysuccinimide ester (MBS)
Carbohydrate moieties	periodate oxidation
Carboxyl groups	1-ethyl-3(3-dimethyl aminopropyl) carbodiimide

After completion of the conjugation reaction, proper recovery of the enzyme-protein conjugate is important. Moreover, it is essential to ensure that the enzymatic activity resides only in the conjugated form and that the solution is free of contaminating native enzyme molecules. The specific activity of the enzyme can be measured by either endpoint or rate analysis. It is necessary to recognize that the optimal conditions of pH, substrate concentration, activators used etc. for the conjugated enzyme can differ from the native enzyme. Thus, the experimental conditions for obtaining maximum activity of the conjugated enzyme in an ELISA may differ from those observed in the fluid phase. The proximity of the solid phase affects the micro-environment of the enzyme and may also lead to conformational changes in the enzyme molecule. It is thus not correct to optimize the conditions in a fluid phase and expect them to hold in ELISA as well (Tijssen, 1985). Furthermore, the antibody part of the conjugate must retain its binding affinity, and this has also to be confirmed in an assay similar to the one for which the conjugate has been prepared, i.e. an ELISA.

The efficiency of conjugation represents the amount of immunoreactive enzyme recovered. Factors that inflence the efficiency are: type of reaction used for conjugation, proportion of reactants, i.e. enzyme and antibody, and heterogeneity/homogeneity of labeling sites for preparation of the immunogen and of the enzyme conjugate. Azimzadeh et al. (1992) have suggested conjugating F(ab)' fragments instead of the whole antibody to the enzyme. This approach has the advantage that the enzyme and antibody fragments are present in the conjugate in a stoichiometric ratio of 1:1 and complications arising from monogamous bivalent binding of the antibody to the antigen (antibody) are eliminated (Azimzadeh et al., 1991).

The antiserum employed in the ELISA is crucial for the specificity of the assay and, by virtue of its affinity for the antigen to be detected in the assay, also for its sensitivity and detection limit. It is therefore evident that the antiserum preparation should be characterized as extensively as possible. This information is often not available for commercial antiserum preparations. Commonly, the only information available is that they are claimed to be affinity purified i.e. to be adsorbed onto affinity columns bearing immobilized, potentially cross-reacting substances. Such preparations should therefore be tested elaborately before use. They must be tested in precipitation based assays as well as in inhibition ELISA. Displacement of a labeled antigen from the complex by competition with increasing concentrations of competing non-labeled antigen, reveals shared or cross-reactivity. Antibodies generally have lower affinities for cross-reactive antigens, so that higher concentrations of these antigens are necessary to obtain maximal inhibition. The degree of maximal inhibtion is dependent on the degree of cross-reactivity between the various antigens. In inhibition-type ELISA a sufficient range of antibody concentrations should be tested on a panel of purified myeloma or hybridoma proteins. The panel should include specimens of every isotype and some of the isotypes should be represented by a lambda or a kappa light chain. Proteins of different idiotypes and allotypes should also be included, certainly when testing the isotype specificity of the antiserum. This is all the more necessary when the preparation is a polyclonal antiserum induced by injecting heterologous animals with purified Ig of the appropriate (sub)class, since under these conditions a substantial part of the antiserum raised can be directed against the allotype, light-chain or idiotype. When tested under such stringent criteria, not all commercially available sera turn out to be suitable for sensitive assays like ELISA.

The methodology for the induction and the purification of the IgG fraction of a specific antiserum by the use of monoclonal antibodies is essentially routine. Monoclonal antibodies are sensitive to purification procedures and the three dimensional structure of the antibody can easily be distorted. Moreover, monoclonal antibody preparations often consist of incomplete chains. This could result in the use of partially denatured and/or incomplete Ig preparations in the raising of the antiserum. The quality of the antibody response can depend upon the immunization conditions and the type of adjuvant used. These factors can therefore affect the quality of the antiserum raised and should be considered while raising antisera for use in ELISA.

Apart from antibody-enzyme conjugates, other ligand-enzyme conjugates are in current use. The biotin-avidin system with a high affinity constant of 10^{15} M^{-1} is one such example (Bayer and Wilchek, 1978). Thus, a system wherein the biotin is conjugated to the specific or detecting antibody or antigen and the avidin is linked to the end-product developing enzyme can be used, especially since biotin bound to a macromolecule retains its high affinity for avidin. Alternatively, biotin can be conjugated to both the detecting antibody and

enzyme and avidin then employed as a bridge between these biotinylated proteins. The use of biotin and avidin ensures that a high degree of enzyme is bound specifically to the Ig in the sample. In recent years the biotin-streptavidin system has found wide application. Biotinylated conjugates of polyclonal and monoclonal antibodies as well as enzymes conjugated to streptavidin are now commercially available, increasing the popularity of the system. Using this system we have achieved a sensitivity of 1-10 ng/ml for our isotype specific microtitre ELISA.

S. aureus protein A and protein G of group G streptococci react with the Fc part of many mammalian species. It is especially useful as it can behave as a purified anti-antibody of restricted specificity with no species specificity. Enzyme-protein A conjugates can therefore be used to detect Ig from samples in ELISA. A sandwich ELISA with enzyme labeled protein A and unlabeled isotype-specific detecting antibody having a high affinity for protein A is currently in use. This method can be useful in assaying Ig with no binding affinity for protein A; e.g. rat monoclonal antibody directed against mouse cell-surface determinants or antigen specific as well as total human or mouse IgE antibody.

4.2 Practical aspects

In our fluorimetric Terasaki-ELISA assays, we have chosen the enzyme ß-galactosidase from *E. coli* (E.C. 3.2.1.23.) for a number of reasons. Though both alkaline phosphatase and ß-galactosidase are widely used in combination with fluorigenic substrates, ß-galactosidase is mostly used if high detectability is required. Also, alkaline phosphatase has the further disadvantage of producing reagent blanks which are 50-fold higher than those of ß-galactosidase, due to the spontaneous degradation of the substrate. Moreover, ß-galactosidase has a high specific activity (400 U/mg), a high turnover number (12,500 substrate molecules transformed per mole of enzyme per min) and can be linked to the antibody by a number of chemical methods with a good degree of retention of its enzymatic activity without altering the immunological activity of the antibody. The conjugate is soluble and stable under the assay conditions and can be stored for prolonged time at 4°C. Last but not least, the enzyme itself, its substrate or factors that interfere with enzyme activity such as inhibitors, are all absent from the samples assayed.

The enzyme is conjugated to the antibody with the one-step glutaraldehyde method of Avrameas et al. (1978; 1983). The antibody to be coupled is extensively dialysed against 0.1 M potassium phosphate buffer (pH 7.8) and a final protein concentration of 4 mg/ml is achieved. 2 mg of ß-galactosidase (specific activity 30 U/mg; Boehringer, Mannheim, FRG) is dissolved in 1 ml of

the above buffer and a reaction mixture is prepared by mixing 1 ml of enzyme solution with 1 ml of antibody solution and 50 µl of 25% (v/v) glutaraldehyde

solution (stored in the dark at 4°C; TAAB laboratories Ltd; Reading, England). The reaction is allowed to occur for 30 min at RT on an end-over-end mixer and thereafter blocked by the addition of 1 ml lysine (Sigma, St. Louis, MO) in the same phosphate buffer and stored overnight at 4°C. After extensive dialysis against PBS, additives such as 0.1% BSA, or 0.2% gelatin or 0.2% glycerol are added to give a 50% (v/v) final concentration. The conjugate is stored at 4°C. The additives make it possible to store the conjugate for a few months, while without them the shelf-life is reduced to few weeks. Ions can act as activators or inhibitors of enzymes. In the case of ß-galactosidase, NH_4^+ and Mn^{2+} ions activate the enzyme while high concentrations of Na^+ and heavy metal ions are inhibitory. Also ß-mercaptoethanol can cause dissociation of the enzyme molecule in the absence of Mg^{2+}, while it is an excellent activator in its presence. These facts therefore need to be taken into account in choosing the conjugate and the substrate buffer (refer Table 4).

Table 4 Physicochemical properties of ß-galactosidase

Name	ß-D-galactoside galactohydrolase (EC 3.2.1.23)
Mass	465,000 Dalton
Molecular form	tetramer (16S) monomers at pH 3.5 or 11.5 or with mercurials
Stability	>30 min at 40°C with pH 6-8 in 100 mM 2-mercaptoethanol and 10 mM $MgCl_2$
Inhibitor	2-mercaptoethanol alone
Isoelectric point	4.6
Specific activity	400 U/mg

5 Substrate reaction and product detection

Assays that utilize enzymatic markers offer the potential for a high degree of assay sensitivity and detectability. However, the detectability of enzyme immunoassays which utilize substrates that generate visibly colored molecules upon enzymatic activation is limited by the detection limit of these relatively low-energy markers. For example, while enzymes in common use have turnover rates of approximately 10^5 substrate molecules transformed per mole of enzyme per min, the fact that some commonly used substrates require concentrations of 10^{-6} mol/l to be detectable by colorimetric instruments limits the usage of standard enzyme immunoassays to 10^{-11} mol/l (Ishikawa et al., 1983). The recent availability of a large number of substrates which generate fluorescent molecules upon enzymatic interaction offers the possibility of the development of an enzyme assay, which utilizes the fluorimetric measurement of the reaction end-point. Moreover, fluorimetry measures a signal increase above relatively low background luminescence while colorimetry measures a small decrease due to absorbance from a large amount of transmitted light. The detection limits of fluorimetry are frequently limited by background fluorescence such as that

arising from serum or other biological samples. For this reason, fluorimetric ELISA methods have become practical only for heterogeneous systems, preferably when a solid phase bound antibody is used to facilitate washing.

This system thus offers the advantage both of the stability and quantitative nature of fluorescence measurement and the catalytic magnification inherent in enzyme-substrate interaction. Since, as discussed above, the detection limit of a fluorigenic substrate can be orders of magnitude lower than that of a chromogenic substrate, this advantage can be used to increase the sensitivity of ELISA, thereby reducing sample sizes, using more dilute reagents, and/or shortening incubation times.

Most researchers using fluorimetric ELISA have employed conventional fluorimeters which require the manual transferring samples to cuvettes and measuring their signals individually. Simply adding a flowcell and autosampler or sipper to a conventional fluorimeter can significantly decrease the labor involved.

Because it is emitted in all directions, there is more versatility in designing detectors for fluorescence than for absorbance. For example, reflectance fluorimetry has been used with thin layer chromatography. A similar detector design could be used for fluorescence measurements directly from the wells of microtitre plates. With laser excitation, fluorescence can be measured from sub-microliter sample volumes. When choosing a fluorigenic substrate, there are several important considerations -

a. The substrate should be readily available in a pure and stable form.
b. It should be nonfluorescent under the detection conditions to be used.
c. It must be efficiently converted by the enzyme label.
d. The resultant product must be stable and highly fluorescent.
e. It should exhibit a large Stokes shift, that is, a significant wave length difference between the product's excitation and emission maxima.
f. It is also preferable to have a long excitation wavelength for the product formed, as there will be lower background fluorescence at lower excitation energies (Milby, 1985).

The most widely used substrates are those which generate the highly fluorescent ketone 4-methyl-umbelliferone (MUF) upon enzymatic cleavage, since this molecule can be measured at concentrations of 10^{-15} to 10^{-18} mol/l. We use MUF-G (4-methyl-umbelliferyl-ß-D-galactoside; Sigma) as our substrate. This ELISA compares favorably with equivalent systems using chromogenic substrates like ortho-nitrophenyl-ß-galactoside that is detectable only at 100-fold higher concentration. The latter has a minimum detection limit of around 10 to 100 ng/ml. In the fluorigenic assay the minimum detection limit has been described to be 10^{-15} mg/ml of IgG (Shalev et al., 1980) and 10^{-10}

mg/ml of IgE (Savelkoul et al., 1989). Crowther et al. (1990) have compared a number of enzyme substrate combinations in ELISA. They have established that the combination of ß-D-galactosidase and MUF-G resulted in maximum sensitivity. The substrate (0.25 mg/ml) is dissolved in 0.05 M potassium phosphate buffer, pH 7.8, with 10 mM $MgCl_2$ by rapid heating till 60°C.

Caution has to be exercised in the heating process as the substrate tends to disintegrate at temperatures higher than 80°C. Alternatively, the substrate can be dissolved to 0.5% in NN-dimethylformamide and diluted to 0.1 mM with 10 mM sodium phosphate, pH 7.0, containing 0.1 M NaCl, 1 mM $MgCl_2$, 0.1% NaN_3 and 0.1% ovalbumin. Following solubilization the substrate solution is rapidly cooled, aliquotted and stored at -20°C. Such aliquots can be used for a few months provided they are reheated till 60°C and rapidly cooled to RT before use. In our experience repeated freezing and thawing of the substrate leads to erraneous results. Also, freshly prepared substrate solution gives less interplate variation. We therefore prefer preparing fresh substrate solution each day.

One of the major points to consider when performing fluorescence based ELISA is the dependence of the resultant fluorescence on the pH of the substrate solution and possible quenching by contaminating impurities. It is of crucial importance to regulate the pH in the substrate solution since by changing the pH, the emission wavelength can shift up to 200 nm or fluorescence can be completely lost by formation of non-fluorescent ions. For MUF-G, the wavelength used for excitation and emission analysis are 360 and 440 or 450 nm, respectively. Secondly, the length of the substrate incubation step and the temperature (60 min, 37°C) are also critical for the fluorescent product formation. Hence, these parameters should be kept exactly constant in order to be able to compare the fluorescence measurements of various ELISA performed on different days.

6 Expression and quantitation of data

6.1 Untransformed data

The most common modes of expressing ELISA results are untransformed absorbance reading at a single sample dilution, end-point antibody titre obtained by direct determination on calibration curves, and antibody-activity unit from a calibrated dose-response curve. Such dose-response curves can be computed employing empirically transformed standard curves or by using equations derived from the Law of Mass Action. Furthermore, for quantitation the data can be expressed in a variety of ways, eg. semi-logarithmic plots, log-log plots, log-logit transformations etc. We shall briefly consider each of these. Any method that one chooses should fulfill two basic criteria:

1. Stability of data under varying conditions such as changes in assay design and minor variations in the experimental conditions.
2. Linearity of response with dilutions of positive sera over a reasonably large interval.

The optimal response and shape of dilution curves are both defined by a multitude of factors related to the main methodological choices made in establishing the ELISA structure as well as to within-method variables such as reagent characteristics and assay conditions which are subject to modifications and not always easy to predict and control. Assay conditions in the ELISA affect the shape of the dilution curve (Malvano et al., 1982). Even with identical assay conditions the shape of the dose-response curves of different serum samples varies in some ELISA (Gripenberg et al., 1979). Also, it is known that antibody avidity and affinity differ between different sera giving different kinds of dose-response curves (De Savigny and Voller, 1980). Thus useful information about antibodies may be lost if ELISA results are derived from a single serum dilution (Lehtonen and Eerola, 1982).

Besides the dependence of signal intensity upon experimental conditions, the non-linear correlation of signal with antibody activity in some regions of the dose response curve sets limits to the use of non-transformed optical responses, despite its immediate availability and wide acceptance in practice. Nevertheless, a simple algorithm is proposed by Franco et al. (1984), wherein multiple categorization of non-transformed absorbance values from ELISA plates is performed under a microprocessor control. The printed output is a pictoral emulation of a 96-well plate with the color intensities represented for each reaction. This method is particularly suited for the screening of mouse hybridoma culture supernatants.

Quantitation by the use of different equations derived from the Law of Mass Action has been extensively tried; but, as a general conclusion, no adaptation has been found suitable to the specific principles of ligand binding assays. Such efforts of obtaining an absolute concentration dependent equation consisted of adapting the Langmuir adsorption isotherm and its consequence: the Scatchard equation. Further adaptation, e.g. the Sips equation, could also not be used with sufficient success.

6.2 End-point titres

Titration of antibody is an established and easy-to-comprehend quantitation method, even for ELISA. If standards calibrated in I.U./ml are not available, titration is often the only generally accepted method.

The need for sequential dilutions of samples for definition and control of a cut-off value are evident disadvantages intrinsic to titration. Other adverse

features are less obvious: the range over which measurements can be made is rigidly defined by the detection system. The readings become increasingly insensitive at either end of this range. The assay precision relates to the sample dilution scale chosen and, when the least dilution still yielding a response above the cut-off value is taken as the titre, the measurement is made close to the detection limit, thus exaggerating the response uncertainty. Moreover, the dilution at which the 'extinction' of response occurs, depends upon the sensitivity of the assay, so that end-point titres reflect variations of sensitivity level under different circumstances.

The expected parallelism between titres and antibody activity appears insufficient to counterbalance the unfavourable aspects, i.e., the high susceptibility to systematic and random variability, the amount of laboratory work involved and the cost of the reagents. This suggests that caution is necessary in considering absorbance readings and end-point titrations as suitable modes of expressing results. The results obtained by the titration method could at best be said to be semi-quantitative.

Dopatka and Giesendorf (1992) have suggested a new method for antibody quantitation in ELISA. Here, the sample is tested in a single dilution and the OD obtained is used in the equation

$$\log_{10} \text{titer} = \alpha.OD^{\beta}$$

where α and ß are constants to be determined for each batch of reagents. Since a single dilution is tested, the criticism above seems to hold for this method as well. Further testing needs to be done before the method can find general application.

6.3 Reference standards

Since most quantitative ELISA are based on the use of calibrators, it is prudent to realize the importance of the standard for determining the quality of the assay and allowing a comparison of the readings made with those obtained previously or in different circumstances. The recovery of the standard Ig is particularly dependent on the diluent used: a regular buffer or a similar matrix in which the sample Ig occurs (serum, liquor, etc.). Therefore, the sample and the standard should preferably be diluted in similar medium. Lyophilized reference samples are more prone to deteriorate, denature and accumulate turbidity as compared to fluid reference standards. It is therefore generally advisable to filter-sterilize, aliquot and freeze the standard samples.

It is also a common practice to prepare standard samples for use in routine assays that are calibrated occasionally on internationally standardized reference preparations. Such routine Ig standards should contain highly purified (sub)class

preparations that have been checked for intact Ig. Generally such standards are obtained by purifying myeloma or hybridoma proteins from which the recovery of intact material is all the more difficult. The Ig preparation should preferably contain members of the particular (sub)class that carry the different light chains and as many allotypes as possible. Also, in the case of hybridoma proteins, different specificities of the Ig produced should be included into the panel. Such sample mixtures can subsequently be tested in various assays for the purity and reactivity against the antiserum preparations used in the ELISA. Next, the protein content in the reference sample can be established and a calibration graph can be constructed by running this standard in the ELISA. Also a standard plot can be obtained in which the sample readings are plotted against the standard concentration. The latter plot can be the basis for further treatment of the data by employing mathematical transformations.

6.4 Data transformation

The use of a reference scale eliminates systematic components of error and gives analytical consistency to the measurement. In this way, normalization between runs, between laboratories and between methods is achieved. Availability of international reference sera greatly facilitates the use of calibration curves. In their absence, however, provisional arbitrary scales for antibody activity can be used. Such procedure based upon interpolation on a calibration curve of a standard sample is, however, hampered by the weak reproducibility of the standard graph, the limited number of standard points to draw graphs and the uncertainty of the geometry of the graph at lower precision of the experimental results.

The calibration curves can be plotted in various ways. Commonly a calibration curve of OD versus log dilution of the standard is plotted. In our experience, however, probably because of differing affinities of the polyclonal Ig for a monoclonal coat, the standard and the sample curves often have different slopes complicating interpretation of the data obtained. Butler et al. (1985; 1992) considered the logarithmic transformation of the Mass Law and arrived at the conclusion that the system can become independent of affinity within certain limits when log-log plots are used. Such log-log plots are also used in the 'Multiple Of Normal Activity method' (Ritchie et al., 1983). This method considers an approximately parabolic relationship between concentration of antibody and the absorbance (A_1 of sample 1 at dilution 1 and A_2 of sample 2 at dilution 2) that will result in a straight line on a log-log plot. The log-log plot will have a slope, m, and this factor is used for the calculation of the dilution factor. This factor can be defined as the number of times a serum should be diluted (D_2) over a reference serum (D_1) to obtain the same absorbance as the reference serum ($= D_2/D_1$).

$$\log\frac{D_2}{D_1} = -\log\frac{A_1/A_2}{m}$$

Characterization of the dose response curve by approximating the dilution curve by a second degree polynomial or a higher degree spline function is also used. Gripenberg and Gripenberg (1983) approximate the function y(x), that is the absorbance (or fluorescence) value obtained in ELISA when the serum dilution factor is 1/x, by the polynomial

$$p(x) = a_0 + a_1 x + a_2 x^2$$

using the least squares method, with equal weights at the discrete measurement values of x. Lehtonen and Viljanen (1982) have used the function

$$kx^{1/mx}$$

Gordon et al. (1985) on the other hand have suggested the use of

$$y = a + b/x + c/x^2$$

Both are empirically found equations where k, m and a, b and c are constants to be arrived at by an iterative process. One advantage of using a polynomial lies in the simplicity of the calculation, since one has only to take a linear combination of the reading values. On the other hand, these polynomials lack monotonicity of the curves and are distorted by outlying values. Alternatively, the standard curve can be transformed into a four-parameter log-logit fit from which the sample Ig concentration can be determined.

6.5 Logistic transformation

For quantitative determination of the Ig concentration, the measured response is plotted in a semi-logarithmic plot versus log dilution (i.e., absolute concentration) of the standard. Such dose-response curves are smooth, symmetrical, and sigmoidal in appearance. The measured response may be in terms of OD (chromogenic microtitre ELISA) or AFU (Arbitary Fluorescence Units; Terasaki-ELISA). The semi-logarithmic curves may be described by the

four-parameter logistic equation

$$y=\frac{a-d}{1+(x/c)^b}+d$$

Here, y represents the response variable, x is the arithmetic dose (absolute lg concentration), d is the response at high dose (upper response plateau), a is the response at zero dose (lower response plataeu), c is the dose resulting in a response halfway between a and d, and b is a slope factor that determines the steepness of the curve. In this equation, y can never exceed d. Therefore, the denominator must be greater than 1, and (x/c) has to be restricted to positive values.

The quantity y increases monotonically since the differential equation, of which the logistic function is the general solution,

$$\frac{dy}{dt}=my(d-y)$$

implies that dy/dt > 0. For t → -∞, y tends to zero, and for t → +∞, y tends to d. The growth starts slowly, then becomes faster and finally tapers off. Growth of the signal is fastest in the neighbourhood of the point of inflection. To get its location, the second derivative y = y(f) has to be equated to zero.

$$\frac{d^2}{dt^2}=m(d-2y)\frac{dy}{dt}$$

This expression can only vanish if d-2y = 0 or y = d/2, that is, the point of inflection is halfway between the lines y = 0 and y = d. To get the abscissa, let y = d/2 in the logistic equation and solve it with respect to t:

$$t=\frac{\ln\ k}{dm}$$

This particular abscissa is positive or negative depending on whether k<1 or k>1.

The four-parameter logistic equation is not fitted to data directly to estimate all four parameters, but a transformation of this equation is commonly used. A new variable Y is defined as Y = (y-d)/(a-d) from which can be derived:

$$\frac{Y}{1-Y} = \frac{1}{(x/c)^b}$$

By taking the natural logarithm, a linear transformation is derived

$$logit(Y) = \ln\frac{(Y)}{(1-Y)} = -\ln(x/c)^b = \ln\ c^b - b\ln\ x$$

Before this linearized equation can be used, estimates of the parameters a and d must be obtained.

Standard linear regression is performed on the logit values of the response versus the log of the standard dilutions. The dilutions of known and unknown samples at which the logit is equal to zero are then compared to determine the concentration of the unknown. The latter plot is also useful to determine the dilution of the standard that gave a half-maximum reading (D_{st}). Given a constant amount of coated protein and constant affinity of the bound Ig versus the coat, the Ig concentration bound to the coat at D_{st} (C_{st}) should be equal to the Ig concentration in the sample (C_{sa}) that is bound to the coat at a certain dilution (D_{sa}). Thus, $C_{st} = C_{sa}$. From the sample response versus dilution factor a similar transformed curve is prepared and the translation factor relative to the dilution factor of the standard that resulted in half-maximum response is determined. By comparison with the known Ig content in the standard, from this translation factor the absolute Ig content can be calculated -

$$C_{sa} = (C_{st} * D_{sa})/D_{st}$$

The complete data handling is generally microprocessor controlled.

The four parameter log-logit transform takes into account the non-Gaussian error distribution of the multiple readings of every standard concentration tested. For every standard concentration tested, unequal weighted arithmetic means of the readings are to be taken, resulting in increasing standard deviations along the standard curve for higher concentrations of standard as

described by Rodbard (1971). This complicates to a large extent the linear regression analysis that has to be performed while constructing a standard graph. For this reason microprocessor-based procedures have been designed to reduce the deviation of the fitted values from the actual readings.

Since it was found that essentially identical results could be obtained by using equal weighted means as well as by unequal weighting, a simplified two parameter log-logit transform was proposed. This method has, however, some serious drawbacks like the strict dependency upon reaching equilibrium at every incubation step and its large systematic errors at either end of the curve. These effects can easily result in non-linear log-logit plots.

6.6 Concentration determination

Controversy has arisen over whether the ELISA measures antibody concentration or antibody affinity. On the one hand, ELISA has been claimed to measure antibody concentration (Engvall and Perlmann, 1971; Butler, 1981; Butler et al., 1985; 1992) and on the other hand to be a measure of antibody affinity or avidity. Moreover, as a discontinuous solid-phase assay comprising of cycles of washes and a second antibody step during which time the first antibody may dissociate, it would not be surprising from first principles that low affinity antibodies may not be detected in this system. It is all the more important to resolve this controversy because low affinity antibodies may predominate early in an immune response (and hence play a role in the early diagnosis of infections) and may be important immunopathologically.

It appears that correlation of ELISA with affinity is associated with the form of data expression chosen. Those reports indicating that ELISA measures antibody concentration use the end-point titration approach, whereas those suggesting that ELISA measures antibody affinity use the direct absorbance approach. From the work of Lehtonen and Eerola (1982) it can be concluded that ELISA absorbances read at low antibody dilution (i.e. antibody excess) preferentially reflect the binding by high affinity antibodies in the preparation whereas absorbances read at high antibody dilution (e.g. antigen excess) allow the detection of low affinity antibody subpopulations as well. It has also been reported that high epitope density minimizes the influence of affinity and should be employed wherever possible. In our opinion, expressing the data in log-logit plots, along with the use of a standardized pure Ig as a reference standard minimizes the influence of affinity and allows normalization between runs. The reference standard is obtained by mixing several purified hybridoma Ig of the same isotype. For antigen specific ELISA the calibrator should consist of a mixture of monoclonals of the same antigenic specificity.

7 Important parameters

Some common characteristics of ligand-binding immunoassays determine the quality and the final applicability of such an assay. These are the specificity, sensitivity, precision and reproducibility, and practicability.

The *specificity* of the assay depends to a large extent on the quality of the detecting antibody employed. Three points need to be borne in mind whilst selecting the detecting reagents -

a. In our experience polyclonal antibodies are better detecting reagents than monoclonals.
b. Generally speaking, the use of enzyme linked $F(ab')_2$ or, better still, Fab fragments is recommended.
c. All the Ig employed in the assay should be explicitly tested for monospecificity.

As mentioned earlier, the detecting antibodies are purified out of hyperimmune sera and need to be of a high affinity to be of use as a detecting reagent. For production of such high affinity sera, some knowledge of affinity maturation is required. It was not until studies of Eisen and Siskind (1964) using the defined DNP-hapten system, that thermodynamically precise measurements of antibody affinity were made. These studies clearly illustrated that the affinity of antibody produced following immunization increases progressively and the rate of affinity maturation is related inversely to antigen dosage. However, affinities do not always mature, as indicated by the persistence of a low affinity population throughout the antibody response, especially in the case of weak immunogens (polysaccharides etc.). These facts should be borne in mind while raising hyperimmune sera.

The direct binding of the conjugate to the solid phase, which is only to some extent reduced by the use of detergents, should be avoided. The conjugate should thus be employed at the highest possible dilution. In a sandwich or two-site assay as described a much better sensitivity is reached by the double recognition of the Ig carrying at least two separate determinants, by the catching antibody or the antigen immobilized on the solid phase and the detecting antibody.

The *sensitivity* of an assay is usually defined as the lowest concentration giving a response which differs significantly from the zero concentration response (detection limit). It would be more appropriate to define sensitivity as the change in response (dR) per unit amount of reactant (dC) and equals dR/dC (Tijssen, 1985). Therefore, on a sigmoid dose-response curve, sensitivity decreases at either end of the curve resulting in an increasingly large error in the estimation of the analyte. *Detectibility* reflects the confidence with which it can

be stated that a certain response is larger than this error. Factors affecting specificity influence sensitivity to a large extent. Assay sensitivity is a function of the analyte concentration, detector sensitivity, and assay imprecision. Other assay conditions also have a role to play in determining the sensitivity. These include washing buffers and the performance of washing steps, nature and molecular weight of the antigen (for antigen-specific assays), ionic strength and pH of the diluent, incubation period and temperature, and the molar ratio of enzyme label per detecting antibody molecule in the conjugate. Ekins (1990) has proposed that maximum sensitivity is dependent on Σ/K, where Σ is the experimental error of measurement and K is the affinity constant. Ekins (1990) has further developed mathematical arguments which show that 'non-specific' binding is one of the important factors that limit the sensitivity of non-competitive ELISA.

The optimal reagent dilutions will also greatly influence the sensitivity and detectability of the assay performed. Firstly, the quantity of immobilized antigen or antibody is critically important. In all probability at high concentrations of the coat protein multilayers are formed so that the actual quantity of protein exposed to the antibodies is not increased. Moreover, the molecules may be packed too close together and therefore are antigenically non-effective due to steric hindrance. On the other hand, when the concentration of the antigen or antibody immobilized is too low, the specific binding capacity is small and the sensitivity of the assay will be low. The optimal coating concentration for each assay system, as well as the optimal dilutions of all the other reagents to be employed in the assay, therefore need to be empirically determined by checkerboard titrations. The efficiency of the reading of the high-energy product formed determines the sensitivity of the assay. Most of the sensitive and quantitative assays described reach detection limits for antibody varying from 2-20 x 10^{-18} mole per ml. The sensitivity in terms of dR/dC, however, is rarely stated in such studies.

The *precision* and *reproducibility* of the assay are reflected by the slope of the log dose-response curve and the standard deviation of the individual reading at a certain dose of antigen. The steeper the log dose-response curve and the smaller the standard deviation of this line, the higher will be the precision of the assay. The general use of standard deviation (SD) is, strictly speaking, not valid since ELISA values for negative reference samples are distributed with a positive skew. Due to this skewness, false positives occur with a significantly higher frequency than expected from a normal distribution. Non-parametric methods would be more accurate but are hardly used since they require larger sample sizes. SD is generally employed, but with a rather limited practical use. More replicates in the assay will only increase the reliability of the estimate for SD, but the spread of the individual remains in principle unchanged. A more practical alternative is to estimate the 95% confidence interval of the arithmetic mean.

The use of ELISA in large scale studies, eg. epidemiological surveys, necessitates adequate assay precision, since in these situations it is not possible to evaluate all samples of interest in a single assay and between-assay variation must be minimised. Sources of between-assay variation include differential adsorptive charactersitics of polystyrene (or PVC) plates, fluctuations in pH and temperature of buffers, errors in reagent preparation, reagent instability, variability in the washing procedure, timing of reactions and volumetric pipetting errors.

Several methods are available for reducing between-assay variation in ELISA. These include - expressing results as a ratio of OD of test sera and the OD of reference sera; expressing results as units read from a standard curve constructed from control samples tested on each plate; use of a plate correction factor (PCF) calculated as the ratio of a single or more control serum's target OD to its actual OD and multiplying the OD of the test sera by the PCF.

Reproducibility of the ELISA method used can be further increased by defining a list of criteria for the standards on which quantitation in the assay is based. Such a list should include: stability, homogeneity, absence of contaminants, accurate division into smaller aliquots, moisture content, identity of properties with the test substance etc. Moreover, quality control samples should be included in the tests to monitor variations at different concentration levels and to ensure the quality of the tests. For regular ELISA users, a quality control chart plotting the results of the control samples over time can provide a simple means of monitoring trends and hence a drift in assay parameters.

The *practicability* of the assay refers not only to the speed and the ease to perform of the assay, but also to the possibility of automation of monotonous steps like washing, addition of reagents whether sample, conjugate, substrate etc., and especially the measurement of the signal and calculation and computation of the results. A range of automated washing as well as measuring systems alongwith software packages for computation of results are available for the microtitre system. For Terasaki-ELISA, on the other hand, only few automation equipment is available. All these parameters must be taken into account while choosing and performing ELISA.

8. References

Ansari, A.A., *et al.* (1985) ELISA solid phase: stability and binding characteristics. J. Immunol. Methods 84, 117-124.

Avrameas, S.A., *et al.* (1983) Immunoenzymatic techniques, Elsevier, Amsterdam.

Avrameas, S.A., *et al.* (1978) Coupling of enzymes to antibodies and antigens. Scand. J. Immunol. 8, 7-23.

Azimzadeh, A., and Van Regenmortel, M.H.V. (1991) Measurement of affinity of viral monoclonal antibodies by ELISA titration of free antibody in equilibrium mixtures. J. Immunol. Methods 141, 199-208.

Azimzadeh, A., *et al.* (1992) Measurement of affinity of viral monoclonal antibodies using Fab'-peroxidase conjugate. Influence of antibody concentration on apparent affinity. Mol. Immunol. 29, 601-608.

Bayer, E.A., and Wilchek, M. (1978) The avidin-biotin complex as tool in molecular biology. Trends Biochem. Sci. 3, 257-259.

Bizollon, C.A. (1984) Monoclonal antibodies and new trends in immunoassay, Elsevier Science Publishers B.V., Amsterdam.

Boudet, F., *et al.* (1991) UV-treated polystyrene microtitre plates for use in ELISA to measure antibodies against synthetic peptides. J. Immunol. Methods 142, 73-82.

Butler, J.E. (1981) The amplified ELISA: principles of and application for the comparative quantitation of class and subclass specific antibodies and the distribution of antibodies and antigens in biochemical separates. In: Methods in enzymology. Van Vunakis, H., Langone, J.J. (Eds), Academic Press, New York, 73, pp 482-523.

Butler, J.E., *et al.* (1985) The amplified immunosorbent assay (a-ELISA). In: Enzyme mediated immunoassay, T.T. Ngo, Lenhoff, H.M. (Eds), Plenum Publishing Corpn., New York, pp 241-276.

Butler, J.E., *et al.* (1992) The physical and functional behavior of capture antibodies adsorbed on polystyrene. J. Immunol. Methods 150, 77-90.

Cantarero, L.A., *et al.* (1980) The adsorptive characteristics of proteins for polystyrene and their significance in solid phase immunoassays. Anal. Biochem. 105, 375-382.

Crowther, J.R., *et al.* (1990) Evaluation of the use of chromogenic and fluorogenic substrates in solid-phase enzyme linked immunosorbent assays (ELISA). Biologicals 18, 331-336.

De Savigny, D., and Voller, A. (1980) The communication of ELISA data from laboratory to clinician. J. Immunoassay 1, 105-128.

Dopatka, H.D., and Giesendorf, B. (1992) Single point quantification of antibody in ELISA without need of a reference curve. J. Clini. Lab. Analysis 6, 417-422.

Eisen, H.N., and Siskind, G.W. (1964) Variations in affinities of antibodies during the immune response. Biochemistry 3, 996-1008.

Ekins, R. (1990) Merits and disadvantages of different labels and methods of immunoasay. In: Principles and practice of immunoassay. Price, C.P., Newman, D.J. (Eds). Stockton Press, New York, pp 96-123.

Engvall, E. (1980) Enzyme immunoassay ELISA and EMIT. In : Methods in enzymology. Van Vunakis H., Langone, J.J. (Eds.) Academic Press, New York 70, pp 419-439.

Engvall, E., and Perlmann, P. (1971) Enzyme-linked immunosorbent assay (ELISA) quantitative assay of immunoglobulin G. Immunochemistry 8, 871-874.

Franco, E.L., *et al.* (1984) Computer assisted multiple categorization of absorbance values in ELISA in pictorial emulation of 96-well plates. J. Immunol. Methods 70, 45-52.

Gordon, J., *et al.* (1985) Immunoblotting and dot immunobinding. In: Rapid methods and automation in microbiology and immunology. Habermahl, K.-O. (Ed), Springer-Verlag, Berlin, pp 103-114.

Gripenberg, M., *et al.* (1979) Demonstration of antibodies against *Yersinia enterocolitica* lipopolysaccharide in human sera by enzyme-linked immunosorbent assay. J. Clin. Microbiol. 10, 279-284.

Gripenberg, M., and Gripenberg, G. (1983) Expression of antibody activity measured by ELISA, anti-DNA antibody activity characterized by the shape of the dose-response curve. J. Immunol. Methods 62, 315-323.

Ishikawa, E., *et al.* (1983) Ultrasensitive enzyme immunoassay using fluorogenic, luminogenic, radioactive and related substrates and factors to limit sensitivity. In: Immunoenzymatic techniques, Avrameas, S.A., Druet, P., Masseyeff, R., Feldmann, G. (Eds), Elsevier, Amsterdam, pp 219-232.

Ivanov, V.S., *et al.* (1992) Effective method for synthetic peptide immobilization that increases the sensitivity and specificity of ELISA procedures. J. Immunol. Methods 153, 229-233.

Kemeny, D.N., *et al.* (1986) The use of monoclonal and polyspecific antibodies in the IgE sandwich ELISA. J. Immunol. Methods 87, 45-50.

Klasen, E., and Rigutti, A. (1983) A solid phase EIA which allows coating of peptides and water-insoluble protein showing no 'hook effect' immunnoreactivity of haemoglobin. In: Immunoenzymatic techniques, Avrameas, S.A., Druet, P., Masseyeff, E., Feldmann, G. (Eds), Elsevier, Amsterdam, pp 159-161.

Koertge, T.E., and Butler, J.E. (1985) The relationship between the binding of primary antibody to solid-phase antigen in microtitre plates and its detection by the ELISA. J. Immunol. Methods 83, 283-299.

Lehtonen, O.-P., and Viljanen, M.K. (1980) Antigen attachment in ELISA. J. Immunol. Methods 34, 61-70.

Lehtonen, O.-P., and Eerola, E. (1982) The effect of different antibody affinities on ELISA absorbance and titre. J. Immunol. Methods 54, 233-240.

Lehtonen, O.-P., and Viljanen, M.K. (1982) A binding function for curve-fitting in enzyme-linked immunosorbent assay (ELISA) and its use in estimating the amounts of total and high affinity antibodies. Int. J. Bio-Med. Comput. 13, 471-479.

Malvano, R., *et al.* (1982) ELISA for antibody measurement: aspects related to data expression. J. Immunol. Methods 48, 51-60.

Milby, K.H. (1985) Fluorometric measurements in enzyme immunoassays. In: Enzyme mediated immunoassay. Ngo, T.T., Lenhoff, H.M. (Eds), Plenum Publishing Corp., New York, pp 325-341.

Morrisey, B.W. (1977) The adsorption and confirmation of plasma protein: a physical approach. Ann. N. Y. Acad. Sci. 283, 50-64.

Nakamura, R.M., *et al.* (1986) Enzyme immunoassays: heterogeneous and homogeneous systems. In: Handbook of experimental Immunology. Weir, D.M. (Ed), Blackwell Science Publications, U.K., pp 27.1-27.20.

Pesce, A., *et al.* (1983) Theories of immunoassay employing labeled reagents with emphasis on heterogeneous enzyme immunoassay. In: Immunoenzymatic techniques, Avrameas, S.A., Druet, P., Masseyeff, R., Feldmann, G. (Eds), Elsevier, Amsterdam, pp 127-138.

Pruslin, F.H., *et al.* (1991) Caveats and suggestions for the ELISA. J. Immunol. Methods 137, 27-35.

Ritchie, D.G., *et al.* (1983) Two simple programs for the analysis of data from enzyme-linked immunosorbent assay (ELISA) on a programmable desk-top calculator. In: Methods in enzymology, Van Vunakis, H., Langone, J.J. (Eds), Academic Press, New York, 92, pp 577-588.

Rodbard, D. (1971) Statistical aspects of radioimmunoassays. In: Principles of competitive protein-binding assays. Odell, W.D., Daughaday, W.H. (Eds), Lippincott, Philadelphia, pp 204-239.

Savelkoul, H.F.J., *et al.* (1989) Terasaki-ELISA for murine IgE-antibodies II. Quantitation of absolute concentration of antigen-specific and total IgE. J. Immunol. Methods 116, 277-285.

Schonheyder, H., and Andersen, P. (1984) Effects of bovine serum albumin on antibody determination by the enzyme-linked immunosorbent assay. J. Immunol. Methods 72, 251-259.

Schuurs, W.H.M., and Van Weemen, B.K. (1977) Enzyme immunoassay. Clin. Chem. Acta 81, 1-40.

Scott, H., *et al.* (1985) Performance testing of antigen-coated polystyrene microplate for measurements of serum antibodies to bacterial and dietary antigens. Acta Path. Microbiol. Immunol. Scand. Sect. C-93, 117-123.

Shalev, A., *et al.* (1980) Detection of attograms of antigen by a high sensitivity enzyme-linked immunosorbent assay (HS-ELISA) using a fluorometric substrate. J. Immunol. Methods 38, 125-139.

Smith, S.C., *et al.* (1993) Pitfalls in the use of ELISA to screen for monoclonal antibodies raised against small peptides. J. Immunol. Methods 158, 151-160.

Tijssen, P. (1985) Practice and theory of enzymeimmunoassays. In: Laboratory techniques in biochemistry and molecular biology. Burdon, R.H., Van Knippenberg, P.H. (Eds), Elsevier Science Publishers B.V., Amsterdam, pp 1-549.

Tsang, V.C.W., *et al.* (1984) Quantitative capacities of glutaraldehyde and sodium m-periodate coupled peroxidase-anti-human IgG conjugates in enzyme-linked immunoassays. J. Immunol. Methods 70, 91-100.

Urbanek, R., *et al.* (1985) Use of the enzyme-linked immunosorbent assay for measurement of allergen-specific antibodies. J. Immunol. Methods 79, 123-131.

Voller, A., *et al.* (1981) (Eds), 'Immunoassays for 80's'. University Park Press, Baltimore, Maryland.

Vos, Q., *et al.* (1987) The effect of divalent and univalent binding on antibody titration curves in solid phase ELISA. J. Immunol. Methods 103, 47-53.

Wisdom, B.G. (1976) Enzyme immunoassay. Clin. Chem. 22, 1243-1255.

CHAPTER 2.2

Journal of Immunological Methods, 116 (1989) 277–285
Elsevier

JIM 05040

Terasaki-ELISA for murine IgE

II. Quantitation of absolute concentration of antigen-specific and total IgE

H.F.J. Savelkoul, P.W.C. Soeting, J.E. De Josselin De Jong and S.S. Pathak

Department of Cell Biology, Immunology and Genetics, Erasmus University, Rotterdam, The Netherlands

(Received 11 July 1988, revised received 22 August 1988, accepted 12 September 1988)

A Terasaki tray-based ELISA system was developed for the quantitative measurement of antigen-specific and total IgE antibodies in 5 μl samples of mouse serum dilutions. The assay was based upon non-competitive binding of mouse IgE antibodies between the immobilized appropriate antigen or capture antibodies and the detecting rabbit antibodies. A conjugate of protein A-labelled β-galactosidase and the fluorigenic substrate methylumbelliferyl-β-D-galactoside were used as a detecting system. The resulted fluorescence could be measured rapidly and automatically using an inverted micro-fluorimeter. These measurements were automatically transformed into absolute concentrations by a microprocessor-based program using a four-parameter logistic function and an absolute IgE standard. The assay was shown to have a detection limit of 0.04 ng/ml and a range of linearity of 0.04–20 ng/ml, which is sufficient to measure IgE concentrations in mouse serum.

Key words: IgE, mouse; Terasaki-ELISA; ELISA, inhibition; Antiserum, commercial; Western blotting

Introduction

In a previous study we have described the production and specificity testing of several mouse IgE-specific antisera that were found to be suitable for enzyme-linked immunosorbent assays (ELISA) of murine IgE (Savelkoul et al., 1989). Using similar approaches, other investigators have also produced heterologous mouse IgE-specific antisera and developed appropriate IgE-specific ELISA systems (Hill and Liu, 1981; Bohn and König, 1982; Bozelka et al., 1982; Giallongo et al., 1982; Maekawa and Ovary, 1984; Coffman and Carty, 1986; Gavériaux et al., 1986). Quantitation of IgE in all of these studies was based on semi-logarithmic standard graphs using the untransformed absorbance readings.

Results obtained in ELISA are generally expressed as graphically determined end point titres (Malvano et al., 1982; Caulfield and Shaffer, 1984), titres based upon linear regression analysis (Hill and Liu, 1981; Sancho et al., 1986) or absolute concentrations using transformed data (Beatty et al., 1987). Probably the most general applicable transformation is based upon a four-parameter logistic equation (Rodbard and McLean, 1977; De Lean et al., 1978; Fernandez et al., 1983).

Correspondence to: H.F.J. Savelkoul, Department of Immunology, Erasmus University, P.O. Box 1738, 3000 DR Rotterdam, The Netherlands.

Abbreviations: IgE, immunoglobulin E; ELISA, enzyme-linked immunosorbent assay; MUF-G, methylumbelliferyl-galactoside; MUF, methylumbelliferon; AFU, arbitrary fluorescence unit.

So far all ELISA systems for detecting murine IgE have been performed in 96-well microtitre plates using at least 100 μl serum dilutions. It is often difficult to measure the very low IgE concentrations since only low dilution factors can be used and a relatively large amount of serum is required. This problem is even more pronounced in longitudinal studies when only limited amounts of serum are available. Therefore, we adapted an ELISA for use in 60-well Terasaki trays so that 5 μl serum dilutions suffice (Pateraki et al., 1981; Van Soest et al., 1984; Labrousse and Avrameas, 1987). Using fluorimetric analysis of β-galactosidase, the sensitivity of the ELISA is sufficient to allow quantitative determination of both antigen-specific and total IgE in mouse serum.

Materials and methods

Mice

Groups ($n = 6–10$) of female mice, 6–12 months of age, were used for serum collection. BALB/c, C57BL/6 and SJL mice were purchased from Bomholtgard (Ry, Denmark). A/J and (C57BL/6 × DBA/2)F_1 mice were purchased from Olac (Bicester, Oxon, U.K.). C3H/HeJ and C3HeB/FeJ mice were obtained from Jackson (Bar Harbor, ME) and AKR mice were purchased from the Radiobiological Institute TNO (Rijswijk, The Netherlands).

Serum samples and standard preparations

Sera from mice were collected and stored at −20 °C. Before use, the samples were spun down in a microfuge. The primary IgE standard used consisted of a mixture of highly purified hybridoma IgE prepared as described before (Savelkoul et al., 1989).

Antisera

The rabbit (RAM/IgE) and goat (GAM/IgE) antisera to murine IgE were produced by immunization with mixtures of several highly purified hybridoma IgE preparations. The IgG fraction of the GAM/IgE and RAM/IgE antisera reacting exclusively with the Fc portion of IgE molecules were purified and used as described elsewhere (Savelkoul et al., 1989). The purified antiserum preparations were adsorbed repeatedly to the reciprocal affinity columns: GAM/IgE and RAM/IgE linked to CNBr-activated Sepharose 4B as prescribed by the manufacturer (Pharmacia, Uppsala, Sweden). Samples were loaded on to the columns in 20 mM Tris-HCl (pH 8.2) and eluted with 0.1 M glycine-HCl (pH 2.3) and washed with 10 mM phosphate-buffered saline (PBS, pH 7.2) containing 0.15 M NaCl. Apart from this adsorption to remove contaminating cross-reacting antibodies, the antisera were adsorbed on a protein A-Sepharose column (Pharmacia). This was prudent since a conjugate of protein A-coupled enzyme was used for detection. For the goat capture antibody the effluent of this column was collected while for the rabbit-detecting antibody the eluted fraction was retained. Both samples were dialysed and concentrated in an ultrafiltration cell equipped with a Diaflow YM-10 membrane (Amicon, Danvers, MA), filter-sterilized through a 0.22 μm filter (Millex GV, Millipore, Milford, MA) and stored in aliquots at −20 °C. In some experiments, a rat monoclonal antibody (mAb) specific for mouse IgE (EM95) (Baniyash and Eshhar, 1984) was used. This mAb was purified from hybridoma supernatant on a goat anti-rat Ig affinity column.

ELISA for quantitation of murine IgE

Clear polystyrene 60-well standard Terasaki trays (type 653180, Greiner, Nürtingen, F.R.G.) were coated with 5 μl/well of 0.5–10 μg/ml of the GAM/IgE antiserum as capture antibodies in 0.1 M carbonate-bicarbonate buffer (pH 9.6) or the mAb EM95 in PBS. Alternatively, wells were coated with 0.5–10 μg/ml of the relevant antigen in coating buffer. In this and every other incubation step distilled water was applied to the tray to prevent drying. The lid on each plate was closed and plates were incubated overnight at 4 °C or 3 h at 37 °C. After coating, plates were used immediately. Trays were washed with PBS containing 0.05% (v/v) Tween 20 (Sigma, St. Louis, MO), with PBS containing 0.02% gelatin (UCB, Brussels, Belgium, PBS-Gel) and wells were filled with PBS-Gel and incubated for 30 min at 37 °C. After washing with PBS containing Tween 20 and gelatin (PBS-Tw-Gel) the plates were dried. The wells were then filled with dilutions of the serum or the

standard preparations. PBS-Gel was added to some wells as a control for non-specific reactions. In this and all subsequent incubation steps plates were incubated for 30 min at 37°C. For the routine testing of sera 2 or 3.3-fold serial dilutions (in four steps) were made while for standard curves eight serial dilution steps were assayed. After extensive washing and removal of liquid from the wells, a conjugate was applied of the enzyme β-galactosidase (Boehringer, Mannheim, F.R.G.) linked to protein A. This reagent was either prepared in-house (Van Soest et al., 1984) or obtained commercially (Amersham, U.K., or Zymed, San Francisco, CA) and was used at an optimal dilution (1/200–1/1000) in conjugate buffer (PBS containing 0.05% Tween 20, 10 mM $MgCl_2$ and 50 mM 2-mercaptoethanol, Eastman Kodak, Rochester, NY). After extensive washing with PBS-Tw-Gel and aspirating the liquid from each well, 5 μl/well (= 3.7 μM) of a solution (0.25 mg/ml) of the highly fluorogenic substrate 4-methylumbelliferyl-β-D-galactopyranoside (MUF-G, Sigma) was applied and plates were incubated for precisely 60 min at 37°C. Finally, to each well 5 μl stopping solution (1 M Na_2CO_3, pH 10.4) was added and the resulting fluorescence was determined in an automatic scanning inverted microfluorimeter (Leitz, Wetzlar, F.R.G.). The instrument was equipped with a photomultiplier and an average value current meter (De Josselin de Jong et al., 1980) and the measured fluorescence intensity was recorded in arbitrary fluorescence units (AFU). A 60 channel 5 μl/well replicator (Biotec, Basel, Switzerland) and a 6 channel Terasaki dispenser (Hamilton, Bonaduz, Switzerland) were used as pipetting devices throughout. For washing the plates a device was constructed consisting of a bottle containing washing buffer and a spraying device that ensured individual washing of every well.

Data analysis and representation

For quantitative determination of IgE concentrations, the measured AFU values were plotted on semi-logarithmic graph papers versus log dilutions (i.e., absolute concentration) of the standard. This yielded dose-response curves which were smooth, symmetrical, and sigmoidal in appearance. These curves may be described by the four-parameter logistic equations:

$$y = \frac{(a-d)}{1+\left(\frac{x}{c}\right)^b} + d$$

where y represents the response variable (AFU), x is the arithmetic dose (absolute IgE concentration), a is the response at high dose (upper AFU plateau), d is the response at zero dose (lower AFU plateau), c is the dose resulting in a response halfway between a and d, and b is a slope factor that determines the steepness of the curve. From this standard plot, log-logit transformation is performed:

$$\text{logit } Y = \ln\left(\frac{Y}{1-Y}\right) = k + (b \times \ln x)$$

in which Y is the percentage response at dilution i ($Y = 100(AFU_i/AFU_{max})$), and k is an unknown constant (De Lean et al., 1978; Beatty et al., 1987). The slope of the log-logit plot corresponds to the slope factor b of the sigmoidal dose-response curve. As a function of the AFU response, the logit equation can be rewritten as:

$$\text{logit } Y = \frac{AFU}{(AFU_{max} - AFU_i)}$$

Standard linear regression was performed on the logit values of the AFU versus the log of the standard dilutions. The dilutions of known and unknown samples at which the logit was equal to zero were then compared to determine the concentration of the unknown. This was based on the notion that the logit zero point represents half the maximum binding of the standard (D_{st}) as well as the sample (D_{sa}). Given a constant amount of coated protein and constant affinity of the bound IgE antibodies to the coat, the IgE concentration bound to the coat at D_{st} (C_{st}) should be equal to the IgE concentration in the sample (C_{sa} at the dilution D_{sa}). Thus at logit zero $C_{st} = C_{sa}$. By comparison with the known IgE content in the standard, the absolute IgE content can be calculated according to:

$$C_{sa} = (C_{st} \times D_{sa})/D_{st}$$

The complete data handling process was microprocessor controlled.

Results

Optimal ELISA conditions

The sample volume (5 μl) used for performing ELISA in wells of a Terasaki tray, is only 5% of that used in a well of a regular microtitre plate (100 μl). Other parameters also play an important role in establishing useful concentrations of reagents in a Terasaki-ELISA. When comparing a well of a standard Terasaki tray with a round bottom well of a microtitre plate with respect to the effective surface area available for coating (Table I), it can be concluded that a different geometry exists in a Terasaki well. Because of the ten times larger effective coating area per volume in a Terasaki well, apart from the optimal coating concentration, the concentrations of all subsequent reagents for performing an ELISA will also differ significantly from those used in the microtitre plate-based ELISA. Therefore, the optimal concentrations of all reagents to be used in a Terasaki-ELISA need to be determined empirically.

The optimal dilutions of all reagents were determined by simple titration and were further refined by chequer-board titrations. The effective coating area per unit volume was such that over a broad range (0.5–8 μg/ml) of coating concentrations of either the capture antibodies (GAM/IgE) or antigen (DNP-BSA) similar readings were obtained when testing serial dilutions of several DNP-specific monoclonal IgE antibodies. Optimal concentrations of either coat were therefore set to 2 μg/ml. In a similar fashion we established the optimal concentration (12.5 μg/ml) of the detecting antibody (RAM/IgE) as well as the optimal working dilution of the protein A-enzyme conjugate (1 in 1500).

TABLE I

COMPARISON OF SOME PHYSICAL CHARACTERISTICS OF ROUND BOTTOM WELLS OF A MICROTITRE PLATE AND THE WELLS OF A STANDARD TERASAKI TRAY

Figures were calculated according to the manufacturer's specifications.

	Microtitre well	Terasaki well
Liquid capacity/well (μl)	317	11.4
Available surface area/well (mm^2)	32.25	12.8
Effective coating area/volume ($mm^2/\mu l$)	0.11	1.14

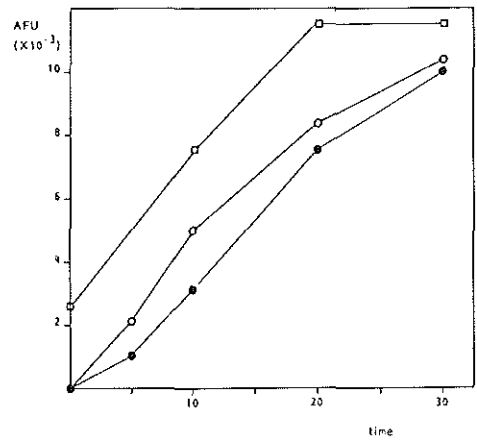

Fig. 1. Determination of the ELISA binding kinetics. Terasaki trays were charged with the IgE standard (□) and after various time intervals the amount of bound IgE was determined. Similarly, RAM/IgE was added for various times to plates coated with either IgE standard (○) or IgE standard bound to the coated GAM/IgE capture antibodies (●). Subsequently, the bound RAM/IgE fraction was determined. The results are expressed as AFU obtained from the bound fractions.

Kinetics of the binding

Next, it was established that equilibrium was reached in this Terasaki-ELISA employing incubation times of 30 min at 37° C. To this end, a regular ELISA was performed for total IgE in which the sample incubation times were increased from 1 min up to 60 min. All other incubation steps remained constant at 30 min. The results (Fig. 1) showed a logarithmically increased signal reaching a plateau value of AFU within 10 min reaction time at 37° C.

Kinetic studies of the substrate incubation times showed a linear increase in time of the reading value of a standard IgE sample in a concentration high enough to reach the plateau value (Fig. 2).

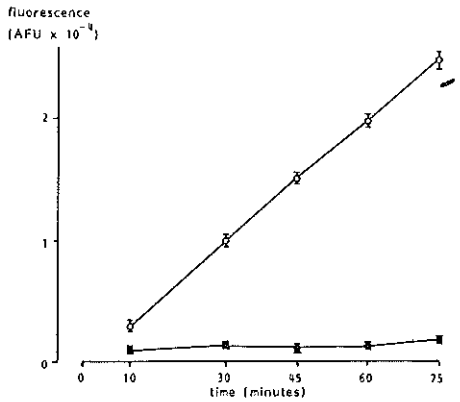

Fig. 2. Kinetics of the product formation (expressed in AFU) by incubating plates charged with a maximum concentration of IgE standard (40 ng/ml) for various periods of time (○). As a negative control plates were charged with PBS-gelatin (●).

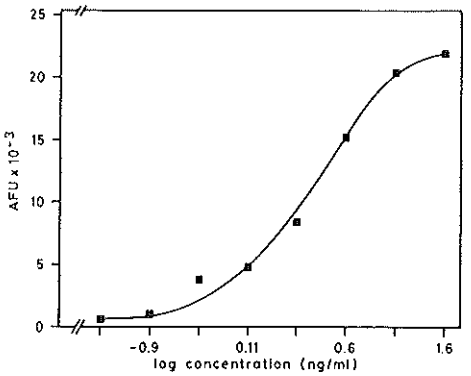

Fig. 4. Standard curve of the absolute IgE standard on plates coated with GAM/IgE capture antibodies. The data represent a semi-logarithmic plot of the various concentrations (0.01–40 ng/ml) of IgE and the extent of binding (expressed in AFU) as determined by Terasaki-ELISA.

This increase was not accompanied by an increase in the negative control. From this experiment an optimal substrate incubation of exactly 60 min was selected in order to be able to compare readings from different experiments. The optimal substrate concentration was determined to be 3.7 μM of MUF-G (data not shown).

Standard curves

An absolute (primary) standard of hybridoma IgE was prepared to permit quantitation of total IgE. This IgE standard contained 40 μg/ml, based upon protein measurement of the purified IgE content (Fig. 3). From the readings of such a standard, a semi-logarithmic plot (Fig. 4) as well as a log-logit plot (Fig. 5) were constructed, show-

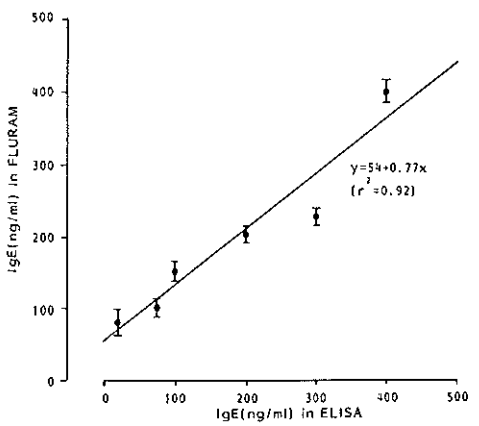

Fig. 3. Standard curve of the absolute IgE standard. The IgE content in various dilutions of the standard was assessed by both the fluorescamin based protein determination and the quantitative Terasaki-ELISA.

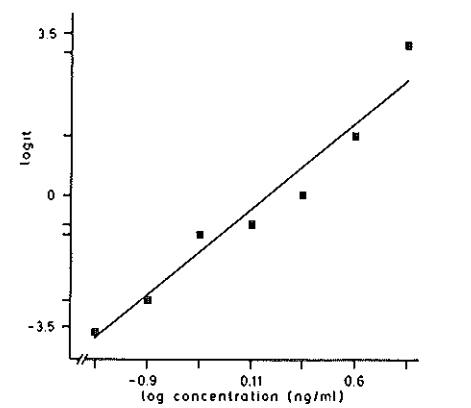

Fig. 5. Log-logit transforms of the data of the standard curves plotted in Fig. 4. Logarithms of the IgE-concentrations at various dilutions of the standard (0.01–40 ng/ml) are plotted against the logit of the corresponding AFU readings.

TABLE II

MONOCLONAL AND POLYCLONAL IgE CONCENTRATION AS DETERMINED IN TERASAKI-ELISA

All figures represent the arithmetic mean of the IgE content in ng/ml ± 1 SD ($n = 4$).

Sample	Origin	IgE content (ng/ml ± SD)
IGEL a4 6.3	Culture supernatant	31 ± 12
IGEL a4 6.5	Culture supernatant	55 ± 14
IGEL b4 1	Ascites	125 ± 25
IGEL b4 14.2	Ascites	8250 ± 167
B53/A4	Culture supernatant	40 ± 9
IgE 14-205	Ascites	90 ± 16
NMS	BALB/c	328 ± 58
NMS	C3H/HeJ	421 ± 36
NMS	C3HeB/FeJ	4 ± 1
NMS	DBA/2	1250 ± 26
NMS	C57BL/6	124 ± 9

ing a straight portion over a sufficiently large range of IgE concentrations (0.04–20 ng/ml). For routine determinations of IgE concentrations in mouse sera a secondary standard consisting of a mixture of partially purified hybridoma IgE was employed in every assay.

In order to test the reproducibility of the Terasaki-ELISA, intra- and interplate variation were repeatedly determined. This was done for the antigen-specific as well as the total IgE standards. It was found that the coefficients of the calculated concentrations were consistently less than 5%.

Concentration of serum IgE antibodies

The Terasaki-ELISA was used to measure IgE concentration in a number of pooled serum samples from mice of several strains (Table II). The results showed that the IgE levels differed significantly amongst the various strains.

Discussion

This paper describes a Terasaki-ELISA for the quantitative determination of murine IgE which combines the measurement of absolute concentration with a small sample size of only 5 μl. The ELISA is performed as a sandwich ELISA employing two non-cross-reacting antisera and a conjugate of protein A linked to the enzyme β-galactosidase. Using a fluorigenic substrate and automatic fluorescence measurement and microprocessor-based data acquisition and transformation, the assay proved to be sensitive and reproducible. The quantitative measurement was based on a standard composed of purified monoclonal IgE proteins from six different hybridomas carrying different idiotypes and allotypes.

The results obtained show that Terasaki trays are well suited to act as a matrix for the performance of an ELISA as was shown previously (Pateraki et al., 1981; Van Soest et al., 1984; Labrousse and Avrameas, 1987). More important, this study reveals that because of the largely increased effective coating area (Horejsi and Matousek, 1985), the Terasaki-ELISA is especially useful for the determination of IgE antibodies that occur at low concentrations.

It has been claimed that up to a certain limit, a constant fraction of the proteins is adsorbed to plastic surfaces with a limit of about 1.5 ng/mm^2 for proteins such as IgM and BSA (Butler, 1981). As these data were obtained in microtitre plates having an effective coating area of around 0.1 mm^2/μl (Table I), this would imply that a maximum protein concentration of 0.2 μg/ml can be employed for coating before steric hindrance occurs. For Terasaki trays, however, the maximum protein concentration for coating is ten times larger and it was this value of 2 μg/ml that was selected for routine coating in this Terasaki-ELISA system. Moreover, this would explain the broad range of coating concentrations that can be used. This and the fact that only seldomly were prozone phenomena observed in the Terasaki-ELISA, led us to believe that a largely increased density of antigenic epitopes is available for binding on these trays compared to microtitre plates. This is in contrast to the prozone phenomenon caused by monovalent binding of antibodies to microtitre plates and observed at similar antigen concentrations (Kemp and Morgan, 1986; Vos et al., 1987).

Although we have tested relatively few batches of trays from one manufacturer, we never observed any variation in the binding capacity of different coating proteins. However, such variation has frequently been described as an edge effect with microtitre plates (Murphy et al., 1980; Shekarchi et al., 1984).

Blocking with gelatin was found to be essential after the coating. Using the same approach as that described for microtitre plates by Vogt et al. (1987) we have tested several blocking agents and found a low concentration of gelatin most efficient.

The sensitivity as well as the specificity of an ELISA assay are largely dependent upon the detecting antibody employed. As described in detail in the accompanying paper (Savelkoul et al., 1989), the specificity of the RAM/IgE antiserum employed has been tested extensively in an inhibition type Terasaki-ELISA. In addition to demonstrating that the antiserum employed was specific for IgE, it was shown that it is also free of any cross-reactivity based on anti-idiotypic, anti-allotypic or anti-light chain contamination.

Detection in this Terasaki-ELISA is based on a conjugate of β-galactosidase-labelled protein A. Protein A is especially useful in ELISA as it can behave as a purified anti-antibody of restricted specificity without species specificity (Engvall, 1978; Surolia and Pain, 1981; Langone, 1982). Such an ELISA can be used for assaying Ig without binding affinity for protein A, e.g., rat monoclonal antibodies directed against cell-surface determinants (Van Soest et al., 1984) or murine IgE (this study).

The present study showed that an incubation time of 30 min at 37°C was sufficient for all binding steps to reach binding equilibrium in this system. This, together with the higher coating efficiency of Terasaki trays, allowed determination of the affinity constants of IgE antibodies in ELISA as described in the accompanying paper.

By employing β-galactosidase-labelled conjugates and fluorimetry as a measuring procedure, the ELISA can be made quantitative to the level at which IgE antibodies occur in mouse serum. It has been claimed that fluorimetric methods offer a 1000-fold higher sensitivity than colorimetric methods (Shalev et al., 1980). In choosing a suitable combination of a fluorigenic substrate and one of the enzymes alkaline phosphatase or β-galactosidase as a label, Ishikawa and Kato (1978) and Neurath and Strick (1981) chose the latter although the β-galactosidase activity for 4-methylumbelliferyl-β-D-galactoside (MUF-G) is lower than the alkaline phosphatase activity for 4-methylumbelliferyl phosphate (MUF-P). The reason that they preferred β-galactosidase in combination with MUF-G was that MUF-P has a significantly higher fluorescence background level than MUF-G. This is probably due to non-enzymatic hydrolysis of MUF-P (Neurath and Strick, 1981).

A further necessity for quantitation in ELISA is an absolute standard for calibration of the assay. Such a standard should consist of a known amount of highly purified and intact IgE (Savelkoul et al., 1987).

In order to adapt the method for broad applicability, microprocessor-based analysis is necessary to compare essentially sigmoidal dose-response curves (when the dose is portrayed on a logarithmic scale) of standard and individual test samples. Irrespective of the type of ELISA and probably generally for ligand-binding assays, a logistic equation is applicable (Rodbard and McClean, 1977; De Lean et al., 1978; Fernandez et al., 1983). Therefore, this method has become standard for radioimmunoassays and was recently also adopted for quantitative analysis in ELISA (Rodbard and McClean, 1977; Fey, 1981; Beatty et al., 1987). The method has the advantage that the absolute concentration of IgE in a sample translates the position of the dose-response curve on the log scale. The method minimizes the influence of the affinity of the sample to the coat and for this reason the shape of the dose-response curve is not significantly different between a sample and the standard or between various samples. This Terasaki-ELISA system has a detection limit that is low enough and a linear measuring scale that is large enough to allow quantitative determination of IgE in mouse serum based upon the log-logit transformation of the data.

It is anticipated that this Terasaki-ELISA system is applicable to a range of situations in which low concentrations of protein molecules have to be quantitatively determined in small sample volumes in an accurate and reliable manner.

Acknowledgements

We thank Prof. Dr. R. Benner for continuous support and Ms. G. De Korte for preparation of the manuscript.

This study was supported by the Netherlands Asthma Foundation.

References

Baniyash, M. and Eshhar, Z. (1984) Inhibition of IgE binding to mast cells and basophils by monoclonal antibodies to murine IgE. Eur. J. Immunol. 14, 799.

Beatty, J.D., Beatty, B.G., Vlahos, W.G. and Hill, L.R. (1987) Method of analysis of non-competitive enzyme immunoassays for antibody quantification. J. Immunol. Methods 100, 161.

Bohn, A. and König, W. (1982) Generation of monoclonal DNP-specific IgM and IgE murine antibodies and the efficacy of hybridization. Mol. Immunol. 19, 193.

Bozelka, B., McCants, M.L., Salvaggio, J.E. and Lehrer, S.B. (1982) IgE suppression in anti-μ-treated mice. Immunology 46, 527.

Butler, J.E. (1981) The amplified ELISA: principles of and applications for the comparative quantitation of class and subclass antibodies and the distribution of antibodies and antigens in biochemical separates. Methods Enzymol. 73, 482.

Caulfield, M.J. and Shaffer, D. (1984) A computer program for the evaluation of ELISA data obtained using an automated microtiter plate absorbance reader. J. Immunol. Methods 74, 205.

Coffman, R.L. and Carty, J. (1986) A T cell activity that enhanced polyclonal IgE production and its inhibition by interferon-gamma. J. Immunol. 136, 949.

De Josselin De Jong, J.E., Jongkind, J.F. and Ywema, H.R. (1980) A scanning inverted microfluorimeter with electronic shutter control for automatic measurements in micro-test plates. Anal. Biochem. 102, 120.

De Lean, A., Munson, P.J. and Rodbard, D. (1978) Simultaneous analysis of families of sigmoidal curves: application to bioassay, radioligand assay, and physiological dose-response curves. Am. J. Physiol. 235, E97.

Engvall, E. (1978) Preparation of enzyme-labelled staphylococcal protein A and its use for detection of antibodies. Scand. J. Immunol. 8 (suppl. 7), 25.

Fernandez, A.A., Stevenson, G.W., Abraham, G.E. and Chiamori, N.Y. (1983) Interrelations of the various mathematical approaches to radioimmunoassay. Clin. Chem. 29, 284.

Fey, H. (1981) Use of a computer to evaluate sigmoidal curves in serology by a new procedure. J. Immunol. Methods 47, 109.

Gavériaux, C., Renard, P., Cammisuli, S. and Loor, F. (1986) A comparison of five different methods for the detection of TNP-specific mouse IgE: ELISA, ELISA on cells, rosetting, granule enzyme release assay and passive cutaneous anaphylaxis. J. Immunol. Methods 93, 107.

Giallongo, A., Kochoumian, L. and King, T.P. (1982) Enzyme and radioimmunoassays for specific murine IgE and IgG with different solid-phase immunosorbents. J. Immunol. Methods 52, 379.

Hill, P.N. and Liu, F.-T. (1981) A sensitive enzyme-linked immunosorbent assay for the quantitation of antigen-specific murine immunoglobulin E. J. Immunol. Methods 45, 51.

Horejsi, V. and Matousek, V. (1985) Equilibrium in the protein-immobilized ligand-soluble-ligand system: Estimation of dissociation constants protein-soluble-ligand complexes from binding-inhibition data. Mol. Immunol. 22, 125.

Ishikawa, E. and Kato, K. (1978) Ultrasensitive enzyme immunoassay. Scand. J. Immunol. 8 (suppl. 7), 43.

Kemp, H.A. and Morgan, M.R.A. (1986) Studies on the detrimental effects of bivalent binding in a microtitration plate ELISA and possible remedies. J. Immunol. Methods 94, 65.

Labrousse, H. and Avrameas, S. (1987) A method for the quantification of colored or fluorescent signal in enzyme immunoassays by photodensitometry. J. Immunol. Methods 103, 9.

Langone, J.J. (1982) Use of labelled protein A in quantitative immunochemical analysis of antigens and antibodies. J. Immunol. Methods 51, 3.

Maekawa, S. and Ovary, Z. (1984) Correlation of murine anti-dinitrophenyl antibody content as determined by ELISA, passive cutaneous anaphylaxis and passive hemolysis. J. Immunol. Methods 71, 229.

Malvano, R., Boniolo, A., Dovis, M. and Zannino, M. (1982) ELISA for antibody measurement: aspects related to data expression. J. Immunol. Methods 48, 51.

Murphy, B.R., Phelan, M.A., Nelson, D.L., Yarchoan, R., Tierney, E.L., Alling, D.W. and Chanock, R.M. (1981) Hemagglutinin-specific enzyme-linked immunosorbent assay for antibodies to influenza A and B viruses. J. Clin. Microbiol. 13, 554.

Neurath, A.R. and Strick, N. (1981) Enzyme-linked fluorescence immunoassays using β-galactosidase and antibodies covalently bound to polystyrene plates. J. Virol. Methods 3, 155.

Pateraki, E., Guesdon, J.-L., Serie, C. and Avrameas, S. (1981) TerELISA: the ELISA test performed in Terasaki plates. J. Immunol. Methods 46, 361.

Rodbard, D. and McClean, S.W. (1977) Automated computer analysis for enzyme-multiplied immunological techniques. Clin. Chem. 23, 112.

Sancho, J., Sánchez-Madrid, F., Felipe, O., Bernabeu, C., Morago, G. and Carreira, J. (1986) Quantitative measurement of human immunoglobulin E using monoclonal antibodies to distinct epitopes. J. Immunol. Methods 90, 71.

Savelkoul, H.F.J., Pathak, S.S. and Van der Linde-Preesman, A.A. (1987) Occurrence of damaged heavy chains during the purification of murine IgE antibodies by fast protein liquid chromatography (FPLC) and their effect on the determination of concentration and affinity in ELISA. Prot. Biol. Fluids 35, 795.

Savelkoul, H.F.J., Soeting, P.W.C., Radl, J. and Van der Linde-Preesman, A.A. (1989) Terasaki-ELISA for murine IgE-antibodies. I. Quality of the detecting antibody: production and specificity testing of antisera specific for IgE. J. Immunol. Methods 116, 265.

Shalev, A., Greenberg, A.H. and McAlpine, P.J. (1980) Detection of attograms of antigen by a high-sensitivity enzyme-

linked immunosorbent assay (HS-ELISA) using a fluorogenic substrate. J. Immunol. Methods 38, 125.

Shekarchi, I.C., Sever, J.L., Lee, Y.J., Castellano, G. and Madden, D.L. (1984) Evaluation of various plastic microtiter plates with measles, toxoplasma, and gamma globulin antigens in enzyme-linked immunosorbent assays. J. Clin. Microbiol. 19, 89.

Surolia, A. and Pain, D. (1981) Preparation of protein A-enzyme monoconjugate and its use as a reagent in enzyme immunoassays. Methods Enzymol. 73, 173.

Van Soest, P.L., De Josselin De Jong, J.E., Lansdorp, P.M. and Van Ewijk, W. (1984) An automatic fluorescence micro ELISA system for quantitative screening of hybridoma supernatants using protein A-β-galactosidase conjugate. Histochem. J. 16, 21.

Vogt, R.F., Phillips, D.L., Henderson, O., Whitfield, W. and Spierto, F.W. (1987) Quantitative differences among various proteins as blocking agents for ELISA microtiter plates. J. Immunol. Methods 101, 43.

Vos, Q., Klasen, E.A. and Haaijman, J.J. (1987) The effect of divalent and univalent binding on antibody titration curves in solid-phase ELISA. J. Immunol. Methods 103, 47.

CHAPTER 2.3

Journal of Immunological Methods, 123 (1989) 71–81
Elsevier

JIM 05302

Terasaki-ELISA for murine IgE

III. Determination of concentration and functional affinity by sequential equilibrium binding analysis

S.S. Pathak, Q. Vos and H.F.J. Savelkoul

Department of Immunology, Erasmus University, Rotterdam, The Netherlands

(Received 11 July 1988, revised received 3 April 1989, accepted 22 May 1989)

A simple Terasaki tray-based ELISA technique with a fluorescent detecting system has been used to determine the affinity of murine IgE antibodies. The system was shown to be sensitive enough to measure affinities in the range of 10^{-6}–10^{-10} M as well as detect IgE antibodies down to a limit of 0.1 ng/ml. The results, expressed as arbitrary fluorescence units (AFU), were compared with those obtained using equilibrium dialysis for several DNP-specific IgE monoclonal antibodies of known affinities yielding K_D values. The relationship between K_{AFU} and K_D established a conversion factor which could then be used to compute K_D from K_{AFU}, provided the detection system remained identical. Based on the equations proposed, an alternative method for the quantitation of murine IgE is described which is independent of the affinity of IgE for the coated antigen.

Key words: Terasaki-ELISA; Sequential equilibrium binding analysis; Affinity; Quantitation

Introduction

Antibody affinity is of crucial importance in the performance of immunoassays. Enzyme-linked immunosorbent assays (ELISA) are generally thought to be too insensitive to detect antibodies of very low affinity (Steward and Lew, 1985). The affinity of an antibody is determined at a state of equilibrium and is expressed as a binding constant. This binding constant (K) is a measure of the strength of the interaction between antigen and antibody, and is a suitable parameter for the specificity of the antibody (Metzger et al., 1984). It therefore directly influences the detection limit of an immunoassay, i.e., the ability to distinguish a low analyte concentration as being statistically different from background.

Several techniques are available for the determination of affinity. Most of these utilize the mathematical theory of Feldman (1972) as a generalization of that of Scatchard (1949). This theory characterizes the equilibrium composition of a multicomponent cross-reactive ligand-binding system by solving the mass action equations. It therefore requires the measurement of bound and free antigen (or antibody) concentrations and the determination of their ratios over a range of antigen (or antibody) concentrations. Equilibrium dialysis

Correspondence to: H.F.J. Savelkoul, Department of Immunology, Erasmus University, P.O. Box 1738, 3000 DR Rotterdam, The Netherlands.

Abbreviations: ELISA, enzyme-linked immunosorbent assay; AFU, arbitrary fluorescence units; MUF-G, methylumbelliferyl-β-galactopyranoside; MUF, methylumbelliferone; IgE, immunoglobulin E; mAb, monoclonal antibody; RAM/IgE, rabbit-anti-mouse-IgE antiserum; OA, ovalbumin; cpm, counts per minute.

is considered to be the most unequivocal of these methods, although it can only be used to determine the affinity of antibodies to small haptens (Steward and Steensgaard, 1983).

Many studies have been conducted on the effect of antibody affinity on ELISA measurements (Lehtonen and Eerola, 1982; Lew, 1984; Nimmo et al., 1984; Steward and Lew, 1985). Competitive ELISA techniques were among the first to use differing input concentrations in the coating solution (Nieto et al., 1984; Beatty et al., 1987). In general non-competitive ELISA have been used for quantitation and avidity determinations are also possible without the need to label the antibodies. However, these techniques require relatively large concentrations of antigen (Lehtonen and Viljanen, 1982; Matikainen and Lehtonen, 1984; Friguet et al., 1985). Alternatively, binding constants may also be estimated from adsorption measurements (Li, 1985).

For the determination of IgE antibodies in ELISA it is common practice to employ sandwich systems because of their increased sensitivity compared to direct ELISA systems (Savelkoul et al., 1989b). We propose that it should be possible to use a simple Terasaki tray-based ELISA technique (Savelkoul et al., 1989a,b) to determine the affinity of murine IgE antibodies without prior purification and even when present in minute quantities as in normal serum. An apparent equilibrium constant (K_{AFU}) was meausred by using the data in two different formulae derived from the Law of Mass Action (see appendix).

Materials and methods

Mice

C57BL/6, DBA/2 and B6D2F1 mice were obtained from Bomholtgard (Ry, Denmark). A/J mice were purchased from Olac (Bicester, Oxon., U.K.). Groups of female mice ($n = 6$–10), 6–12 months old, were used for serum collection. Serum samples were collected and stored at −20°C. Before use, the samples were spun in a microfuge.

Reagents

Monoclonal anti-DNP IgE antibodies (mAb) (clone IgE 53.169) and anti-ovalbumin IgE (clone IgE 14-205) (Böttcher and Hammerling, 1978) were obtained from Sera Lab (Crowly Down, Sussex, U.K.). Anti-TNP IgE IGEL b4 14.2, b4 1, a4 6.3, a4 6.5 (Rudolph et al., 1981) were a kind gift from Dr. M.R. Wabl (San Francisco, CA, U.S.A.). Anti-DNP IgE HI-ε-26 (Liu et al., 1980) was kindly provided by Dr. S.B. Lehrer (New Orleans, LA). Anti-DNP IgE B53/A4 (Böttcher et al., 1980) and rat-anti-mouse IgE EM95 (Baniyash and Eshhar, 1984) were kindly donated by Dr. R.L. Coffman (Palo Alto, CA) and Dr. Z. Eshhar (Israel), respectively.

The samples used were either crude supernatants, ascitic fluids or purified IgE as indicated in the results section. Purification was performed as previously described (Savelkoul et al., 1987).

A conjugate of sheep anti-rabbit-β-galactosidase (ShAR-β-gal) was obtained from MIAB Laboratories (Uppsala, Sweden). Bovine serum albumin (type V, Sigma Chemicals, St. Louis, MO) was dinitrophenylated to a level of 27 DNP molecules (DNP27-BSA) per protein molecule (as determined spectrophotometrically) using dinitrobenzenesulfonic acid (Eastman Kodak Co., Rochester, NY) as described (Koch et al., 1981). Fraction VII ovalbumin (OA) was obtained from Sigma Chemicals. 2,4-[3,5-^{3}H]dinitrofluorobenzene was obtained from NEN Research Products (NET 363, Dreieich, F.R.G.).

Terasaki-ELISA

The Terasaki-ELISA was performed as described by Savelkoul et al. (1989b). Clear 60-well Terasaki trays were coated overnight at 4°C with 2 μg/ml of DNP27-BSA, OA or the capture mAb rat anti-mouse IgE EM95 (Baniyash and Eshhar, 1984) in 0.05 M phosphate-buffered saline, pH 7.2 (PBS). Plates were blocked with PBS containing 0.05% Tween 20 (Sigma) and 0.02% gelatin (UCB, Brussels, Belgium) for 30 min at 37°C. The same buffer was also used to wash the plates between each incubation step. Next, 5 μl replicates of serial dilutions of the sample were added to the plates. Plates were incubated in a humidified atmosphere for 30 min since it has been shown previously that this time is sufficient to establish binding equilibrium in these plates (Savelkoul et al., 1989b). Subsequently, the plates were treated with the detecting antibody RAM/IgE diluted optimally

(1/200) and the conjugate ShAR-β-gal, diluted 1/1000 in PBS containing 10 mM $MgCl_2 \cdot 6H_2O$ and 0.02% Tween. The fluorigenic substrate 4-methylumbelliferyl-β-galactopyranoside (MUF-G, Sigma) was added to the wells and the plates were incubated at 37°C for precisely 60 min. The reaction was terminated by adding 1 M Na_2CO_3 stop buffer, pH 10.4. The resulting fluorescence was measured in an automated microfluorimeter (Leitz, Wetzlar, F.R.G.). The data obtained were subsequently presented as mean arbitrary fluorescence units (AFU). Controls for non-specific binding of reagents to the coat (negative control) and non-specific substrate reactions (background) were also included.

The detecting antibody used was a polyclonal RAM/IgE antiserum (2 mg purified IgG fraction/ml). It was prepared, purified and tested for its affinity as previously described (Savelkoul et al., 1989a). Moreover, the monospecificity of the antiserum was assessed in immunoblotting and in inhibition ELISA employing purified hybridoma and myeloma proteins of IgE as well as other (sub)classes, including both heavy and light chains.

Binding analysis and determination of K_{AFU}

The Terasaki-ELISA as described above was adapted for affinity determinations. Following the first incubation with the sample, the liquid in the wells was carefully removed with an automatic replicator (Biotec, Basel, Switzerland) and transferred to a fresh plate that had been previously identically coated and blocked for non-specific interactions. The second plate was then incubated at 37°C for 30 min to allow the equilibrium to be reached once again. Sequential transfers were performed a number of times to establish the validity of appendix equation 9. The plates were further treated with the developing reagents identically as described above. The fluorescence developed (AFU value) in the first plate was a direct measure of the paratopes that had complexed with the epitopes, i.e., x_1 of equation 8 (see appendix). The sum of x_2 (AFU value in the second plate) + x_3 (AFU value of the third plate) + ...x_n (AFU value in the n^{th} plate) gave the Σx_2 value of equation 8 for every dilution of the IgE containing sample tested.

Equilibrium dialysis

Equilibrium dialysis was performed essentially as described by Fazekas de St. Groth (1979) and Lehtonen and Eerola (1982). Briefly, 1 ml screw-capped tubes (Nunc, Roskilde, Denmark) were used as dialysis chambers. These were treated overnight with PBS-Tw-Gel containing 0.1 M sodium azide (NaN_3) to reduce non-specific binding and to prevent microbial growth. The tubes were then shaken dry and 1.3 ml of a range of various concentrations of the labeled hapten dinitrofluorobenzene in PBS-NaN_3 was added to them. 200 μl of various concentrations of DNP-specific IgE (B53/A4) diluted in PBS-NaN_3 were added to the lids. They were then covered with a double layer of the dialysis membrane (cut-off 6–8 kDa, BRL, Bethesda, MD) and closed tightly, taking care to exclude air from the reaction chambers. The tubes were then sealed carefully and incubated at 37°C with intermittent shaking for 48 h. The liquid in the chambers was then checked for volume and 50 μl of the liquid from both of the compartments were transferred to 20 ml Instagel (Packard, IL, U.S.A.), shaken and the cpm measured in a liquid scintillation counter (Tricarb, Model 1500, Packard, IL, U.S.A.). A plot of the ratio of bound (x) to free hapten ($E - x$) versus the bound hapten (x) was then constructed and the K_D of the antibody was calculated from the slope of the curve. Considering E total antigenic epitopes and n paratopes per antibody molecule ($P = nA$), the equilibrium equation used was:

$$\frac{(E - x)(nA - x)}{x} = K$$

(Fazekas de St. Groth, 1979).

Results

Determination of K_{AFU}

Based on equations 7 and 8 of the appendix, we determined in sequential binding steps the affinity of a monoclonal anti-DNP IgE (B53/A4) for DNP-BSA. It was observed that the signal reached a plateau in the first few dilutions of the IgE on the first plate (Table I). The x_1 and x_2 values were almost equal at the highest input concentra-

TABLE I

RESULTS OF SEQUENTIAL BINDING ANALYSIS OF A MONOCLONAL IgE ON DNP-BSA COATED TERASAKI PLATES

Sample dilution [a]	Arbitrary fluorescence units (AFU) [b]			
	x_1	x_2	x_3	Σx_2
1/2	17210	16962	12753	43503
1/4	17621	15065	9357	28422
1/8	17663	14296	8411	26213
1/16	16490	11781	5890	19671
1/32	14639	8890	3720	12590
1/64	11248	5463	1910	7373
1/128	9825	4390	–	4390
1/256	6333	2226	–	2226

[a] Dilutions of the sample were added to the coated and blocked plate and incubated at 37° C for 30 min. The sample was then carefully removed and added to a second identically coated and blocked plate. The sequential transfers were continued until the AFU in the highest IgE input reached the level of the negative control. The AFU value in the first plate was x_1, in the second one x_2, in the third x_3...etc. The summation of x_2, $x_3 \ldots x_n$ gave Σx_2.

[b] All figures were corrected for background and non-specific fluorescence.

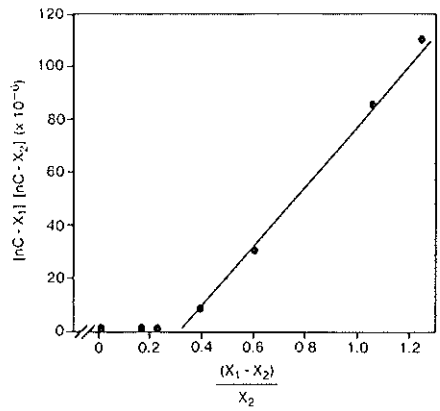

Fig. 1. Determination of K_{AFU} based upon approximation of nC. Dilutions of anti-DNP IgE B53/A4 were added to DNP-BSA coated trays. Following the first incubation, the sample was removed, added to a second identically coated tray and reincubated. The signal obtained in the first tray was x_1 (AFU) and that obtained in the second was x_2. The AFU value of the plateau region of the dilution curve gave the approximate value of nC. A plot of $(nC - x_1)(nC - x_2)$ $(\times 10^{-6})$ vs. $(x_1 - x_2)/x_2$ was then constructed.

tion. The x_1 value remained on the same plateau over a range of sample dilutions whereas x_2 was already decreasing within this range. This suggested that nC, the concentration of antigenic sites available in the wells, was limiting at these input concentrations of IgE and x_1 tending towards nC. This gave the approximate value of nC in AFU. Using this value of nC, a plot of $(nC - x_1)(nC - x_2)$ vs. $(x_1 - x_2)/x_2$ was constructed (Fig. 1). The slope of this graph is $K_{AFU} * nC$ as outlined in appendix equation 7. The K_{AFU} obtained was 4.2×10^3.

If a plateau is not reached at the highest input concentration of the IgE, the value of nC cannot be estimated and equation 7 is inapplicable. In order to apply equation 8, a series of equilibria between the mAb IgE (B53/A4) and the DNP-BSA coat was established to meet the condition $(P_1 - x_1) = x_2 + x_3 \ldots + x_n$ of equation 7a. The plot of x_1 vs. $x_1/\Sigma x_2$ was then constructed (Fig. 2). The inverse of the slope of this graph yielded a K_{AFU} of 4.5×10^3.

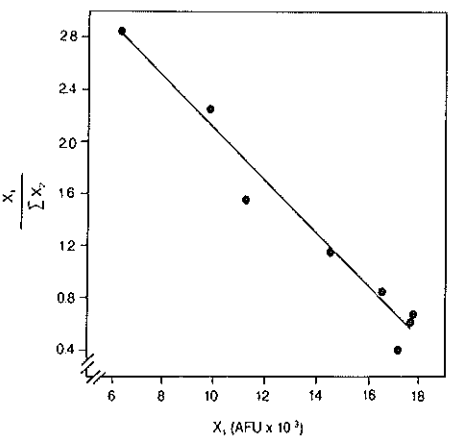

Fig. 2. Determination of K_{AFU} without the use of nC. Sequential equilibria were established between DNP-BSA (coat) and the IgE sample. The AFU obtained in the first plate was x_1. The summation of AFU for the remaining plates was Σx_2. A plot of $x_1/\Sigma x_2$ vs. x_1 was then constructed. The inverse of the slope of this graph gave the K_{AFU}.

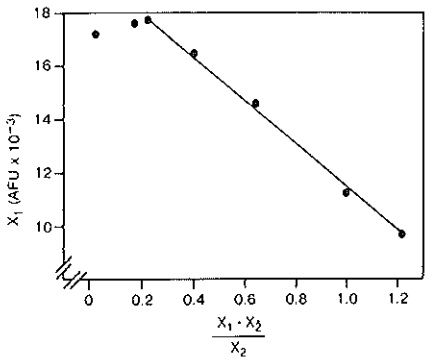

Fig. 3. Sequential equilibria for the prediction of Σx_2. The x_1 and x_2 values were determined as outlined in the legend to Fig. 1. A plot of x_1 vs. $(x_1 - x_2)/x_2$ was then constructed. Such plots were used to predict the values of x_3, $x_4 \ldots x_n$.

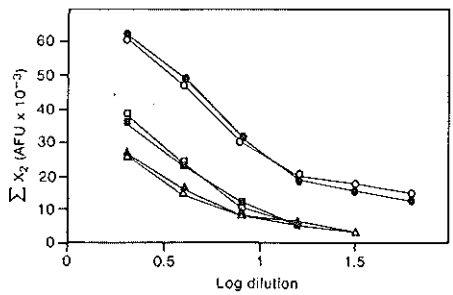

Fig. 4. Comparison of actual and predicted Σx_2 values. Sequential equilibria were established between IgE samples and the coat. A summation of AFU values of plates 2, 3, 4... n, gave the experimental Σx_2 (closed symbols). The AFU values of the first and the second plates were inserted in equation 9 to arrive at the predicted Σx_2 values (open symbols). A plot of Σx_2 vs. log dilution was then constructed. The IgE samples were mAb IGEL b4 1 on a DNP-BSA coat (▲, △), normal serum from A/J mice on EM95 coat (■, □), and anti-ovalbumin IgE (clone IgE 14-205) on EM95 coat (●, ○).

Determination of Σx_2

As an alternative to the series of sequential equilibria required for equation 8, the empirical equation 9 may be used to obtain the x_2 value. The AFU values obtained after the first and the second incubations, x_1 and x_2, were used to construct a plot of x_1 vs. $(x_1 - x_2)/x_2$. Fig. 3 shows a typical result of this analysis for the mAb B53/A4. Such plots were used to predict the x_3, $x_4, \ldots, x_n$ values for equation 8. Plotting the log of dilution of the samples against these predicted and experimentally determined values of Σx_2 shows the close agreement between these values (Fig. 4). Similar results were obtained with other mAb: anti-TNP IgE (IGEL a4 6.5, b4 14.2), anti-OA IgE (14-205), anti-DNP IgE (53.169) as well as with polyclonal IgE antibodies (sera of DBA/2 and B6D2F1 mice) on various different coats (mAb anti-IgE EM95, DNP-BSA and OA). These results established the applicability of the equation (data not shown).

Determination of K_{AFU} of a different IgE mAb

The K_{AFU} values of the complete panel of six mAb anti-DNP IgE were then computed by determining the x_1 and x_2 values of these monoclonals on a DNP-BSA coat. The data were fitted in equations 7, 8 and 9. Table II lists the K_{AFU} values obtained.

Applicability

The method was also used to determine the equilibrium constant of a reaction involving two immunoglobulins. Plates were coated with 2 μg/ml of EM95. They were charged with various mono-

TABLE II

K_{AFU} AND K_D OF A PANEL OF ANTI-DNP IgE FOR DNP-BSA AT 37°C AS DETERMINED IN TERASAKI-ELISA

Monoclonal IgE	Nature	K_{AFU} [a]		K_D [b]
		per equation 7	per equation 8	
IGEL b4 1	Supernatant	3.3×10^{3}	3.6×10^{3}	6.9×10^{-9}
IGEL b4 14.2	Ascites	ND [c]	7.5×10^{3}	1.5×10^{-8}
IGEL a4 6.5	Supernatant	3.2×10^{3}	3.5×10^{3}	6.7×10^{-9}
IGEL a4 6.3	Supernatant	ND	2.0×10^{3}	4.0×10^{-9}
Clone 53.169	Purified	ND	2.2×10^{4}	4.4×10^{-8}
HI-ε-26	Purified	1.4×10^{4}	1.6×10^{4}	3.0×10^{-8}

[a] All K_{AFU} values are an average of three readings obtained on three separate occasions.

[b] K_D is equal to K_{AFU} * conversion factor (2×10^{-12}), has the dimensions of mol/l and is an average of the two K_{AFU} values wherever applicable.

[c] Not determined.

TABLE III

K_{AFU} AND K_D OF IgE FOR THE MONOCLONAL ANTI-IgE ANTIBODY EM95 AT 37°C AS DETERMINED IN TERASAKI-ELISA

Sample	Nature	K_{AFU} [a]	K_D [a,b]
IgE B53/A4	Purified	2.9×10^{3}	5.8×10^{-9}
IGEL a4 6.5	Supernatant	4.0×10^{3}	8.0×10^{-9}
IGEL b4 1	Supernatant	3.0×10^{4}	6.0×10^{-9}
C57BL/6	Serum	6.2×10^{4}	1.2×10^{-7}
DBA/2	Serum	1.3×10^{4}	2.6×10^{-8}
B6D2F1	Serum	2.5×10^{4}	5.0×10^{-8}
A/J	Serum	1.0×10^{4}	2.0×10^{-8}

[a] All values are an average of three readings obtained in three independent experiments.

[b] K_D is equal to K_{AFU} • conversion factor (2×10^{-12}) and has the dimensions of mol/l.

clonal and polyclonal samples. The x_1 and x_2 values obtained after developing the plates were then used in equations 7, 8 and 9. Table III lists the K_{AFU} values obtained. In general polyclonal IgE had a lower affinity for EM 95 than the monoclonals tested. The monoclonal IgE tested had an affinity in the range of 10^{-9} M.

Effect of various coat concentrations on K_{AFU}

Essentially similar results were obtained when analyzing the effect of various inputs of the antigen and antibody in the coating solutions. The shape of the dilution curve, the plateau reached, and the K_{AFU} were not significantly affected by the input concentration in the coating solutions over the range of concentrations investigated (data not shown). The K_{AFU} values for these different coating concentrations were found to be 3.6×10^{3}, 4.3×10^{3}, 4×10^{3}, at input concentrations of 0.5, 2, and 8 μg/ml of DNP-BSA, respectively.

Equilibrium dialysis

A Scatchard plot of the experimental data (data not shown) gave a K_D value of 8.6×10^{-9} M for the mAb IgE B53/A4. This value was used to

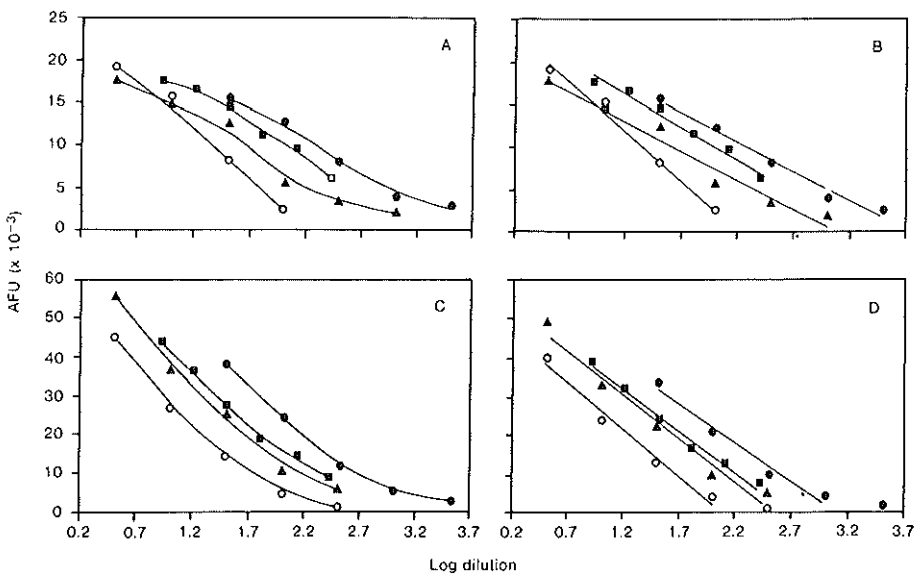

Fig. 5. Comparison between x_1 (AFU on the first plate) and Σx (total AFU) generated for the quantitation of IgE samples. The AFU generated on the first plate were plotted against the log of dilution as a curve (*A*) and in the linearly regressed form (*B*). The total AFU generated ($x_1 + x_2 + \ldots + x_n$) were similarly plotted in *5C* and *5D*, respectively. The IgE samples used were mAb B53/A4 on the DNP27-BSA (○) and EM95 coat (■), normal serum from DBA/2 mice on the EM95 coat (△), and anti-ovalbumin IgE (clone 14-205) on the ovalbumin coat (●).

calculate the conversion factor required to establish the relationship between K_D (in mol/l) and K_{AFU} (in AFU). The conversion factor was 2×10^{-12}. Tables II and III list the K_D values of mAbs and polyclonals calculated on the basis of this conversion factor. Equilibrium dialysis was also performed on a sample of the anti-DNP HI-ε-26 IgE hybridoma. A K_D value of 7.3×10^{-9} M was obtained which resulted in a similar conversion factor (data not shown).

Quantitation

The appendix equation 7a can be used to obtain the total AFU generated by the original concentration of the Ig [P] added to the wells. This value – Σx – can therefore be used in quantitation of the Ig independent of the affinity for the coat. Figs. 5*A*–5*D* are plots of log dilution vs. either AFU obtained in the first plate, i.e., x_1 (Figs. 5*A* and 5*B*) or Σx i.e., $x_1 + \Sigma x_2$, the total AFU values (Figs. 5*C* and 5*D*). The parallellism observed in Figs. 5*C* and 5*D* indicates that the system measured the total AFU for a given IgE, independent of the affinity for the coat. The lines in the linearly regressed plot shown in Fig. 5*D* have similar slopes which permit the determination of IgE concentration. The absolute concentration of IgE in the DBA/2 mouse serum (Fig. 5*D*) on the EM95 coat was calculated on the basis of the IgE standard (B53/A4) and was found to be 1.08 μg/ml.

TABLE IV

INDEX OF AFFINITY OF IgE FOR VARIOUS COATS

Sample	Nature	Index of affinity [a]	
		EM 95 coat	DNP-BSA coat
DBA/2	Serum	3.95, 3.4, > 4, 3.6	ND [b]
IGEL b4 1	Supernatant	2.05, > 4, 2.7, 0.75	2.375, > 4.325
IgE B53/A4 anti-OVA	Purified	0.4, > 4	2.9, 0.5, 1.6
IgE [c]	Supernatant	3.15, 3.6, 2.12, > 4	ND

[a] The figures indicate results obtained on different days.
[b] Not determined.
[c] Anti-OVA IgE, clone IgE 14-205.

Discussion

Antibody affinity measurement may be influenced by immunoassay methodology. It is therefore important to determine this parameter under the conditions of the assay used. The sequential equilibrium binding analysis in Terasaki-ELISA necessitated the setting up of a series of binding equilibria between the antigen and the antibody and determining the concentrations (in AFU) of the complexes formed. In the plateau region of the dilution curve (at the highest input concentration of IgE), the value of x_1 was sometimes lower than at lower IgE concentrations (the steep part of the dilution curve). In this region, x_2 may also be greater than x_1. This may be due to the plateau region of the dilution curve being the antibody excess zone with only one antibody binding site complexed with the antigen (Vos et al., 1987). Alternatively, due to steric hindrance, detecting reagents cannot bind or bind weakly to the IgE, leading to a deviation from linearity in the dose-response curve on the first plate (Butler et al., 1986).

The nature of ELISA determines that in every sequential incubation more ligand binds to the coat nonspecifically than specifically (Butler, 1988). The washing procedure, however, ensures that the nonspecifically bound ligand is not detected. Moreover, as in every ELISA only that proportion of the total antibody population present is detected which is able to bind under the particular assay conditions. For this reason, Σx_2 is generally much smaller than the total antibody concentration applied. From the data presented in Table I it is clear that the ratio $\Sigma x_2/x_1$ decreases linearly with the concentration of x_1, indicating that with regard to the detectable specific antibody binding the assumption $P_2 = P_1 - x_1$ (appendix equation 3) is valid.

It has been described that the upper plateau in ELISA dilution curves is more dependent on antibody affinity than concentration, with high-affinity antibodies reaching higher plateau values than antibodies of lower affinity (Butler, 1988). Therefore, this plateau value would not be a useful estimate for *nC*. However, IgE antibodies, whether mono- or polyclonal, generally tend to be of relatively high affinity (Liu et al., 1980; Prahl and

Nexo, 1982). Moreover, employing both Terasaki trays with a high effective coating area (Savelkoul et al., 1989b) and high epitope density hapten-carrier proteins establish conditions for bivalent binding, provided that no prozone phenomena occur (Vos et al., 1987). These conditions were found to be responsible for losing differential upper plateau levels when employing mAb of identical isotype, differing 100-fold in their affinity for the same antigen (Lew, 1984; Nimmo et al., 1984). These considerations and the fact that markedly different upper plateau levels were not observed in the dilution curves of IgE Terasaki-ELISA (Savelkoul et al., 1989b), validated the assumption that the intercept of the plot of x_1 vs. $x_1/\Sigma x_2$ can be used to estimate the value of nC.

When the concentration of the antibody is not high enough, an estimate of nC cannot be made on the basis of the data available. Appendix equation 8 is then again used. This makes it necessary to determine (in AFU) the amount of paratope that remains unreacted at each successive equilibrium, until the value reaches that of the negative control, i.e., the detection limit of the system. The values of x_3, $x_4 \ldots x_n$ can either be determined practically or predicted using the empirical equation 9. In Fig. 3 the close agreement of these values determined in both ways is demonstrated.

The K_{AFU} values obtained have to be further converted to the dimensions of mol/l (K_D) using a conversion factor. This factor (2×10^{-12}) was determined by equilibrium dialysis on an IgE sample (B53/A4). The K_D value obtained was 8.6×10^{-9} M at 37°C, which was in close agreement with the 3.3×10^{-9} M at 37°C established by RIA (Hirayama et al., 1982). The conversion factor was found to be dependent on the detecting and measuring system used and will be unique for a particular assay design. The K_D values of another IgE sample (anti-DNP IgE HI-ε-264 IgE) for its hapten was found, using equilibrium dialysis and this conversion factor, to be also in close agreement with its reported value (Liu et al., 1980). Using this procedure the K_D value of the reaction between various mAb IgE samples and the mAb anti-IgE EM95 were determined. The values obtained were again found to fall within the range reported (Baniyash and Eshhar, 1984). Using the conversion factor the method was capable of determining K_D values in the region of 10^{-9} M, the range within which human and murine IgE antibodies often fall (Liu et al., 1980; Prahl and Nexo, 1982).

Equation 7a also contains useful information for the quantitation of [P], independent of the affinity of the paratope for the epitope. A semilogarithmic plot of log dilution against the response obtained in the first plate (x_1 of equation 2) in an ELISA results in a sigmoid curve and is concentration as well as affinity dependent. Within limits, logistic transformation can be used for concentration determination as this reduces the effect of the affinity of the antibody for the coat by taking into account only the slope of the dilution curve. Again, using Terasaki trays and high epitope density hapten-carrier proteins different upper plateau levels are not markedly present (Butler, 1988; Savelkoul et al., 1989b).

As shown in Figs. 5*C* and 5*D*, this method is independent of the influence of the coat and applicable in both monoclonal and polyclonal situations for the determination of IgE concentration, since the slope of the graph depends on the affinity of the detecting reagents only. By carefully selecting these detecting reagents for a sufficiently high affinity and specificity, the slope of the graph remains similar for different antibody populations (Savelkoul et al., 1989b). The method presented here will therefore have more general applicability for the determination of affinity constants and concentrations of rare serum antibodies, such as IgE.

Appendix

The quantitative relationship of the interaction between antigen and antibody at equilibrium is governed by the Law of Mass Action. This can be represented in various forms, one of them being (Fazekas de St. Groth, 1979)

$$\frac{[nC-x][P-x]}{[x]} = K_D \qquad (1)$$

where [C] = original concentration of antigen molecules with n epitopes/molecule; [P] = original

concentration of paratopes; [x] = concentration of complex formed at equilibrium; and K_D = equilibrium constant. All the concentrations are expressed in mol/l. K_D has the dimension of mol/l. Thus, when [nC] is constant, but [P] varies, we arrive at,

$$\frac{[nC-x_1][P_1-x_1]}{[x_1]} = \frac{[nC-x_2][P_2-x_2]}{[x_2]} = K_D \qquad (2)$$

where $[x_1]$, $[x_2]$ = the concentrations of complexes formed at $[P_1]$ and $[P_2]$ concentrations of the paratopes, respectively.

Imposing the condition that $[P_2] = [P_1 - x_1]$, equation (2) can be rewritten as

$$\frac{[nC-x_1][P_1-x_1]}{[x_1]} = \frac{[nC-x_2][P_1-x_1-x_2]}{[x_2]} = K_D \qquad (3)$$

or,

$$[P_1-x_1] = \frac{K_D * [x_1]}{[nC-x_1]} \qquad (4)$$

and

$$[P_1-x_1-x_2] = \frac{K_D * [x_2]}{[nC-x_2]} \qquad (5)$$

Subtracting equation (5) from equation (4) results in:

$$[x_2] = \frac{K_D * [x_1]}{[nC-x_1]} - \frac{K_D * [x_2]}{[nC-x_2]} \qquad (6)$$

or,

$$[nC-x_1][nC-x_2] = K_D * nC\frac{[x_1-x_2]}{[x_2]} \qquad (7)$$

This equation can be employed in practice within certain limits. Though theoretically [nC] will never be equal to $[x_1]$, practically [nC] tends towards $[x_1]$ when [nC] is limiting and $[x_1]$ and/or $[x_2]$ tend to zero at the upper and the lower plateaus of the dilution curve, respectively. Thus there is a suitable range within which this equation can be used. Also, reconsidering equation 2, and extending the condition

$[P_1-x_1] = [P_2]$,

$[P_2-x_2] = [P_3]$,

$[P_3-x_3] = [P_4] \ldots [P_n]$

where $[x_n] \to 0$, we arrive at

$$[P_1-x_1] = [x_2]+[x_3]+\ldots[x_n] \qquad (7a)$$

$[x_2]$, $[x_3], \ldots [x_n]$ being the concentrations of the complexes formed at successive equilibrium steps, with the original concentration of paratopes, $[P_1]$. The total concentration of epitopes [nC] is being kept constant at each step. Therefore equation 2 can be rewritten as,

$$\frac{[nC-x_1][x_2+x_3+\ldots]}{[x_1]} = K_D$$

or,

$$\frac{[nC]}{K_d} - \frac{[x_1]}{K_D} = \frac{[x_1]}{[x_2+x_3+\ldots]} = \frac{[x_1]}{[\Sigma x_2]} \qquad (8)$$

Both equations 7 and 8 give a straight line in the range under consideration. They can be used to determine the value of K_D. Thus the slope of the plot of $(nC-x_1)(nC-x_2)$ vs. $(x_1-x_2)/x_2$ will be $nC * K_D$. The inverse of the slope of the plot of $x_1/\Sigma x_2$ vs. x_1 will give the K_D. The intercept on the y axis can be used to arrive at the value of nC. The first condition of equation 2 can be met in an ELISA by transferring the liquid in the wells after equilibrium has been reached to a fresh plate, previously coated and blocked as in the initial case and incubating the second plate until equilibrium is once again established. The process can be repeated a number of times to get the values required for equation 8. However, in the repeated transferring of the sample the systematic error in the measurement will be amplified and the loss of minute amounts of the sample (from an original 5 μl sample) in each successive transfer will further distort the signal obtained. We therefore suggest the use of an empirical equation that can be used to predict the values of x_3, $x_4, \ldots$ etc., once the values of x_1 and x_2 have been

established. This equation is of the form $y = mx + c$

$$x_1 = m * \frac{(x_1 - x_2)}{x_2} + c \qquad (9)$$

All the variables in equations 8 and 9 are expressed in terms of arbitrary fluorescence units (AFU). The K_{AFU} value so determined therefore will also be in these terms and a conversion factor will have to be determined to arrive at a K_D in mol/l using mAb with predetermined affinity constants for their haptens based upon equilibrium dialysis.

A number of assumptions have to be made when applying the above equations to ELISA.

(1) The binding of antibody to the antigen coat is governed by the Law of Mass Action.

(2) The reaction reaches an equilibrium.

(3) The antigenic epitopes remain essentially unaltered after adsorption to the solid phase, so that the behavior of the paratopes and therefore the K_D remains unaffected.

(4) The epitopes bound to the solid phase behave independently of each other and there is no cooperation between the two identical binding sites of the antibody.

(5) The coating of the solid phase is uniform, i.e., the average number of epitopes that can react with the paratopes/well is the same for a given antigenic input in the coating solution.

Acknowledgements

We thank Prof. R. Benner for his continuous support and Ms. G. De Korte for typing the manuscript.

This study was supported by the Netherlands Asthma Foundation.

References

Baniyash, M. and Eshhar, Z. (1984) Inhibition of IgE binding to mast cells and basophils by monoclonal antibodies to murine IgE. Eur. J. Immunol. 14, 799.

Beatty, D.J., Beatty, B.G. and Vlahos, W.G. (1987) Measurement of monoclonal antibody affinity by non-competitive enzyme immunoassay. J. Immunol. Methods 100, 173.

Böttcher, I. and Hammerling, G. (1978) Continuous production of monoclonal mouse IgE antibodies with known allergenic specificity by a hybrid cell line. Nature 275, 761.

Böttcher, I., Ulrich, M., Hirayama, N. and Ovary, Z. (1980) Production of monoclonal mouse IgE antibodies with DNP specificity by hybrid cell lines. Int. Arch. Allergy Appl. Immunol. 61, 248.

Butler, J.E. (1988) The amplified ELISA (a-ELISA): Immunochemistry and applications. In: D.M. Kemeny and S.J. Challacombe (Eds.), ELISA and Other Solid Phase Immunoassays. Wiley, London, p. 107.

Butler, J.E., Spradling, J.E., Suter, M., Dierks, S.E., Heyerman, H. and Peterman, J.H. (1986) The immunochemistry of sandwich ELISAs. I. The binding characteristics of immunoglobulins to monoclonal and polyclonal capture antibodies adsorbed on plastic and their detection by symmetrical and asymmetrical antibody-enzyme conjugates. Mol. Immunol. 23, 971.

Fazekas de St. Groth, S. (1979) The quality of antibodies and cellular receptors. In: I. Lefkovits and B. Pernis (Eds.), Immunological Methods, Vol. 1. Academic Press, New York, p. 1.

Feldman, H.A. (1972) Mathematical theory of complex ligand binding systems at equilibrium. Some methods for parameter fitting. Anal. Biochem. 48, 317.

Friguet, B., Chaffote, A.F., Lisa, D.-O. and Goldberg, M.E. (1985) Measurements of true affinity constant in solution of antigen-antibody complexes by enzyme-linked immunosorbent assay. J. Immunol. Methods 77, 305.

Hirayama, N., Hirano, T., Köler, G., Kurata, A., Okumura, K. and Ovary, Z. (1982) Biological activities of antitrinitrophenyl and antidinitrophenyl mouse monoclonal antibodies. Proc. Natl. Acad. Sci. U.S.A. 79, 613.

Koch, G., Osmond, D.G., Julius, M.H. and Benner, R. (1981) The mechanism of thymus-dependent antibody formation in bone marrow. J. Immunol. 126, 1447.

Lehtonen, O.P. and Eerola, E. (1982) The effect of different antibody affinities on ELISA absorbance and titer. J. Immunol. Methods 54, 233.

Lehtonen, O.P. and Viljanen, M.K. (1982) A binding function for curvefitting in enzyme-linked immunosorbent assay (ELISA) and its use in estimating the amounts of total and high affinity antibodies. Int. J. Bio-Med. Comput. 13, 471.

Lew, A.M. (1984) The effect of epitope density and antibody affinity on the ELISA as analysed by monoclonal antibodies. J. Immunol. Methods 72, 171.

Li, C.K.N. (1985) ELISA-based determination of immunological binding constants. Mol. Immunol. 22, 321.

Liu, F.-T., Bohn, J.W., Ferry, E.L., Yamamoto, H., Molinaro, C.A., Sherman, L.A., Klinman, N.R. and Katz, D.H. (1980) Monoclonal dinitrophenyl-specific murine IgE antibody: Preparation, isolation and characterization. J. Immunol. 124, 2728.

Matikainen, M.-T. and Lehtonen, O.-P. (1984) Relation between avidity and specificity of monoclonal anti-chlamydial antibodies in culture supernatants and ascitic fluids determined by enzyme immunoassay. J. Immunol. Methods 72, 341.

Metzger., D.W., Chong, L.-K., Miller, A. and Sercarz, E.E. (1984) The expressed lysozyme-specific B cell repertoire. I. Heterogeneity in the monoclonal anti-hen egg white lysozyme specificity repertoire, and its difference from the in situ repertoire. Eur. J. Immunol. 14, 87.

Nieto, A., Gaya, A., Jansa, M., Moreno, C. and Vives, J. (1984) Direct measurement of antibody affinity distribution by hapten-inhibition enzyme immunoassay. Mol. Immunol. 21, 537.

Nimmo, G.R., Lew, A.M., Stanley, C.M. and Steward, M.W. (1984) Influence of antibody affinity on the performance of different assays. J. Immunol. Methods 72, 177.

Prahl, P. and Nexo, E. (1982) Human serum IgE against two major allergens from cow hair and dander. Allergy 37, 49.

Rudolph, A.K., Burrows, P.D. and Wabl, M.R. (1981) Thirteen hybridomas secreting hapten-specific immunoglobulin E from mice with Ig^a or Ig^b heavy chain haplotype. Eur. J. Immunol. 11, 527.

Savelkoul, H.F.J., Pathak, S.S. and Van der Linde-Preesman, A.A. (1987) Occurrence of damaged heavy chains during purification of murine IgE antibodies by fast protein liquid chromatography (FPLC) and their effect on the determination of concentration and affinity in ELISA. Prot. Biol. Fluids 35, 375.

Savelkoul, H.F.J., Soeting, P.W.C., Radl, J. and Van der Linde-Preesman, A.A. (1989a) Terasaki-ELISA for murine IgE antibodies. I. Quality of the detecting antibody: Production and specificity testing of mouse epsilon-chain antisera. J. Immunol. Methods 116, 265.

Savelkoul, H.F.J., Soeting, P.W.C., De Josselin De Jong, J.E. and Pathak, S.S. (1989b) Terasaki-ELISA for murine IgE antibodies. II. Quantitation of absolute concentration of antigen-specific and total IgE. J. Immunol. Methods 116, 277.

Scatchard, G. (1949) The attractions of proteins for small molecules and ions. Ann. N.Y. Acad. Sci., 51, 660.

Steward, M.W. and Lew, A.M. (1985) The importance of antibody affinity in the performance of immunoassays for antibody. J. Immunol. Methods 78, 173.

Steward, M.W. and Steensgaard, J. (1983) Antibody affinity. Thermodynamic aspects and biological significance. CRC Press, FL.

Vos, Q., Klasen, E.A. and Haaijman, J.J. (1987) The effect of divalent and univalent binding on antibody titration curves in solid-phase ELISA. J. Immunol. Methods 103, 47.

CHAPTER 2.4

Mixing of two monoclonal IgE antibodies increases the functional affinity of the mixture for the antigen

S.S. Pathak and H.F.J. Savelkoul

Department of Immunology, Erasmus University Rotterdam, The Netherlands

Abstract

Using a simple, rapid and reliable method, the relative affinity of mixtures of monoclonal IgE for DNP was determined in Terasaki-ELISA. Some of the mixtures (notably a mixture of IGEL b4.1 and B53/A4) showed a relative affinity at least ten-fold greater than either of the individual components while others (e.g. IGEL a4 6.5 and b4.1) do not. A decrease in the hapten density did not affect the K_{rel} of the individual mAbs, but did affect the K_{rel} of the mixtures. The relative affinity of these mixtures for the cross-reacting antigen NIP was also determined. Our results point towards non-specific interaction of the Fc regions of the purified IgE molecules as a possible reason for the increased affinity.

Introduction

Determination of the affinity of a monoclonal antibody (mAb) for its antigen is of considerable importance as it is the basic experimental parameter which serves to characterize the strength of the antigen-antibody reaction (Goldberg and Djavadi-Ohaniance, 1993). The interaction between one antigen-combining site of an antibody molecule with the corresponding antigenic determinant can be expressed in quantitative, thermodynamic terms. The energy of the interaction is referred to as the equilibrium constant (K_D). However, it is not possible to make measurements at the level of a single site and interacting with a single determinant, but measurements are done using populations of sites and determinants, by allowing them to interact under controlled conditions of temperature, ionic strength etc. The final result, the antibody affinity represents an average of all interactions in the system (Macario and de Macario; 1975). Thermodynamically speaking, K_D can only be interpreted rigorously for an equilibrium in homogenous solutions. When it is being determined with methods such as ELISA or RIA, other factors may influence equilibrium, and the stability of the complex is best described by an appropriate operational parameter that is strictly dependent on experimental conditions and is best described by the word 'functional affinity' (Goldberg and Djavadi-Ohaniance, 1993).

We have earlier developed an ELISA based method for the relative affinity (K_{rel}) ranking of mAb (Pathak et al., 1989). Initial observations made during investigations of the K_{rel} of IgE mAb indicated that some of the IgE mAb, when mixed together, displayed a functional affinity that is much greater than that of the individual components. This phenomenon has been noted earlier. Howard et al. (1979) have reported that certain mixtures of mAb result in a much greater lysis of erythrocytes than the individual components. The fact that some mAbs show synergistic activity has been used in the development of radioimmunometric assays of increased specificity (Haber et al., 1981). Ehrlich et al. (1982) have reported an increased functional affinity of mAb mixtures and suggested that this was due to a non-specific co-operative interaction of the Fc region involving multi-antibody-antigen complexes. In this paper we report on the behaviour of purified DNP-specific IgE mAb mixtures in ELISA.

Materials and methods

Monoclonal antibodies

IGEL b4.1, IGEL a4 6.5, IGEL b4 14.2, and IGEL a4 6.3 hybridomas (Rudolph et al., 1981), were the kind gift of Dr. M.R. Wabl (University of California, San Francisco, CA). The hybridomas were maintained *in vitro*. The IgE-rich supernatant of the B53/A4 hybridoma as well as the rat-anti-mouse IgE mAb EM 95 (Baniyash and Eshhar, 1984), were the kind gift of Dr. R.L. Coffman (DNAX, Palo Alto, CA). The mAbs were purified as described (Savelkoul et al., 1987). The mAbs were combined in various molecular ratios for testing (1:1, 1:5,..to 1:100).

Preparation of antigen

Bovine serum albumin (BSA; type V; Sigma, St. Louis, MO) was dinitrophenylated to levels of 28 or 17 dinitrophenol (DNP) molecules per protein molecule (as determined spectrophotometrically) by using dinitrobenzenesulfonic acid (Eastman Kodak Co., Rochester, NY) according to Koch et al. (1981). 4-hydroxy-5-iodo-3-nitrophenyl protein ($NIP_{13}BSA$) was prepared by using NIP-succinimide ester (Biosearch, San Rafel, CA) in dimethylformamide (BDH, Poole, England) as described (Hudson and Hay, 1976; Haas, 1979).

Sequential equilibrium binding analysis

Sequential equilibrium binding analysis was performed to determine the K_{rel} of the reaction as described previously (Pathak et al., 1989). Briefly, clear 60 well Terasaki trays (Type 653180; Greiner, Nürtingen, FRG) were coated overnight at 4°C with 2 µg/ml of protein (DNP-BSA, NIP-BSA or the rat anti-mouse IgE EM 95). The trays were washed, blocked for non-specific

interaction with 0.02% (w/v) gelatin in PBS, charged with 5 µl of dilutions of the IgE samples and incubated at 37°C for 30 min for the equilibrium to be reached. Following the first incubation with the sample, the liquid in the wells was removed carefully using an automatic replicator (Biotec, Basel, Switzerland) and transferred to an identically coated and blocked plate. The second plate was also incubated at 37°C for 30 min for the equilibrium to be re-established. Subsequently, the plates were developed using the detecting antibody (rabbit anti-mouse IgE; RAM/IgE), enzyme-antibody conjugate sheep anti-rabbit-ß-galactosidase (MIAB Lab., Uppsala, Sweden) and the substrate, 4-methylumbelliferyl-ß-galactopyranoside (MUF-G; Sigma). The resulting fluorescence was measured as arbitrary fluorescence unit (AFU) on a Leitz inverted automated microfluorimeter (Leitz, Wetzlar, FRG). We have previously established that this ELISA has a detection limit of 0.04 ng/ml and a linearity range of 0.04 ng to 20 ng/ml (Savelkoul et al., 1989a). The RAM/IgE has been extensively tested in our laboratory, and has been established to be free of anti-idiotypic antibodies (Savelkoul et al., 1989b). The fluorescence developed in the first plate (x_1) as well as that in the second plate (x_2) for every dilution of the sample was then fitted in an equation derived from the Law of Mass Action to obtain the K_{rel} value. We have previously established that 2% ethanol helps disperse aggregates formed by IgE as detected by ion-exchange chromatography (Savelkoul et al., 1987). The mixtures that showed an increased K_{rel} as well as the individual mAbs were diluted in 2% ethanol and sequential binding analysis performed as above.

The sequential equilibrium binding analysis is based on equations derived from the Law of Mass Action.

$$\frac{[nC]}{K_D} - \frac{x_1}{[x_2+x_3+\ldots+x_n]} = \frac{x_1}{\Sigma x_2} \qquad (1)$$

Where,

nC is the concentration of antigen molecules adsorbed to the plate.

$x_1, x_2, \ldots x_n$ are the complexes formed at equilibrium by $P_1, P_2 \ldots P_n$ concentrations of paratopes with the epitopes respectively, provided the concentration of nC is kept constant and $P_1 - x_1 = P_2$, $P_2 - x_2 = P_3, \ldots P_{n-1} - x_{n-1} = P_n$; P_n and therefore $x_n \rightarrow 0$.

Σx_2 is the summation of $x_2 + x_3 + \ldots + x_n$

K_D is the equilibrium constant.

Multiple sequential transfers of the liquid in the wells following the attainment of equilibrium is necessary to satisfy the condition $P_1 - x_1 = P_2$, $P_2 - x_2 = P_3$, etc. This can be circumvented by using the empirical formula (eq. 2 below) to predict the x_3, x_4, x_n values, once x_1 and x_2 are determined.

$$X_1 = m * \frac{(X_1 - X_2)}{X_2} + C \qquad (2)$$

x_1 and x_2 being the AFU values obtained for every dilution of the sample in the first and second plate, respectively, while m and C are constants.

The inverse of the slope of the graph of x_1 versus $x_1/\Sigma x_2$ (eq. 1) gives the K_D value. All the concentrations in this equation are molar, K_D therefore has the same dimension. When applying this equation to the Terasaki-ELISA all the values are in AFU and the K_{rel} has these dimensions. Lower the K_{rel} greater the affinity. A conversion factor has to be used to convert the K_{rel} to K_D. Thus, $K_D = K_{rel} *$ conversion factor. However, we find the value of this conversion factor to be very large, increasing the chances of distortions and/or amplification of small errors. We therefore restrict the use of sequential equilibrium binding analyisis for relative ranking only.

Results

Determination of K_{rel} of monoclonal IgE and their mixtures for $DNP_{28}BSA$ and EM 95

Sequential equilibrium binding analysis of five DNP-specific IgE mAb as well as their combinations over a wide range of concentrations was performed to determine their relative affinity for DNP-BSA. Some mixtures of IgE mAb showed an increased relative affinity for the antigen (b4.1 + B53/A4, a4 6.5 + B53/A4, b4.1 + b4 14.2, cf. Table 1). This increase was calculated with respect to the component displaying the greatest affinity for the hapten. The mixture b4.1 + B53/A4 in particular showed a 16 times increased affinity for $DNP_{28}BSA$. Figure 1 shows a typical plot of x1 vs $x1/\Sigma x2$ of the mAbs as well as their mixture. The inverse of the slope of this graph gave the K_{rel} of the samples. The enhanced relative affinity was observed over a range of proportions of the components, with a particular combination showing the maximum enhancement (Table 2). Thus, in the case of b4.1 + B53/A4, a maximum enhancement was observed when the two mAbs were added in the proportion of 50:1. When sequential equilibrium binding analysis was performed with PBS + 2% ethanol as the diluent, the K_{rel} of the individual mAbs was not affected by the diluent employed indicating that the functional sites of the antigen and antibody remained undisturbed. In the case of the mixtures, however, the plot of $x_1/\Sigma x_2$ was curvilinear suggesting that the mixtures behaved as a combination of antibodies with differing affinities (data not shown).

Table 1 K_{rel} of monoclonal IgE and their mixtures for DNP-BSA and NIP-BSA[a]

IgE	K_{rel}		
	$DNP_{28}BSA$	$DNP_{17}BSA$	$NIP_{13}BSA$[a]
b4.1	3.5×10^3	3.3×10^3	8.0×10^3
a4 6.5	3.3×10^3	3.3×10^3	8.0×10^3
a4 6.3	2.0×10^3	n.d.[b]	n.d.
B53/A4	4.3×10^3	4.2×10^3	5.0×10^3
b4 14.2	1.2×10^4	1.1×10^4	2.5×10^5
a4 6.5 + b4.1[c]	4.1×10^3	n.d.	n.d.
b4.1 + b4 14.2 (1:10)	4.4×10^2 (7.9)[d]	4.5×10^3 < 1	4.0×10^3 < 1
b4.1 + B53/A4 (1:50)	2.1×10^2 (16.4)[d]	4.1×10^3 < 1	8.0×10^5 <
a4 6.3 + B53/A4[c]	2.8×10^3 < 1	n.d.	n.d.
a4 6.5 + B53/A4 (1:20)	1.2×10^3 (2.9)[d]	1.0×10^3 (3.3)[d]	5.0×10^2 (10)[d]

a. All the readings are the average of three experiments performed on three different days.
b. n.d. = not done
c. All combinations tested
d. Figures in brackets indicate enhancement factor calculated against the mAb showing the greatest affinity.

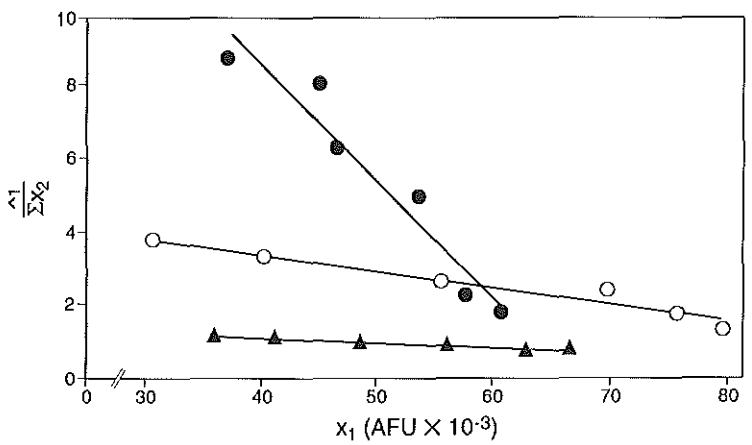

Figure 1 Sequential equilibrium binding analysis of individual IgE mAb specific for $DNP_{28}BSA$ and their mixture. The mAb used were b4.1 (○), b4 14.2 (▲) and their mixture (●).

Table 2 K_{rel} of mixtures of the IgE mAb b4.1 and B53/A4 for $DNP_{28}BSA$

IgE	K_{rel}
1 : 1	5.5×10^2
5 : 1	1.6×10^3
10 : 1	5.0×10^2
50 : 1	2.1×10^2
1 : 5	6.0×10^2
1 : 10	8.0×10^2

All the readings are the average of three experiments performed on three different days.

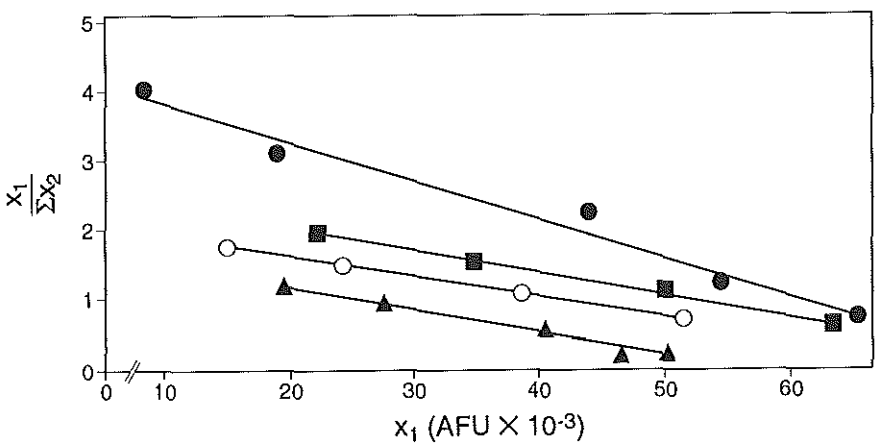

Figure 2 Sequential equilibrium binding analysis of individual IgE mAb and their mixture for rat anti-mouse anti-IgE EM 95. The samples used were B53/A4 (○), b4.1 (■), B53/A4 + b4.1 (▲), and a4 6.5 + B53/A4 (●).

To confirm that the Fc regions of the mAb used in this study were functionally intact, we performed an ELISA with immobilised mAb EM95 that interacts with the Fc region of IgE. Further, sequential equilibrium binding analysis was also performed. Figure 2 shows a typical plot of x_1 vs $x_1/\Sigma x_2$ obtained for two mAb (B53/A4, b4.1) and two mixtures (B53/A4 with b4.1, and B53/A4 with b4 14.2). The K_{rel} of the individual mAbs as well as the mixtures for EM 95 were not significantly different, all of them being in the range of 2.0 to $4.5 * 10^3$.

The influence of hapten density on K_{rel}

After first establishing that the hapten density/protein molecule did not significantly affect the K_{rel} of the individual mAb (Table 1), we proceeded to

determine its effect on the relative affinity of the mixtures. As appears from Table 1, antigen density affected the K_{rel} of the mixture to a varying degree. A fall in the hapten density from 28 to 17 DNP molecules led to a decreased relative affinity in the case of two of the mixtures (viz. mixture of b4.1 + b4 14.2 and b4.1 + B53/A4) suggesting the described aggregation of the antibody molecules as a possible mechanism underlying the increased affinity.

Determination of K_{rel} of monoclonal IgE and their mixtures for $NIP_{13}BSA$

The influence of mixing the mAbs on their K_{rel} to the cross-reacting antigen $NIP_{13}BSA$ was next investigated. The results (Table 1) showed a lowered affinity of the mAb for NIP, though the mixtures varied in this respect. Two out of the three combinations that showed an increase in relative affinity for DNP, displayed an increased affinity for NIP as well. The lack of increase in the case of the third mixture may be attributed to the lower hapten density of NIP on BSA (13 units/BSA) since this mixture also showed a decrease in relative affinity for DNP at a density of 17 DNP units/BSA molecule.

Discussion

ELISA based methods of affinity determination offer many advantages over conventional methods such as equilibrium dialysis in that they require only minute quantities of the mAb, do not need costly equipment, eliminate the need to label the primary reactants, and can be used to determine the affinity of a mAb to macromolecular antigens (Beatty et al., 1987; Nieto et al., 1984; Fedorov et al., 1992). We have previously described a Terasaki tray based non-competitive ELISA system that allows determination of relative affinity binding constants by sequential equilibrium binding analysis (Pathak et al., 1989). In this paper we show the application of this method to study relative affinities of mixtures of IgE mAb. We found that some mixtures show an increase in the relative affinity.

Monoclonal IgE antibodies directed against either TNP or DNP were used in the present study. It was observed that mixing these IgE sometimes resulted in a far greater relative affinity for $DNP_{28}BSA$ than would be expected from the K_{rel} of the components. Previous reports suggested either complexes formed via the Fc region or formation of circular complexes between antigen and antibody molecules as possible explanations for the apparent increase in the average affinity (Ehrlich et al., 1982, 1983; Moyle et al., 1983). The antigen-antibody interaction, like any other biochemical reaction, undergoes a continuous association-dissociation process. The multiple bonds formed by a complex will not separate synchronously, making it less likely that the complex becomes separated, thus giving a higher equilibrium constant (Tijssen, 1985). However, we think formation of circular complexes as an

unlikely mechanism of the apparent increase in functional affinity for a number of reasons. In the present study, we have studied the functional affinity of a mixture of mAbs to an antigen with a high density of identical epitopes (28 molecules of DNP per molecule of BSA). The increase in functional affinity of the mixture was affected by the hapten density, while that of the individual mAbs were not. A fall in the density of DNP units from 28 to 17 led to a decrease in the functional affinity of 2 of the 3 mixtures. This would not be expected to happen if circular complexes were formed between the antigen and the antibody. Moreover, we find the phenomenon selective. If formation of circular complexes between antigen and antibody was indeed responsible for the apparent increase in the functional affinity of the mixture, all the combinations tested should show this increase, which is at variance with our results. We therefore favor the Fc interaction hypothesis.

The functional intactness of the Fc region of the IgE mAb used in the mixtures was first established. EM 95 is directed against the Fc region of IgE (Baniyash and Eshhar, 1984), hence, the binding of the EM 95 to IgE mAb was taken as indicative of a functionally intact Fc region. In addition, we also established the K_{rel} of the mixtures for cross-reacting antigen. Furusawa and Ovary (1988) have reported cross-reactivity between anti-DNP/anti-TNP IgE and NIP. This is not surprising as 1 in every 20 splenic B cells in normal mice is NIP specific, while 1 in every 100 is TNP specific (Hooijkaas et al., 1983). The mixtures showed an increased affinity for this antigen as well, when compared to the component mAb. Only aggregate formation via the Fc region can explain the observed results.

Murine IgE is a heavily carboxylated glycoprotein with a carbohydrate content of about 13%. We have previously established that some of these carbohydrates are stripped off from the molecules during the process of purification (unpublished observations). Removal of the glycoside side-chains may lead to a conformational change in the molecule and different mAbs will show such changes to a varying degree. Such conformational changes due to the loss of COOH-terminal glycosylation with a concomitant increase in affinity have been reported for IgM μ chains (Bazin et al., 1992). If such changes indeed occur, they may promote aggregate formation between particular mAb combinations and not others. The extent to which the K_{rel} is affected will then depend upon the nature of the aggregation. It has been previously shown by us, that the use of 2% ethanol in the buffer effectively decreases the extent of aggregation of IgE as seen on fast protein liquid chromatography columns (Savelkoul et al., 1987). When 2% ethanol was used in the buffer, a curvilinear plot of $x_1/\Sigma x_2$ was obtained. This curvilinear nature could be attributed to partial breakdown of the aggregates, so that the mixture behaved as a combination of antibodies with different affinities. Thus, the observed increase in functional affinity seems to be due to a

potential artefact due to the method of purification. Further studies at the molecular level are being undertaken in our laboratory to confirm our hypothesis.

Acknowledgment

We thank Prof. R. Benner for his continuous support and for critically reviewing the manuscript.

References

Baniyash M. and Eshhar Z. (1984) Inhibition of IgE binding to mast cells and basophils by monoclonal antibodies to murine IgE. *Eur. J. Immunol.* **14**, 799-807.

Bazin R., Darveau A., Martel F., Pelletier A., Piche L., S-Lauren M.,Thibault M., Demers A., Boyer L., Lemeiux G., et al. (1992) Increased affinity of mutant IgM antibodies caused by the absence of COOH-terminal glycosylation of the μ chain. J. Immunol. **149**, 3889-3993.

Beatty J. D., Beatty B. G. and Vlahos W.G. (1987) Measurement of monoclonal antibody affinity by non-competitive enzyme immunoassay. *J. Immunol. Methods* **100**, 173-179.

Ehrlich P. H., Moyle W. R., Moustafa Z. A. and Canfield R.E. (1982) Mixing two monoclonal antibodies yeilds enhanced affinity for antigen. *J. Immunol.* **128**, 2709-2713.

Ehrlich P. R., Moyle W. R. and Moustafa Z. A. (1983) Further characterization of co-operative interactions of monoclonal antibodies. *J. Immunol.* **131**, 1906-1911.

Fedorov A. N., Friguet B., Djavadi-Ohaniance L., Alakhov Y. B. and Goldberg M. E. (1992) Folding on the ribosome of Escherichia coli tryptophan synthase subunit nascent chains probed with a ß conformation-dependent monoclonal antibody. *J. Mol. Biol.* **228**, 351-358.

Furusuwa S. and Ovary Z. (1988) Heteroclitic antibodies: Differences in fine specificities between monoclonal antibodies directed against dinitrophenyl and trinitrophenyl haptens. *Int. Archs. appl. Immunol.* **85**, 238-243.

Goldberg M. E. and Djavadi-Ohaniance L. (1993) Methods of antibody/antigen affinity based on ELISA and RIA. *Curr. Opin. Immunol.* **5**, 278-281.

Haas W. (1979) Hapten-gelatin gels used as adsorbents for separation of hapten-specific B lymphocytes. In *Immunological Methods* (Edited by Lefkovits, I. and Pernis, B.). Academic Press, New York, p. 269-273.

Haber E., Donahoe P., Ehrlich P., Hurrell J., Katus H., Khaw B. A., Margolles M. N., Mudgett-Hunter M. and Zurawski V.R. (1981) Resolving antigenic sites and purifying proteins with monoclonal antibodies. In *Monoclonal Antibodies in Endocrine Research.* Miller J. (Ed), Raven Press, New York, p. 1-23.

Howard J. C., Butcher G. W., Galfre G., Milstein C. and Milstein C. P. (1979) Monoclonal antibodies as tools to analyze the serological and genetic complexities of major transplantation antigens. *Immunol. Rev.* **47**, 139-174.

Hooijkaas H., Benner R., Pleasants J. R. and Wostmann B. S. (1984) Isotypes and specificities of immunoglobulins produced by germfree mice fed chemically defined ultrafiltered 'antigen-free' diet. *Eur. J. Immunol.* **14**, 1127-1130.

Hudson L. and Hay F. C. (1976) Initial preparations. *Practical Immunology*, Blackwell Scientific Publications, Oxford, London, p. 1-24.

Koch G., Osmond D. G., Julius M. H. and Benner R. (1981) The mechanism of thymus-dependent antibody formation in bone marrow. *J. Immunol.* **126**, 1447-1451.

Macario A.J.L. and de Macario E.C. (1975) Sequential changes and persistence of antibody molecules during the immune response with a special reference to the binding properties of the antigen-combining site. *Immunochem.*, **12**, 249-262.

Moyle W.R., Lin C., Corson L. and Ehrlich P.H. (1983) Quantitative explanation for increased affinity shown by mixtures of monoclonal antibodies: importance of a circular complex.

Mol. Immunol. **20**, 439-444.

Nieto A., Gaya A., Jansa M., Moreno C. and Vives J. (1984) Direct measurement of antibody affinity distribution by hapten inhibition ELISA. *Mol. Immunol.* **21**, 537-542.

Pathak S. S., Vos Q. and Savelkoul H.F.J. (1989) Terasaki-ELISA for murine IgE: III. Determination of absolute concentration and functional affinity by sequential equilibrium binding analysis. *J. Immunol. Methods* **123**, 71-81.

Rudolph A. K., Burrows P. D. and Wabl M. R. (1981) Thirteen hybridomas secreting hapten-specific immunoglobulin E from mice with Ig^a or Ig^b heavy chain haplotype. *Eur. J. Immunol.* **11**, 527-529.

Savelkoul H. F. J., Soeting P. W. C., De Josselin de Jong J. E. and Pathak S. S. (1989a) Terasaki-ELISA for murine IgE antibodies: II. Quantitation of absolute concentration of antigen-specific and total IgE. *J. Immunol. Methods* **116**, 277-285.

Savelkoul H. F. J., Soeting P. W. C., Radl J. and Van der Linde-Preesman A. A. (1989b) Terasaki-ELISA for murine IgE antibodies: I. Quality of the detecting antibody: Production and specificity testing of antisera specific for IgE. *J. Immunol. Methods* **116**, 265-275.

Savelkoul H. F. J., Pathak S. S. and Van der Linde-Preesman A. A. (1987) Occurrence of damaged heavy chains during purification of murine IgE antibodies by fast protein liquid chromatography (FPLC) and their effect on the determination of concentration and affinity in ELISA. *Prot. Biol. Fluids.* **35**, 375-385.

Tijssen P. (1985) Practice and theory of enzyme Immunoassays. In *Lab. Tech. in Biochem. and Molecular Biology*, Burdon, R.H. and Van Knippenberg, P.H. (Eds), Elsevier Science Publishers B.V., Amsterdam, pp. 1-549.

CHAPTER 2.5

Determination of relative affinity and affinity distributions in ELISA

S.S. Pathak and H.F.J. Savelkoul

Department of Immunology, Erasmus University Rotterdam, The Netherlands

Abstract

Quantitation of immune memory responses is important in developing new vaccines and demonstrating the phenomenon of affinity maturation. Developing immune responses can be analyzed by ranking the average affinities of the serum samples during the response. For a detailed insight into the affinity maturation, however, the distribution of antigen-specific antibodies over predefined affinity classes should be determined at various time points. Also, when developing hybridomas for monoclonal antibody production, a simple method is desired for relative ranking of affinities of the different monoclonal antibodies produced. In this paper, we describe simple microtitre ELISA based methods that permit determination of relative affinity as well as affinity distributions of serum antibodies. The relative affinity determination was done by sequential equilibrium binding analysis that permits both concentration and affinity determination in the same aliquot of the sample. A simple competitive ELISA was used for determining the affinity distributions.

Introduction

The development of an immune response to T cell dependent antigens involves both antigen-dependent selection of particular gene segment combinations and a selection of structural variants i.e. somatic mutants (Manser et al., 1985). It is now clear that antigenic activation is necessary to induce hypermutation in B cells and that somatic mutations accumulate only in the antigen-dependent expansion of B cell clones (Berek, 1993). As a result of hypermutation and affinity selection, the average affinity of antigen-specific antibodies produced later in the immune response is greater than in the initial phase. Though the phenomenon of affinity maturation has been studied at the molecular level, determining the absolute value of the affinity of the serum as well as affinity distributions of serum antibody subpopulations requires special methodology (Steward and Steensgaard, 1983; Berek et al., 1991; Randen et al., 1992; Yee, 1991). Often only relative ranking of the sera or supernatant from hybridoma cell lines is desired and special instrumentation or methodology for affinity determinations proves

expensive.

In this paper we report the use of simple ELISA-based techniques to measure the concentration, relative affinity as well affinity distributions of antigen-specific serum IgG1 antibodies. The relative affinity of the serum TNP-specific IgG1 was determined by sequential equilibrium binding analysis as described earlier (Pathak et al., 1989). The method is essentially similar to a normal sandwich ELISA. However, once the equilibrium is reached in the first plate, the liquid in the wells is transferred to a second identically treated plate. The optical density (OD) developed in each plate can then be fitted in equations to arrive at the relative affinity of the sample. For determining affinity distributions we have adapted a simple hapten inhibition ELISA that permits determination of affinity distributions in serum samples (Rizzo et al., 1992).

Materials and methods

Mice

Female BALB/c mice (age 12-16 weeks) were bred and maintained in the animal facilities of our own department under conventional conditions under a protocol approved by the local Animal Welfare Committee.

Reagents and immunization

Keyhole limpet hemocyanin (KLH; Pierce, Rockford, IL) was trinitrophenylated to a level of 25 TNP residues per 10^5 Da molecular mass of KLH as determined spectroscopically (Hudson and Hay, 1976) by using trinitrobenzenesulfonic acid (Eastman Kodak, Rochester, NY).

Mice were injected i.p. with 0.2 ml phosphate buffered saline (PBS) containing 100 μg/ml of TNP-KLH adsorbed on 2 mg alum (n=5). Sera were collected on days 14 and 120. Secondary immunization followed after 4 months with a booster of 0.2 ml PBS containing 10 μg/ml TNP-KLH (adsorbed on 2 mg alum) i.p. Serum was collected on day 30 thereafter.

Evaluation of relative affinity of antigen-specific serum IgG1 antibodies

96 well microtitre plates (Nunc, Roskilde, Denmark) were coated overnight with TNP-KLH (0.3 μg/ml), blocked with PBS containing 1% bovine serum albumin (BSA) and incubated with 100 μl of appropriate dilutions of the serum for 3 hrs at room temperature. The samples were then removed carefully and added to an identically coated and blocked plate and incubated for a further 3 hrs. After washing with PBS containing 0.1% BSA and 0.1% Tween 20, both sets of plates were treated with biotinylated goat anti-

mouse-IgG1 (GAM/IgG1; Southern Biotechnology, Birmingham, AL), streptavidin-horseradish peroxidase (SA-HRP) (Jackson Immunoresearch, West Grove, PA) and the substrate 2,2'-azino-bis(3-ethylbenz-thiazoline-6-sulfonic acid) (ABTS; Sigma, St. Louis, MO). The OD developed in the first plate was called the x_1 value while that in the second plate the x_2. These values were then fitted in the following equations to arrive at the K_{rel}. The equations have already been validated (Pathak et al., 1989).

$$\frac{[nC]}{K_D} - \frac{X_1}{K_D} = \frac{X_1}{[x_2+x_3+\ldots+x_n]} = \frac{X_1}{\Sigma x_2} \qquad (1)$$

where

nC - is the concentration of antigen molecules adsorbed to the plate.
x_1, x_2,...x_n - are the complexes formed at equilibrium by P_1, P_2.... P_n concentrations of paratopes with the epitopes, respectively, provided the concentration of nC is kept constant and the condition $P_1 - x_1 = P_2$; $P_2 - x_2 = P_3$,...$P_{n-1} - x_{n-1} = P_n$; P_n and therefore $x_n \rightarrow 0$ is fulfilled.
$\Sigma x_2 = x_2 + x_3 + \ldots + x_n$.
K_D - is the equilibrium constant.

Multiple sequential transfers of the liquid in the wells following the attainment of equilibrium is necessary to satisfy the condition $P_1 - x_1 = P_2$; $P_2 - x_2 = P_3$ etc. This can be circumvented by using an empirical formula (eq. 2 below) to predict the x_3, x_4,..x_n values, once x_1 and x_2 are determined.

$$x_1 = m * \frac{(x_1 - x_2)}{x_2} + C \qquad (2)$$

x_1 and x_2, being the OD values obtained for every dilution of the sample in the first and second plate, respectively, while m and C are constants.

The inverse of the slope of the graph of x_1 versus $x_1/\Sigma x_2$ (eq. 1) gives the K_D value. When all the concentrations in this equation are molar, K_D has the same dimension. When applying this equation to microtitre ELISA, all the values are in OD and a conversion factor can be used to convert the K_{rel} to K_D. However, the use of this large conversion factor is likely to introduce a large error and we use the method essentially for the relative ranking of affinities.

Determination of affinity distributions

The affinity distributions of anti-TNP IgG1 antibodies were determined in a TNP-specific isotype specific competitive ELISA (Rizzo et al., 1992). Dilutions of serum samples were incubated overnight (4°C) with increasing concentrations of the monovalent hapten N-ε-DNP-L-lysine HCl (DNP-lys; 10^{-4} to 10^{-11} M; Sigma) in PBS. The mixtures were transferred to ELISA plates coated with TNP-KLH. After incubation for 3 hrs the plates were washed and the amount of TNP-specific antibody established by using GAM/IgG1, SA-HRP and ABTS. The high affinity antibodies are inhibited from binding to the plates by low concentrations of free hapten. As the free hapten concentration increases incrementally, lower affinity antibody is inhibited until theoretically, at sufficiently high hapten concentrations, all DNP-specific antibody binding is inhibited.

Results

Determination of concentration and K_{rel}

The concentration of the serum TNP-specific IgG1 was determined using the OD developed in the first plate. The concentration of serum antigen-specific IgG1 increased in relation to time after immunization with TNP-KLH. It was below the detection limit (0.2 μg/ml) on day 0. At day 14 the response reached 248±36 μg/ml and remained at that level till day 120 of primary immunization. At day 30 after the secondary immunization the concentration was found to be 2.4±1.6 mg/ml (data not shown).

In the sequential equilibrium binding analysis, data for the relative affinity of the serum can be derived from the same aliquot of sample used for concentration determination by applying equation 1. To arrive at the value of Σx_2, needed for equation 1, we use equation 2. The validity of this equation was established in the Terasaki system by performing a series of sequential transfers and comparing the actual and predicted values (Pathak et al., 1989). Essentially similar results were also obtained in the microtitre system (data not shown). The relative affinity of the serum antibodies (K_{rel}) is essentially a reflection of K_D; affinity increases as the K_{rel} decreases. Figure 1 shows a typical plot of x_1 vs $x_1/\Sigma x_2$ for a serum sample of a single animal. Similar results were obtained for the other animals in the group. As is observed from the plot, the relative affinity of the sera increased in the primary immune response (from 5.5 on day 14 to 1.1 on day 120) and further increased to 0.34 in the secondary response; i.e. an increase of 16 fold over the value for day 14 of the primary immune response.

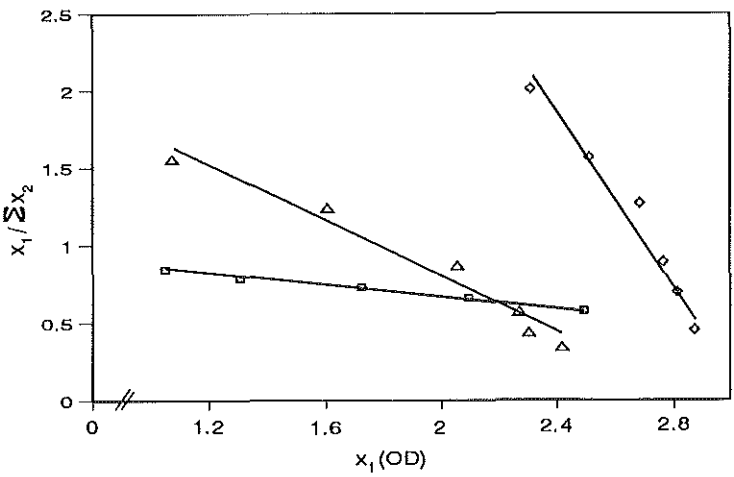

Figure 1 Determination of K_{rel}. Sequential equilibrium binding analysis was performed on serum samples obtained at different time points after primary immunization (days 14 and 120) and secondary immunization (day 30). Microtitre plates were coated with TNP-KLH, blocked and incubated with serum dilutions for 3 hours. The samples were then carefully removed and added to an identically coated and blocked plate and incubated for a further 3 hrs. The plates were developed with GAM/IgG1, SA-HRP and ABTS. The signal developed in the first plate was x_1 while that in the second plate was x_2. These values were fitted in equations 1 and 2. The inverse of the slope of the graph of x_1 vs $x_1/\Sigma x_2$ gives K_{rel}.

Determination of relative affinity distributions

In the competitive ELISA for affinity distributions, increasing amounts of the hapten DNP-lys was added to serum aliquots and incubated overnight. The mixture was then run in a regular ELISA using a coat of the same hapten conjugated to a protein. High affinity antibodies will be inhibited from reacting with the coat at low concentrations of the free hapten, while low affinity antibodies will require a much higher concentration of free hapten for inhibition. The affinity distributions of the serum subpopulations of antigen-specific antibodies at various time points after immunization are shown in Figure 2. The histograms clearly establish that affinity maturation occurred both in the primary and secondary immunization scheme employed. Primary day 14 serum contained a major fraction (68%) of antibodies that were inhibited only at the high free hapten concentration of 10^{-4} M DNP-lys. Affinity increased thereafter as seen from the emergence of high affinity subpopulations at day 120. The primary day 120 serum showed a predominance of a single high affinity group (48%) that is represented by inhibition by 10^{-8} M free DNP-lys. At day 30 in the secondary response the serum showed a small fraction of low affinity antibodies, along with a population of antibodies (20%) of a very high affinity.

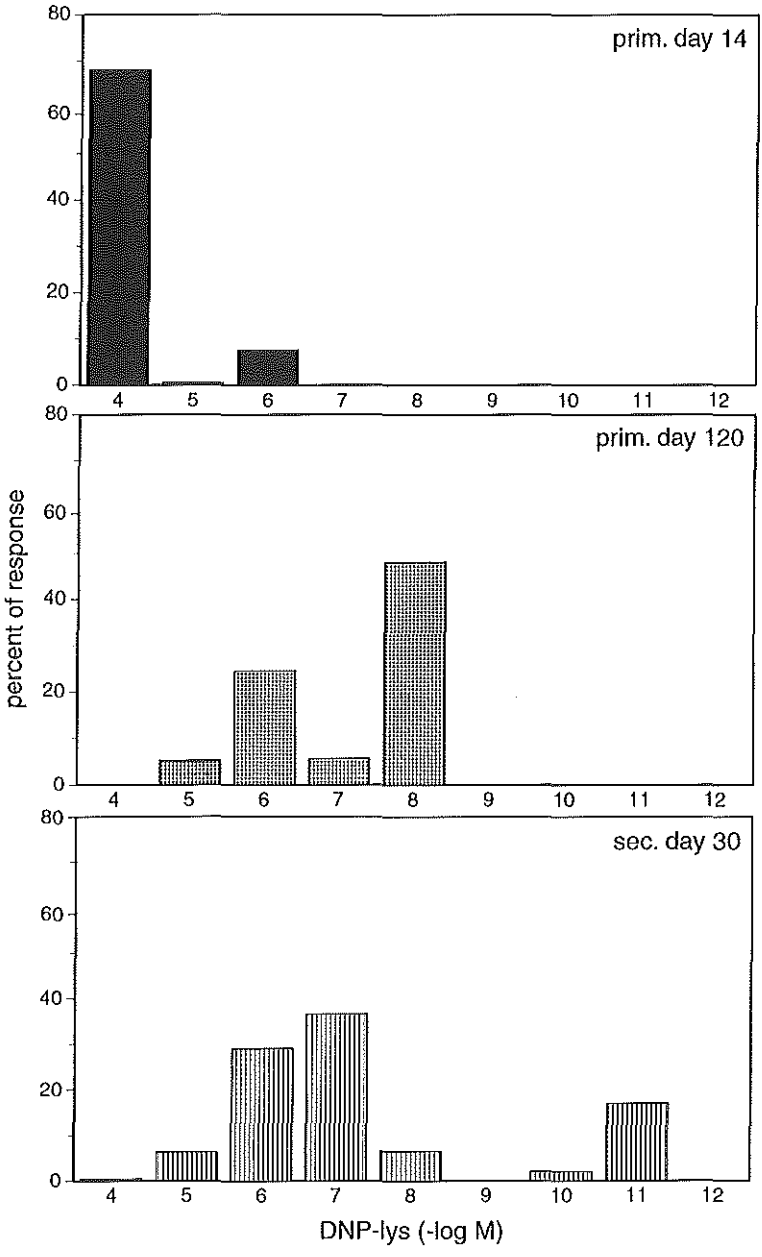

Figure 2 Affinity distributions of serum TNP-specific IgG1 antibodies. Serum samples were collected on days 14 and 120 after primary immunization and day 30 after secondary immunization and run in a competitive inhibition ELISA. The abscissa indicates the concentration of free DNP-lys (−log M) used for inhibition. Affinity increases to the right. The ordinate shows the percentage of antibody present in each affinity sub-group. Each histogram represents the results of a typical analysis of serum of one animal.

Discussion

In this paper we demonstrate the application of simple ELISA-based methodology to determine the concentration, increase in relative affinity as well as affinity distributions of anti-DNP IgG1 antibodies in sera of immunized mice. Quantitation of immune memory responses is important in developing new vaccines and demonstrating the phenomenon of affinity maturation. One of the parameters often used to establish memory is the concentration determination. But, it is not enough to establish an increase in the concentration of antigen-specific antibodies during immunization, one must also show an increase in the average or functional affinity of the antibodies produced. However, this value by itself may not be sufficient to demonstrate affinity maturation as it is an average value that does not reflect the affinity distributions of antibody subpopulations present. The efficacy of immunization can only be demonstrated by the appearance of antibody populations with an increased affinity later in the response, i.e. by determining the affinity distributions in ongoing immune responses.

Determining average affinity and affinity distributions in sera is difficult, especially for large proteinic antigens. A variety of mathematical functions have been used to determine the heterogeneity index (Scuitto et al., 1987; reviewed in Day, 1990). These are based on the assumption that the affinity distributions are Gaussian in nature. Attempts have also been made to determine affinity distributions from data obtained in RIA, fluorescence quenching etc. (Flanagan et al., 1978; Munson and Rodbard, 1980; Thakur et al., 1980). It is virtually impossible to determine true affinity distributions in polyclonal sera since it requires the separation of the different antibody subpopulations, a process that is highly labor intensive and expensive in terms of the amount of serum and reagents required. Using the simple hapten-based ELISA proposed by us, it is possible to determine the relative affinity distributions in polyclonal immune responses. Using this technique, we have established that the immunization protocol used by us was successful in inducing affinity maturation as judged from the affinity distributions of serum DNP-specific IgG1 antibodies.

We have previously demonstrated the use of sequential equilibrium dialysis for affinity analysis in Terasaki-ELISA. We now demonstrate that it is equally applicable in the microtitre system. In the case of Terasaki-ELISA, the K_{rel} determination is not significantly affected by the input concentrations of the coating solutions (Pathak et al., 1989). In the mictotitre system, however, we found the input concentration in the coating solution important for reproducible affinity determinations (data not shown). Terasaki trays have a higher coating efficiency and a Terasaki-ELISA shows a relative independence of the coating concentration (Savelkoul et al., 1989). However, the microtitre plates have a 10 times less coating area so that at high input

coating concentrations, multiple protein layers are likely to be formed. In performing sequential binding equilibrium analysis in the microtitre system, therefore, careful titration of the input concentration is needed.

This method is being used routinely in our laboratory to evaluate immunization protocols, as well as for the relative ranking of panels of monoclonal antibodies. Here, we show that the immunization protocol used led to an increase in the concentration of the antigen-specific antibodies. It was also successful in inducing affinity maturation in both primary and secondary immune responses. This is reflected in the average affinity value as well as the affinity distributions of the secondary serum sample. The method calls for no special equipment, and determines both relative affinity and affinity distributions in small amounts of the sample.

References

Berek, C., Berger, A. and Apel M. (1991) Maturation of the immune response in the germinal centers. Cell 67, 1112.

Berek, C. (1993) Somatic mutation and memory. Curr. Opin. Immunol. 5, 218.

Day, E.D. (1990) Affinity. In: Advanced Immunochemistry. Wiley-Leiss, USA, p. 295.

Flanagan, M.T., Tattam, F.G. and Green, N.M. (1978) The characterization of heterogeneous antibody hapten interaction using nonlinear regression analysis on fluorescence quenching curves. Mol. Immunol. 15, 261.

Hudson, L. and Hay, F.C. (1976) Initial preparations. In: Practical Immunology. Blackwell Scientific Publications, Oxford, London, p.1.

Manser, T., Wysocki, L.J., Gridley, L.J., Near, R.I. and Gefter, M.L. (1985) The molecular evolution of the immune response. Immunol. Today 6, 94.

Munson, P.J. and Rodbard, D. (1980) Ligand: a versatile computerized approach for characterization of ligand-binding systems. Analyt. Biochem. 107, 220.

Pathak, S.S., Vos, Q. and Savelkoul, H.F.J (1989) Terasaki-ELISA for murine IgE: III. Determination of absolute concentration and functional affinity by sequential equilibrium binding analysis. J. Immunol. Methods, 123, 71.

Randen, I., Brown, D., Thompson, K.M., Hughes-Jones, N., Pascaul, V., Victor, K., Capra, J.D., Foorre, O.O. and Natvig, J.B. (1992) Clonally related rheumatoid factors undergo affinity maturation in the synovial tissue. J. Immunol. 148, 3296.

Rizzo, L.V., Dekruyff, R.H. and Umetsu, D.T. (1992) Generation of B cell memory and affinity maturation. Induction with Th1 and Th2 clones. J. Immunol. 148, 3733.

Savelkoul H. F. J., Soeting P. W. C., De Josselin de Jong J. E. and Pathak S. S. (1989) Terasaki-ELISA for murine IgE antibodies: II. Quantitation of absolute concentration of antigen-specific and total IgE. J. Immunol. Methods 116, 277-285.

Scuitto, E., Garat, E., Ortega, E. and Larralde, C. (1987) Antibody heterogeneity: theoretical and experimental evaluation of a simple procedure to describe differing affinities in hapten binding reactions. Mol. Immunol. 24, 577.

Steward, M.W. and Steensgaard, J. (1983) Antibody affinity: thermodynamic aspects and biological significance. CRC Press, Boca Raton, FL. p. 170.

Thakur, A.K., Munson, P.J., Hunston, D.L. and Rodbard, D. (1980) Characterization of ligand-binding systems by continuous affinity distributions of arbitrary shape. Analyt. Biochem. 103, 240.

Yee, E. (1991) Reconstruction of the antibody distribution from the experimental data using minimum cross-entropy procedure. J. Theor. Biol. 153, 205.

KINETIC INTERACTION ANALYSIS WITH A BIOSENSOR

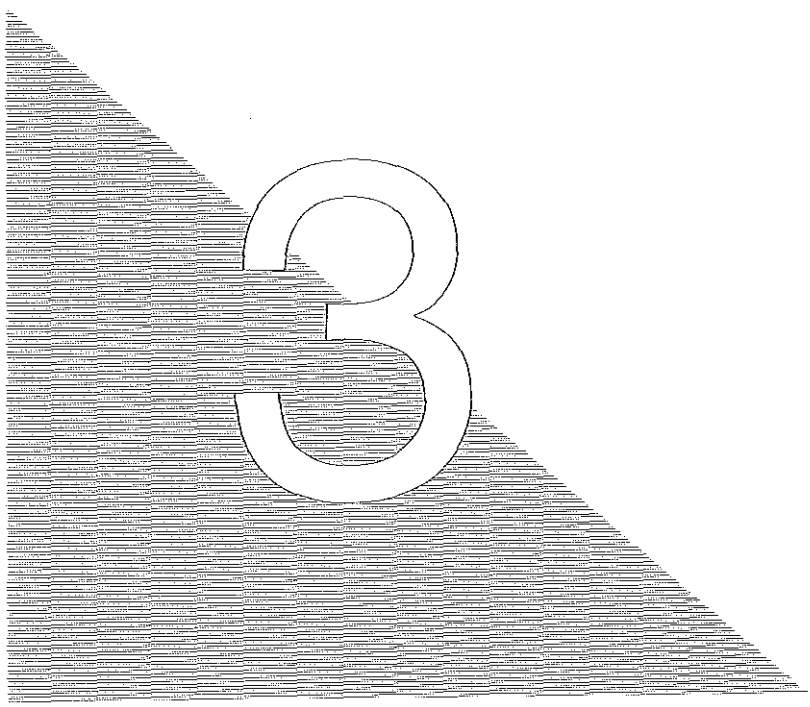

Kinetic interaction analysis with a biosensor

CHAPTER 3.1

Determination of antibody affinity and affinity distributions

S.S. Pathak, G.J.M. Tibbe and H.F.J. Savelkoul

Department of Immunology, Erasmus University, P.O. Box 1738,
3000 DR Rotterdam, The Netherlands

1 Introduction

Like any other biochemical reaction antibody-antigen reactions are reversible and can be characterized by measuring both association and dissociation constants. In the case of a monovalent antibody site reacting with a monovalent determinant, the equilibrium constant is conventionally defined as the 'affinity' of the antibody. It is therefore a ratio of the molecular association and dissociation rates. Thus, if we consider the equation

$$Ag + AB \underset{k_2}{\overset{k_1}{\rightleftharpoons}} Ag.Ab$$

then, the affinity = equilibrium constant = $\frac{k_2}{k_1} = K_d = \frac{1}{K_a}$

When both the antibody and the antigen are multivalent the equilibrium constant has been termed the 'avidity' of the antibody. Avidity, thus, depends upon affinity but also involves other contributing factors such as valency, the method of measurement etc., that are not necessarily concerned with the primary antibody-antigen reaction. In a polyclonal situation, eg. estimation of the affinity of antisera, the situation is further complicated by the fact that the serum is a mixture of antibodies of different affinities. Thus, the affinity of the serum is a kind of 'average affinity' or the 'functional affinity'. The fuctional affinity is influenced by the affinity distribution of the various antibodies capable of reacting to the same epitope in the serum as well as the method of determination.

The experimental determination of the affinity of a monocloal antibody for its antigen is of considerable importance. It is the basic experimental parameter in a variety of studies, eg. the use of monoclonal antibodies as conformational probes, the thermodynamical approach to the study of the molecular basis of the antigen-antibody interaction etc. (Goldberg and Djavadi-Ohaniance, 1993). Antibody screening as well as ranking of antibodies with regard to their reactivity to a tumor associated antigen is a common assay in the production

of monoclonal antibodies for diagnosis and therapy. The knowledge of the functional affinity as well as the affinity distribution patterns of the various antibody populations in the serum is important in the study of ongoing immune responses and especially the phenomenon of affinity maturation.

The possibility that variation in the binding affinity of antibody can influence the biological properties of antisera was recognized several years ago. A range of factors are known to influence antibody affinity. These include the dose and nature of the immunogenic stimulus, the immunization scheme, genetic factors, qualitative and quantitative aspects of lymphocyte function, dietary and hormonal factors, reticulo-endothelial function and the effects of free antibody and antigen-antibody complexes in the micro-environment. The mechanisms by which these factors affect affinity are not clear, particularly since the cellular basis of the control of affinity has not been fully characterized.

2 Methods of affinity determination

It is clear from the equation above, that the determination of antibody affinity requires the measurement, at equilibrium, of antibody-bound and free antigen or the measurement of antigen-bound and free antibody. The methods used must obviously not disturb the equilibrium and should not preferentially detect antibodies of a particular affinity. In practical terms the analysis requires the availability of large amounts of purified labeled (radio-, enzyme- or fluorescence-labeled) ligand, undamaged by the labeling procedures.

A variety of methods have been used to measure antibody avidity or average affinity. The most accepted amongst them is equilibrium dialysis, in which the reactants are separated by a semi-permeable membrane which allows movement of one of the reactants (the labeled antigen), but not the other (antibody). The amount of label at either side of the membrane at equilibrium is then quantitated. Affinity can then be calculated by the Scatchard equation. The obvious disadvantage of this method viz. the strict requirement for small haptens, however, limits its usage.

A number of different methods have therefore been employed to generate the data required for the Scatchard analysis. These include precipitation by ammonium sulfate or polyethylene glycol, electrophoresis in agarose gels, radioimmuno assay and, recently, ELISA (Gaze et al., 1973; Nimmo et al., 1984; Friguet et al., 1985; Heegaard and Bjerrum, 1991). However, strictly speaking, the K_d can be rigorously be determined only for an equilibrium in homogeneous solution and no straight forward thermodynamic theory can describe the equilibrium in heterogeneous phase systems.

A different approach to the determination of antibody avidity is the use of agents that disrupt the already formed antigen-antibody complexes, eg.

temperature, chaotropic ions such as thiocyanate, perchlorate, iodide, low pH buffers etc. (Lee et al., 1974; Germuth et al., 1979). Especially chaotropic ions exhibit a remarkable capacity to modify ionic forces responsible for stabilization of the tertiary structure of many molecules and can disrupt or modify the intermolecular interactions between antigen and antibody that are mediated by such forces and have been recognized as promising for the study of antibody affinity.

Lately, the biosensor technology has made it possible to measure antigen-antibody reactions in real-time as they are occurring (refer section 4.).

3 Affinity determination

3.1 Calculations

In calculating the affinity constant for polyclonal serum antibodies and more recently for monoclonal antibodies, the most frequently used method has been that of Scatchard (Scatchard, 1949; Soos and Siddle, 1982; Steward and Lew, 1985). Scatchard analysis allows estimation of antibody affinity by the regression analysis of bound over free ligand (antigen) concentration versus the bound ligand concentration, under circumstances where the ligand concentration is variable and the antibody concentration is constant. From the application of the Law of Mass Action to antigen-antibody interaction, the following form of the Langmuir Adsorption Isotherm may be derived

$$\frac{[Ab\text{-}Ag]}{[Ab]} = r = \frac{nK_a[Ag]}{1+K_a[Ag]}$$

where r = moles antigen bound per mole of antibody; [Ab-Ag] = bound antigen concentration; [Ab] = free antibody concentration; [Ag] = free antigen concentration (at equilibrium); n = antibody valence; K_a = association constant or affinity. From this equation we arrive at

$$\frac{r}{[Ag]} = nK_a - rK_a = K_a(n-r)$$

being the Scatchard equation. Therefore, a plot of r/[Ag] versus r over a range of free antigen concentrations allows values of K_a and n to be assessed. When half the divalent antibody (n = 2) binding sites are bound (r = 1) then

$$\frac{1}{[Ag]} = 2K_a - K_a = K_a$$

and thus K_a equals to the reciprocal of the free concentration at equilibrium when half the antibody sites are antigen-bound. Alternatively, the free antigen ([Ag]) at equilibrium is determined by subtracting the bound antigen from the total antigen. The reciprocals of bound antigen (1/[Ab-Ag]) and free antigen (1/[Ag]) are plotted according to the Langmuir equation

$$\frac{1}{[Ab\text{-}Ag]} = \frac{1}{K_a.[Ag][Ab_t]} + \frac{1}{[Ab_t]}$$

to obtain a value for the total amount of antibody present, expressed as total antigen binding sites Ab_t. Thus, when 1/[Ag] = 0, then (1/[Ab-Ag] = ($1/Ab_t$)); Ab_t may be determined by extrapolation of the linear portion of the plot directly by determining the value of 1/[Ag] when 50% of the total antigen binding sites are bound. The relationship must be linear over a range of ligand concentration, at least one order of magnitude on either side of the K_a value. If linearity is not observed over this range, the assumptions made in deriving the Scatchard formula do not apply and the calculated K_a value is not meaningful. Regrettably, frequently a portion of the plot, often covering only a narrow range of antigen concentration, is found to be roughly linear and arbitrarily chosen for the calculation. Furthermore, even when using isolated and purified anti-hapten antibodies, these plots frequently deviate from linearity due to the existence of heterogeneity of antibody affinities within an antibody population. This heterogeneity makes it necessary for the equilibrium concentrations of bound and free antigen (or antibody) to be determined over a range of free antigen (or antibody) concentrations. The interpretation of the results is thus based on the overall affinity estimation and is therefore often called 'average' affinity, although the value estimated empirically may not represent the mean, mode or median.

3.2 Affinity determination in ELISA

Though many studies have been conducted on the effect of antibody affinity on ELISA measurements, application of non-competitive ELISA for affinity measurement has been limited (Nimmo et al., 1984; Steward and Lew, 1985). ELISA have been mainly used for quantitation. Friguet et al. (1985) have used this technique to determine the amount of unreacted antibody that is left in the

reaction mixture after the antigen-antibody reaction in the fluid phase and performed Scatchard analysis on the data obtained. Alternatively, a mathematical approach involving curve fitting procedures for estimating avidity from ELISA dilution curve data has been explored. Binding constants have also been estimated from adsorption kinetics data (Matikainen and Lehtonen, 1984; Li, 1985). Recently, Beatty et al. (1987a; 1987b) have used the approach of determining relative affinities by varying the input concentration in the coating solution. Competitive EIA techniques have also been employed (Nieto et al., 1984). These methods, however, require special methodology and are not universally applicable, especially where the antibody is present in minute quantities as is the case with IgE (< 1 µg/ml in normal mouse serum). Moreover, some of these techniques are laborious and often require partial purification and concentration determination of the Ig involved.

The major drawback of applying general ELISA techniques for affinity measurement is the fact that though it is possible to determine the input concentration of the ligand in the coating solution, it is almost impossible to determine the amount of ligand that has been actually adsorbed to the wells, even if one assumes such adsorption to be uniform all over the plate and therefore the concentration of ligand/well to be identical. The approach of Scatchard requiring the determination of bound over free antigen or antibody ratios cannot be easily adapted to the ELISA system since the molar concentration of antibody that complexes with the antigen cannot be easily computed. The reaction developed is proportional to the complex formed, so that it is not possible to determine the amount of free antibody (antigen) on the solid phase. Moreover, low affinity antibodies are said to be preferentially underestimated in ELISA. Also, independent of its affinity, subpopulations of <10% concentrations could not be detected in ELISA. It is especially difficult to measure the affinity constant of a reaction where both the reactants are Ig. Nevertheless, because of its ease and simplicity, ELISA remains a popular method of quantitation and affinity determination.

We have proposed the use of a simple binding analysis - sequential equilibrium binding analysis to determine the 'functional affinity' of Ig without prior purification and even when present in minute quantities (Pathak et al., 1989). An apparent equilibrium constant - K_{rel}, is measured by fitting the ELISA data in two different formulae derived from the Law of Mass Action. The relation between the K_{rel} and K_d, the conversion factor, is then established. Once established the relation can be employed for computing K_d from K_{rel}, provided the detection system remains identical.

The quantitative relationship of the interaction between antigen and antibody at equilibrium is governed by the Law of Mass Action (Fazekas De St. Groth, 1979). It is represented in various forms, one of them being

$$\frac{[nC-x][P-x]}{[x]}=K_d \qquad (1)$$

where

C - original concentration of antigen molecules with n epitopes/molecule.
P - original concentration of paratopes.
x - concentration of complex formed at equilibrium.
K_d - equilibrium constant = $1/K_a$
All the concentrations are expressed in Moles/litre. K_d has the dimension of Moles/litre.

Thus, when the concentration of [nC] is constant, but the concentration of [P] varies, we arrive at

$$\frac{[nC-x_1][P_1-x_1]}{[x_1]}=\frac{[nC-x_2][P_2-x_2]}{[x_2]}=K_d \qquad (2)$$

$[x_1]$,$[x_2]$ - are the complexes formed at $[P_1]$ and $[P_2]$ concentrations of the paratopes, respectively.

Upon imposing the condition that $[P_2] = [P_1 - x_1]$, equation (2) can be rewritten as

$$\frac{[nC-x_1][P_1-x_1]}{[x_1]}=\frac{[nC-x_2][P_1-x_1-x_2]}{[x_2]}=K_d \qquad (3)$$

or

$$[P_1-x_1]=\frac{K_d*[x_1]}{[nC-x_1]} \qquad (4)$$

and

$$[P_1 - x_1 - x_2] = \frac{K_d * [x_2]}{[nC - x_2]} \tag{5}$$

Subtracting eq. (5) from eq. (4) results in

$$[x_2] = \frac{K_d * [x_1]}{[nC - x_1]} - \frac{K_d * [x_2]}{nC - x_2]} \tag{6}$$

or

$$[nC - x_1][nC - x_2] = K_d * nC \frac{[x_1 - x_2]}{[x_2]} \tag{7}$$

This equation can be employed in practice within certain limits. Though theoretically nC will never be equal to x_1, practically nC tends towards x_1 when nC is limiting and x_1 and/or x_2 tend to zero at the upper and the lower plateaus of the dilution curve, respectively. We thus have a range within which this equation can be used.

Also, reconsidering eq. (2), and extending the condition

$[P_1 - x_1] = [P_2]$,
$[P_2 - x_2] = [P_3]$,
$[P_3 - x_3] = [P_4] \ldots [P_n]$
where $[x_n] \rightarrow 0$,

we arrive at $[P_1 - x_1] = [x_2] + [x_3] + \ldots . [x_n]$ (7a)

$[x_2]$, $[x_3]$, $\ldots [x_n]$ being the complexes formed at successive equilibrium steps, with the original concentration of paratopes $[P_1]$, and the total concentration of epitopes [nC] kept constant at each step. Therefore eq. (2) can be rewritten as

$$\frac{[nC - x_1][x_2 + x_3 + ..]}{[x_1]} = K_d$$

or

$$\frac{[nC]}{K_d} - \frac{[x_1]}{K_d} = \frac{[x_1]}{[x_2+x_3+...]} \qquad (8)$$

Both eq. (7) and (8) give a straight line in the range under consideration. They can be used to determine the value of K_d. Thus the slope of the plot of $[x_1-x_2]/x_2$ vs $[nC-x_1][nC-x_2]$ will be $nC*K_d$. The inverse of the slope of the plot of $x_1/\Sigma x_2$ vs x_1 will give the K_d, the intercept on the Y axis can be used to arrive at the value of nC (Figure 1). The first condition of eq. (2) can be met in an ELISA by transferring the liquid in the wells after equilibrium has been reached to a fresh plate previously coated and blocked as the intial one and incubating the second plate until equilibrium is once again established.

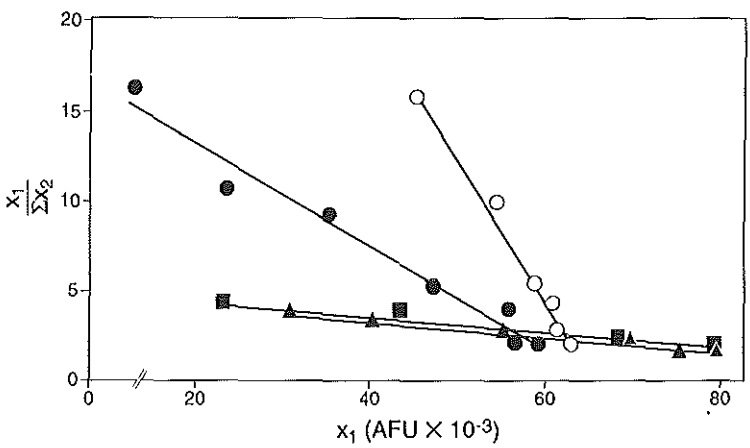

Figure 1 Sequential equilibrium binding analysis for affinity ranking in ELISA. Four individual monoclonal anti-TNP antibody preparations were tested on plates coated with the antigen. The product developed in each plate (OD or AFU) was fitted in eq. 8. Affinities can be ranked in decreasing order (○, ●, ■ and ▲).

It is essential to determine the value of nC - the maximum number of epitopes that are available for reaction with the paratopes in each well in order to allow the aplication of eq. (7). When nC becomes limiting, i.e. in the plateau region of the dilution curve, x_1 tends towards nC, and the values of x_1 and x_2 are approximately equal. These values of x_1 remain unchanged over a range of decreasing concentrations of P, while the value of x_2 decreases. The response value of x_1 in this region is approximately equal to nC. The value of x_1 in the plateau region of the dilution curve (at the highest concentration of Ig) is sometimes lower than that obtained at lower Ig concentrations (the steep part of the curve). Similarly, x_2 is sometimes found to be greater than x_1 in this region. On purely theoretical grounds, two explanations are possible. Firstly, the plateau region of the dilution curve is the antibody excess zone so that only one

antibody site can complex with the antigen, leading to a loose binding. Some of this Ig will be lost in the subsequent washing steps giving a reduced signal. Alternatively, the detecting reagents either cannot bind or bind loosely to the Ig due to steric hindrance, leading to a deviation from linearity in the dose response curve on the first plate.

The process of liquid transfer can be repeated a number of times to get the values required for eq. (8). However, the repeated transfer of the liquid is a tedious and laborious process. The systematic error in the measurement will also be amplified and loss of minute amounts of the liquid in each successive transfer will further distort the signal obtained. We therefore suggest the use of an empirical equation that can be used to predict the values of x_3, x_4, etc., once the values of x_1 and x_2 are established. A close agreement of the predicted and the experimentally determined values is generally observed (Figure 2).

$$x_1 = m * \frac{x_1 - x_2}{x_2} + c \qquad (9)$$

All the variables in equations (8) and (9) are expressed in terms of response (e.g. optical density). The K_{rel} value so determined therefore will also be in these terms and a conversion factor will have to be determined to arrive at K_d in Moles/litre. This conversion factor is dependent on the detecting and measuring system used and will be unique for a particular system.

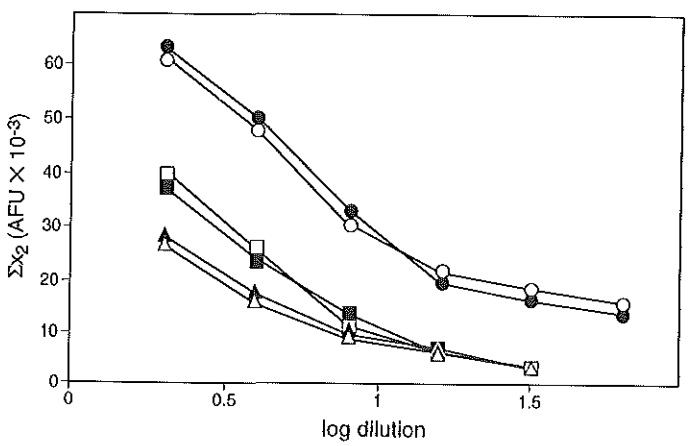

Figure 2 Comparison of the actual and predicted Σx_2 values. Sequential equilibria were established between a coat and three different monoclonal antibodies. A summation of the response values (OD or AFU) of plates 2,3,4...,n, gave the experimental Σx_2 (closed symbols). The response values of the first and second plates were fitted in eq. 9 to arrive at the predicted Σx_2 values (open symbols). A plot of Σx_2 vs log dilution was then constructed.

A number of assumptions have to be made for applying the above equations to ELISA -

1. The antigen-antibody interaction wherein the antigen is bound to the solid phase and the antibody is in the liquid phase is governed by the Law of Mass Action.
2. The reaction reaches an equilibrium and this equilibrium is not substantially affected by the binding of the antibody to the immobilized antigen and it's consequential removal from the fluid phase.
3. The antigenic epitopes remain essentially unaltered after adsorption to the solid phase, so that the behaviour of the paratopes and therefore the K_d remains unaffected in this system.
4. The epitopes bound to the solid phase behave independently of each other and there is no cooperative binding between the two identical binding sites of the antibody.
5. The coating of the solid phase is uniform, i.e. the average number of epitopes that can react with the paratopes/well is the same for a given antigenic input in the coating solution.

It is possible to determine the K_{rel} (and K_d) of reactions between antigen and antibody as well as between anti-Ig antibodies and Ig by the sequential equilibrium binding analysis. A large conversion factor is required to arrive at the K_d from K_{rel}. However, the use of this large factor is likely to introduce/amplify errors and we restrict the usage to relative ranking only. We have used this system extensively for evaluating immunization protocols as well as relative ranking of monoclonal antibodies. In our experience, the system works best for monoclonal antibodies and for polyclonal sera consisting of relatively simple affinity distributions. When the serum consists of a wide range of affinities, e.g. late secondary or tertiary responses, the K_{rel} can only be determined over a very small range of dilutions, and caution needs to be exercised in evaluating the results.

3.3 Determination of affinity distributions

It is known that the binding of antibodies produced by the immune system in response to 'foreign' antigens is heterogeneous and that the distribution of association constants of the antigen-antibody reaction evolves in time under various circumstances (Eisen and Siskind, 1964). The study of the antibody distribution pattern as a function of time after immunization is useful for the quantitation of the immune memory (Yee, 1991).

The affinity constants of polyclonal serum antibodies represent the overall binding properties of a normally heterogeneous population of antigen-specific antibodies and have limited usage (Bruderer et al., 1992). An accurate assessment of affinity distributions within polyclonal populations of antigen-

specific antibodies depends either on the isolation of antibody populations according to differences in affinity, or on the detectability of these populations in the presence of additional populations with the same specificity. Such isolation and quantitation of antigen-specific antibodies requires large samples and is difficult and labor intensive. Moreover, an accurate detection of the affinity populations in polyclonal samples is problematic due to the complexity of the populations to be analyzed and the multiplicity of the possible interactions.

Several ELISA based assays have been described for the measurement of affinity distributions (Nieto et al., 1984; Rath et al., 1988; Van Dam et al., 1989). We have adapted a simple competitive inhibition ELISA method for the relative determination of affinity distribution patterns in a polyclonal serum using a previously described protocol (Rizzo et al., 1992). Increasing amounts of the hapten are added to serum aliquots and incubated overnight. The mixture is then run in a regular ELISA using the same hapten-protein conjugate as the coat. In this type of an assay, the high affinity antibody is inhibited from binding to the ELISA plates by the low concentrations of the free hapten. As the free hapten concentration is incremently increased, lower affinity antibody is inhibited, until at sufficiently high hapten concentrations all hapten-specific antibody is inhibited. The results are expressed in an histogram (Figure 3).

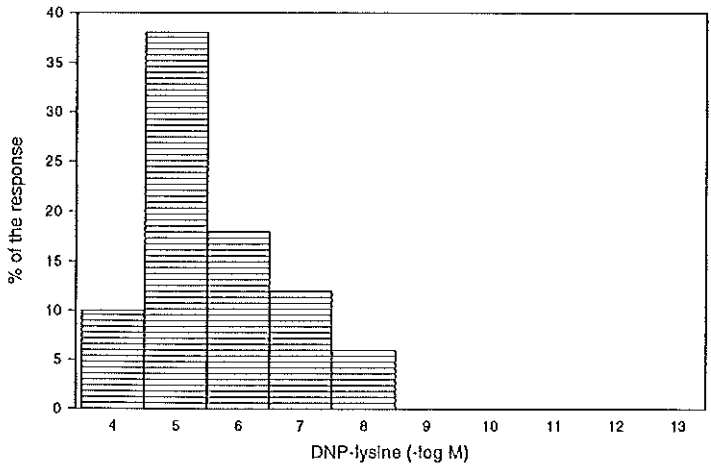

Figure 3 Histogram of the affinity distributions of DNP-specific serum antibodies. Sera were collected at certain days after immunization and run in a competitive inhibition ELISA. The abscissa indicates the concentration of free DNP-lys (-log M) used for inhibition. Affinity increases to the right. The ordinate shows the percentage of antibody present in each affinity subgroup.

4 Application of biosensors to interaction kinetics

For the understanding of structure-function relationships in biomolecular interactions and for the technical use of these biomolecules, the characteristic properties of the interaction must be known. Ideally, it should be possible to characterize the reaction between unlabeled reactants, but this has proved difficult by traditional methods (Karlsson et al., 1991). Evanescent optical sensing techniques are finding increasing applications for the monitoring of biomolecular interactions. They offer the ability to perform real-time quantitative assays allowing for the kinetic analysis of interactions, and are generic techniques applicable to a wide range of assays. They exploit the ability to perform assays at solid surfaces and use evanescent fields to probe changes in refractive index, layer thickness, absorption or fluorescence caused by reactions occurring within a few hundred nm of the sensor surface.

Two main types of optical evanescent sensors are commercially available: those based on surface plasmon resonance (SPR), and those based on waveguiding techniques (resonant mirror). Here we focus on the resonant mirror biosensor. The basic principle of the evanescent sensors is similar. When light travels through an optically denser medium, e.g. a glass prism, it is totally reflected back into the prism when reaching an interface to an optically less dense medium, provided that the angle of incidence is larger than the critical angle. This phenomenon is known as total internal reflection. Although the light is said to be totally reflected, a component of the incident light momentum, called the evanescent wave penetrates a distance of the order of one wavelength into the less dense medium to give the evanescent field. Both the commercially available optical biosensor types (IAsys^{tm} biosensor, Fisons plc, Applied Sensor Technology, Cambridge, UK; BIAcore^{tm} biosensor, Pharmacia Biosensor AB, Uppsala, Sweden) exploit this phenomenon of evanescent wave generation.

4.1 The resonant mirror biosensors

In the wave guiding technique devices, the sensing layer is placed in the evanescent region of guided mode propagating in a dielectric waveguide structure. The resonant mirror biosensor is essentially similar in structure to an SPR device. Light is totally internally reflected from the sensing surface by means of a prism. At the sensing surface, a dielectric resonant layer of high refractive index that is separated from the prism by a layer of low refractive index, is present. This low refractive index layer is sufficiently thin (around 1 μm) that light may couple into the resonant layer via the evanescent field. Efficient coupling occurs only for certain resonant angles, where phase matching between the incident beam and the resonant modes of high index layer is achieved. At the resonant point, light couples into the high index layer and propagates some distance along the sensing interface before coupling back in the prism. The angle of excitation of resonance is sensitive to changes at the

sensing interface. By monitoring shifts in the resonance angle, changes occurring as a result of binding or dissociation of biomolecules can be measured in real-time. The IAsys biosensor is a cuvette system based on the resonant mirror waveguiding technique (Figure 4). It includes a sensor device with integrated optics incorporated in a reinsertable micro-cuvette sample cell, a resonance angle detector and a microprocessor based system controller. A micro-stirrer in the instrument ensures efficient transport of reagents and analytes to the sensor surface for kinetic analysis on the instrument. The inner surface of the micro-cuvette, i.e. the sensor surface, is coated with carboxymethylated dextran (CMD). This provides a hydrophilic and flexible matrix suitable for studies of biomolecular interactions and for efficient immobilization of ligands through covalent linkage of target molecules. Alternatively, cuvettes coated with silane are also available. The cuvette design minimizes sample requirements and offers the possibilities of sample recovery and re-insertion of the sample cells. The coated sample cells can be stored at refrigeration temperatures in between runs. This design also permits the operator to use a range of ligate volumes (50 to 200 µl). The change in the angle of resonance can be directly related to the presence and concentration of biomolecules in real-time. The instrument records this change in resonance angle in terms of arc-sec.

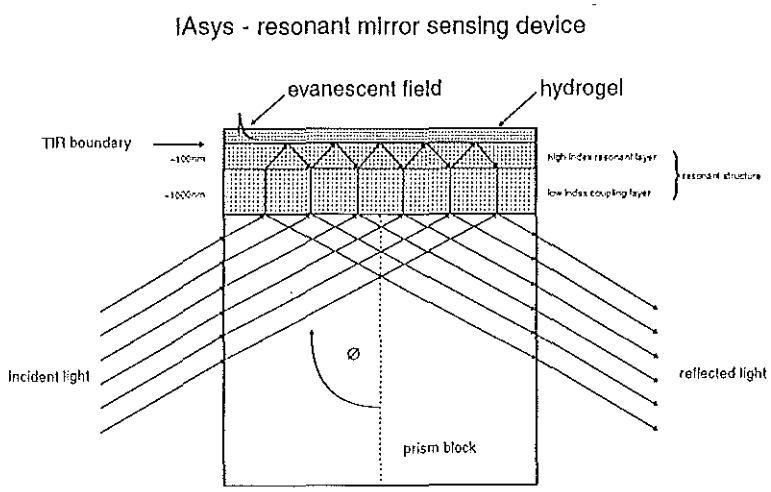

Figure 4 Schematic representation of the IAsys resonant mirror sensing device built in a disposable cuvette.

4.2 Immobilization of the ligand

For the biosensor, it is possible to immobilize various molecules to the CMD layer by conventional chemical methods. The ligand may be one of the reactants in the interaction of interest or a capture antibody having a high affinity for one of the reactants. In order to optimize the immobilization

procedure, the electrostatic uptake characteristics of the ligand should be evaluated with respect to concentration and immobilization pH. This allows sufficient concentration of protein available for immobilization onto the matrix. Buffer selection is dependent on the iso-electric point of protein to be immobilized. Generally, proteins are coupled most efficiently at pH close to their isoelectric point (pI). Proteins or peptides of interest can be immobilized by using simple carbodiimide chemistry (Lofas et al., 1991). The dextran surface is activated by adding a mixture of N-ethyl-N' (dimethyl-aminopropyl)carbodiimide and N-hydroxysuccinimide. Next, the protein/peptide of interest is added to the dextran layer. A covalent bond is formed between the free amines (e.g. lysine, arginine, histidine) or N-terminus on the peptide and the reactive ester group. The remaining activated groups are then deactivated by reaction with ethanolamine. A final wash with acid/alkali removes any unreacted but non-specifically bound molecules and the sensor is ready for studying biomolecular interactions. The immobilization step itself can be monitored in real-time allowing quantitation of the surface concentration of the immobilized ligand (Figure 5).

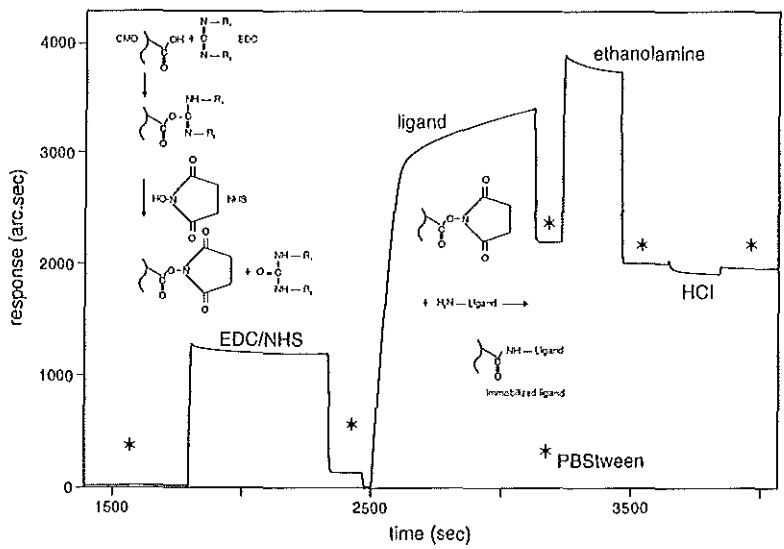

Figure 5 Profile of immobilization of ligand (protein) to CMD coated cuvette. The CMD is activated by the addition of EDC and NHS. The primary amino groups in the protein bind covalently to the carboxyl groups on the CMD. The surface is deactivated with ethanolamine and regenerated with HCl.

Ligand purity and homogeneity, proper choice of immobilization buffer, the extent of the electrostatic uptake, concentration of the ligand and the time of incubation of the various immobilization reagents are all critical for the successful application of biosensor and have to be carefully standardized. The immobilized cuvette can be used for multiple runs. An appropriate reagent

(acid/alkali/urea) can be used for regeneration. The measurement of the resonance signal is volume-dependent up to a volume of 50 µl per cuvette after which the measurement becomes volume-independent. We therefore consider it essential to consistently use a constant volume in the cuvette. Moreover, a total volume exchange for running buffer with sample has to be avoided as it causes extensive baseline shifts.

The binding stoichiometry is calculated by the formula:

$$analyte{:}ligand = \frac{analyte\ response}{analyte\ MW} : \frac{ligand\ response}{ligand\ MW}$$

Multiple parameters are important in studying interaction analysis with the biosensor -

a. The quality of the ligand - Apart from factors like purity and homogeneity, the sensitivity of the ligand to the process of immobilization will affect the quality of the assay. The extent of denaturation and/or alteration in conformation may result in non-homogeneous ligand sites.
b. Immobilization - The gentleness and randomness of immobilization will affect the quality of the analysis. The level of immobilization is also important and will be dictated by the ligand-ligate system to be studied as well as the desired application.
c. The quality of the ligate - Purity of the ligate is not essential but desirable. Various proteins may react non-specifically with the coat, and the absence of such reaction must be ensured. If the preparation contains aggregates or fragments, the ligate may display a heterogeneity with respect to binding properties and complicate data interpretation. Non-specific binding is of special importance when the ligate is present in a complex protein mixture such as serum or supernatant.
d. Controls - Proper positive and negative controls must be included in the experiments. These can be used for correction of the non-specific binding as well as ensuring quality of immobilized cuvette even after multiple runs.
e. Method of regeneration - Ideally regeneration should be as gentle as possible, but at the same time, the agent must regenerate the entire surface. Repeated regenerations may affect the quality of the immobilized ligand. Often, for complex protein mixtures, one reagent may not be sufficient, and a combination of reagents could be investigated (HCl, EDTA, urea, high salt buffers, etc.).
f. Method of data analysis - It is possible to use either linear or non-linear regression for data analysis. However, the reaction between the immobilized ligand and the solution phase ligate can not be described by a simple linear equation and hence non-linear regression analysis is to be

preferred.

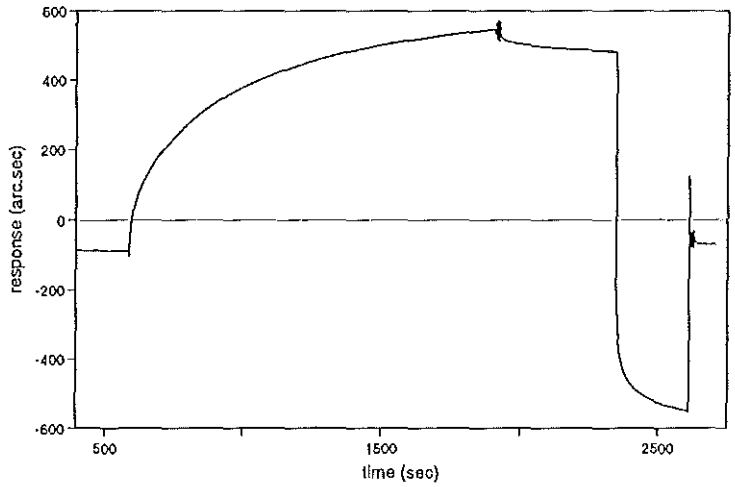

Figure 6 A typical dose response curve obtained on a biosensor. Goat anti-mouse-IgG was immobilized to the sensor surface. After establishing a base line, 50 µg/ml of mouse-IgG was added to it. The sample was replaced with PBS and allowed to dissociate for 4 min. The sensor surface was regenerated with an acid wash.

4.3 Interaction kinetics

Antigen-antibody interactions have been traditionally measured using a variety of methods such as radioimmunoassay, ELISA, fluorescence quenching, etc. All these approaches have many theoretical and practical drawbacks (Nygren et al., 1987; Malmborg et al., 1992). When information regarding the kinetics of the reaction *per se* is required, e.g. for studying affinity maturation, the binding characteristics of recombinant antibody fragments, the selection of monoclonal antibodies etc., rapid kinetic measurements are desired and the traditional methods are not suitable (Lofas et al., 1991). Biosensors have been successfully used for such measurements (reviewed in Malmqvist, 1993). Various dilutions of the ligate are added to the ligand-immobilized cuvette and the association kinetics followed in time. Replacing the ligate with buffer allows the dissociation kinetics to be studied in real-time as well. Figure 6 shows a typical dose-response curve obtained on a biosensor. This primary biosensor data can be treated in various ways to arrive at the kinetic constants. Most of the published studies use the traditional method involving linear transformations of the primary biosensor data for the determination of kinetic constants. However, linear transforms also transform the parameter-associated errors (Malmqvist, 1993). Accordingly, the use of non-linear regression are increasingly in use (O'Shannessy et al., 1993; Edwards et al., 1995).

4.4 Theoretical considerations

A detailed theoretical consideration of kinetic analysis is given elsewhere (Karlsson et al., 1991; O'Shannessy et al., 1993). Here, only the linear and non-linear regression analysis methods are briefly outlined. The monovalent homogeneous binding between monoclonal antibody (B) and its antigen (A) to form the complex (AB) can be expressed by the equation

$$[A]\ [B] \underset{k_{diss}}{\overset{k_{ass}}{\rightleftharpoons}} [AB] \tag{10}$$

The net rate of complex formation is given by

$$\frac{d[AB]}{dt} = k_{ass}[A]_t[B]_t - k_{diss}[AB]_t \tag{11}$$

When A is immobilized on the sensor surface, and the concentration of B is in large excess and continuously replenished at the boundary layer, a pseudo first order reaction results. The complex AB is monitored by the biosensor directly as the change in response against time, and the rate of change of response (R) with time can be given by

$$\frac{dR}{dt} = k_{ass}[B](R_{max} - R_t) - k_{diss}R_t \tag{12}$$

where

[B] - is the concentration of the ligate in the free solution

R_{max} - total number of binding sites for B on the immobilized ligand A expressed in the biosensor response R,

R_t - number of binding sites on A occupied at time t expressed as biosensor response

dR/dt - the rate of formation of the complex AB expressed as response R per second.

Rearrangement of the equation gives

$$\frac{dR}{dt} = k_{ass}[B]R_{max} - k_{ass}[B]R_t - k_{diss}R_t \tag{13}$$

When the response R is measured for varying dilutions of the sample (thus varying [B]), dR/dt can be calculated. The slope of a plot of dR/dt vs R, K' = k_{ass}[B] + k_{diss}. When these K' values are plotted against [B], a straight line results. The slope of this line is k_{ass} and the intercept is k_{diss}. The units of the association constant k_{ass} are $M^{-1}s^{-1}$. In general, when the k_{diss} is expected to be low (as is the case for antigen-antibody reactions) the intercept value is too close to zero and the error on the value too large to give a true k_{diss}. The dissociation of the complex [AB] is observed as a decrease in response when sample is replaced by a buffer. At this point the concentration of the free molecule [B] is zero, and from the above equation we arrive at

$$\frac{dR}{dt} = -k_{diss}R_t \tag{14}$$

When the conditions at the sensor are such that it can be assumed that there is no reassociation of the complex AB from the released B

$$\ln\frac{R_{t1}}{R_{tn}} = k_{diss}(t_n - t_1) \tag{15}$$

where

R_{t1} - response at starting time 1.. t_1,
R_{tn} - response at time n..t_n

A plot of decrease in response vs time yields a slope = k_{diss} in s^{-1}. The association constant can be calculated as $K_a = k_{ass}/k_{diss}$ in M^{-1}.

As noted earlier, linear transforms, such as those described above, also transform the errors in the primary data. In addition, little information is obtained to define the reproducibility or the certainty of the derived parameters. Non-linear regression helps circumvent these problems. It is not necessary to rearrange the original experimental results prior to analysis and so there is no distortion of the original error distributions (Leatherbarrow, 1990).

For non-linear regression analysis, the integrated form of the rate equation has to be used. In the cuvette (B) can be considered constant as it is added in large excess, and efficient stirring ensures that the concentration remains constant throughout the cuvette. Then, the concentration of antigen at time t ($[A]_t$) is given by

$$[A]_t=[A]_o-[AB]_t \tag{16}$$

$$\frac{d[AB]}{dt}=k_{ass}[B]([A]_o-[AB]_t)-k_{diss}[AB]_t \tag{17}$$

$$\frac{d[AB]}{dt}=k_{ass}[B][A]_o-[AB]_t(k_{ass}[B]+k_{diss}) \tag{18}$$

Separating the terms in $[AB]_t$ and t and integration yields

$$\int\frac{[AB]_t}{k_{ass}[B][A]_o-[AB]_t(k_{ass}[B]+k_{diss})}=\int dt \tag{19}$$

$$\frac{\ln(k_{ass}[B][A]_o-[AB]_t(k_{ass}[B]+k_{diss}))}{-(k_{ass}[B]+k_{diss})}=t+c \tag{20}$$

At

$$t=0,\ [AB]=0\ ,\quad \therefore\quad c=\frac{\ln(k_{ass}[B][A]_o)}{-(k_{ass}[B]+k_{diss})} \tag{21}$$

$$\frac{\ln(k_{ass}[B][A]_o - [AB]_t(k_{ass}[B]+k_{diss}))}{-(k_{ass}[B]+k_{diss})} = t - \frac{\ln(k_{ass}[B][A]_0)}{k_{ass}[B]+k_{diss}} \quad (22)$$

or

$$\frac{k_{ass}[B][A]_o - [AB]_t(k_{ass}[B]+k_{diss})}{k_{ass}[B][A]_o} = e^{-(k_{ass}[B]+k_{diss})t} \quad (23)$$

$$\therefore \quad [AB]_t = \frac{k_{ass}[B][A]_o}{k_{ass}[B]+k_{diss}}(1-e^{-(k_{ass}[B]+k_{diss})t}) \quad (24)$$

The term

$$\frac{k_{ass}[B][A]_o}{k_{ass}[B]+k_{diss}}$$

can be rearranged as

$$\frac{k_{ass}[B][A]_o}{k_{ass}[B]+k_{diss}} = \frac{[B][A]_o}{[B]+\frac{k_{diss}}{k_{ass}}} = \frac{[B][A]_o}{[B]+K_d} \quad (25)$$

This is equivalent to the Michaelis-Menten equation, and gives the [AB] at equilibrium ($[AB]_\infty$)

$$[AB]_t = [AB]_\infty (1-e^{-k_{on}t}) \quad (26)$$

where k_{on} is the observed pseudo first order constant.

[AB] at equilibrium can be termed the extent (E) of the reaction. Thus the association of the antibody with the immobilized antigen can be described by

the following pseudo first order equation

$$R_t = R_O + E\,(1 - e^{k_{on}t}) \tag{27}$$

where R_0 is the initial response and E is the extent of the change in response.

However, the instrument response does not always increase in a single exponential manner, and frequently at least two distinguishable phases are observed. This biphasic response is better described by

$$R_t = R_O + E_1(1 - e^{k_{on(1)}t}) + E_2(1 - e^{k_{on(2)}t}) \tag{28}$$

where E_1 is the extent of the first association phase characterized by the rate constant $k_{on(1)}$ and E_2 is the extent of the second association phase characterized by the rate constant $k_{on(2)}$.

To facilitate the calculations, the biosensor comes along with the necessary software packages that allow the use of non-linear regression analysis to fit the association phase of the interaction profiles to the equations above, eliminating the need for equilibrium binding to occur. The appropriate association phase data are selected and monophasic and biphasic fits are performed to arrive at an apparent on rate (k_{on}). The residual error plot, also produced by the program, allows the selection of the k_{on}. By determining the k_{on} for various concentrations of the ligate (minimum 5), a linear regression plot of k_{on} vs [B] is constructed. The slope of this plot is k_{ass} as described by the equation

$$k_{on} = k_{ass}[B] + k_{diss} \tag{29}$$

The intercept of the plot is k_{diss}. However, as suggested earlier, calculation of k_{diss} from such plots is likely to be erroneous. Data transformation needed in the linear regression analysis also transforms the error in the primary data. It is therefore better to calculate k_{diss} by non-linear regression analysis using the integrated rate equation

$$R_t = E.e^{-k_{diss}t} + R_f \qquad (30)$$

where

R_t - is the instrument response at time t after replacing ligate with buffer,
R_f - is the final response after dissociation is complete, and
E - is the extent of change in response.

Edwards et al. (1995) have investigated in details the application of biosensors to biomolecular interaction analysis. They have investigated the kinetic behaviour of biomolecules in biosensors and compared them to the behaviour in liquids. It is suggested that the biphasic responses observed in biosensors seem to be intrinsic to CMD surfaces (Malmqvist, 1993). The observed biphasic interaction is most probably due to steric hindrance caused by ligate binding to ligand immobilized to the CMD on the sensor surface. In such cases, the fast phase of the binding profiles should be directly comparable to the situation in free solution.

A number of precautions need to be taken while determining kinetic constants in biosensors. However, with an understanding of the possible artefacts that can interfere with biosensor measurements, it is possible to obtain relevant kinetic information even with unpurified material. Association rate constants in the range 10^3 to 10^6 $M^{-1}sec^{-1}$ and dissociation rates of 10^{-5} to 10^{-2} sec^{-1} are within the instruments capability, whereas determining equilibrium constants of molecules with high dissociation rates is especially difficult with conventional techniques (Nygren et al., 1987).

5 Conclusions

Biosensors can be defined as devices that combine a biological recognition mechanism with a suitable transducer, which generates a measurable signal in response to changes in concentration of a given biomolecule at the detector surface. They offer the possibility of characterizing biomolecular interactions in real-time without the need to label either of the reactants. Furthermore, due to the possibility of visualizing each step, complex assays can be relatively easily performed and controlled. In the conventional techniques, the quality of such assays can only be judged by the final step, and the defects, if any, in the intermediate steps cannot be identified easily. With adequate precautions and proper knowledge of the possible artefacts, this technology promises to open avenues of research that were hitherto inaccessible or could be approached only very indirectly.

For the determination of functional affinity and avidity of Ig specific for macromolecular antigens, both ELISA and biosensor technology are available. Under these conditions conventional affinity determination by equilibrium dialysis is not feasible. ELISA-based affinity measurement is particularly helpful when ranking large series of e.g. monoclonal antibodies for their affinity for the same antigen. This method is less suitable for functional affinity determination because of the need for a generally large conversion factor. This conversion factor is based upon a comparison between the K_{rel} arrived at in ELISA with that measured in equilibrium dialysis or some such unequivocal method. Again this is not feasible for macromolecular antigens. The advent of the biosensor technology has enabled absolute affinity determination by permitting kinetic binding analysis by highly sensitive measurement of binding events on a sensor surface. This combined with the development of software enabling non-linear regression analysis of binding data has made measurements of association and dissociation rate constants possible. We see multiple applications of this methodology in typing monoclonal antibodies, following ongoing immune responses, characterization of receptor-ligand interactions and the binding of molecules to living cells, etc.

6 References

Beatty, J.D., *et al.* (1987) Method of analysis of non-competitive enzyme-immunoassays for antibody quantification. J. Immunol. Methods 100, 161-172.

Beatty, J.D., *et al.* (1987) Measurement of monoclonal antibody affinity by non-competitive enzyme immunoassay. J. Immunol. Methods 100, 173-179.

Bruderer, U., *et al.* (1992) Analyses of affinity distributions within polyclonal populations of antigen-specific antibodies. J. Immunol. Methods 151, 157-164.

Edwards, P.R., *et al.* (1995) Kinetics of protein-protein interactions at the surface of an optical biosensor. Anal. Biochem. in press.

Eisen, H.N., and Siskind, G.W. (1964) Variations in affinities of antibodies during the immune response. Biochemistry 3, 996-1008.

Fazekas De St. Groth, S. (1979) Quality of antibodies and cellular receptors. In: Immunological Methods, Vol. I. Lefkovits, I., Pernis, B. (Eds.) Academic Press, New York, pp 1-42.

Friguet, B., *et al.* (1985) Measurements of true affinity constant in solution of antigen-antibody complexes by enzyme-linked immunosorbent assays. J. Immunol. Methods 77, 305-319.

Gaze, S.N., *et al.* (1973) The use of a double-isotope method in the determination of antibody affinity. J. Immunol. Methods 3, 357-364.

Germuth, F.G., *et al.* (1979) Passive immune complex glomerulonephritis in mice models for various lesions found in human disease. 1. High avidity complexes and mesangiopathic glomerulonephritis. Lab. Invest. 41, 360-365.

Goldberg, M.E., and Djavadi-Ohaniance, L. (1993) Methods for measurement of antibody/antigen affinity based on ELISA and RIA. Curr. Opin. Immunol. 5, 278-281.

Heegaard, N.H.H., and Bjerrum, O.J. (1991) Affinity electrophoresis for determination of binding constants for antibody-antigen reactions. Anal. Biochem. 195, 319-326.

Karlsson, R., *et al.* (1991) Kinetic analysis of monoclonal antibody-antigen interactions with a new biosensor based analytical system. J. Immunol. Methods 145, 229-240.

Leatherbarrow, R.J. (1990) Using linear and non-linear regression to fit biochemical data. Trends Biochem. Sci. 15, 455-458.

Lee, R.G., *et al.* (1974) Competitive adsorption of plasma proteins on to polymer surfaces. Thromb. Res. 4, 485-490.

Li, C.K. (1985) ELISA-based determination of immunological binding constants. Mol. Immunol. 22, 321-327.

Lofas, S., *et al.* (1991) Bioanalysis with surface plasmon resonance. Sensors Actuators 5, 79-84.

Malmborg, A.-C., *et al.* (1992) Real-time analysis of antibody-antigen reaction kinetics. Scand. J. Immunol. 35, 643-650.

Malmqvist, M. (1993) Surface plasmon resonance for detection and measurement of antibody-antigen affinity and kinetics. Curr. Opin. Immunol. 5, 282-286.

Matikainen, M.T., and Lehtonen, O.-P. (1984) Relation between avidity and specificity of monoclonal anti-chlamydial antibodies in culture supernatants and ascitic fluids determined by enzyme immunoassay. J. Immunol. Methods 72, 341-347.

Nieto, A., *et al.* (1984) Direct measurement of antibody affinity distribution by hapten-inhibition enzyme immunoassay. Mol. Immunol. 21, 537-542.

Nimmo, G.R., *et al.* (1984) Influence of antibody affinity on the performance of different antibody assays. J. Immunol. Methods 72, 177-187.

Nygren, H., *et al.* (1987) Kinetics of antibody binding to solid-phase-immobilised antigen. Effect of diffusion rate limitation and steric interaction. J. Immunol. Methods 101, 63-71.

O'Shannessy, D.J., *et al.* (1993) Determination of rate and equilibrium binding constants for macromolecular interactions using surface plasmon resonance: Use of non-linear least square analysis methods. Analyt. Biochem. 212, 457-468.

Pathak, S.S., *et al.* (1989) Terasaki-ELISA for murine IgE: III. Determination of absolute concentration and functional affinity sequential equilibrium binding analysis. J. Immunol. Methods 123, 71-81.

Rath, S., *et al.* (1988) An inhibition enzyme immunoassay for estimating relative antibody affinity and affinity heterogeneity. J. Immunol. Methods 106, 245-249.

Rizzo, L.V., *et al.* (1992) Generation of B cell memory and affinity maturation. Induction with Th1 and Th2 T cell clones. J. Immunol. 148, 3733-3739.

Scatchard, G. (1949) The attraction of protiens to small molecules and ions. Ann. N. Y. Acad. Sci. 51, 660-672.

Soos, M., and Siddle, K. (1982) Characterization of monoclonal antibodies directed against human thyroid-stimulating hormone. J. Immunol. Methods 51, 57-68.

Steward, M.W., and Lew, A.M. (1985) The importance of antibody affinity in the performance of immunoassays for antibody. J. Immunol. Methods 78, 173-190.

Van Dam, G.J., *et al.* (1989) Estimation of the avidity of antibodies in polyclonal antisera against *Streptococcus pneumoniae* type 3 by inhibition ELISA. Mol. Immunol. 26, 269-274.

Yee, E. (1991) Reconstruction of the antibody affinity distribution from the experimental data by a minimum cross-entropy procedure. J. Theor. Biol. 153, 205-227.

CHAPTER 3.2

Application of a resonant mirror biosensor to the determination of functional affinity of monoclonal and polyclonal antibodies

S.S. Pathak, G.J.M. Tibbe and H.F.J. Savelkoul

Department of Immunology, Erasmus University, P.O. Box 1738, 3000 DR Rotterdam, The Netherlands

Abstract

A biosensor based on optical resonance was evaluated for its usability for the determination of functional affinity of monoclonal and polyclonal antibodies. After establishing important parameters for the immobilization of various proteins to the cuvette-shaped sensor surface, the biosensor was employed for affinity determinations. The affinity of antigen-specific antibodies was determined using a direct method. A sandwich format was adopted for the measurement of the interaction constant K_A of TNP-specific IgG1 in mouse serum. The data obtained was evaluated by non-linear regression analysis. We found that it was possible to determine the affinity of the reaction between the antigen and monoclonal or polyclonal antibodies by the biosensor. The K_A of the antibody preparations was found to be between 3.3×10^6 and 3.6×10^7 M^{-1}. Data regarding the relative affinity distributions of antigen-specific IgG1 was obtained by competitive elution. The affinity distributions determination, however, took a rather long time and did not compare favorably with other methods for determination of relative affinity distributions, such as ELISA.

Introduction

Antibody-antigen interactions are reversible and can be characterized by measuring both the association and dissociation rate constants. The resulting equilibrium constant is conventionally defined as affinity in case of a monovalent antibody binding site reacting with a monovalent determinant. When both antibody and antigen are multivalent, the equilibrium constant has been termed avidity. Avidity, thus, depends upon affinity but also involves other contributory factors such as valency, the method of determination, etc. that are not necessarily concerned with the primary antibody-antigen reaction. In a polyclonal situation, eg. estimation of the affinity of antisera, the situation is further complicated by the fact that the serum is a mixture of antibodies of different affinities. Thus, the affinity of all the antigen-specific antibodies in the serum is an average or functional affinity (Steensgaard et al., 1980). This functional affinity is influenced by the affinity distributions of the various

antibodies capable of reacting with the same epitope as well as the method of determination.

It is known that the binding of antibodies produced by the immune system in response to foreign antigens is heterogeneous and that the distribution of association constants of the antigen-antibody reaction evolves in time under various circumstances (Eisen and Siskind, 1964). The study of the antibody distribution patterns as a function of time after immunization is useful for the quantitation of the immune memory (Werblin and Siskind, 1972; Yee, 1991). The affinity constants of polyclonal serum antibodies represent the overall binding properties of a normally heterogeneous population of antigen-specific antibodies and have limited usage (Bruderer et al., 1992). An accurate assessment of affinity distributions within polyclonal populations of antigen-specific antibodies depends either on the isolation of antibody populations according to differences in affinity, or on the detectability of these populations in the presence of additional populations with the same specificity. Such isolation and quantitation of antigen-specific antibodies requires large samples and is difficult and labor intensive. Moreover, an accurate detection of the affinity populations in polyclonal samples is problematic due to the complexity of the populations to be analyzed and the multiplicity of the possible interactions.

Conventionally, the determination of antibody affinity requires the measurement, at equilibrium, of antibody-bound and free antigen or antigen-bound and free antibody. Only those methods that do not disturb the equilibrium and do not preferentially detect antibodies of a particular affinity can be employed for such determinations. In practical terms the analysis requires the availability of large amounts of purified (radio-, enzyme- or fluorescent-) labeled ligand, undamaged by the labeling procedure. Determination of affinity distributions has proved to be even more problematic, though several ELISA based assays have been described for the measurement of relative affinity distributions (Nieto et al., 1984; Rath et al., 1988; Van Dam et al., 1989; Pathak and Savelkoul, 1995).

Recently, biosensor technology has made it possible to measure the kinetics of antigen-antibody interactions in real-time. None of the reactants need to be labeled in this system. The optical resonant mirror biosensor measures optical phase changes with respect to the angle of incidence occurring when an analyte binds to its partner immobilized on a sensor surface (Buckle et al., 1993). The sensing surface is present in the form of a disposable cuvette. A microstirrer ensures efficient transport of the analyte to the immobilized ligand, minimizing mass transport limitations making the system suitable for kinetic analysis (Karlsson et al., 1991). Such analysis can only be performed when the concentration of antigen-specific antibodies has been determined previously. The optical biosensor permits both concentration and affinity determinations.

This study reports the use of optical biosensor technology for the determination of functional affinity of interactions between haptens and immunoglobulins (Ig) as well as Ig and anti-Ig. Furthermore, we demonstrate the use of this system for determinations of relative affinity distributions of antigen-specific serum antibodies.

Materials and methods

Mice

Female BALB/c mice (age 12-16 weeks) were bred and maintained in the animal facilities of our department under conventional conditions under a protocol approved by the local Animal Welfare Committee.

Reagents and immunization

Chicken gamma globulin (CGG) was dinitrophenylated to a level of 5 dinitrophenyl (DNP) residues per molecule using dinitrobenzenesulfonic acid (Eastman Kodak, Rochester, NY) according to Koch et al. (1981). Keyhole limpet hemocyanin (KLH; Pierce, Rockford, IL) was trinitrophenylated to a level of 25 trinitrophenyl (TNP) residues per 10^5 Da molecular mass of KLH as determined spectroscopically (Hudson and Hay, 1976) by using trinitrobenzenesulfonic acid (Eastman Kodak). Polyclonal goat-anti-mouse-IgG1 (GAM/IgG1) was obtained from Southern Biotechnology Associates (SBA; Birmingham, AL). N-ε-DNP-L-lysine HCl was obtained from Sigma (St. Louis, MO). The rat IgG1 monoclonal antibodies 11B11 and XMG1.2 were the kind gift of Dr. R. L. Coffman (DNAX, Palo Alto, CA). The RG11/39.4 hybridoma was obtained from ATCC (Rockville, MD).

Mice were injected i.p.with 100 μg of TNP-KLH adsorbed on 2 mg of alum in 0.2 ml PBS (n = 5). Sera were collected by tail bleeding on day 120.

Measurement using biosensor technology

The IAsys^{tm} biosensor system (Fisons, Applied Sensor Technology, Cambridge, UK) is a cuvette system capable of real-time measurements of the reaction between biomolecules. It is thus an equilibrium non-dependent system that allows the measurement of the forward and reverse reaction rates and is therefore much quicker than the conventional methods. The sensing surface consists of a 100 - 200 nm thick carboxymethylated dextran hydrogel to which a protein can be immobilized. This sensing surface lies on the top of the resonant mirror of a high refractive index material that is placed on a low refractive index material which is in turn on the top of a prism block. The entire device is contained in a disposable cuvette. When laser light is totally internally reflected from the prism surface, at one unique angle, the resonant angle, the

light tunnels through the coupling layer and propagates along the waveguide before tunneling back rapidly through the coupling layer. The resonant light that propagates along the mirror produces an evanescent field that extends to the distance of one wavelength into the hydrogel thereby probing the sensor surface. Alterations in the refractive index and thickness of this layer influence the evanescent wave and so alter the resonant angle of the mirror. The shift in the angle of resonance occurring as a result of biomolecules binding to or dissociating from the surface can be monitored in real-time (Buckle et al., 1993). The IAsys allows the sampling of the resonant angle at predetermined time intervals and the response measured is expressed in arc.sec. We sampled the resonant angle every 0.2 seconds. The IAsys sensing chamber is connected to a circulating water bath allowing the choice of a range of temperatures. It was set at 25°C for all the experiments. All samples and buffers were also equilibrated to this temperature.

Immobilization of the ligand

The cuvette of the IAsys system is coated with high-molecular weight carboxymethylated dextran. It is possible to immobilize various molecules to this layer by conventional chemical methods (Fisons, 1993). It is essential to determine the optimal pH of the buffer to be used prior to immobilization. This was achieved by following the electrostatic uptake of the protein at various pH below the pI of the protein. The ideal concentration for immobilization was next determined by using the selected immobilization buffer and varying the concentrations of the protein.

Optimal immobilization conditions (as indicated in the results section) were used to coupe TNP-KLH or GAM/IgG1 or RG11/39.4 to the dextran via an amino-coupling method wherein the ligand amino groups are coupled to carboxyl groups of the dextran. The dextran was activated by adding 200 µl of a mixture containing a final concentration of 0.2 M N-ethyl-N'(dimethylaminopropyl)carbodiimide (EDC) and 0.05 M N-hydroxysuccinimide (NHS) for 8 min. Next, appropriate concentrations of the proteins to be immobilized (TNP-KLH, GAM/IgG1 or RG11/39.4), were added to the cuvette and the reaction was allowed to occur for various time periods. The surface was then deactivated by allowing it to react with 200 µl of 1 M ethanolamine, washed with 10 mM HCl to remove any unreacted protein and stabilized in PBS containing 0.1% Tween 20 (PBS/T). The cuvettes were then ready to study kinetic interactions.

Determination of K_A

Various samples of proteins (normal mouse serum, NMS; bovine serum albumin, BSA; KLH, etc) were added to the cuvette to determine the specificity of the reaction. Both direct and sandwich systems were used for affinity determinations. In the direct method, dilutions of the samples were added to

TNP/KLH or RG11/39.4 immobilized cuvette surface and allowed to react for a minimum of 5 minutes. The sample was aspirated, replaced by PBS/T and the dissociation studied for a further 5 min. To ensure isotype specificity of the reaction studied, a sandwich system was adopted. Dilutions of the serum were added to a GAM/IgG1 immobilized cuvette and allowed to react for precisely 5 min. After aspirating the sample, PBS/T was added to the cuvette (5 min) and a baseline established. DNP-CGG was next added to the cuvette and the association kinetics were followed for 5 min. The antigen was aspirated, replaced by PBS/T and the dissociation kinetics followed for a further 5 min.

The association rate of monovalent homogeneous binding between antibodies and their ligand can be described by an equation containing one exponential term

$$R_t = R_o + E(1 - e^{-k_{on}t}) \tag{1}$$

where R_t is the response at time t, R_0 is the initial response, E is the extent of change in response and k_{on} is the apparent on-rate.

However, when dealing with antibody populations, the association is better described by an equation containing two exponential terms

$$R_t = R_o + E_1 (1 - e^{-k_{on(1)}t} + E_2 (1 - e^{-k_{on(2)}t}) \tag{2}$$

where E_1 is the extent of the first association phase, which is characterized by the rate constant $k_{on(1)}$, and E_2 is the extent of the second phase having a rate constant $k_{on(2)}$.

Experimental data from the IAsys instrument were analyzed by a data analysis program (FASTfit, Fisons Applied Sensor Technology, Cambridge). This program uses non-linear regression analysis to fit the association phase of interaction profiles to the equations shown above, thus eliminating the need for equilibrium binding to occur. The user selects the baseline region (routinely 30 sec), the association phase (generally 300 sec) and the dissociation phase (also 300 sec). Monophasic (equation 1) and biphasic (equation 2) fits are performed to arrive at the apparent on-rates. The residual error plot, produced by the program, allows the selection of the k_{on} from the relevant equation. If the data are found to be best described by a biphasic equation, thus producing two k_{on} values ($k_{on(1)}$ and $k_{on(2)}$), then $k_{on(1)}$ is used (Edwards et al., 1995). Interaction profiles

of at least five different predetermined concentrations of ligate are used to determine five different k_{on} values. These k_{on} values are then used to construct a plot of k_{on} at various ligate concentrations. Upon linear regression of this plot the association rate constant (k_{ass}) is found from the slope and the dissociation rate constant (k_{diss}) from the intercept. However, when dealing with ligates with a high affinity for the ligand, the k_{diss} value will be small and therefore the value obtained from the intercept is likely to contain a potential error. It is therefore advisable to determine the k_{diss} value form direct dissociation and fitting this experimental data by non-linear regression using the following equation

$$R_t = R_\infty + E \cdot e^{-k_{diss}t} \tag{3}$$

where R_t is the instrument response at time t, R_∞ is the final response after dissociation is complete, E is the extent of change in response and k_{diss} is the dissociation rate constant.

Determination of relative affinity distributions of anti-TNP serum IgG1

TNP-KLH was immobilized to the dextran layer as described. Appropriate dilution of the serum was added to the cuvette and allowed to react for 10 min. The serum was then aspirated and replaced by PBS/T. Increasing concentrations of free DNP-lysine were added to the buffer and elution was allowed to occur for 7 min. At lower concentrations of the hapten, lower affinity antibodies would be eluted from the coat, while high affinity antibodies would require much higher competing concentrations of the hapten for elution. A similar experiment was performed using 30 min reaction time and 40 min elution time.

Results

Electrostatic uptake

In order to optimize the immobilization procedure, the electrostatic uptake characteristics of the ligand should be evaluated with respect to concentration and pH of immobilization. The pH chosen must allow sufficient concentration of protein to be available on the matrix. When immobilizing TNP-KLH, several pH buffers starting 0.5 pH unit below the iso-electric point (pI = 6.5) were used to evaluate the capacity of the dextran layer in the cuvette to bind the TNP-KLH hapten-carrier complex. The results (Figure 1A) show that a pH of 4.5 was suitable to immobilize TNP-KLH since it allows a high electrostatic uptake of the complex onto the matrix. The results also showed that at a concentration

of 25 µg/ml an optimal electrostatic uptake of TNP-KLH was achieved (Figure 1B). When evaluating the electrostatic uptake of polyclonal antisera (with the pI of the various IgG subclasses ranging between 6 and 8), on the other hand, the maximum electrostatic binding was obtained with 25 µg/ml at pH 5.0 (Table 1). At higher pH a significant drop in the electrostatic uptake capacity of the hydrogel was observed.

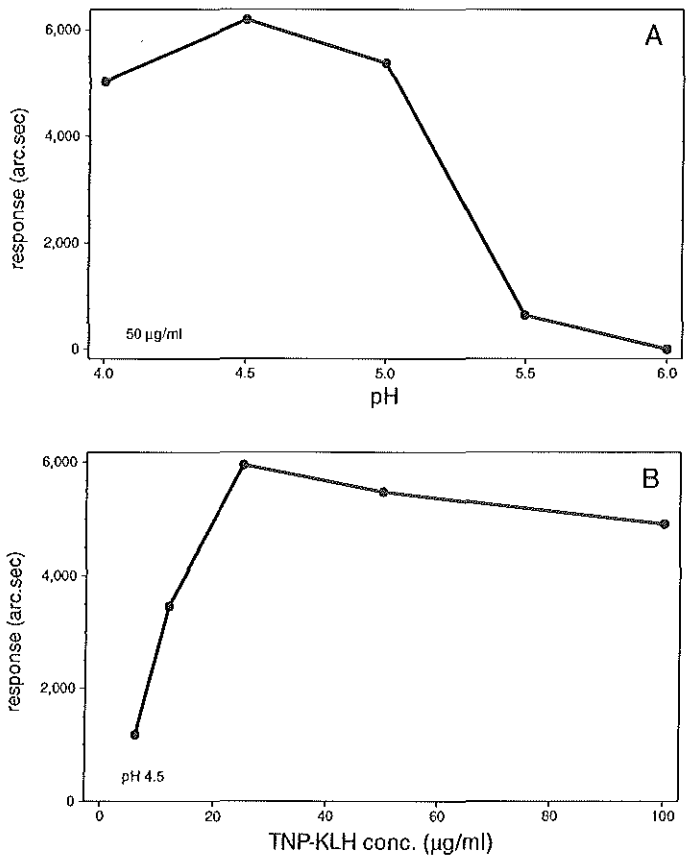

Figure 1 Electrostatic uptake of TNP-KLH by the dextran layer of the biosensor cuvette. 200 µl of 50 µg/ml of TNP-KLH in 10 mM sodium acetate buffers of varying pH were added to the cuvette (A). A buffer of pH 4.5 was used to make up various concentrations of TNP-KLH (B).

Immobilization

Immobilization of the ligand was carried out after establishing suitable coating conditions on the basis of the results obtained for the electrostatic uptake. After the coating, the resonance signal was evaluated in order to establish the baseline. When comparing the various resonance results from the electrostatic uptake conditions with the resonance signals obtained after the coating for several antibodies, we observed that the after-coating resonance signal

reflected on average 29.7 % (± 6.1, n = 6) of the electrostatic uptake resonance signal (data not shown).

Table 1 Electrostatic uptake of rabbit antibodies at different pH

pH	plateau level
3.5	5124
4.0	6228
4.5	7266
5.0	7833
5.5	6117
6.0	1154

Polyclonal rabbit antibodies specific for rat Ig were diluted to 25 µg/ml in 50 mM sodium acetate of different pH. Electrostatic uptake was determined after 5 min reaction time in a fresh uncoated cuvette.
Plateau levels in arc.sec were corrected for background (PBS/T) values.

Adjusting the time and concentration of the ligand to be immobilized can control the level of immobilization. For example, addition of 10 µg/ml of antibody (GAM/IgG1) for 75 seconds in 10 mM sodium acetate, pH 5.0, gave an immobilization level of 155 arc.sec, while a solution of 25 µg/ml of antibody (GAM/IgG1) for 8 min represented a level of 1680 arc.sec. The binding stoichiometry was calculated by the formula:

$$\text{analyte : ligand} = \frac{\text{analyte response}}{\text{analyte MW}} : \frac{\text{ligand response}}{\text{ligand MW}}$$

Characteristics of the immobilized cuvette

A high degree of non-specific binding was observed when the TNP-KLH coated cuvette was exposed to solutions containing 1% ($^{w}/_{v}$) BSA or 2% ($^{v}/_{v}$) NMS. This non-specific binding could be removed by washing with PBS/T (Figure 2). The BSA signal was completely removed after washing for about 200 seconds, while the NMS signal could only be partially removed in this time span. Buffer optimization (addition of varying concentrations of non-specific proteins, changes in concentration of Tween 20, etc.) was undertaken to reduce this non-specific binding. Moreover, the degree of immobilization influenced the non-specific reaction. It was especially pronounced at higher levels of immobilization (2500 arc.sec). At low levels of immobilization (120 - 200 arc.sec), however, the non-specific binding was negligible.

The stability of the immobilized surfaces was monitored by including the respective positive controls in the runs. When any immobilized surface was found to degenerate because of repeated acid washes (> 10% shift in arc.

sec), a fresh cuvette was immobilized. Routinely, this happened after approximately 40 acid washes.

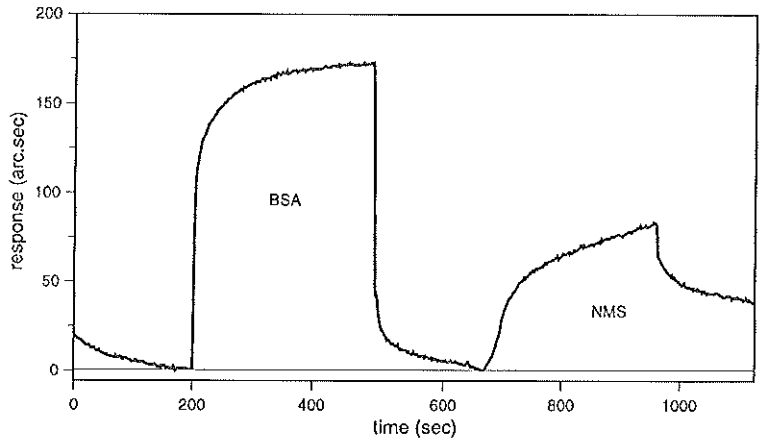

Figure 2 Profile of non-specific binding of 1% BSA or 2% NMS to a TNP-KLH immobilized cuvette.

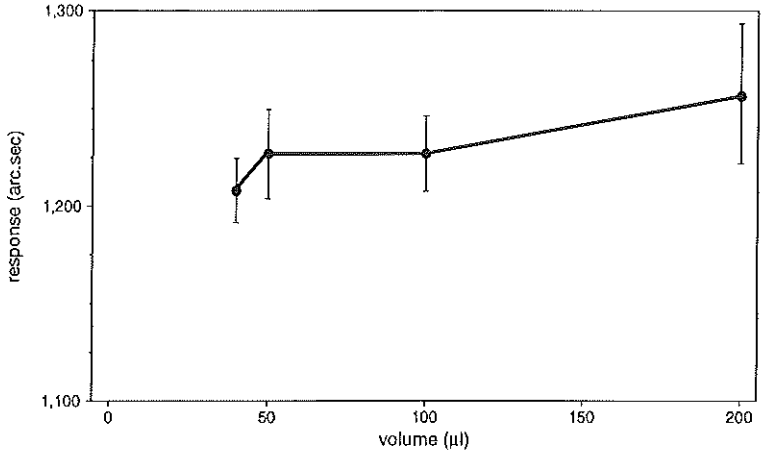

Figure 3 Volume dependence of response (arc.sec) measured in a GAM/IgG1 coated cuvette. Various volumes of 25 µg/ml of IgG1 were added to the cuvette and the maximum response was measured at 300 sec.

A cuvette containing immobilized antibody (GAM/IgG1) was used to determine the volume dependence of the cuvette system (Figure 3). The measurement of the resonance signal turned out to be volume-dependent up to a volume of 50 µl per cuvette after which the measurement became volume-independent. The refractive index is temperature sensitive. A total volume exchange for running

buffer with sample has to be avoided as it causes temporary, but extensive, baseline shifts (data not shown). To avoid fluctuations in temperature, we considered it essential to consistently use a constant basal volume (190 µl) in the cuvette and dilute the samples (10 µl) into it.

Table 2 The influence of immobilization on K_A determination

Level of immobilization (arc.sec)	K_A obtained (M^{-1})	Variance %	Binding Stoichiometry	Occupancy rate* (ng/mm^2)
150	3.27×10^6	8.5	1.3	0.92
500	3.47×10^6	20.1	0.47	3.25
1000	1.58×10^6	29.7	0.33	6.13

* The occupancy rate was calculated on the basis that 163 arc.sec represent 1 ng/mm^2 protein (Fisons, 1993)

The detection limit of the coated cuvette is partially dictated by the time of interaction. We found that at the level of immobilization achieved by us, the detection limit was between 10 to 100 µg/ml and was dependent on the interaction time. To allow accurate measurements at or near the detection limit of the system the baseline obtained with running buffer should be stable. With the cuvettes currently available, a stable baseline with a typical drift of about ± 2 response units per min was observed. Even a shift of 10-12 arc.sec due to the specific binding between the antigen and antibody was therefore measurable being significantly above the baseline. The cuvette was wrapped in parafilm and stored at 4°C in between runs. Addition of sodium azide to the cuvette did not influence results, although we preferred to leave azide out of the immobilization procedure (data not shown).

Determination of K_A

Various dilutions of the monoclonal antibodies were added to the cuvette and the association observed for 5 min. After aspirating the liquid and replacing by PBS/T, the dissociation was also observed for 5 min. The FASTfit program was used to fit the association curves to the pseudo first order equations described above. The k_{on} was plotted against the concentration (Figure 4). The slope of the graph gives the k_{ass}. We found that the level of immobilization was important in kinetic interaction analysis. High levels of immobilization resulted in a non-linear plot of k_{on} vs ligand concentration. The reproducibility of the data was also affected (Table 2). Though the detection limit of the analysis was affected by the amount of immobilized protein, the extent of the response did not increase linearly with the level of immobilization (Figure 5). An immobilization level of between 120 to 150 arc.sec was therefore selected for interaction analysis. In the direct method, dilutions of the serum were added to

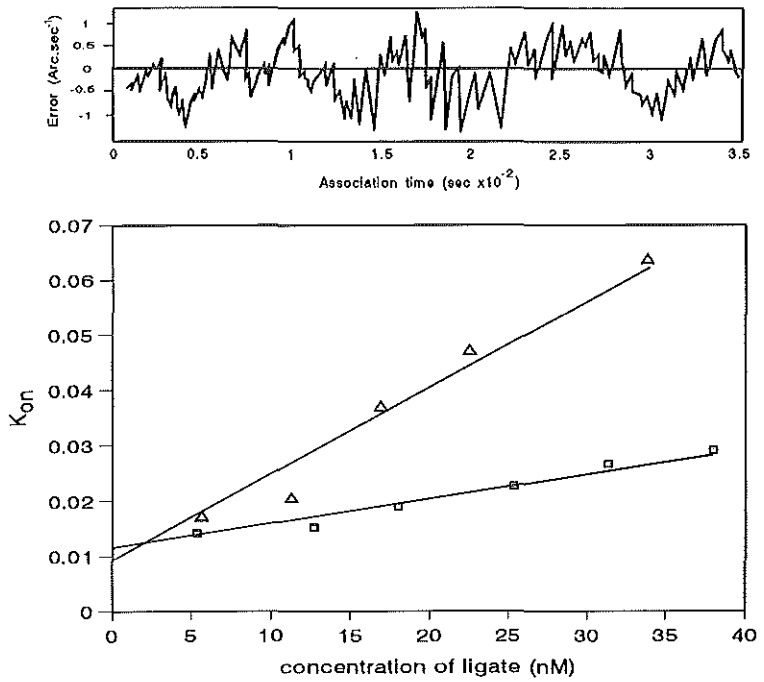

Figure 4 Plot of k_{on} against antibody concentrations for 11B11 (Δ) and XMG1.2 (□). Interaction profiles at five different concentrations of the ligate are used to arrive at the five k_{on} values. These were plotted against the antibody concentrations. The slope of the line gives the k_{ass} and the intercept the k_{diss}. The residual error plot of one such measurement is also shown.

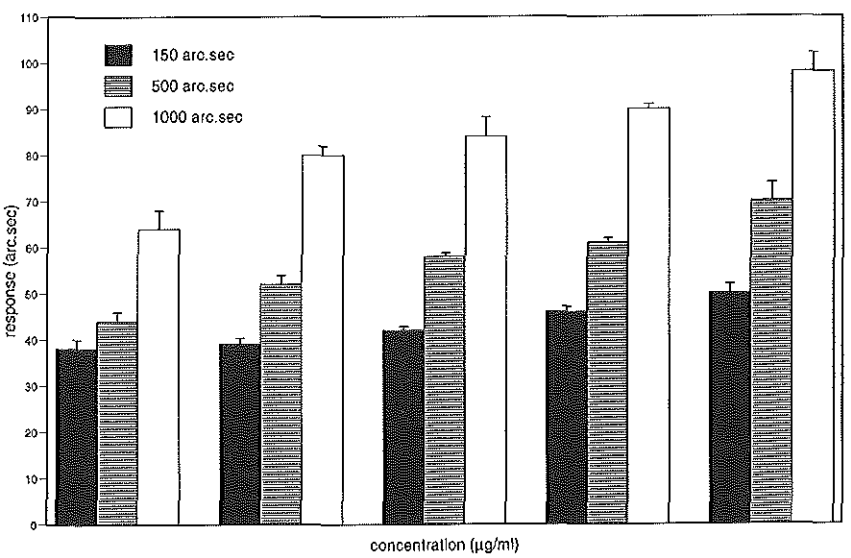

Figure 5 Influence of immobilization level on concentration determination. The ordinate indicates the response obtained with the biosensor in arc.sec. The abscissa indicates concentration of monoclonal antibody (µg/ml) added to the cuvette. Each bar represents the response obtained at the end of 5 min reaction time.

a TNP-KLH coated cuvette and the response noted for 5 min. The sample was replaced by PBS/T and the response followed for a further period of time. Figure 6 illustrates the determination of K_A from a typical run. Figure 6, left, demonstrates the responses of the different dilutions of the sample. The k_{on} values obtained by data fitting in the FASTfit program were plotted against the concentration of the antigen-specific IgG1 to yield a straight line (Figure 6, right).

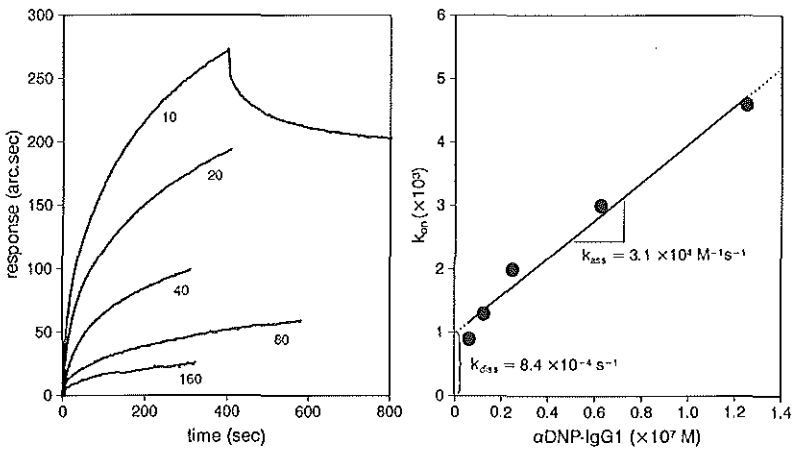

Figure 6 Determination of K_A of TNP-specific serum antibodies by the optical biosensor. Two-fold dilutions starting at a 1:20 dilution of serum in PBS/T were added to the cuvette for 5 min. The sample was aspirated and replaced with PBS/T. Subsequently, DNP-CGG was added to the cuvette. The response (R in arc.sec) was plotted against time (sec) for every serum dilution (*left*). Figures 10, 20, 40, 80, 160 represent reciprocal serum dilutions. From the 10-fold diluted serum the dissociation was also observed after replacing the sample with PBS/T. Interaction profiles at five different concentrations of the ligate were used to arrive at the five k_{on} values. The serum k_{on} values were plotted against the various serum anti-TNP IgG1 antibody concentrations (*right*). The slope of this graph is the k_{ass} (in $M^{-1}sec^{-1}$) while the intercept is k_{diss} (in sec^{-1}).

In the sandwich system, various dilutions of the serum were added to a GAM/IgG1 immobilized cuvette and the response profile measured for 5 min. The time of this first interaction was kept exactly constant ensuring that the amount of IgG1 binding to the immobilized GAM/IgG1 was a function of the serum concentration. The serum was then aspirated, PBS/T was added to the cuvette and allowed to equilibrate for 5 min. The interaction between DNP-CGG was then followed for a further 5 min. Figure 7 shows a typical interaction analysis profile of a sample run obtained. The results are tabulated in Table 3.

No appreciable dissociation was observed for both the monoclonal and polyclonal antibodies within the experimental time. The k_{diss} was therefore calculated from the intercept. In our limited experience the k_{diss} determination by the dissociation approach was consistently not significantly different from the intercept of a plot of k_{on} vs ligand concentration. Similar results have been

obtained by other workers (J. Aherne, personal communications).

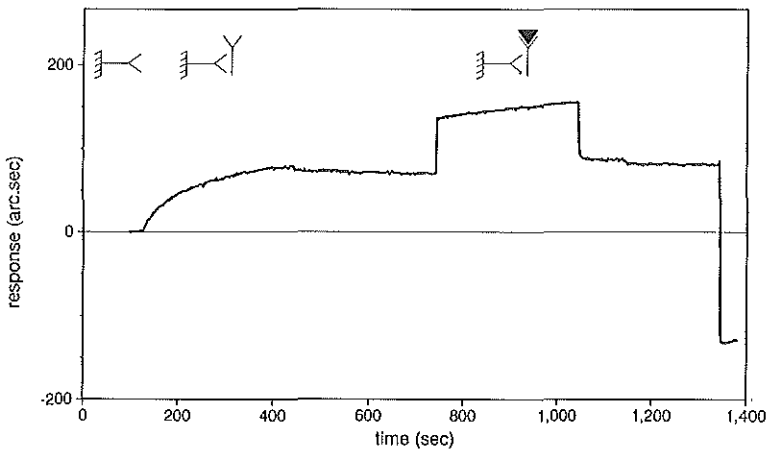

Figure 7 Interaction profile of a dilution of serum IgG1 with TNP-KLH. GAM/IgG1 was immobilized on the biosensor cuvette. An appropriate dilution of the serum sample was added to the cuvette and allowed to react for 5 min, the liquid was aspirated, PBS/T added and allowed to equilibrate. DNP-CGG was next added to the cuvette. The liquid was aspirated, PBS/T added and the dissociation recorded for 5 min.

Table 3 K_A determination of monoclonal and polyclonal antibodies

Antigen	Antibody	k_{ass} (M^{-1} sec^{-1})	k_{diss} (sec^{-1})	K_A (M^{-1})
TNP-KLH	serum IgG	3.1×10^4	8.4×10^{-4}	3.6×10^7
DNP-CGG	serum IgG1	2.7×10^3	8.3×10^{-5}	3.3×10^7
RG11/39.4	XMG1.2	3.3×10^4	1.0×10^{-2}	3.3×10^6
RG11/39.4	11B11	1.2×10^5	5.5×10^{-3}	2.0×10^7

Relative affinity distributions of anti-TNP serum IgG

For determining affinity distributions in the IAsys, it was necessary to establish conditions for binding and elution that permit repeated determinations with one sample in a reasonable time span. The serum from the immunized mice was added in an appropriate dilution to a TNP-KLH immobilized cuvette. TNP-specific IgG antibodies in the serum were thus bound out of the serum. The reaction was allowed to proceed for 10 and 30 min. The process of association was very quick and incubation for the longer time (30 min) did not appreciably increase the signal obtained. Incrementally increasing concentrations of free DNP-lysine (10^{-8} to 10^{-4} M) were next added to the cuvette. Two different elution times were used (7 and 40 min). Lower concentrations of free hapten eluted out low affinity fractions of antibodies, while higher concentrations were

required to elute out higher affinity subgroups. The percentage of antibodies in each affinity subgroup are represented in Figure 8. As is seen from the histogram, essentially similar results were obtained for both time schemes employed.

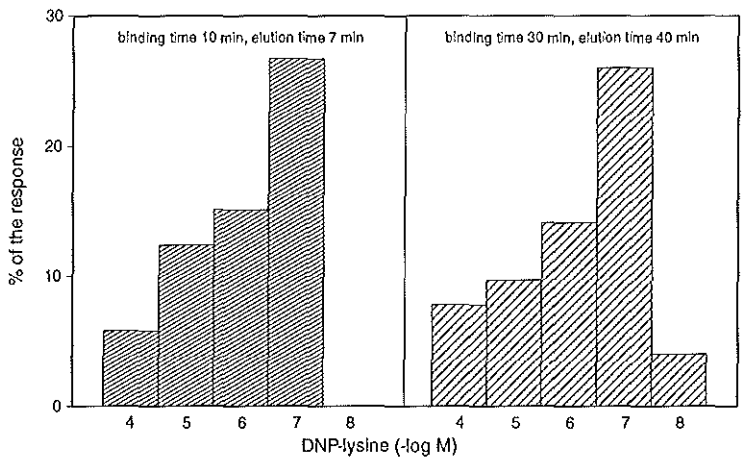

Figure 8 Relative affinity distribution of TNP-specific serum IgG antibodies as determined in biosensor. Serum (day 120) of mice immunized with TNP-KLH was added to a TNP-KLH immobilized cuvette. The association was allowed to occur for 10 (left) or 30 (right) min. Increasing increments of free DNP-lysine were then added to the cuvette and the elution was allowed to proceed for 7 (left) or 40 (right) min. The abscissa represents the concentration of free DNP-lysine (-log M) used for the elution. The ordinate shows the percent of antibody in each affinity subgroup.

Discussion

In this paper we demonstrate the potential application of a resonant mirror biosensor to establish the affinity constants of interactions between antigen-specific IgG1 antibodies and either the relevant antigen or isotype-specific antibodies. The study of interactions between such macromolecules is especially difficult by conventional techniques. We investigated the interaction of the antigen with both monoclonal and polyclonal antibodies. We also show that this method permits analysis of the distribution of antigen-specific antibodies belonging to various predefined affinity subgroups. It therefore promises to have a great potential in evaluation of ongoing immune responses.

The resonant mirror biosensor reported in this study is a cuvette-based stirred instrument that allows the study of biomolecular interactions in real-time. The ligand of interest is directly bound to the flexible hydrophilic matrix by a defined covalent linkage. Immobilization is therefore possible even at low concentrations (Fortune, 1993). The ligand is then accessible to three dimensional antibody interactions. The cuvette design minimizes sample requirements and dead volume. The stirrer ensures efficient mixing which should, together with the

open structure of the gel, minimize mass transport dependence. The change in the refractive index caused by the binding of the ligate to the ligand is measured by the instrument. This response is not dependent on absorption, emission of electromagnetic radiation etc., obviating the need for a detecting antibody or labeling.

We have earlier developed an ELISA based method for the relative affinity determination of monoclonal and polyclonal antibodies (Pathak et al., 1989). However, ELISA based methods of affinity measurement have many limitations. The kinetics of the interaction between an antibody and the solid phase bound ligand differ from the kinetics of the corresponding liquid phase reaction in several respects. The initial forward reaction often becomes diffusion rate limited (Stenberg et al., 1982; Nygren et al., 1987). Also, antigen-antibody reactions at solid-liquid interfaces can often be considered as practically irreversible and limited by mass transport or steric interactions (Stenberg and Nygren, 1988). The flexible dextran layer as well as the presence of the stirrer in the biosensor cuvette help overcome these difficulties. The immobilization procedure, however, may affect the three-dimensional conformation of the ligand, and hence influence the affinity of the reaction.

The cuvettes used in this study were coated with high molecular carboxymethylated dextran. In order to immobilize biomolecules efficiently (even at low concentrations of 10 µg/ml), sufficient concentration of the biomolecule is necessary in the dextran matrix. This can be achieved by electrostatic uptake. Electrostatic concentration relies upon the attraction between the negatively charged carboxyl groups on the dextran and the net positive charge on the biomolecule. The extent of electrostatic uptake is determined by the ionic strength and the pH of the immobilization buffer used. As reported, we find that the pH of the buffer should be above the pK_A of the carboxyl groups on the dextran and below the pI of the biomolecule. The ionic strength should be low. The extent of immobilization needs to be standardized for the desired application. We find that a low level of immobilization (120 - 150 arc.sec) best suited for interaction analysis. At high levels of immobilization factors other than the primary antigen-antibody interaction probably come into play as suggested by Edwards et al. (1995).

The biomolecular interaction at the sensor surface leads to a change in the angle of resonance. The interaction can therefore be followed in real-time. Factors other than the interaction process itself may contribute to the interaction profiles produced by the instrument. The change in the bulk refractive index and sample dispersion may distort the profile at the time of sample addition. Hence routinely the association analysis region was selected such that the first point was 5 sec after the addition of the antibody sample. Also, mass transfer processes may limit transfer of analyte to and from the sensor surface. Adjusting the stirrer speed helps minimize these restrictions.

The software supplied with the instrument allows relatively rapid data analysis. Error plots produced by the program helps ensuring that there are no major or systematic deviations of the data from the fitted curve. Typically, the errors were within 1 arc second and were randomly distributed. Unlike ELISA, the biosensor has no built in specificity. If K_A determination of a particular Ig isotype antibody for its antigen is desired, specificity has to be introduced in the system. The sandwich system adopted by us offers the advantage of ensuring that the k_{on} measured was specifically due to the reaction between antigen-specific antibody of a particular isotype and the hapten-carrier conjugate. We have tried to establish the k_{diss} by allowing the antibody to dissociate in PBS/T for 5 min. However, in all the cases studied, we failed to achieve appreciable dissociation. It is possible that the antibodies had indeed a low dissociation rate or, alternatively, reassociated with the bound antigen because the diffusion of the unbound ligate away from the surface was rate-limiting. The k_{diss} was therefore calculated from the intercept of k_{on} vs concentration plot.

We attempted to study the relative affinity distributions in a serum sample by a process of competitive elution. Varying binding times of the primary reactants were tested. The bound antigen-specific antibody was eluted by addition of increasing amounts of the free hapten. We find that it is possible to study affinity distributions by this method. The elution profiles were not significantly affected by increasing either the binding time or the elution time. However, the time required for such an analysis is rather long. This, together with the high detection limit of the system, does not compare favorably with other methods of relative affinity distributions such as competitive ELISA.

In conclusion, the methods described in this study using the IAsys optical biosensor with a cuvette-shaped sensor surface permit the determination of affinity constants and the analysis of affinity distributions of antigen-specific antibodies. We propose to use this system in studies of affinity maturation during ongoing immune responses.

Acknowledgements

We thank drs. D. Wenham, P. Edwards, and P. Buckle (FAST, Cambridge, UK) for helpful advice and discussions, Mr. S. Erkeland for technical assistance and Mr. T.M. van Os for preparation of the figures.

References

Bruderer, U., Deusinger, M., Schurch, U. and Lang, A.B. (1992) Analyses of affinity distributions within polyclonal populations of antigen-specific antibodies. Evaluation of their accuracy in population detection using monoclonal antibodies. J. Immunol. Methods 151, 157.

Buckle, P.E., Davies R.J., Kinning, T., Yeung, D., Edwards, P.R. and Pollard-Knight D. (1993) The resonant mirror: a novel optical sensor for direct sensing of biomolecular interactions Part II: Applications. Biosensors and Bioelectronics 8, 355.

Edwards, P.R., Gill, A., Pollard-Knight, D.V., Hoare, M., Buckle, P.E., Lowe, P.A., Leatherbarrow, R.J. (1995) Kinetics of protein-protein interactions at the surface of an optical biosensor. Anal. Biochem. (in press).

Eisen, H.N. and Siskind, G.W. (1964) Variations in affinities of antibodies during the immune response. Biochemistry 3, 996.

Fisons Applied Sensor Technology (1993) IAsys Methods Guide.

Fortune, D. (1993) Binding and kinetics-new dimensions in optical biosensor analysis. Biosens. Bioelectr. 8, xxxii.

Hudson, L. and Hay, F.C. (1976) Initial preparations. In: Practical Immunology, Blackwell Scientific Publications, Oxford, London, p. 1.

Karlsson, R., Michaelsson, A. and Mattson, L. (1991) Kinetic analysis of monoclonal antibody-antigen interactions with a new biosensor based analytical system. J. Immunol. Methods 145, 229.

Koch, G., Osmond, D., Julius, M.H. and Benner, R. (1981) The mechanism of thymus-dependent antibody formation in bone marrow. J. Immunol. 126, 1447.

Nieto A., Gaya A., Jansa M., Moreno C., Vives J. (1984) Direct measurement of antibody affinity distribution by hapten-inhibition enzyme immunoassay. Mol. Immunol. 21, 537.

Nygren H., Werthen M. and Stenberg M. (1987) Kinetics of antibody binding to solid-phase-immobilized antigen. Effect of diffusion rate limitation and steric interaction. J. Immunol. Methods 101, 63.

Pathak, S.S., Vos, Q. and Savelkoul, H.F.J. (1989) Quantitation of concentration and functional affinity of immunoglobulins with special reference to Terasaki-ELISA. J. Immunol. Methods 123, 71.

Pathak S.S. and Savelkoul, H.F.J. (1995) Determination of relative affinity and affinity distributions in ELISA. (submitted)

Rath, S., Stanley, C.M. and Steward, M.W. (1988) An inhibition enzyme immunoassay for estimating relative antibody affinity and affinity heterogeneity. J. Immunol. Methods 106, 245.

Steensgaard, J., Steward, M.W. and Frich, J.R. (1980) The significance of antibody affinity heterogeneity in antigen-antibody reactions demonstrated by computer stimulation. Mol. Immunol. 17, 689.

Stenberg M. and Nygren H. (1988) Kinetics of antigen-antibody reactions at solid-liquid interface. J. Immunol. Meth. 113, 3.

Stenberg M., Elwing H. and Nygren H. (1982) Kinetics of reaction zone formation with radial diffusion of ligands over a receptor-coated surface. J. Theor. Biol. 113, 589.

Steward, M.W. and Steensgaard J. (1983) Antibody affinity: thermodynamic aspects and biological significance. CRC Press, Boca Raton, FL, p. 170.

Van Dam, G.J., Verheul, A.F.M., Zigterman, G.J.W.J., De Reuver, M.J. and Snippe, H. (1989) Estimation of the avidity of antibodies in polyclonal antisera against *Streptococcus pneumoniae* type 3 by inhibition ELISA. Mol. Immunol. 26, 269.

Werblin, T.P. and Siskind, G.W. (1972) Distribution of antibody affinities techniques of measurement. Immunochemistry 9, 987.

Yee, E. (1991) Reconstruction of the antibody affinity distributions from the experimental data by a minimum cross-entropy procedure. J. Theor. Biol. 153, 205.

CHAPTER 3.3

Interleukin-4 influences the pace of affinity maturation of IgG1 antibodies

S.S. Pathak, A.E.C.M. Vredendaal, R. Van Ommen and H.F.J. Savelkoul

Department of Immunology, Erasmus University, P.O. Box 1738, 3000 DR Rotterdam, The Netherlands

Abstract

The phenomenon of affinity maturation is observed only in the response to T cell dependent antigens. This phenomenon can be established by demonstrating changes in the affinity distributions of the antigen-specific antibodies with respect to time as well as showing an increase in the average affinity of the serum. Interleukin-4 (IL-4) is a multipotent cytokine that can influence isotype switching, germinal center formation as well as proliferation and survival of germinal center B cells. In this paper we investigate the influence of exogenous IL-4 on the process of affinity maturation, specifically the functional affinity and the affinity distributions of antigen-specific IgG1 in serum. A resonant mirror optical evanescent field sensory device was used to measure the functional affinity of the serum. The relative affinity distributions of subpopulations of antigen-specific IgG1 during the primary and secondary immune response to TNP-KLH was determined by using a hapten inhibition ELISA. Our results establish that affinity maturation clearly occurs during the production of IgG1 anti-TNP antibodies. This is reflected in the functional affinity and affinity distributions of the serum IgG1 antibodies. We found that exogenous IL-4 markedly influenced the affinity distributions, but not the functional affinity of the antigen-specific IgG1 response. A clear shift towards higher affinity subpopulations was observed in the TNP-specific serum IgG1 antibodies of mice implanted with alginate encapsulated CV-1/IL-4 cells that produce IL-4. The possible role of IL-4 in the process of affinity maturation is discussed.

Introduction

B cells undergo clonal expansion and later terminal differentiation on primary exposure to the antigen. The clonal expansion occurs in the germinal centers in the spleen and lymph nodes, and can only be observed in immune responses to T cell dependent (TD) antigens (Kroese et al., 1990; MacLennan et al., 1992). Antigen-induced B cell proliferation in the germinal centers activates a hypermutation mechanism by which point mutations are introduced into the

rearranged variable regions (Kocks and Rajewsky, 1988; Liu et al., 1992; Nossal, 1992). This, along with antigen selection of the B cells carrying the mutated V regions, leads to the phenomenon of affinity maturation, i.e. an increase in the average affinity of the antigen-specific antibody molecules with time (Sharon et al., 1989; Berek and Zeigner, 1993). During an induced immune response, the resulting serum is heterogeneous, consisting of a spectrum of different sub-populations of antigen-specific antibodies having different affinities (Varitek and Day, 1979; Berek and Milstein, 1987). The study of the antibody affinity distributions after immunization is useful for the quantitation of the generation of immune memory and is of particular interest in ongoing immune responses (Yee, 1991).

Interleukin-4 (IL-4) is known to be a pluripotent cytokine. It is necessary for isotype switching to IgG1 and IgE (Coffman and Carty 1986; Savelkoul et al., 1988; Coffman et al., 1993), the development of germinal centers (Butch et al., 1993), rescue of germinal center B cells from apoptosis (Thorbecke et al., 1994) and their continued proliferation (Butch and Nahm, 1992). However, the effect of IL-4 on the affinity maturation of serum IgG1 antibodies is not established. We have previously demonstrated that IL-4 leads to an increase in the concentration of total IgG1 in serum, but leads to a decrease in the IgG1 responses (Van Ommen et al., 1994). In this paper, we carry these studies further to demonstrate that IL-4 increases the pace of affinity maturation by shifting the affinity distributions of IgG1 antibodies to increased affinity subpopulations.

We investigated the use of a resonant mirror optical biosensor for functional affinity determinations in ongoing immune responses. The resonant mirror optical biosensor measures optical phase changes with respect to the angle of incidence occurring when an analyte binds to its partner immobilized to the sensor surface (Buckle et al., 1993). The sensing surface is present in the form of a disposable cuvette. A microstirrer ensures the efficient transport of the analyte to the immobilized ligand, minimizing mass transport limitations, so that the system is uniquely suitable for kinetic analysis. A competitive ELISA was used for the estimation of relative affinity distributions of the serum IgG1 antibodies. The validity and the applicability of this method has already been established (Rizzo et al., 1992; Pathak et al., 1995a).

Materials and methods

Mice

Female BALB/c mice (age 12-16 weeks) were bred and maintained in the animal facilities of our department under conventional conditions under a protocol approved by the local Animal Welfare Committee.

Preparation of antigens

Keyhole limpet haemocyanin (KLH; Pierce, Rockford, IL) was trinitrophenylated to a level of 25 TNP residues per 10^5 Da molecular mass of KLH as determined spectroscopically (Hudson and Hay, 1976) by using trinitrobenzenesulphonic acid (Eastman Kodak, Rochester, NY). Chicken gamma globulin (CGG) was dinitrophenylated to a level of 5 dinitrophenol (DNP) residues per protein molecule (DNP-CGG) by using dinitrobenzenesulfonic acid (Eastman Kodak) according to Koch et al. (1981).

IL-4 treatment

Mice were implanted with 2 x 10^6 CV-1/IL-4 cells encapsulated in alginate, every 2 weeks as described by Savelkoul et al. (1994). The monkey CV-1 cells stably transfected with the murine IL-4 gene under the control of SV40 promotor were a kind gift of Dr. N. Arai (DNAX Research Institute, Palo Alto, CA). The cells were grown on Cytodex 3 beads (Pharmacia, Uppsala, Sweden). Fully covered beads were harvested after 3 days of culture, washed with sterile saline, mixed with equal volumes each of sterile saline and 1.2% sterile cell-prep alginate (FMC, Bioproducts, Rockland, PA) and squirted through a 25 gauge needle into fresh 80 mM $CaCl_2$ solution. The encapsulated cells were washed with sterile saline (3x) and 2 x 10^6 encapsulated cells in 1 ml were injected i.p. with a 19-gauge needle. Empty beads encapsulated in alginate were used as control for IL-4 treatment. No immunological effects were observed after injection of alginate encapsulated beads (Savelkoul et al., 1994). The injection of CV-1/IL-4 cells was repeated every 2 weeks, since it has been established that IL-4 production starts declining after day 15 and IL-4 mRNA is no longer detectable in the encapsulated cells after day 18 post-implantation (Savelkoul et al., 1994).

Experimental design

The mice were divided into 3 groups (n = 5). The first group of mice were immunized i.p. with 0.2 ml of phosphate buffered saline (PBS) containing 100 µg of TNP-KLH adsorbed on 2 mg alum. Secondary immunization (0.2 ml of 10 µg TNP-KLH adsorbed on 2 mg alum; i.p.) followed after 120 days. Half of the group was treated with CV-1/IL-4 cells, while the other half (control) received empty beads. Sera were collected 14, 58 and 120 days after the primary immunization, and on day 4, 7, 11, 21 and 30 after secondary immunization.

The second group of mice were immunized 5 times with 0.2 ml of saline containing 100 µg of TNP-KLH (adsorbed on 2 mg alum) i.p. every 14 days. Half the group was treated with IL-4, while the other half received empty beads. Serum was collected on day 14 and 56.

The third group of mice were implanted with CV-1/IL-4 cells on day 0. They received 0.2 ml of PBS containing 100 µg/ml of TNP-KLH adsorbed on 2 mg alum i.p. on the same day. Serum was collected on days 14 and 56.

Determination of affinity distributions

The affinity distributions of IgG1 anti-TNP antibodies were determined in a TNP-specific isotype specific competitive ELISA (Rizzo et al., 1992; Pathak and Savelkoul, 1995). Serum samples were diluted and incubated overnight (4°C) with increasing concentrations of the monovalent hapten N-ε-DNP-L-lysine HCl (DNP-lys; 10^{-13} to 10^{-4} M in PBS; Sigma, St. Louis, MO). The mixtures were then transferred to ELISA plates coated with TNP-KLH. After incubation for 3 hrs the plates were washed and the amount of TNP-specific antibody was established by using biotinylated goat anti-mouse IgG1 (GAM/IgG1, Southern Biotechnology, Birmingham, AL), horseradish peroxidase conjugated streptavidin (Southern Biotechnology) and the substrate 2,2'-azino-bis(3-ethylbenz-thiazoline-6-sulfonic acid) (ABTS; Sigma). In this type of ELISA, the high affinity antibodies are inhibited from binding to the plates by low concentrations of free hapten. As the free hapten concentration increases incremently, lower affinity antibodies are inhibited until theoretically, at sufficiently high hapten concentrations, all DNP-specific antibodies are inhibited from binding.

Measurement of K_A using the IAsys applied biosensor technology

Instrumentation

The IAsys^{tm} biosensor system employed (Fisons plc, Applied Sensor Technology, Cambridge, UK) is a cuvette system capable of real-time measurements of reaction between biomolecules. It is an equilibrium non-dependent system that allows the measurement of the forward and reverse reaction rates and therefore is much quicker than the conventional methods. It includes a sensor device, the carboxymethylated dextran coated sample cell which includes integrated optics, a resonance angle detector instrument, and a micro-processor based instrument controller. Light is totally internally reflected from the sensing surface by a prism which is integrated in the disposable cuvette. When light irradiated at an appropriate angle of incidence at an high/low refractive index interface is totally internally reflected, an electromagnetic component of the light, the evanescent field, is generated (Cush et al., 1993). The sensing surface is prepared from a dielectric material of a high refractive index which is separated from the prism by a low refractive index layer. At discrete angles of incidence light couples into the high refractive index layer and propagates along the sensing layer before coupling back out again. The angle at which this occurs, is extremely sensitive to the refractive index and thickness at the sensor surface. The shift in

the angle of resonance (in arc.sec) occurring as a result of biomolecules binding to or dissociating from the surface can be monitored in real-time (Buckle et al., 1993).

Various molecules can be immobilized to a dextran coated cuvette. For immobilization, the dextran was activated by adding 200 µl of a mixture of equivalent amounts of N-ethyl-N'(dimethylaminopropyl)carbodiimide (EDC) and N-hydroxysuccinimide (NHS) for 8 min. GAM/IgG1 (10 µg/ml, in 10 mM acetate buffer, pH 5) was added to the cuvette for 75 sec. The surface was then deactivated with 200 µl of 1M ethanolamine, washed with 10 mM HCl and stabilized in PBS containing 0.1% Tween 20 (PBS/T). An immobilization level of 120 to 150 arc.sec was used for affinity determinations since we have previously established that this level of immobilization is suited for studying interaction kinetics (Pathak et al., 1995a). The detection limit of the GAM/IgG1 immobilized cuvettes was 10 - 100 µg/ml (Pathak et al., 1995a)

Determination of K_A of TNP-specific serum IgG1

The functional affinity of the TNP-specific IgG1 from the sera of the immunized mice was determined using a sandwich format as described elsewhere (Pathak et al., 1995a). Briefly, dilutions of the serum samples were added to the cuvette surface and allowed to react with the catching antibody for precisely 5 min. The sample was aspirated, PBS/T was added to the cuvette (5 min) and a baseline established. DNP-CGG was next added to the cuvette and the association kinetics were followed for 5 min. The antigen was aspirated and replaced with PBS/T. The dissociation kinetics were then followed for a further period of 5 min. Interaction profiles were established for at least five different concentrations of ligate and the experimental data analyzed by a data analysis program that is available with the instrument (FASTfit, Fisons Applied Sensor Technology). This program uses non-linear regression analysis to fit the association phase of interaction profiles to two different equations (for a monophasic or a biphasic fit) to arrive at an apparent on-rate (k_{on}) as described (Pathak et al., 1995b).

After setting the appropriate baseline (30 sec of flat baseline), the association analysis region was selected. Routinely, the first point of data analysis was chosen 5 sec after the addition of the ligate to allow for the bulk refractive index shift, caused by the change in buffer. The residual error plot, produced by the program, allows the selection of k_{on} from the relevant equation. If the data were found to be best described by a biphasic equation, thus producing two k_{on} values ($k_{on(1)}$ and $k_{on(2)}$), then $k_{on(1)}$ was used (Edwards et al., 1995). The slope of the linearly regressed plot of k_{on} versus the ligate concentrations gives the association rate constant (k_{ass}) and intercept gives the dissociation rate constant (k_{diss}).

Results

Relative affinity distributions of IgG1 antibodies in primary and secondary anti-TNP responses

To allow determination of affinity and affinity distributions, it was necessary to determine the concentration of the TNP-specific IgG1 antibodies in the sera. The results are tabulated in Table 1.

Table 1 Concentrations of TNP-specific serum IgG1 in immunized mice

Immunization	Treatment	Primary response			Secondary response	
		day 14	day 58	day 120	day 7	day 30
TNP-KLH twice	none	248±36	310±25	335±82	1272±277	2174±795
TNP-KLH twice	IL-4 continuous	318±23	598±133	47±5	639±53	2403±1010
		Days after treatment				
		day 14	day 56			
TNP-KLH 5 times	none	1544±59	31360±4335			
TNP-KLH 5 times	IL-4 continuous	488±348	8693±781			
TNP-KLH once	IL-4 once	440±15	470±198			

All the concentrations are in µg/ml ± SEM.

Figure 1 shows the relative affinity distributions of the IgG1 anti-TNP antibodies at various time points in the control group. The histogram represents the affinity distribution profile of one animal. Essentially similar profiles were obtained for other animals of the group as well. We were interested in the overall pattern of affinity distributions in predefined classes at various time points after immunization. We wanted to establish whether this pattern changed, and whether new subgroups appeared or disappeared at later stages of immunization. Repeated testing of the sera gave an acceptable level of variation in the individual inhibition subgroups (± 10%). Though a variation was observed in individual mice belonging to a particular group in terms of the extent of inhibition at a particular concentration of free DNP-lys, the overall affinity subgroups spanned by them did not differ more than one inhibition class. The sera of the primary day 14 immune response consisted

of a population of antibodies that were inhibited only at the highest concentration of DNP-lysine (10^{-4} M) employed, indicating the presence of very low affinity antibodies. The shift to higher affinity antibody classes was clearly seen in the primary response when sera from different time points were compared. The affinity changed from very low to higher affinity subclasses at day 58 and 120. The major population of antibodies in the primary response seemed to lie in an affinity range indicated by inhibition between 10^{-5} to 10^{-8} M DNP-lysine. The sera from the secondary day 7 immune response, on the other hand, had almost no very low affinity sub-classes (Figure 1). The majority of the antibodies lied in the inhibition range of 10^{-8} and 10^{-9} M DNP-lys. The low affinity antibodies reappeared at day 30 of the secondary response along with a population of very high affinity antibodies (11% inhibited by 10^{-13} M DNP-lys).

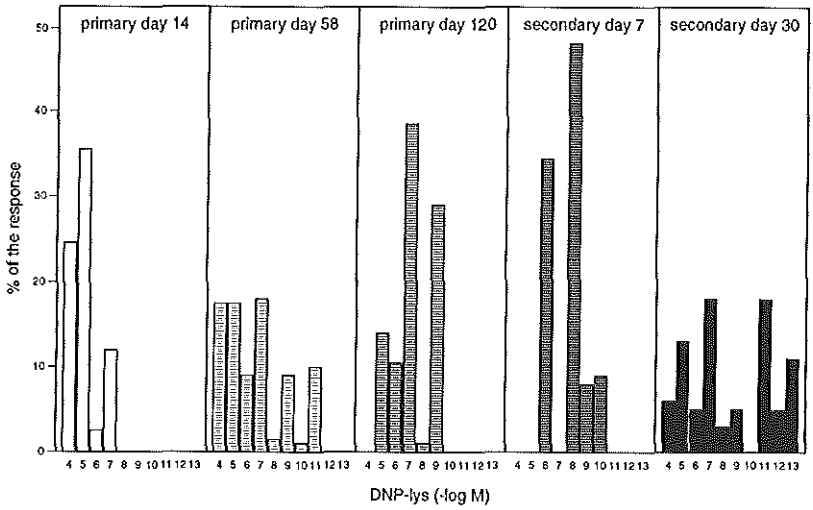

Figure 1 Relative affinity distributions of TNP-specific IgG1 antibodies. Female BALB/c mice were immunized (i.p.) with 100 µg of TNP-KLH on alum. Serum was collected on days 7, 58 and 120. The animals were boosted with 10 µg of the antigen and serum collected on days 7 and 30. Relative affinity was determined in an inhibition ELISA. The abscissa represents the concentration of free DNP-lysine (-log M) used for inhibition. Affinity increases to the right. The ordinate shows the percentage of antibody present in each affinity subgroup.

The findings of the affinity distributions of TNP-specific serum IgG1 of continuously IL-4 treated mice are summarized in the histogram of Figure 2. The effect of the IL-4 treatment was already observed on day 14 of the primary response. The serum showed a range of affinities represented by inhibition at 10^{-5} to 10^{-11} M DNP-lysine. At day 58 of the primary response, a mixture of antibodies of varying affinities ranging from low to very high affinity subclasses were observed. Day 120 serum showed, like the non-IL-4 treated group, an absence of high affinity subgroups. On secondary stimulati-

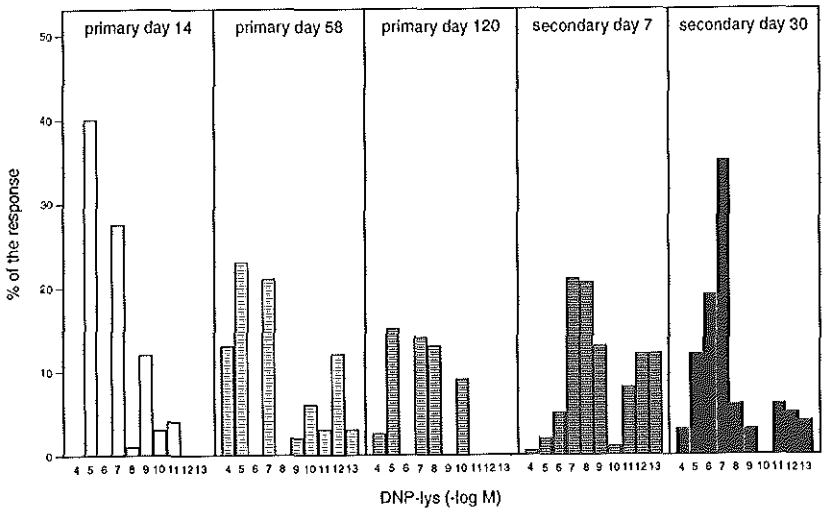

Figure 2 Relative affinity distributions of TNP-specific IgG1 antibodies in continuously IL-4 treated mice. Female BALB/c mice implanted with alginate encapsulated CV-1/IL-4 cells (every 14 days) were immunized (i.p.) with 100 µg of TNP-KLH on alum. Serum was collected on days 7, 58 and 120. The animals were boosted with 10 µg of the antigen and serum collected on days 7 and 30. Relative affinity was determined in an inhibition ELISA. The abscissa represents the concentration of free DNP-lysine (-log M) used for inhibition. Affinity increases to the right. The ordinate shows the percentage of antibody present in each affinity subgroup.

on, the major population of antibodies (approx. 40%) lied in the very high affinity subgroup (inhibited at 10^{-11} to 10^{-13} M DNP-lysine). The day 30 serum of the secondary response showed the presence of a broad spectrum of affinity ranges with subpopulations in all affinity subgroups tested.

A single administration of alginate encapsulated CV-1/IL-4 cells in mice immunized with a single dose of TNP-KLH was sufficient to shift the affinity distributions towards higher affinity subgroups (Figure 3). Repeated antigen administration either with or without exogenous IL-4 did not influence the process of affinity maturation to any appreciable degree in the time span tested (Figures 4 and 5), since the affinity profiles of these groups of mice were essentially similar.

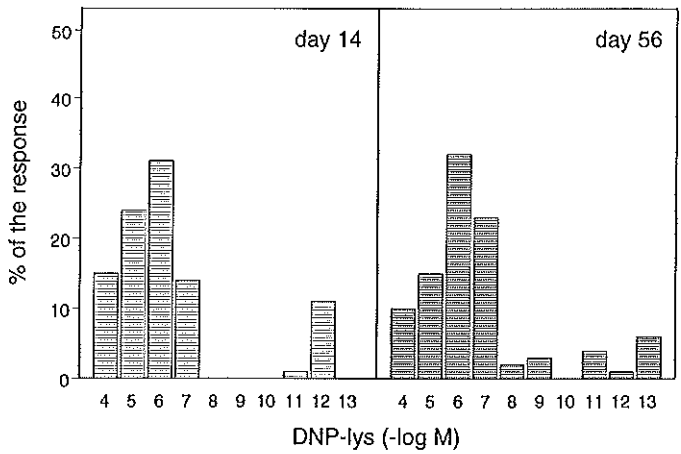

Figure 3 Relative affinity distributions of TNP-specific IgG1 mice treated with IL-4 only once. Female BALB/c mice implanted with alginate encapsulated CV-1/IL-4 cells were immunized (i.p.) with 100 µg of TNP-KLH on alum. Serum was collected on days 7 and 56. Relative affinity was determined in an inhibition ELISA. The abscissa represents the concentration of free DNP-lysine (-log M) used for inhibition. Affinity increases to the right. The ordinate shows the percentage of antibody present in each affinity subgroup.

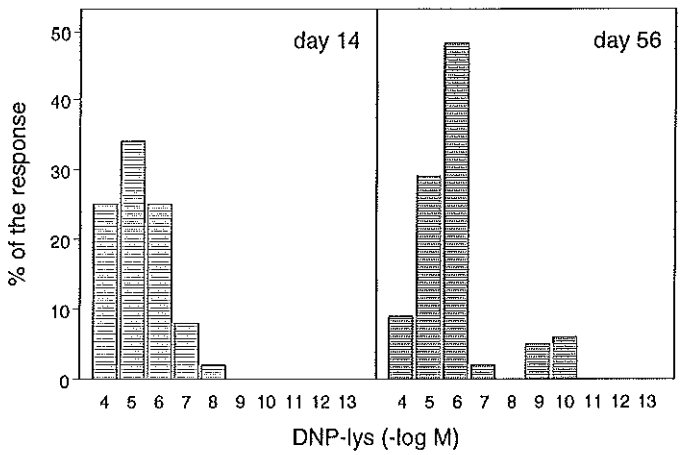

Figure 4 Relative affinity distributions of TNP-specific IgG1 in repeatedly immunized mice. Female BALB/c mice were immunized (i.p.; 5 times) with 100 µg of TNP-KLH on alum, every 14 days. Serum was collected on days 14 and 56. Relative affinity was determined in an inhibition ELISA. The abscissa represents the concentration of free DNP-lysine (-log M) used for inhibition. Affinity increases to the right. The ordinate shows the percentage of antibody present in each affinity subgroup.

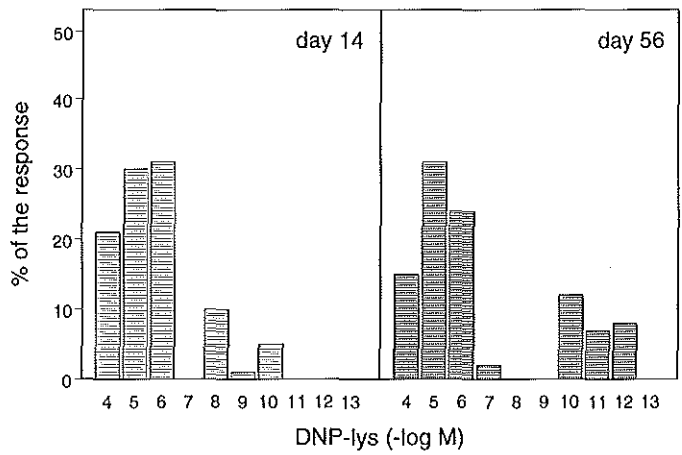

Figure 5 Relative affinity distributions of TNP-specific IgG1 in IL-4 treated repeatedly immunized mice. Female BALB/c mice implanted with alginate encapsulated CV-1/IL-4 cells every 14 days were immunized (i.p., 5 times) with 100 µg of TNP-KLH on alum. Serum was collected on days 14 and 56. Relative affinity was determined in an inhibition ELISA. The abscissa represents the concentration of free DNP-lysine (-log M) used for inhibition. Affinity increases to the right. The ordinate shows the percentage of antibody present in each affinity subgroup.

Table 2 K_A of TNP-specific IgG1 antibodies of control mice

Days after immunization		K_A (M^{-1})	Increase*
Primary	day 14	1.21×10^7	-
	day 58	8.33×10^7	6.9
	day 120	3.25×10^8	27.0
Secondary	day 30	5.80×10^8	48.3

* The increase was calculated with respect to the day 14 value.

K_A determination by IAsys optical sensor

The functional affinity of the TNP specific IgG1 antibodies of the control mice increased with time (Table 2). An almost fifty fold increase in affinity was observed when the functional affinity of serum from primary day 14 was compared with that of day 30 after secondary immunization. The increases in K_A presented in Table 2 were calculated relative to the day 14 value. Similar results were obtained for the CV-1/IL-4 treated group (Table 3). The K_A values in the secondary responses of both the treated and untreated groups seemed to reach a plateau and did not differ significantly in relation to time. The IgG1 anti-TNP antibody responses of both the control

Table 3 K_A (M^{-1}) **of TNP-IgG1 antibodies in secondary immunization**

Days after immunization	Control treated	IL-4 treated
day 4	4.8×10^8	2.1×10^8
day 11	3.1×10^8	5.6×10^8
day 21	3.9×10^8	4.8×10^8
day 30	5.8×10^8	6.2×10^8

treated and CV-1/IL-4 treated mice were essentially similar with respect to their functional affinity.

Discussion

Affinity maturation is an operational definition that implies a shift towards high affinity sub-populations of the antigen-specific antibodies later in the immune response (Steiner and Eisen, 1967). The major driving force in affinity maturation is somatic hypermutation along with antigen-driven selection of high affinity B cells in the germinal centers. This study shows that affinity maturation is observed for the TNP-specific IgG1 antibody formation after immunization of BALB/c mice with TNP-KLH. Analysis of serum samples obtained at days 14, 58 and 120 after primary immunization clearly demonstrated this phenomenon. This was reflected in the relative affinity distributions of the TNP-specific antibodies. Day 14 samples consisted almost entirely of low affinity subpopulations since high concentrations of DNP-lysine (10^{-7} to 10^{-4} M) were required to inhibit their interaction with the TNP-KLH coat. The day 58 serum showed the presence of a range of affinity subclasses. On day 120, however, the higher affinity antibodies disappeared and a major fraction of moderate affinity predominated. The shift towards lower affinity populations later in the primary response has been noted earlier. Doria et al. (1972) have reported that an initial rise in antibody affinity may be followed by a later fall. Such changes in affinity with respect to time is thought to be partly dependent on the type of antigen (Kimball et al., 1972). Determination of the concentration of the anti-TNP antibodies indicates that the immune response is well in decline at day 120 of the primary response. The absence of high affinity sub-populations at this time point could be attributed to the clearance of antigen-antibody complexes from the circulation (Klaus, 1977). The high affinity antibodies will form more stable complexes with the antigen, and would therefore be removed faster from circulation. Formations of anti-idiotypic antibodies later in the immune response may also play a role in this process (Taylor, 1982). This absence of high affinity antibodies later in the immune response was observed for both for the IL-4 treated and untreated groups.

In the early primary response, the process of hypermutation is still in its early phase resulting in medium affinity clones. In the secondary response, these

memory B cells of moderately high affinity will be initially activated, resulting in relatively homogeneous affinity distributions at day 7. Later in the secondary responses, the distribution is more heterogeneous due to the presence of further matured very high affinity clones along with very low affinity clones, the latter perhaps due to newly recruited naive B cells. It has been recognized that even in mice forming mainly high affinity antibodies, continuing synthesis of considerable amounts of very low affinity antibodies is observed (Klaus, 1977; Kim et al., 1994). Berek and Milstein (1987) have also reported finding low affinity hybridomas along with higher affinity hybridomas at all stages of the immune response. Our findings of presence of low affinity subgroups at day 30 of the secondary response, both in IL-4 treated and untreated mice are in agreement with the above suggestion of recruitment of naive B cells. The affinity distribution patterns remained essentially unchanged, even with repeated antigen administration for the time span tested.

Exogenous IL-4 seemed to increase the pace of affinity maturation of the IgG1 isotype. We have previously noted that the kinetics of the IgG1 response changes after IL-4 treatment (Van Ommen et al., 1994). The CV-1/IL-4 alginate encapsuled cells continue IL-4 synthesis for up to 18 days (Savelkoul et al., 1994). Our findings suggest that the presence of exogenous IL-4 in the first 14 days after immunization is enough to shift the system to high affinity antibodies, since even a single administration of the cells results in a shift to higher affinity subgroups in the primary response. We now establish that, though prolonged *in vivo* IL-4 treatment inhibits antigen-specific IgG1 formation, the resulting serum consists of higher affinity subpopulations. Primary day 14 and 58 sera of the IL-4 treated group showed a range of affinity subgroups as in the control group, but with a definite shift to higher affinity subpopulations. The secondary day 7 serum showed the presence of very high affinity subgroups resembling the day 30 picture in the non-IL-4 treated mice.

The functional affinity of the serum was measured by a resonant optical mirror biosensor. This instrument is uniquely suited for rapid evaluation of antigen-antibody interaction kinetics. The ligand of interest can be immobilized to the sensor surface either directly or indirectly via a catching antibody. We preferred to use a catching antibody for immobilization of the ligand to ensure isotype specificity of the reaction studied. Antigen was then added to the sensor and kinetic analysis performed using a software program provided with the instrument. Thermodynamically speaking, K_A can only be interpreted rigorously for an equilibrium in homogeneous solutions. Also, though biosensors are increasingly being used for interaction analysis (Fagerstam et al., 1992; Wohlheuter et al., 1994), correlation between other techniques and biosensors has yet to be established (Malmqvist, 1993). In the absence of such data, we prefer to describe the affinity constants arrived at as 'functional affinity'. In the case of ongoing immune responses, the resulting

serum consists of subpopulations of antibodies of varying affinities. However, the functional or average affinity is an overall affinity estimation and may not represent the mean, mode or median (Klotz, 1982). The functional affinity of the TNP-specific IgG1 antibodies in the control group was seen to increase in time. An almost fifty fold increase in K_A was observed from primary to secondary responses. Also, the K_A of serum IgG1 anti-TNP antibodies of the IL-4 treated group was not significantly different from the control group at all time points tested. It has been recognized that serum samples may be indistinguishable with regard to their functional affinity, but differ significantly with respect to the actual distribution of antibody affinities (Kim et al., 1974). Our observations are in agreement with this finding.

We find that when dealing with polyclonal antibodies such as sera, the initial steep part of the binding curve has a large influence on the k_{on} measurement. It is recommended that the first 5 sec data be omitted from data analysis to minimize the influence of bulk refractive index changes (Fastfit training manual, 1995). However, this procedure is likely to skew negatively towards high affinity antibodies, especially when present along with a large population of low affinity antibodies. This can result in an underestimation of the functional affinity early in the immune response. Moreover, the presence of large amounts of non-specific protein in the serum is also likely to increase mass transfer limitations. Also, with longer times of analysis, conformational changes may occur in the antigen-antibody complexes, besides multivalency and/or cooperativity in antibody binding. Finally, aggregates of antibodies, if present, may also influence kinetic determinations. The determination of the k_{on} value was observed to be more difficult for sera (containing polyclonal antibodies) than for pure monoclonal antibody preparations of similar concentrations. We therefore think that the polyclonal nature of the antigen-specific antibody populations present in the serum samples make it sometimes impossible to construct reliable k_{on} vs ligand concentration curves and thereby compromise the determination of k_{ass} and k_{diss}. Further studies on the kinetic analysis of serum samples are being undertaken in our laboratory.

Administration of exogenous IL-4 can result in an increase in the number of activated B cells. If this was the only mechanism of action of IL-4, the increase in number of activated B cells would lead to an increase in the entire range of affinity subgroups observed. But this is at variance with our results, which clearly show that IL-4 treatment shifts the affinity distributions to higher affinities. It is also possible that the exogenous IL-4 acts indirectly in that it leads to a preferential outgrowth of Th2 helper cells. IL-4 is also known to increase CD23 and MHC class II expression on follicular dendritic cells (FDC) (Kosco-Vilbois et al., 1993) as well as B7 (CD80/CD86) on B cells (Valle et al., 1991), thereby increasing T-B cell interaction. Such increased T cell help will also provide the CD40-CD40L interaction that is important in germinal center reactions (Clark et al., 1992; Callard et al.,

1993; Foy et al., 1994). It has been suggested that IL-4 and activated T cells together can stimulate FDC proliferation (Kim et al., 1994). Both these processes will lead to a better interaction between the antigen immobilized on the FDC and the B cell and/or a stronger selection process for cells carrying high affinity surface-receptors on their membrane. Such interaction and/or selection can explain the observed shift to higher affinities.

We therefore propose that IL-4 may lead to the observed shift to higher affinities by a combination of a number of different mechanisms. Firstly, IL-4 may induce proliferation and rescue from apoptosis of activated B cells, and increased expression of CD86/CD80. Secondly, it may lead to a selective outgrowth of Th2 cells. Thirdly, it may also cause an indirect induction of FDC proliferation and increased expression of CD23 and MHC class II molecules by these cells. Together these processes could induce the B cells to undergo multiple rounds of hypermutation, with a concomitant shift to higher affinities.

Acknowledgments

We thank Prof. R. Benner for critically reviewing and Ms. P.C. Assems for preparation of the manuscript. The help of Mr. T.M. van Os in the preparation of the figures is gratefully acknowledged.

References

Berek C. and Milstein, C. (1987) Mutation drift and repertoire shift in the maturation of immune response. *Immunol. Rev.* 96:23.

Berek C. and Ziegner, M. (1993) The maturation of the immune response. *Immunol. Today* 14:400.

Buckle P. E., Davies R. J., Kinning T., Yeung D., Edwards P. R. and Pollard-Knight D. (1993) The resonant mirror: a novel optical sensor for direct sensing of biomolecular interactions Part II: Applications. *Biosens. Bioelectr.* 8:355.

Butch A.W., Chung G-H., Hoffman J.W. and Nahm M. (1993) Cytokine expression by germinal centre cells. *J. Immunol.* 150:39.

Butch A.W. and Nahm M.H. (1992) Functional properties of human germinal centre B cells. *Cell. Immunol.* 140:331.

Callard R.E., Armitage R.J., Fanslow W.C. and Spriggs M.K. (1993) CD40 ligand and its role in X-linked hyper-IgM syndrome. *Immunol. Today* 14:559.

Clark E.A., Grabstein K.H. and Shu G.L. (1992) Cultured human follicular dendritic cells. Growth characteristics and interactions with B lymphocytes. *J. Immunol.* 148:3327.

Coffman R.L. and Carty J. (1986) A T cell activity that enhances polyclonal IgE production and its inhibition by interferon-gamma. *J. Immunol.* 136:949.

Coffman R.L., Lebman D. and Rothman P. (1993) Mechanisms of immunoglobulin isotype switching. Adv. Immunol. 54:229.

Cush R., Cronin J. M., Stewart W. J., Maule C. H., Molloy J. O. and Goddard N. J. (1993) The resonant mirror : a movel optical sensor for the direct sensing of biomolecular interactions. Part I: Principle of operation and associated instrumentation. *Biosens. Bioelectr.* 8:347.

Doria G., Schiaffin G., Garavini M. and Mancini C. (1972) The rise and fall of antibody avidity at the level of single immunocytes. *J. Immunol.* 109:1245.

Edwards P.R., Gill A., Pollard-Knight D.V., Hoare M., Buckle P.E., Lowe P.A. and Leatherbarrow R.J. (1995) Kinetics of protein-protein interactions at the surface of an optical biosensor *Anal. Biochem.* (in press).

Fagerstam, L.G., Frostell-Karlsson, A., Persson, B. and Ronnberg, I. (1992) Biospecific interaction analysis using surface plasmon resonance detection applied to kinetic, binding site and concentration analysis. *J. Chromatogr.* 597:397.

Fastfit Training Manual (1995) Fisons Applied Sensor Technology, Cambridge.

Foy T.M., Laman J., Ledbetter J., Aruffo A., Claasen E. and Noelle R.J. (1994) gp39-CD40 interactions are essential for germinal centre formation and development of B cell memory. *J. Exp. Med.* 180:157.

Hudson, L. and Hay F. C. (1976) Initiated preparations In: *Practical Immunology*, Blackwell Scientific Publications, Oxford, London, p. 1.

Kim Y.T., Werblin, T.P. and Siskind G.W. (1974) Distribution of antibody affinities - II. Fractionation of antibody with respect to its hapten binding affinity. *Immunochem.* 11:685.

Kim H-S., Zhang X. and Choi Y.S. (1994) Activation and proliferation of follicular dendritic cell-like cells by activated T lymphocytes. *J. Immunol.* 153:2951.

Kimball J.W. Maturation of the immune response to type III pneumococcal polysaccharide. *Immunochem.* 9:1169.

Klaus G.G.B. (1977) B cell maturation: its relationship to immune induction and tolerance. In: *B and T cells in immune recognition.* Loor F. and Roelants G.E. (Eds), John Wiley and Sons, London. p. 235.

Klotz I.M. (1982) Number of receptor sites from Scatchard graphs: facts and fantasies. *Science* 217:1247.

Koch G., Osmond D., Julius M. H. and Benner R. (1981) The mechanism of thymus-dependent antibody formation in bone marrow. *J. Immunol.* 126:1447.

Kocks C. and Rajewsky K. (1988) Stepwise intraclonal maturation of antibody affinity through somatic hypermutation. *Proc. Natl. Acad. Sci. USA* 85:8206.

Kosco-Vilbois M.H., Gray D., Scheidegger D. and Julius M. (1993) Follicular dendritic cells help resting B cells to become effective antigen-presenting cells: induction of B7/BB1 and upregulation of major histocompatibility complex class II molecules. *J. Exp. Med.* 178:2055.

Kroese, F. G. M., Timens, W. and Nieuwenhuis, P. (1990) Germinal center reaction and B lymphocytes: morphology and function. *Curr. Top. Path.* 84:103.

Kroese F.G.M., Wubbena A.S. and Nieuwenhuis P. (1986) Germinal centre formation and follicular antigen trapping in the spleen of lethally X-irradiated and reconstituted rats. *Immunology* 57:99.

Liu, Y-J., Johnson, G. D., Gordon, J. and MacLennan, I. C. M. (1992) Germinal centres in T-cell dependent antibody responses. *Immunol. Today* 17:17.

MacLennan, I. C., Liu, Y-J. and Johnson, G. D. (1992) Maturation and dispersal of B-cell clones during T cell-dependent antibody responses. *Immunol. Rev.* 126:143.

Malmqvist M. (1993) Surface plasmon resonance for detection and measurement of antibody - antigen affinity and kinetics. *Curr. Opin. Immunol.* 5:282.

Nossal, G. J. V. (1992) The molecular and cellular basis of affinity maturation in the affinity response. *Cell* 68:1.

Pathak S.S. and Savelkoul (1995) Determination of affinity and affinity distributions in ELISA (*submitted for publication*).

Pathak S.S., Tibbe G.J.M. and Savelkoul H.F.J. (1995a) Application of a resonant mirror biosensor to the determination of functional affinity and affinity distributions in monoclonal and polyclonal systems (*submitted for publication*).

Pathak S.S., Tibbe G.J.M. and Savelkoul H.F.J. (1995b) Antibody affinity determination in ELISA and biosensor. In: Manual of Immunological Methods. I. Lefkovits (Ed) (in press).

Rizzo, L. V., Dekruyff, R. H. and Umetsu, D. T. (1992) Generation of B cell memory and affinity maturation. Induction with Th1 and Th2 T cell clones. *J. Immunol.* 148:3733.

Savelkoul H.F.J., Lebman D.A., Benner R. and Coffman R.L. (1988) Increase of the precursor

frequency and clonal size of murine immunoglobulin E-secreting cells by interleukin-4. *J. Immunol.* 141:749.

Savelkoul H.F.J., Van Ommen R., Vossen A.C.T.M., Breedland E.G., Coffman R.L. and Van Oudenaren A. (1994) Modualtion of systemic cytokine levels by implantation of alginate encapsulated cells. *J. Immunol. Methods* 170:185.

Sharon, J., Gefter, M. L., Wysocki, L. J. and Margolies, M. N. (1989) Recurrent somatic mutations in mouse antibodies to p-azophenylarsonate increase affinity for hapten. *J. Immunol.* 142:696.

Steiner L.A. and Eisen H.N. (1967) Sequential changes in the relative affinity of antibodies synthesized during immune response. *J. Exp. Med.* 126:1185.

Taylor R.B. (1982) Regulation of antibody response by antibody towards the immunogen. *Immunol. Today* 3:47.

Thorbecke G.J., Amin A.R. and Tsiagbe V.K. (1994) Biology of the germinal centre in the lymphoid tissue. *FASEB J.* 8:832.

Valle A., Aubry J-P., Durand I. and Banchereau J. (1991) IL-4 and IL-2 upregulate the expression of antigen B7, the B cell counterstructure to T cell CD28: an amplification mechanism for T-B cell interactions. *Int. Immunol.* 3:229.

Van Ommen R., Vredendaal A.E.C.M. and Savelkoul H.F.J. (1994) Prolonged *in vivo* IL-4 treatment inhibits antigen-specific IgG1 and IgE formation. *Scand. J. Immunol.* 40:1.

Varitek, V. A. and Day, E. D. (1979) Relative affinity of antisera for myelin basic protein (MBP) and degree of affinity heterogeneity. *Molec. Immunol.* 16:163.

Wohlhueter RM, Parekh K, Udhaykumar V, Fang S. and Lal AA (1994) Analysis of binding of monoclonal antibody to a malarial peptide by Surface Plasmon Resonance biosensor and integrated rate equation. *J. Immunol.* 153:181.

Yee, E. (1991) Reconstruction of the antibody affinity distribution from the experimental data by a minimum cross-entropy procedure. *J. Theor. Biol.* 153:205.

DISCUSSION

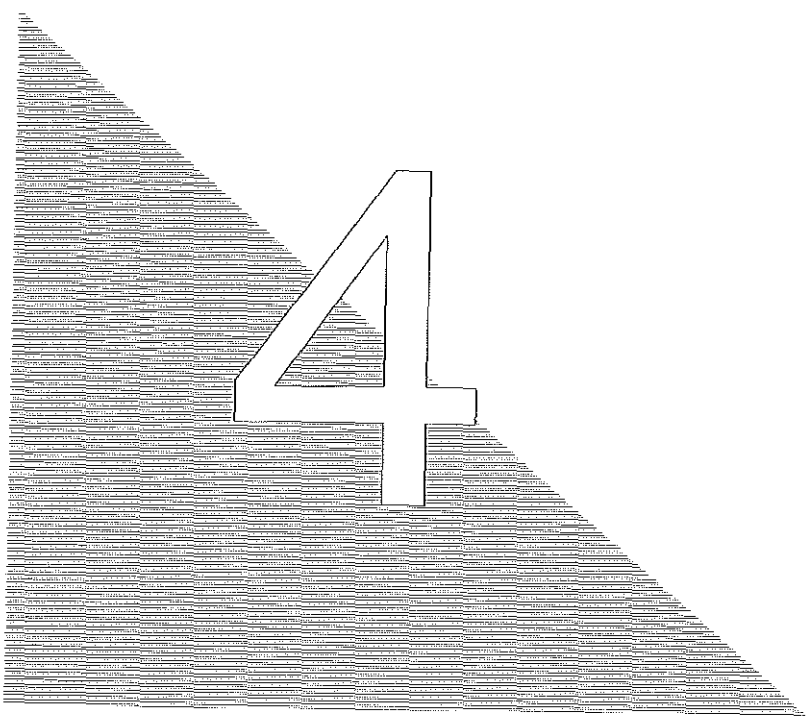

CHAPTER 4

Discussion

Affinity maturation is a T cell dependent, antigen-driven process, wherein the affinity of the antibodies produced later in the immune response is higher than that in the initial stages. This increase in affinity occurs due to somatic hypermutation and concomitant affinity selection. It is now established that germinal centers are the most likely site of somatic hypermutation, isotype switch and memory B cell formation.

The aim of this thesis was to gain insights in the process of affinity maturation of IgG1 and IgE antibody responses at the serum level. IL-4 is known to have a crucial role in both the process of isotype switching as well as prevention of apoptosis in the germinal centers. We were therefore interested in elucidating the effect of addition of exogenous IL-4 on the functional affinity and affinity distributions of antigen-specific serum IgG1 and IgE. The questions we aimed to address were -

- Is it possible to determine the affinity and affinity distributions of serum antibodies in ongoing immune responses?
- Does affinity maturation occur in primary and secondary IgG1/IgE responses and what is the extent of this maturation?
- Does prolonged IL-4 treatment affect this process of affinity maturation?

4.1 Application of ELISA

Affinity determination

Affinity is the measure of the strength of binding between a monovalent antigen and a single binding site of an antibody and is denoted by K_A or K_D. Serum, however, contains a heterogeneous mixture of antibodies. Under such conditions, the kinetics is best described by an operational parameter that is dependent on defined experimental conditions (Joshi et al., 1992). Therefore, the term functional affinity or average affinity is often used to describe the technique-dependent, quantitative assignment of a value to the strength of binding between a multivalent antigen and the multivalent antibody populations in serum (Hornick and Karush, 1972).

To answer the questions raised above, it was necessary to establish reliable methods for the measurement of affinity and affinity distributions of polyclonal antibody populations in sera. Both equilibrium dependent and independent systems were investigated. Chapter 2 of this thesis deals with affinity determinations in ELISA. Chapter 2.1. reviews some of the important parameters that can affect the performance of ELISA. A Terasaki-ELISA capable

of measuring IgE in nanogram ranges and in minute volumes of the sample (5 µl) was developed and is described in chapter 2.2. We extended the use of this ELISA for affinity determinations as well (chapter 2.3). During these investigations we established that some monoclonal IgE mixtures exhibited an increased affinity for the relevant antigen. In chapter 2.4 we report on this phenomenon. Our results point towards non-specific interaction of the Fc regions of the purified IgE molecules as a possible reason for the increased affinity. The applicability of the equations developed to relative affinity determinations in ongoing immune responses is demonstrated in chapter 2.5.

A variety of approaches have been used for affinity determinations in ELISA. Direct ELISA methods require the labeling of one of the reactants in the antigen-antibody interaction. Such labeling may affect the conformation of the reactants and hence their kinetics. A sandwich system is therefore preferred. One of the major problems with using ELISA for affinity determination is that though one may know the input concentration of the antibody, it is not possible to determine the amount of ligand that has been actually adsorbed to the wells (Lehtonen, 1981). It is therefore difficult to determine the concentration of the unreacted ligand required for Scatchard analysis. Mathematical approaches that determine affinity from dilution curves or approaches that use the concentration of ligand that gives half saturation of the coat as a measure of affinity, are therefore theoretically unacceptable (Goldberg and Djavadi-Ohaniance, 1993). We used a sandwich format for affinity determinations in ELISA. In sequential equilibrium binding analysis, a series of equilibria are set up between the solid-phase antigen/antibody and the liquid-phase antibody/antigen. The fraction of unreacted ligate in the liquid at each stage is a function of the concentration of the antibody/antigen transferred to the plate as well as the affinity. It is therefore possible to compute relative affinity from this data using equations derived from the Law of Mass Action. By using a conversion factor, it would be possible to arrive at absolute value from this relative affinity value. However, this conversion factor is very large, and is likely to magnify errors in the primary data. Also, there are some other valid criticisms about using ELISA for affinity determinations. First and foremost, equilibrium is attained at solid-liquid interface, and these kinetics, though reflecting what happens in solution, may be different from them (Goldberg and Djavadi-Ohaniance, 1993). Secondly, adsorbing the antigen to plastic may severely affect its conformation, resulting in altered kinetics (Butler et al., 1992). Also, the method suffers from mass-transport limitations (Nygren et al., 1987). Moreover, it has been suggested that ELISA tests are skewed towards detection of high affinity antibodies (Nimmo et al., 1984). Taking into consideration the limitations of the technique, we restrict the use of sequential equilibrium binding analysis to relative affinity determinations only. We find this method especially suitable in situations where a quick and easy method for relative ranking is desired, e.g. when evaluating immunization protocols or investigating the affinity of antibodies present in supernatants from hybridoma cell lines etc.

Affinity distributions

In polyclonal situations, the observed equilibrium constant is a central measure of an unknown distribution of particular equilibrium constants K_i ($1 \leq i \leq n$), where the number of n itself is not known. To estimate the effect of a treatment on affinity maturation, therefore, it is not enough to determine the functional or average affinity, but it is desirable to study the affinity distributions of antigen-specific serum antibodies as well. A variety of mathematical functions (based on a Gaussian distribution or a Sips function, as reviewed in Day, 1990) have been used to determine a heterogeneity index of antigen-specific serum antibodies. The Gaussian and Sipsian functions describe similar symmetrical distribution curves. However, it is now known that affinity distributions are not Gaussian or Sipsian in nature. Attempts have also been made to determine affinity distributions from data obtained in fluorescence quenching, temperature-jump relaxation, RIA etc. (reviewed in Day, 1990). Thus, no straight forward method of determining affinity heterogeneity in polyclonal sera is available, since it requires the separation of the different antibody subpopulations present, a process that is highly labor intensive and expensive in terms of the amount of serum and reagents required. Chapter 2.5 demonstrates the use of a simple inhibition ELISA-based technique for relative affinity distributions. In this method, dilutions of the serum are incubated with incremently increasing concentrations of free hapten. The mixture is then added to an ELISA plate coated with the antigen (hapten-carrier conjugate). High affinity antibodies in the serum will be inhibited by low concentrations of the hapten. The affinity distributions of serum antibodies can thus be represented in terms of the concentration of hapten used for the inhibition. We used a hapten range of 10^{-4} to 10^{-13} M. We considered the arbitrarily chosen 10^{-1} M increments small enough for the relative discrimination of the various affinity subgroups and large enough to cover the range of affinity classes present in the serum. However, this method is only applicable when the epitopes on the antigen are well defined and available in large quantities. Using the above technique, we ascertained that higher affinity populations predominate in the secondary response while only lower affinity populations are found early in the primary response.

4.2 Application of biosensor

The advent of optical biosensors has paved the way for kinetic analysis of antigen-antibody interaction. In chapter 3 we report on the application of an optical resonant mirror biosensor for studying the qualitative and quantitative aspects of antibodies in ongoing immune responses. Chapter 3.1. reviews the application of biosensors to kinetic interaction analysis. The mathematical treatment of primary data to arrive at the K_A value is also extensively covered in this chapter. The methodology for the application of the biosensor for determination of functional affinity of monoclonal and polyclonal antibody

populations is described in chapter 3.2. In this chapter we also discuss a method for determining relative affinity distributions with a biosensor. Finally, in chapter 3.3, we report our findings on the effect of IL-4 treatment on the process of affinity maturation of IgG1 anti-TNP antibodies.

The IAsys^{tm} biosensor (Fisons, Applied Sensor Technology, Cambridge, UK) is a cuvette system based on the resonant mirror waveguiding technique that can monitor shifts in the resonance angle due to changes occurring as a result of binding or dissociation of biomolecules at the sensor surface. The sensing surface is present in the form of a disposable cuvette. A microstirrer ensures efficient transport of the analyte to the immobilized ligand, minimizing mass transport limitations making the system suitable for kinetic analysis (Karlsson et al., 1991). The ligand of interest is directly bound to the flexible hydrophilic matrix by a defined covalent linkage. The ligand is then accessible to three dimensional antibody interactions. The change in resonance angle occurring as a result of biomolecules binding to or dissociating from the surface can be monitored in real-time in terms of a binding curve (Buckle et al., 1993). In ELISA, a coat as well as appropriate detecting reagents ensure the specificity of the final response. However, the biosensor does not have this kind of in-built specificity. Since we desired to study affinity maturation of a particular isotype, we chose a sandwich format for interaction analysis in the biosensor. Moreover, we found that the dextran at the sensor surface could reversibly bind non-specific proteins. This non-specific binding could potentially interfere with kinetic interaction analysis. A sandwich system helps to minimize the influence of such non-specific binding as well.

We established that the K_A of the TNP-specific IgG1 response increases with time. An almost 50 fold increase was observed when the K_A of secondary day 30 sera were compared with that of primary day 14. In the secondary response, however, the K_A value did not differ significantly with respect to time. Recently, several studies have reported the use of biosensors in interaction kinetics (Davies et al., 1994; George et al., 1995). However, most of these studies investigated the interaction between monoclonal antibody preparations and their antigens. We find that when dealing with polyclonal systems such as sera, the determination of kinetic constants is more complicated as indicated in chapter 3.3. Overall, we find the system and the analysis software most suited for affinity determinations of monoclonal preparations at this point of time. With the advent of new sensor surfaces and more sophisticated data analysis programs, it should be possible to use this system for measurement of interaction of polyclonal antibodies with their antigen in the near future.

We envisage that the biosensor technology could then be applied to the study of atopic patients characterized by the presence of the allergen-specific IgE in the serum. This would require the monitoring of time-dependent changes in the functional affinity and affinity distributions of the allergen-specific IgE

antibodies. Two major problems have to be overcome to enable these determinations. Firstly, IgE is present in very low concentrations in normal human sera. Thus, to be able to detect IgE, it would be necessary to lower the detection limit of the system. The use of gold enhancement techniques could help in achieving this to some extent. Secondly, one must also be able to determine K_A of IgE antibodies in the presence of a large excess of other antigen-specific isotypes. The use of high affinity catching antibodies along with a combination of techniques that allow the enrichment of IgE should help in meeting this objective.

Such studies may help in understanding the progressively lower allergen challenge needed, and increased severity of symptoms observed, in patients with allergic manifestations. It should hopefully help in exploring avenues to limit the progress of sometimes crippling disorders such as asthma.

4.3 IL-4 treatment and affinity maturation

Having established the techniques that enable us to study the process of affinity maturation at the serum level, we wished to study the affinity maturation of the IgG1 and IgE isotypes. We also wanted to study the effect of exogenous IL-4 on the affinity maturation of these isotypes. IgE is present in nanogram levels in normal mouse sera. Even with protocols designed for induction of a predominant IgE response, a peak concentration of around 150 µg/ml of antigen-specific IgE was obtained at the height of the response (Van Ommen et al., 1994). Affinity maturation of this isotype could therefore not be studied at this point of time. However, because both these isotypes are linked in their response to IL-4 dependence, it is our conviction that observations for the IgG1 isotype will also hold for the IgE isotype. The DNP/TNP anti-DNP/TNP system has been extensively studied for affinity maturation. We have chosen this system to study the IgG1 and IgE responses in the murine model with the ultimate aim of utilizing the model for investigating clinical situations. So far, we have concentrated on evaluating the effects of exogenous IL-4 treatment on affinity maturation at the serum level. Future work must also investigate the effect of IL-4 treatment at the cellular level.

We established that the process of affinity maturation is clearly observed for the IgG1 isotype. Control mice injected with 100 µg of TNP-KLH adsorbed on alum showed predominantly low affinity TNP-specific antibodies in their sera early in the primary immune response (chapter 3.3). A shift to higher affinity subpopulations was observed later in the primary response. This shift was reflected both in the functional affinity as well as the affinity distribution of TNP-specific IgG1. On secondary immunization, a further shift to higher affinities was observed, along with reappearance of lower affinity clones. Such presence of low affinity antibodies in the presence of high affinity antibodies has also been reported in the literature (reviewed in Klaus, 1977).

IL-4 is a pluripotent cytokine secreted predominantly by Th2 cells. It is known to be important in isotype switching to IgG1 and IgE (Coffman et al., 1993). IL-4 has also been shown to be important in the development and maintenance of germinal center reactions (Tsiagbe et al., 1992; Butch et al., 1993). Germinal centers are thought to be the site of isotype switching, hypermutation and antigen selection of high affinity variants, as well as generation of memory B cell responses.

We found that IL-4 increases the pace of affinity maturation of the IgG1 isotype. Affinity maturation is essentially an operational definition implying a shift to higher affinities in the later stages of the immune response. Somatic hypermutation along with antigen-driven selection are thought to be the two main mechanisms underlying affinity maturation. This simplistic view of the clonal selection theory would imply an absence of low affinity antibodies later in the immune response. However, this is in contradiction to observations of many investigators who report the occurrence of low affinity antibodies throughout the immune response (Berek and Milstein, 1987). Our report is in agreement with these investigations. Low affinity antibodies were observed in the sera of both IL-4 treated and untreated animals even in the later stages of the secondary response. It is possible that primary B cells are recruited throughout the immune response as a source of potentially useful new germ-line gene combinations necessary for continued affinity maturation. The low affinity antibodies are an outcome of this recruitment.

The observed increased affinity maturation due to exogenous IL-4 could be a result of a number of different phenomena, all of them not mutually exclusive. Firstly, IL-4 may increase the rate of proliferation and survival of the germinal center B cells. Administration of exogenous IL-4 can therefore result in an increase in the number of activated B cells. If this were the only mechanism of action of IL-4, the increase in number of activated B cells should lead to an increase in the entire range of affinities observed in the control group. But this is at variance with our results which clearly show that IL-4 treatment shifts the affinity distributions to higher affinities. Hence increased proliferation and survival could not be the only mechanism of action of IL-4.

The exogenous IL-4 may also act indirectly in that it leads to a preferential outgrowth of Th2 helper cells. Moreover, IL-4 is known to increase CD86/CD80 (B7) expression on B cells (Valle et al., 1991). Taken together, these two phenomena would result in increased T cell-B cell interaction. Such increased T cell help will also provide the CD40-CD40L interaction that is reported to be important in germinal center reaction (Callard et al., 1993; Foy et al., 1994). This interaction has been shown to be important in memory B cell formation as well as expression of bcl-2 protein that is linked to protection of germinal center cells from apoptosis. Cells rescued from apoptosis in this way have been reported to be maintained in cell cycle by the addition of recombinant IL-4 (Liu

et al., 1991). Together these processes could induce the B cells to undergo multiple rounds of hypermutation and clonal selection, with a concomitant shift to higher affinities. It has been suggested that IL-4 and activated T cells together can stimulate follicular dendritic cells (FDC). Such stimulation will lead to a better interaction between the antigen immobilized on the FDC and the B cell and/or a stronger selection process for cells carrying high affinity surface-receptors on their membrane. FDC are also known to help B cells to become effective antigen-presenting cells. According to a model suggested by Van Seventer et al. (1991), bilateral dialogue between specific T cells and antigen-presenting B cells would lead to both B cell activation and germinal center formation together with T cell activation and production of T cell cytokines required for FDC to promote B cell differentiation. Taken together such interactions can explain the observed shift to higher affinities. To summarize, IL-4 may lead to the observed shift to higher affinities by a combination of the following mechanisms -

a. induced proliferation and rescue from apoptosis of activated B cells, along with increased expression of CD86/CD80,
b. selective outgrowth of Th2 cells, and
c. indirect induction of FDC proliferation and increased expression of CD23 and MHC class II molecules by these cells.

4.5 Conclusions

In this thesis we have reached to the following conclusions pertaining to the questions raised -

- A simple method like ELISA can be used for relative affinity determinations and affinity ranking of monoclonal and polyclonal antibody populations. It can also be used for determining the affinity distributions of antigen-specific antibodies in ongoing immune responses.
- It is also possible to determine both the functional affinity and affinity distributions by a resonant mirror optical biosensor.
- Affinity maturation is observed in primary and secondary TNP-specific IgG1 responses in mice.
- Exogenous IL-4 treatment increases the pace of affinity maturation of these IgG1 anti-TNP antibodies.

4.6 References

Berek C. and Milstein C. (1987) Mutation drift and repertoire shift in the maturation of the immune response. Immunol. Rev. 96:23.

Buckle P. E., Davies R. J., Kinning T., Yeung D., Edwards P. R. and Pollard-Knight D. (1993) The resonant mirror: a novel optical sensor for direct sensing of biomolecular interactions. Part II: Applications. Biosens. Bioelectr. 8:355.

Butch A.W., Chung G-H., Hoffman J.W. and Nahm M. (1993) Cytokine expression by germinal center cells. J. Immunol. 150:39.

Butler J.E., Ni L., Nessler R., Joshi K.S., Suter M., Rosenberg B., Chang J., Brown W.R. and Cantarero L.A. (1992) The physical and functional behaviour of capture antibodies adsorbed to polystyrene. J. Immunol. Methods 150:77.

Callard R.E., Armitage R.J., Fanslow W.C. and Spriggs M.K. (1993) CD40 ligand and its role in X-linked hyper-IgM syndrome. Immunol. Today 14:559.

Coffman R.L., Lebman D. and Rothman P. (1993) Mechanisms of immunoglobulin isotype switching. Adv. Immunol. 54:229.

Davies R.D., Edwards P.R., Watts H.J., Lowe C.R., Buckle P.E., Yeung D., Kinning T. and Pollard-Knight D., (1994) The resonance mirror: a versatile tool for the study of biomolecular interactions. Techniques in Protein Chemistry V:285.

Day E. (1990) Affinity. Advanced Immunochemistry. Wiley-Liss, NY, USA. p. 295.

Foy T.M., Laman J., Ledbetter J., Aruffo A., Claassen E. and Noelle R.J. (1994) gp39-CD40 interactions are essential for germinal center formation and development of B cell memory. J. Exp. Med. 180:157.

George A.G.T., French R.R. and Glennie M.J. (1995) Measurement of kinetic binding constants of a panel of anti-saporin antibodies using a resonant mirror biosensor. J. Immunol. Methods 183:51.

Goldberg M.E. and Djavadi-Ohaniance L. (1993) Methods for measurement of antibody/antigen affinity based on ELISA and RIA. Curr. Opin. Immunol. 5:278.

Hornick C.L. and Karush F. (1972) Antibody affinity. III. The role of multivalence. Immunochemistry 9:325-340.

Joshi K.S., Hoffman L.G. and Butler J.E. (1992) The immunochemistry of sandwich ELISAs. V. The capture antibody performance of polyclonal antibody-enriched fractions prepared by various methods. Mol. Immunol. 29:971.

Karlsson R., Michaelsson A. and Mattieson L. (1991) Kinetic analysis of monoclonal antibody-antigen interactions with a new biosensor based analytical system. J. Immunol. Methods 145:229.

Klaus G.G.B. (1977) B cell maturation: its relationship to immune induction and tolerance. In: B and T cells in immune recognition. Loor F. and Roelants G.E. (Eds), John Wiley and Sons, London. p. 235.

Lehtonen O.-P. (1981) Immunoreactivity of solid phase hapten measured by a hapten binding plasmocytoma protein (ABPC 24). Mol. Immunol. 18:323.

Liu Y.-J., Cairns J.A., Holder M.J., Abbot S.D., Jansen K.U., Bonnefoy J.-Y., Gordon J. and MacLennan I.C.M. (1991a) Recombinant 25kDa CD23 and interleukin-1 alpha promote the survival of germinal center B cells: evidence for bifurcation in the development of centrocytes rescued from apoptosis. Eur. J. Immunol. 21:1107.

Nimmo G.R., Lew A.M., Stanley C.M. and Steward M.W. (1984) Influence of antibody affinity on the performance of antibody assays. J. Immunol. Methods 72:177.

Nygren H., Werthen M. and Stenberg M. (1987) Kinetics of antibody binding to solid-phase-immobilized antigen. Effect of diffusion rate limitation and steric interaction. J. Immunol. Methods 101:63.

Tsiagbe V.K., Linton P-J. and Thorbecke G.J. (1992) The path of memory B cell development. Immunol. Rev. 126:113.

Valle A., Aubry J-P., Durand I. and Banchereau J. (1991) IL-4 and IL-2 upregulate the expression of antigen B7, the B cell counterstructure to T cell CD28: an amplification mechanism for T-B cell interactions. Int. Immunol. 3:229.

Van Ommen R., Vredendaal A.E.C.M. and Savelkoul H.F.J. (1994) Prolonged *in vivo* IL-4 treatment inhibits antigen-specific IgG1 and IgE formation. Scand. J. Immunol. 40:1.

Van Seventer G.A., Shimuzu Y. and Shaw S. (1991) Roles of multiple accessory molecules in T cell activation: bilateral interplay of adhesion and costimulation. Curr. Opin. Immunol. 3:294.

SUMMARY

SAMENVATTING

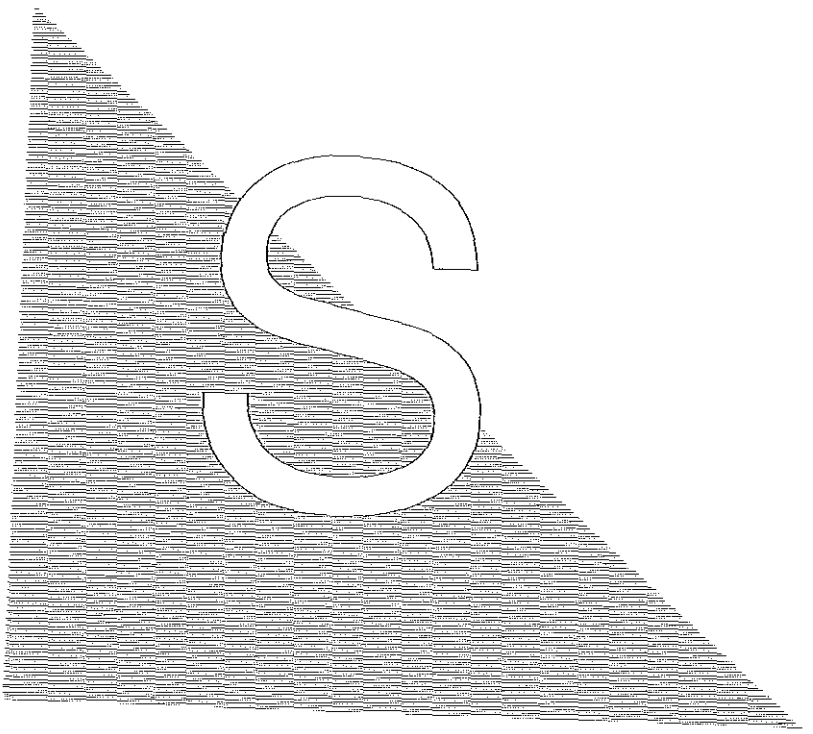

Summary

Molecular recognition guides the selective interaction of macromolecules in essentially all biological processes. This process of selective interaction is dependent on complementarity between the moieties involved, and is responsible for the strength of the binding (called affinity in the case of antigen-antibody interaction). It has been recognized for many years that secondary humoral immune responses are faster, of an increased magnitude, of a different isotype and consist of antibodies with a higher affinity for the antigen than primary humoral immune responses. The increase in affinity of the antibodies later in the immune response, i.e. affinity maturation, is due to the process of hypermutation and antigen-driven selection in the germinal centers. The end result is an improved complementarily between the paratopes of the antibody and the epitopes on the antigen. Germinal centers are also thought to be the site of isotype switching. Interleukin 4 (IL-4) is known to have a crucial role in the development of germinal centers, rescue of antigen-selected B cells from apoptosis and their continued proliferation. In mice it is also known to selectively induce isotype switching to IgG1 and IgE. We were therefore interested in studying the influence of exogenous IL-4 on the process of affinity maturation on the antigen-specific serum IgG1/IgE antibodies in the murine model, with the hope of ultimately extending our studies to humans.

The first chapter of this thesis reviews the main features of the immune system and the mechanism underlying the specificity, diversity and memory of the humoral immune response. The process of somatic hypermutation and antigen-driven selection is also described in this chapter. A brief description of the germinal centers, which are thought to be the site of clonal expansion of B cells, their differentiation, generation of antigen-induced diversity and isotype switching, is also included.

Chapter 2 deals with the application of ELISA to the quantitation of concentration and affinity of antibodies. ELISA is one of the simplest yet most versatile tool that has a variety of applications in immunology. Chapter 2.1 deals with concentration determination in ELISA. Important parameters that can affect the performance of ELISA as well as various methods of data handling are also discussed in this chapter. In chapter 2.2 we describe a Terasaki-ELISA that can be used for the quantitation of the concentration of total and antigen-specific murine IgE. This Terasaki-ELISA has a detection range of 1-10 ng/ml and requires only 5 µl of sample. By sequential equilibrium binding analysis, we extended the use of the non-competitive Terasaki-ELISA to affinity determinations (chapter 2.3). In this method a series of equilibria are set up between the antigen immobilized to the wells of a Terasaki tray and the antigen-specific antibodies in the supernatant in the wells. We derived equations from the Law of Mass Action that could be used

to arrive at a relative affinity constant (K_{rel}) from this data. A conversion factor is needed to arrive at the equilibrium constant (K_D) from the K_{rel}. During our work with monoclonal IgE antibodies, we found that some mixtures of purified IgE antibodies displayed an apparent increase in their affinity for the antigen. Our investigations are reported in chapter 2.4. We suggest that the observed apparent increase was an artefact of the purification process. In chapter 2.5 we extend the applicability of the sequential equilibrium binding analysis to microtitre ELISA. We have used this technique for evaluation of immunization protocols. To document the process of affinity maturation, it is not enough to establish the average affinity constant, but one must also be able to show a shift to higher affinity subpopulations later in the immune response. Accordingly, in chapter 2.5, we also describe a simple hapten-inhibition ELISA to determine the relative affinity distributions of subpopulations antigen-specific antibodies in sera.

We find that sequential equilibrium binding analysis is best suited for affinity ranking of antibodies. The large conversion factor needed to arrive at the absolute K_D value from the K_{rel}, is likely to magnify primary errors in the data. Also, being a discontinuous, heterogeneous phase, equilibrium-dependent assay, data obtained in an ELISA may not reflect homogeneous interactions. We therefore also investigated a biosensor for affinity determinations.

Chapter 3 describes the use of optical biosensor technology (IAsys^{tm}, Fisons Applied Sensor Technology) to kinetic interaction analysis. The resonant mirror biosensor used, is a cuvette system based on the resonant mirror waveguiding technique. The ligand of interest is directly bound to the sensor surface. The change in resonance angle occurring as a result of biomolecules binding to or dissociating from the surface can be monitored in real-time in terms of a binding curve. All traditional methods of affinity determination are equilibrium-dependent methods, that arrive at the K_D indirectly from the concentration of the reactants/products at equilibrium. Biosensors, on the other hand, offer the unique opportunity of monitoring the interaction in real-time, and hence actually measuring both the association and dissociation rate constants.

Chapter 3.1 gives an overview of methods of affinity determinations with special reference to the biosensor. The mathematical basis of data analysis is also extensively discussed in this chapter. Various parameters that can affect the performance and analysis with a biosensor are also considered. The application of biosensor to interaction analysis between the antigen and monoclonal and polyclonal antibodies is reported in chapter 3.2. In this chapter we also demonstrate the possibility of determining affinity distributions of antigen-specific antibodies in sera by the application of a biosensor. However, because of the rather long time required for such distribution analysis, it does not compare favorably with other methods for determining

relative affinity distributions, such as ELISA.

Having established the methods that enabled us to study affinity maturation, we studied the influence of exogenous IL-4 on the functional affinity as well as affinity distributions of TNP-specific serum IgG1 antibodies in primary and secondary responses of BALB/c mice (chapter 3.3). We established that IL-4 increased the pace of affinity maturation of the IgG1 isotype. The functional affinity of these antibodies did not change significantly when compared with the non-treated group. The affinity distributions, however, shifted to higher affinity subgroups. We think that IL-4 may lead to the observed shift to higher affinities by a combination of mechanisms that lead to an increased T-B cell co-operation as well as increased follicular dendritic cell and B cell interaction in the germinal centers.

In summary, in this study we demonstrate the use of relatively simple as well as sophisticated methods for determining the affinity and affinity distributions of antigen-specific serum antibodies. We find that the non-competitive ELISA developed by us best suited for relative affinity ranking of monoclonal antibodies and determinations of relative affinity distributions. Biosensors, on the other hand, are very useful to determine the K_A of monoclonal antibodies and show promise for K_A determination of polyclonal antibodies as well. We established that IL-4 increases the pace of affinity maturation of the IgG1 isotype. Since the IgG1 and the IgE isotype are linked to IL-4 in their responses, we think that this study may also help understand the progressively lower allergen challenge needed, and increased severity of symptoms observed, in patients with allergic manifestations. It should hopefully help in exploring avenues to limit the progress of these sometimes crippling disorders.

Samenvatting

Moleculaire herkenning stuurt de selectieve interactie van macromoleculen in alle biologische processen. Dit proces van selectieve interactie is afhankelijk van de *complementariteit* van de twee betrokken biomoleculen en is verantwoordelijk voor de sterkte van de binding (affiniteit genoemd i.g.v. antigeen-antistof interactie). Het is reeds jaren bekend dat secundaire humorale immuunreakties sneller op gang komen, sterker zijn, en bestaan uit antistoffen met een andere isotype en van hogere affiniteit voor het antigeen dan primaire immuunreakties. De verhoging in affiniteit van de antistoffen in de loop van een immuunreaktie (affiniteitsmaturatie), wordt veroorzaakt door hypermutatie en antigeen-gestuurde selectie in de kiemcentra. Het eindresultaat is een verbeterde complementariteit tussen de paratopen van de antistoffen en de epitopen van het antigeen. Kiemcentra zijn waarschijnlijk de plaats waar isotype switching en hypermutatie plaatsvinden. Het is bekend dat interleukine-4 (IL-4) een cruciale rol speelt in de ontwikkeling van kiemcentra, bij het voorkomen van apoptose van antigeen-geselecteerde B-cellen, en bij hun verdere proliferatie. IL-4 induceert in muizen een selectieve isotype switching van IgM antistoffen naar IgG_1 en IgE. In dit proefschrift wordt onderzoek beschreven naar de invloed van extra toegediend IL-4 op het proces van affiniteitsrijping van antigeen-specifieke IgG_1 antistoffen in het serum van muizen. Uiteindelijk hopen we onze studies uit te breiden naar de regulatie van de affiniteitsrijping bij de mens.

Het eerste hoofdstuk van dit proefschrift beschrijft de belangrijkste kenmerken van het immuunsysteem en het mechanisme dat ten grondslag ligt aan specificiteit, diversiteit en geheugen van de humorale immuunreaktie. De processen van somatische hypermutatie en antigeen-gedreven selectie worden tevens beschreven in dit hoofdstuk. Ook worden de kiemcentra kort beschreven, waar de klonale expansie en differentiatie van B cellen, de somatische hypermutatie en de isotype switching plaatsvinden.

Hoofdstuk 2 behandelt de toepassing van ELISA om de concentratie en affiniteit van antistoffen te bepalen. ELISA is een van de meest eenvoudige immunologische technieken, met een grote variëteit aan toepassingen in tal van vakgebieden. Hoofdstuk 2.1 behandelt de concentratiebepaling van biomoleculen m.b.v ELISA. Belangrijke parameters die de uitvoering van een ELISA kunnen beïnvloeden en verschillende methoden van databewerking worden bediscussiëerd in dit hoofdstuk. In hoofdstuk 2.2 beschrijven we een Terasaki-ELISA die gebruikt kan worden om de concentratie van totaal IgE en antigeen-specifieke IgE antistoffen te meten. Deze Terasaki-ELISA heeft een detectielimiet van 1-10 ng/ml en verbruikt maar 5 µl monster. Voor *sequentiële evenwichts-bindingsanalyse* hebben we de niet-competitieve Terasaki-ELISA aangepast voor affiniteitsbepalingen (hoofdstuk 2.3). Bij deze methode laten we een aantal malen bindingsevenwicht tot stand komen tussen het

geïmmobiliseerde antigeen op de bodem van de putjes in een Terasakiplaat en de antigeen-specifieke antistof in het supernatant in het putje. Uit de wet van de Massawerking van Goldberg en Waage, volgens welke de snelheid van een reaktie evenredig is met het produkt van de concentraties der reagerende stoffen, werd een vergelijking afgeleid die gebruikt kan worden om een relatieve affiniteitsconstante (K_{rel}) te berekenen. Via een omrekeningsfactor is de evenwichtsconstante (K_D) uit de K_{rel} te berekenen. Gedurende onze studie met monoklonale IgE antistoffen vonden we dat sommige mengsels van gezuiverde IgE antistoffen een opvallende verhoging in hun affiniteit voor het antigeen vertoonden. Deze resultaten staan vermeld in hoofdstuk 2.4. Wij suggereren dat de waargenomen verhoging een artefact van het zuiveringsproces is. In hoofdstuk 2.5 hebben we de sequentiële evenwichts-bindingsanalyse toegepast in de microtiter ELISA. Wij hebben deze techniek gebruikt voor de evaluatie van immunisatieprotocollen. Om het proces van affiniteitsmaturatie te beschrijven, is het niet voldoende om de gemiddelde affiniteitsconstante te bepalen, maar moet tevens een verschuiving naar subpopulaties antistoffen van een hogere affiniteitsklasse later in de immuunreaktie worden aangetoond. Daarom wordt in hoofdstuk 2.5 een eenvoudige hapteen inhibitie-ELISA beschreven, die geschikt is om de relatieve affiniteitsdistributie van subpopulaties van antigeen-specifieke antistoffen in sera te bepalen.

Wij hebben gevonden dat sequentiële evenwichts-bindingsanalyse het meest geschikt is voor het in volgorde plaatsen van antistoffen naar een toenemende affiniteit. De grote omrekeningsfactor, die nodig is om de absolute K_D waarde te berekenen uit de K_{rel}, vergroot gemakkelijk de primaire fouten in de resultaten. Daarom is een ELISA voor een absolute K_D bepaling niet geschikt.
Daarnaast is een ELISA een discontinue, heterogene evenwichtsafhankelijke test en geven de zo verkregen gegevens mogelijk geen homogene interacties weer. Op basis van deze problemen hebben we tevens een biosensor gebruikt voor affiniteitsbepalingen.

Hoofdstuk 3 beschrijft het gebruik van optische biosensortechnologie (IAsys^{tm}, Fisons Applied Sensor Technology) voor interactie-analyse. De resonantie spiegelbiosensor, die gebruikt werd, is een cuvet systeem gebaseerd op de "resonantiegolf" techniek. De te bestuderen verbinding (ligand) is direct gebonden aan het sensoroppervlak. De verandering van resonantiehoek, die optreedt door biomoleculen die binden of dissociëren van het oppervlak, kan gevolgd worden in de tijd en kan worden weergegeven in de vorm van een bindingscurve. Alle traditionele methoden van affiniteitsmetingen zijn evenwichtsafhankelijke methoden. Biosensoren daarentegen, geven de unieke gelegenheid om de reactie te volgen in de tijd, en dus om de werkelijke associatie en dissociatie snelheidsconstanten te bepalen.

Hoofdstuk 3.1 geeft een overzicht van methoden voor affiniteitsbepalingen met speciale aandacht voor de biosensor. De wiskundige basis van data analyse wordt eveneens uitvoerig besproken in dit hoofdstuk. Verschillende parameters, die de uitvoering en de analyse met een biosensor kunnen beïnvloeden, worden ook beschreven. De toepassing van een biosensor bij interactie-analyse tussen het antigeen en de monoklonale en polyklonale antistoffen wordt beschreven in hoofdstuk 3.2. In dit hoofdstuk tonen wij tevens aan dat met behulp van een biosensor de affiniteitsdistributie van antigeen-specifieke antistoffen in sera kan worden gemeten. Desondanks, vanwege de lange tijd die distributie-analyse in beslag neemt, kiezen wij voor een andere methode om de relatieve affiniteitsdistributie te bepalen, namelijk de ELISA.

Nadat wij de methoden, die het mogelijk maken affiniteitsmaturatie te bestuderen, ontwikkeld en geoptimaliseerd hadden, onderzochten we de invloed van IL-4 toediening op zowel de functionele affiniteit als de affiniteitsdistributies van TNP-specifieke serum IgG_1 antistoffen in primaire en secundaire reakties in BALB/c muizen (hoofdstuk 3.3). We stelden vast dat IL-4 de snelheid van affiniteitsmaturatie van IgG_1 antistoffen verhoogt. De functionele affiniteit van antistoffen in IL-4 behandelde muizen was niet significant verschillend van die van onbehandelde muizen. De affiniteitsdistributies verschoven echter naar hogere affiniteits-subgroepen. We denken dat IL-4 de waargenomen verschuiving naar hogere affiniteiten veroorzaakt door een combinatie van mechanismen die leiden tot een verhoogde interactie tussen zowel T- en B-cellen als folliculaire dendritische cellen en B-cellen in de kiemcentra.

Samengevat kan worden gesteld, dat zowel relatief eenvoudige als zeer verfijnde, recent ontwikkelde technieken geschikt zijn voor de bepaling van de affiniteit en affiniteitsdistributie van serum antistoffen. Uit onze resultaten blijkt dat de niet-competitieve ELISA, zoals door ons ontwikkeld, het meest geschikt is voor de indeling van monoklonale antistoffen op basis van hun relatieve affiniteit en voor de bepaling van relatieve affiniteitsdistributies van polyklonale antistoffen.

Biosensoren zijn op hun beurt goed te gebruiken voor de absolute bepaling van de K_A van monoklonale antistoffen en geven tevens een goede indicatie voor de K_A van polyklonale antistoffen. Wij stelden vast dat IL-4 de snelheid van de affiniteitsmaturatie van IgG_1 antistoffen verhoogt. Omdat de vorming van zowel IgG_1 als IgE afhankelijk is van IL-4, zijn we van mening dat deze studie mogelijk kan helpen meer inzicht te krijgen in allergische aandoeningen bij patiënten. Hopelijk helpt deze studie bij het vinden van nieuwe wegen om de ontwikkeling en de verergering van deze soms ernstige aandoeningen te beperken.

Abbreviations

5-AS	aminosalicylic acid
A	adenine
ABTS	2,2'-azino-bis(3-ethylbenz-thiazoline-6-sulfonic acid)
AFU	arbitrary fluorescence units
APC	antigen-presenting cells
BSA	bovine serum albumin
BSAP	B cell-specific transcription factor
C	cytosine
CDR	complementarity determining regions
CGG	chicken gamma globulin
C_H	constant region, immunoglobulin heavy chain domain
CMD	carboxymethylated dextran
DNP	dinitrophenyl
DNP-lys	N-ε-DNP-L-lysine-HCl
EDC	N-ethyl-N'(dimethylaminopropyl)carbodiimide
ELISA	enzyme-linked immunosorbent assay
Fc	fragment crystallizable
FDC	follicular dendritic cells
FM-P	fluorescein methyl phosphate
FRW	frame work
FV	heterodimer of V_H and V_L domain
G	guanine
GAM	goat-anti-mouse
GC	germinal center
H chain	immunoglublin heavy chain
His	histidine
HPA	hydroxyphenylacetic acid
hrs	hours
Ig	immunoglobulin
IgE	immunoglobulin E
IgG^+ cells	immunoglobulin G positive cells
IgM^+ cells	immunoglobulin M positive cells
IL-4	interleukin 4
J chain	joining chain
K_A/K_D	affinity constant
k_{ass}	association rate constant
k_{diss}	dissociation rate constant
KLH	keyhole limpet hemocyanin
k_{on}	apparent on rate
K_{rel}	relative affinity constant
L chain	immunoglobulin light chain
mAb	monoclonal antibody
MBS	M-maleimidebenzoyl-N-hydroxysuccinimide ester

min	minutes
MUF-P	methyl umbelliferyl phosphate
MUF-G	4-methyl umbelliferyl-ß-galactopyranoside
NADH	nicotinamide adenine dinucleotide
NHS	N-hydroxysuccinimide
NMS	normal mouse serum
OD	optical density
ONPG	ortho nitrophenyl galactose
ONPP	ortho nitrophenyl phosphate
OPD	orthophenylene diamine
PALS	periarteriolar lymphatic sheath
PBS	phosphate buffered saline
PBS/T	PBS containing 0.1% Tween 20
PCF	plate correction factor
Phe	phenylalanine
phOX	2-phenyloxazolone
PNA	peanut agglutinin
PVC	polyvinylchloride
RAM	rabbit-anti-mouse
RIA	radio-immune assay
RT	room temperature
SA-HRP	streptavidin-horseradish peroxidase
SD	standard deviation
sec	seconds
sIg	surface immunoglobulin
SPDP	succinimidyl-3-(2-pyridyldithiopropionate)
T	thymine
TD	T cell dependent
Th cells	T helper cells
TNP	trinitrophenyl
TW20	Tween 20
V region	variable region of immunoglobulin

Glossary

Association rate constant (k_{ass}) - Forward velocity rate constant of a chemical reaction.

Dissociation rate constant (k_{diss}) - Backward velocity rate constant of a chemical reaction.

Affinity - Refers to the strength of the interaction between a single antigen-binding site of an antibody and an antigenic determinant. It can be given in terms of the equilibrium constant K_A (M^{-1}) which is the ratio of the velocity rates (k_{ass}/k_{diss}) at equilibrium. K_D (M) equals K_A^{-1}.

Avidity - Is the strength of the binding between a multivalent antigen and a multivalent antibody.

Functional affinity - The term functional affinity is used to describe the technique-dependent, quantitative assignment of a value to the strength of binding between multivalent antigen and multivalent antibody populations, e.g. in serum. Since parameters other than the primary antigen-antibody interaction influence its determination, it is not, thermodynamically speaking, an absolute value.

Biosensor - A biosensor is an analytical microelectronic device that uses biological detector molecules as sensing or signal transducing elements. The device detects chemicals or biomolecules by virtue of chemical, physical or electronic changes occurring as a result of the binding.

ELISA - Enzyme-linked immunosorbent assays are heterogeneous immunosorbent assays, in which the ligand is attached to a solid phase and the bound and free fraction of the ligate (either antigen or antibody) are physically separated by a washing procedure. An enzyme label is used for subsequent detection.

Dankwoord

A number of people have helped me directly and indirectly in my work. It is impossible to mention all of them. I take this opportunity to thank those who have been directly involved and gratefully acknowledge their contribution and help.


Prof. dr. O. Vos: For making this possible.


Prof. dr. Benner, Rob: For going far beyond the call of duty in giving help and encouragement. But for you, this would have been just a dream.


Dr. Savelkoul, Huub: For the trust and confidence in me; for being such an encouraging and enthusiastic guide. A kinder boss I could not have hoped for.


John Tibbe and Astrid Vredendaal: For the hard work; for being so 'aardig', supportive and helpful; for all the 'gezellige' lunches.


Ann Vossen and Miranda Baert: For putting up with me; for all the 'steun' and help when I got into a dip phase.


My lab-genotes - A3, Willy, Hedda, Rene, Kimberley, Marika, Stefan: For the help; the gezelligheid; the warmth and the kindness.


Rianne van der Linde-Preesman: For the companionship in k738; for showing me the ropes when I was a novice in the Netherlands.


Afdeling Immunologie: For the kindness, the interesting give and take.


Petra Assems and Geertje de Korte: For helping with the manuscripts.

Tom Vermetten and Henk Janse: For taking care of the administrative matters.

Tar van Os: For the beautiful figures and slides.

My Parents: I want to thank you for so many things, where do I start? Above all, thank you for giving me legs to stand on.

Sanjeev: Thanking you feels odd, its like thanking a part of myself! Thank you all the same for granting me all the space I need, for patiently putting up with the 2 a.m. brainwaves; for always being there.

Gauri: Being so young, I am sure you found it difficult to understand my need to keep going on, for space. Thank you, my dear, for granting it to me all the same.

Curriculum vitae

30-01-1955	Born at Sangli, Maharashtra, India
1960 - 1971	Secondary School Certificate
1971 - 1975	Bachelor of Science (principal subject: Microbiology; subsidiary subject: Chemistry)
1975 - 1977	Master of Science in Microbiology
1978 - 1985	Lecturer in Microbiology University of Bombay, India
1985 - 1995	Research in Immunology for a Ph.D. degree at the Department of Immunology, Erasmus University, Rotterdam, The Netherlands
1988 onwards	Consultant Microbiologist and Immunologist Guest-lecturer at the University of Bombay for M.Sc. course in Microbiology.

Publications

1. Kane S.M.* (1977) Microbial aspects of export-quality frozen frog-legs. Dissertation submitted to the University of Bombay in partial-fulfillment of the requirement for M.Sc. degree in Microbiology.
2. Pathak S.S. (1980) Notes in Microbiology. Schola Mundi, London, UK.
3. Savelkoul H.F.J., Pathak S.S. and Van der Linde-Pressman A.A. (1987) Rapid purification of mouse IgE antibodies by multi-column liquid chromatography. In: 'Proceedings Second FPLC Symposium', Pharmacia Nederland. p. 83-93.
4. Savelkoul H.F.J., Pathak S.S. and Van der Linde-Preesman A.A. (1987) Occurrence of damaged heavy chains during purification of murine IgE antibodies by fast protein liquid chromatography (FPLC) and their effect on the determination of concentration and affinity in ELISA. Prot. Biol. Fluids 35:375-382.
5. Savelkoul H.F.J., Pathak S.S., Sabbele N.R. and Benner R. (1988) Generation and measurement of antibodies. In: 'The Pharmacology of Lymphocytes'. Handbook of Pharmacology, Vol. 85, Morley, J. and Bray, M.R. (Eds.) Springer Verlag, Heidelberg. p. 141-185.
6. Savelkoul H.F.J., Soeting P.W.C., De Josselin-De Jong J.E. and Pathak S.S. (1989) Terasaki-ELISA for murine IgE antibodies. II. Quantitation of absolute concentration of antigen-specific and total IgE. J. Immunol. Methods 116:277-285.
7. Pathak S.S., Vos Q. and Savelkoul H.F.J. (1989) Terasaki-ELISA for murine IgE. III. Determination of concentration and functional affinity by sequential equilibrium binding analysis. J. Immunol. Methods 123:71-81.
8. Savelkoul H.F.J. and Pathak S.S. (1994) The IAsys biosensor for affinity measurements of antibodies in immune responses. Fusion 7:10-11.
9. Pathak S.S. and Savelkoul H.F.J. (1995) Quantitation of concentration and functional affinity of immunoglobulins with special reference to Terasaki-ELISA. Life Science Advances, CSI, Trivandrum. In press.
10. Pathak S.S. and Palan U.N. (1995) Immunology: A comprehensive textbook. B.I. Publications Pvt. Ltd., New Delhi. In press.
11. Pathak S.S., Van Oudenaren A. and Savelkoul H.F.J. (1995) Quantitation of immunoglobulin concentration by ELISA. In: 'Manual of Immunological Methods'. I. Lefkovits (Ed), Academic Press, London. In press.
12. Pathak S.S., Tibbe G.J.M., Savelkoul H.F.J. (1995) Antibody affinity determination by ELISA and biosensor. In: 'Manual of Immunological Methods'. I. Lefkovits (Ed), Academic Press, London. In press.
13. Pathak S.S., Tibbe G.J.M. and Savelkoul H.F.J. (1995) Application of a resonant mirror optical biosensor to the determination of functional affinity in monoclonal and polyclonal antibody systems. Submitted.
14. Pathak S.S. and Savelkoul H.F.J. (1995) Biosensors and their potential

uses. Submitted.
15. Pathak S.S. and Savelkoul H.F.J. (1995) Mixing two monoclonal IgE antibodies increases the functional affinity of the mixture for the antigen. Submitted.
16. Pathak S.S., Vredendaal A., Van Ommen R. and Savelkoul H.F.J. (1995) Interleukin-4 influences the pace of affinity maturation of IgG1 antibodies. Submitted.
17. Pathak S.S. and Savelkoul H.F.J. (1995) Determination of relative affinity and affinity distributions in ELISA. Submitted.

* S.M. Kane is the maiden name of S.S. Pathak